

AD-A013 923

EXPLORATORY DEVELOPMENT OF WELD QUALITY DEFINITION AND  
CORRELATION WITH FATIGUE PROPERTIES

Robert Witt, et al

Grumman Aerospace Corporation

Prepared for:

Air Force Materials Laboratory

April 1975

DISTRIBUTED BY:

**NTIS**

National Technical Information Service  
U. S. DEPARTMENT OF COMMERCE

245095

AFML-TR-75-7

AD A 0 1 3 9 2 3

**EXPLORATORY DEVELOPMENT OF  
WELD QUALITY DEFINITION AND  
CORRELATION WITH FATIGUE PROPERTIES**

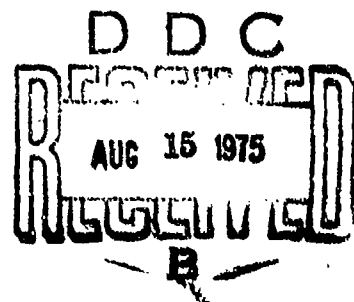
GRUMMAN AEROSPACE CORPORATION  
BETHPAGE, NEW YORK 11716

APRIL 1975

TECHNICAL REPORT AFML-TR-75-7

FINAL REPORT FOR PERIOD SEPTEMBER 1972-NOVEMBER 1974

Approved for public release; distribution unlimited.



AIR FORCE MATERIALS LABORATORY  
AIR FORCE WRIGHT AERONAUTICAL LABORATORIES  
AIR FORCE SYSTEMS COMMAND  
WRIGHT-PATTERSON AIR FORCE BASE, OHIO 45433

Reproduced by  
NATIONAL TECHNICAL  
INFORMATION SERVICE  
US Department of Commerce  
Springfield, VA. 22151

NOTICE

When Government drawings, specifications, or other data are used for any purpose other than in connection with a definitely related Government procurement operation, the United States Government thereby incurs no responsibility nor any obligation whatsoever; and the fact that the government may have formulated, furnished, or in any way supplied the said drawings, specifications, or other data, is not to be regarded by implication or otherwise as in any manner licensing the holder or any other person or corporation, or conveying any rights or permission to manufacture, use, or sell any patented invention that may in any way be related thereto.

This technical report has been reviewed and is approved for publication.

APPROVED FOR	
THIS	White Staff <input checked="" type="checkbox"/>
BY	DISPATCH <input type="checkbox"/>
UNCLASSIFIED	<input type="checkbox"/>
CLASSIFICATION	
BY	
DISTRIBUTION/AVAILABILITY CODES	
Dist.	AVAIL. and/or SPECIAL
A	

Paul L. Hendricks  
PAUL L. HENDRICKS  
Project Engineer  
Corrosion Control & Failure Analysis

FOR THE COMMANDER  
T. D. Cooper  
T. D. COOPER, Chief  
Aeronautical Systems Branch  
Systems Support Division  
Air Force Materials Laboratory

Copies of this report should not be returned unless return is required by security considerations, contractual obligations, or notice on a specific document.

UNCLASSIFIED

SECURITY CLASSIFICATION OF THIS PAGE (When Data Entered)

REPORT DOCUMENTATION PAGE		READ INSTRUCTIONS BEFORE COMPLETING FORM
1. REPORT NUMBER AFML-TR-75-7	2. GOVT ACCESSION NO.	3. RECIPIENT'S CATALOG NUMBER
4. TITLE (and Subtitle) Exploratory Development of Weld Quality Definition AND CORRELATION WITH FATIGUE PROPERTIES		5. TYPE OF REPORT & PERIOD COVERED Final Report September 1972 - November 1974
7. AUTHOR(s) R. Witt and O. Paul		6. PERFORMING ORG. REPORT NUMBER
9. PERFORMING ORGANIZATION NAME AND ADDRESS Grumman Aerospace Corporation Bethpage, New York 11714		8. CONTRACT OR GRANT NUMBER(s) F33615-72-C-2039
11. CONTROLLING OFFICE NAME AND ADDRESS Air Force Materials Laboratory Air Force Systems Command Wright-Patterson Air Force Base, Ohio 45433		10. PROGRAM ELEMENT, PROJECT, TASK AREA & WORK UNIT NUMBERS Project Nr. 7381 Task Nr. 738107 Work Unit Nr. 73810739
14. MONITORING AGENCY NAME & ADDRESS (if different from Controlling Office)		12. REPORT DATE April 1975
		13. NUMBER OF PAGES 240
		15. SECURITY CLASS. (of this report) Unclassified
		15a. DECLASSIFICATION/DOWNGRADING SCHEDULE
16. DISTRIBUTION STATEMENT (of this Report) Approved for public release; distribution unlimited.		
17. DISTRIBUTION STATEMENT (of the abstract entered in Block 20, if different from Report)		
18. SUPPLEMENTARY NOTES		
19. KEY WORDS (Continue on reverse side if necessary and identify by block number) Welding                      Nondestructive Inspection                      Electron-Beam Welding Titanium                      Metallography                      Plasma-Arc Welding Weld Defects                      Mechanical Properties                      Gas-Tungsten-Arc Welding Defect Production Techniques                      Gas-Metal-Arc Welding		
20. ABSTRACT (Continue on reverse side if necessary and identify by block number) The purpose of this program was to conduct an exploratory evaluation of the effects of typical weld anomalies on fatigue endurance of Ti-6Al-4V titanium alloy weldments and to propose criteria for acceptance/rejection of titanium fusion welds.		

DD FORM 1473 1 JAN 73

EDITION OF 1 NOV 68 IS OBSOLETE  
S/N 0102-014-6601

1-a

UNCLASSIFIED

SECURITY CLASSIFICATION OF THIS PAGE (When Data Entered)

The program objectives were as follows:

- Determine the feasibility of producing typical defects in Ti-6Al-4V titanium alloy weldments by intentional variation of processing parameters. Ti-6Al-4V (STOA) plates were utilized as base materials.
- Evaluate the effect of flaws produced intentionally in experimental welds by electron-beam (EB), plasma-arc (PA), gas-tungsten-arc (GTA), and gas-metal-arc (GMA) welding on fatigue endurance.
- Propose acceptance criteria for titanium fusion weldments based on correlation of fatigue test results with both nondestructive inspection and fractographic findings.

The welding parameters used to generate intentional flaws were intended to simulate conditions which could inadvertently occur in production welding. The types of defects and the welding processes used to generate them included porosity (EB, PA, GTA, and GMA), bursts (EB), inclusions (GTA), mismatch (EB, PA and GTA), undercuts (PA and GTA), underfills (EB, PA and GTA), reinforcements (EB, PA and GTA), lack of penetration (EB and GMA), surface contamination (EB, PA and GTA) and cracks (GTA).

The fatigue endurance of weldments containing these defects was determined and correlated with pretest radiographic and fractographic findings. Corresponding flawless-weld and base-metal properties were evaluated at various stress intensity ( $K_t$ ) levels. The fatigue endurance of EB welds repaired by both mechanized and manual GTA welding techniques was characterized.

Proposed acceptance criteria for titanium fusion welds were prepared. Data generated to support the proposed standards and to determine the degree of compliance with proposed specifications were analyzed.

## FOREWORD

This Final Technical Report covers all work performed under Contract F33615-72-C-2039 from 29 September 1972 through 31 October 1974. The report was released by the authors in November 1974.

This Contract with Grumman Aerospace Corporation, Bethpage, New York, was initiated under task number 738107 "Exploratory Development of Weld Quality Definition and Correlation with Fatigue Properties." The work was administered under the technical direction of Mr. Paul L. Hendricks (AFML/MXA) of the Aeronautical Systems Branch, Systems Support Division, Air Force Materials Laboratory, Wright-Patterson Air Force Base, Ohio.

The program was directed by Mr. Robert Witt, Program Manager, and Mr. Olev Paul, Project Engineer. Others assisting on the project were Messrs. Albert Flescher, Joel Magnuson, Harold Ellison, Vincent Sgro and Salvatore Stracquadaini of Advanced Materials and Processes Development; Messrs. David Layton, Peter Donohue, Robert Zoellner and Robert Wigger of Elements and Materials Testing; Messrs. Robert Messler, Jr., and Robert Knappe of Metallurgy and Welding Engineering; and Mr. Dennis Becker of the Quality Control Laboratory.

This project was accomplished as part of the Air Force Manufacturing Methods Program, the primary objective of which is to develop on a timely basis, manufacturing processes, techniques and equipment for use in economical production of aircraft materials and components.

## CONTENTS

Section		Page
I	INTRODUCTION . . . . .	1
	A. BACKGROUND . . . . .	1
	B. OBJECTIVES . . . . .	1
	C. PROGRAM SCOPE . . . . .	2
II	EXPERIMENTAL PROCEDURES . . . . .	5
	A. MATERIALS . . . . .	5
	1. Phase I . . . . .	5
	2. Phase II . . . . .	5
	B. PROCESSING OF TEST SPECIMENS . . . . .	5
	1. Machining of Weld Blanks . . . . .	5
	2. Joint Preparation . . . . .	7
	3. Acid Cleaning . . . . .	7
	4. Welding . . . . .	7
	5. Weld Characterization . . . . .	11
	6. Identification of Test Specimen Configurations . . . . .	12
	7. Fatigue Tests . . . . .	13
III	DEVELOPMENT OF PARAMETERS FOR INTENTIONAL PRODUCTION OF WELD DEFECTS - Phase I . . . . .	15
	A. PROCEDURES . . . . .	15
	1. Porosity . . . . .	15
	2. Mismatch . . . . .	15
	3. Underfill . . . . .	15
	4. Surface Contamination . . . . .	16
	5. Lack of Penetration . . . . .	16
	6. Reinforcement . . . . .	16
	7. Undercut . . . . .	16
	8. Inclusions . . . . .	16
	9. Bursts . . . . .	16
	10. Cracks . . . . .	16
	11. Base Metal Fatigue Endurance . . . . .	17

CONTENTS (Continued)

Section	Page
III	
B. DEMONSTRATION OF THE FEASIBILITY OF GENERATING INTENTIONAL DEFECTS . . . . .	17
1. Porosity . . . . .	17
2. Lack of Penetration . . . . .	19
3. Undercut . . . . .	22
4. Underfill . . . . .	22
5. Inclusions . . . . .	22
6. Mismatch . . . . .	26
7. Reinforcement . . . . .	24
8. Surface Contamination . . . . .	24
9. Cracks . . . . .	24
10. Bursts . . . . .	31
11. Flawless Welds . . . . .	38
IV	
FATIGUE ENDURANCE OF GTA WELDMENTS . . . . .	39
A. INTRODUCTION . . . . .	39
B. GENERAL FABRICATION PROCEDURE . . . . .	39
C. FLAWLESS GTA WELDMENTS . . . . .	39
1. 0.080-Inch Thick Welds . . . . .	39
2. 0.25-Inch Thick Welds . . . . .	39
D. POROUS GTA WELDS . . . . .	41
1. .080-Inch Thick Welds . . . . .	41
2. 0.25-Inch Thick Welds . . . . .	41
E. REINFORCED GTA WELDS . . . . .	45
1. 0.080-Inch Thick Welds . . . . .	45
2. 0.25-Inch Thick Welds . . . . .	45
F. MINOR UNDERFILLS . . . . .	50
1. 0.080-Inch Thick Welds . . . . .	50
2. 0.25-Inch Thick Welds . . . . .	50

CONTENTS (Continued)

Section	Page
IV	<ul style="list-style-type: none"> <li>G. MINOR UNDERCUT, 0.080-Inch Thick Welds . . . . . 55</li> <li>    1. 0.25-Inch Thick Welds . . . . . 55</li> <li>    2. Evaluation of Fatigue Data . . . . . 55</li> </ul>
H.	<ul style="list-style-type: none"> <li>TUNGSTEN INCLUSIONS IN GTA WELDS . . . . . 59</li> <li>    1. Fabrication of Experimental Welds . . . . . 59</li> <li>    2. Evaluation of Fatigue Data . . . . . 59</li> </ul>
I.	<ul style="list-style-type: none"> <li>MISMATCH . . . . . 59</li> <li>    1. Fabrication of Experimental Welds . . . . . 59</li> <li>    2. Mismatched - 0.25-Inch Thick Welds . . . . . 64</li> </ul>
J.	<ul style="list-style-type: none"> <li>GTA WELDS PRODUCED UNDER INTENTIONALLY INADEQUATE SHIELDING CONDITIONS . . . . . 64</li> <li>    1. 0.080-Inch Thick Welds . . . . . 64</li> <li>    2. 0.25-Inch-Thick Welds . . . . . 69</li> </ul>
K.	<ul style="list-style-type: none"> <li>0.25-INCH THICK GTA WELDS CONTAINING TRANSVERSE CRACKS . . . . . 69</li> <li>    1. Fabrication of Experimental Welds . . . . . 69</li> <li>    2. Evaluation of Fatigue Data . . . . . 73</li> </ul>
L.	<ul style="list-style-type: none"> <li>GTA-REPAIRED 0.25-INCH THICK ELECTRON-BEAM WELDS . . 73</li> <li>    1. Fabrication of Experimental Welds . . . . . 73</li> <li>    2. Evaluation of Fatigue Data . . . . . 73</li> </ul>
M.	<ul style="list-style-type: none"> <li>SUMMARY . . . . . 76</li> </ul>
V	<ul style="list-style-type: none"> <li>FATIGUE CHARACTERISTICS OF ELECTRON BEAM (EB) WELDMENTS PHASE II . . . . . 77</li> <li>    A. INTRODUCTION . . . . . 77</li> <li>    B. FLAWLESS WELDS . . . . . 77</li> <li>        1. Fabrication of Experimental Weldments (0.080 and             0.25-Inch Thick) . . . . . 77</li> <li>        2. Fatigue Endurance of 0.080-Inch Thick Flawless Welds . . . . . 77</li> <li>        3. Fatigue Endurance of 0.25-Inch Thick Flawless Welds . . . . . 77</li> <li>        4. Radiographically and Ultrasonically Flawless 1.5-Inch             Thick EB Welds . . . . . 78</li> </ul>

CONTENTS (Continued)

Section	Page
V	<ul style="list-style-type: none"> <li>C. POROSITY-CONTAINING WELDS . . . . . 80                             <ul style="list-style-type: none"> <li>1. 0.080-Inch Thick Welds . . . . . 81</li> <li>2. 0.25-Inch Thick Welds . . . . . 83</li> <li>3. 1.5-Inch Thick Welds . . . . . 89</li> </ul> </li> <li>D. MISMATCH - 0.25-Inch Welds . . . . . 100                             <ul style="list-style-type: none"> <li>1. Fabrication of Test Specimens . . . . . 100</li> <li>2. Fatigue Tests . . . . . 100</li> </ul> </li> <li>E. INTENTIONAL UNDERFILL, 0.25-Inch Thick Welds . . . . . 100                             <ul style="list-style-type: none"> <li>1. Fabrication of Experimental Weldments . . . . . 100</li> <li>2. Fatigue Test Results . . . . . 100</li> </ul> </li> <li>F. SURFACE CONTAMINATION - 0.25-Inch Thick Welds . . . . . 104                             <ul style="list-style-type: none"> <li>1. Fabrication of Experimental Weldments . . . . . 104</li> <li>2. Evaluation of Fatigue Test Results . . . . . 104</li> </ul> </li> <li>G. LACK OF PENETRATION - 1.5-INCH THICK WELDMENTS . . . . . 104                             <ul style="list-style-type: none"> <li>1. Fabrication of Experimental Welds . . . . . 104</li> <li>2. Evaluation of Fatigue Data . . . . . 104</li> </ul> </li> <li>H. FATIGUE ENDURANCE OF EB WELDMENTS CONTAINING BURSTS . . . . . 109                             <ul style="list-style-type: none"> <li>1. Fabrication of Experimental Welds . . . . . 109</li> <li>2. Evaluation of Fatigue Data . . . . . 109</li> </ul> </li> <li>I. SUMMARY . . . . . 113</li> </ul>
VI	<ul style="list-style-type: none"> <li>FATIGUE ENDURANCE OF MECHANIZED PLASMA-ARC WELDED (PAW) 0.25-INCH THICK WELDMENTS PHASE II . . . . . 115                             <ul style="list-style-type: none"> <li>A. INTRODUCTION . . . . . 115</li> <li>B. FLAWLESS WELDS . . . . . 115                                     <ul style="list-style-type: none"> <li>1. Fabrication Procedure . . . . . 115</li> <li>2. Evaluation of Fatigue Data . . . . . 115</li> </ul> </li> <li>C. POROUS WELDS . . . . . 116                                     <ul style="list-style-type: none"> <li>1. Fabrication Procedure . . . . . 116</li> <li>2. Evaluation of Fatigue Data . . . . . 116</li> </ul> </li> <li>D. MISMATCH . . . . . 117                                     <ul style="list-style-type: none"> <li>1. Fabrication Procedure . . . . . 117</li> <li>2. Evaluation of Fatigue Data . . . . . 118</li> </ul> </li> </ul> </li> </ul>

CONTENTS (Continued)

Section		Page
VI	E. WELDS WITH UNDERFILL AND UNDERCUT DEFECTS . . . . .	121
	1. Fabrication Procedure . . . . .	121
	2. Evaluation of Fatigue Data . . . . .	121
	F. REINFORCED WELDS . . . . .	122
	1. Fabrication Procedure . . . . .	122
	2. Evaluation of Fatigue Data . . . . .	122
	G. SURFACE-CONTAMINATED WELDS . . . . .	126
	1. Fabrication Procedure . . . . .	126
	2. Evaluation of Fatigue Data . . . . .	126
	H. SUMMARY . . . . .	129
VII	FATIGUE CHARACTERISTICS OF 0.25-INCH THICK GAS-METAL- ARC (GMA) WELDMENTS - PHASE II . . . . .	131
	A. INTRODUCTION . . . . .	131
	B. WELDMENT PREPARATION . . . . .	131
	C. FLAWLESS WELDS . . . . .	131
	1. Fabrication Procedure . . . . .	131
	2. Evaluation of Fatigue Data . . . . .	131
	D. WELDS WITH UNDERCUT AND LACK-OF-PENETRATION DEFECTS . . . . .	132
	1. Fabrication Procedure . . . . .	132
	2. Evaluation of Fatigue Data . . . . .	134
	E. FATIGUE ENDURANCE OF POROSITY-CONTAINING WELDS . . . . .	134
	1. Fabrication Procedure . . . . .	134
	2. Evaluation of Fatigue Data . . . . .	134
	F. SUMMARY . . . . .	134
VIII	CRITERIAL FOR ACCEPTANCE OF TITANIUM FUSION WELDS . . . . .	139
	A. SCOPE . . . . .	139
	B. PROPOSED ACCEPTANCE STANDARDS FOR TITANIUM FUSION WELDS . . . . .	139
	1. Visual Inspection . . . . .	139
	2. Nondestructive Inspection . . . . .	140

CONTENTS (Continued)

Section	Page
VIII C. GUIDELINES FOR PROPOSED ACCEPTANCE STANDARDS FOR TITANIUM FUSION WELDS . . . . .	141
1. Visual Inspection . . . . .	141
2. Nondestructive Inspection . . . . .	145
IX CONCLUSIONS AND RECOMMENDATIONS . . . . .	149
A. CONCLUSIONS . . . . .	149
1. General . . . . .	149
2. Weld Defect-Fatigue Endurance Correlation . . . . .	149
B. RECOMMENDATIONS . . . . .	152
REFERENCES . . . . .	153
APPENDIX A DATA - PHASE I . . . . .	155
APPENDIX B TEST DATA SUMMARY (PHASE 2) . . . . .	197

## ILLUSTRATIONS

Figure	Page
1 Processing Flow Chart for Weld Defect Specimens . . . . .	6
2 30-KW Sciaky Electron-Beam Welding Unit . . . . .	9
3 Automatic Plasma Arc Welding Unit . . . . .	9
4 Radiography Equipment for Inspection of Weld Quality Weldments . . . . .	9
5 36' X 12' X 6' Ultrasonic Inspection Tank . . . . .	9
6 Sontag Constant-Amplitude Fatigue Machines and Multipliers . . . . .	9
7 One-Million-Pound MTS Testing Machine . . . . .	13
8 Typical Weld Profile for 0.090-Inch Thick Gas-Tungsten-Arc Porosity Specimen (6X MAG) . . . . .	18
9 Photomicrograph of Porosity in 9GTA-PX-1 Weld (250 MAG) . . . . .	18
10 Cross Section of 9GTA-PX-2 Weld Showing 0.015 Inch Pore Formed by Hydrocarbon Oil Contamination (10 X MAG) . . . . .	18
11 Weld 4EB-PX-1 One Sided Placement of Porosity, Resulting From Abrasive Grit Blast Residue (10X MAG) . . . . .	18
12 Weld 4EB-PX-6 Scattered Linear Porosity Throughout the Weld Showing the Effect of Cut Edges Without Acid Cleaning (10X MAG) . . . . .	18
13 Cross Section of a 4GMA-2-PX-Type Weld Showing Induced Porosity (10X MAG) . . . . .	18
14 Weld 4EB-PX-19 Porosity Generated by Saw Cut Edges, Insufficient Cleaning and Increased Welding Speed (10X Mag) . . . . .	20
15 Weld 4EB-PX-21 Porosity Generated by Addition of Cutting Oil to Milled Edges and Increased Weld Speed in Weld 4EB-PX-21 (10X MAG) . . . . .	20
16 Plane View of Root Surface Showing EB weld Porosity (10X MAG) . . . . .	20
17 The Profile of Weld 4-PAW-PX3. . . . .	20
18 Weld 4PAW-PM-2 . . . . .	20
19 Weld 4PAW-PM-3 . . . . .	20
20 Weld 4EB-LPX-1 Showing Lack of Penetration (6X MAG) . . . . .	21
21 Weld 4EB-PLX-3 Showing Lack of Penetration (6X MAG) . . . . .	21
22 Lack of Penetration as Produced by Variations in Beam Power, Weld 4EB-LPX-4 (10X MAG) . . . . .	21
23 Lack of Penetration as Produced by Variation in Beam Power, Weld 4EB-LFX-5 (6X MAG) . . . . .	21
24 Slight Undercut in Weld 4PAW-UCX-3 (6X MAG) . . . . .	23

ILLUSTRATIONS (Continued)

Figure		Page
25	Intermediate-Depth Undercut in Weld 4PAW-UCX-4 (10X MAG) . . . . .	23
26	Extensive Undercut in Weld 4PAW-UCX-5 (10X MAG) . . . . .	23
27	Underfill in Welds 9GTA-UFX-1 and -2 (5.5X MAG) . . . . .	23
28	Metallographic Section of a GTA Test Weld Showing Tungsten Inclusions (2.6C MAG) . . . . .	23
29	Metallographic Section of Welds 9GTA-M5X-1, 2 Showing the Intended Mismatch (4X MAG) . . . . .	23
30	Microhardness Studies on Electron-Beam Welded Surface Contamination-Type Specimen . . . . .	25
31	Weld 4EB-SUX-4. Microhardness Traces on Weld Cross Section (10X MAG) . . . . .	26
32	Weld 4PAW-SUX-1. Surface Contamination Resulting from Gas-Flow-Rate Variation . . . . .	26
33	Weld 4PAW-SUX-2. Surface Contamination Resulting from Gas-Flow-Rate Variation . . . . .	26
34	Weld 4PAW-SUX-3. Surface Contamination Resulting from Gas- Flow-Rate Variation <sup>1</sup> . . . . .	26
35	Cross Section of Weld 4PAW-SUX-1 (10X MAG) . . . . .	27
36	Cross Section of Weld 4PAW-SUX-2 (10X MAG) . . . . .	27
37	Cross Section of Weld 4PAW-SUX-3 . . . . .	27
38	Weld 4PAW-SUX-3 Hardened Surface Layer and Microhardness Indications. (250X MAG) . . . . .	27
39	Microhardness Studies on Plasma-Arc Welded Surface Contamination-Type Specimens . . . . .	28
40	View of Weld Assembly Showing Back Plate and Weld Specimen Used for the Production of Cracks . . . . .	30
41	Weld 4EB-CX-2 After the Eleventh Weld Pass (10X MAG) . . . . .	30
42	Configuration of Experimental Assembly Utilized in Stressing of Existing Welds . . . . .	30
43	Overall View of Configuration 1 Utilized for Burst Defect Generation . . . . .	33
44	Overall View of Configuration 2 Utilized for Burst Defect Generation . . . . .	33
45	Configuration 3 - Burst Generation . . . . .	33

ILLUSTRATIONS (Continued)

Figure		Page
46	Configurations 4 and 5 - Burst Generation . . . . .	33
47	Weld 4EB2-BX-16 . . . . .	33
48	Mechanism of Burst Formation During EB Welding . . . . .	34
49	Configuration of Experimental Weld Blank to Determine Burst Formation Mechanism During EB Welding . . . . .	35
50	Contoured Welding Blank Used in Burst-Generation Studies . . . . .	36
51	Radiographs Showing Indication of Burst (5 X MAG) . . . . .	37
52	Fatigue Endurance of Flawless 0.080-Inch-Thick GTA-Welded Specimens . . . . .	40
53	Typical Surface Failure Initiation Site in Flawless 0.080-Inch-Thick GTA Weldment (20 X MAG) . . . . .	40
54	Fatigue Endurance of Flawless 0.25-Inch-Thick GTA Welds . . . . .	42
55	Fatigue Endurance of Porous 0.090-Inch-Thick GTA Weldments . . . . .	43
56	0.007-Inch Pore at Failure Initiation Site in Specimen F7 (20 X MAG) . . . . .	43
57	Fatigue Endurance of 0.25-Inch-Thick GTA Welds Containing Porosity . . . . .	44
58	Multiple Failure Initiation Encountered in 0.25-inch-Thick Porous GTA Specimens with Fatigue Endurance in the $K_t = 2$ to $K_t = 3$ Range (20 X MAG) . . . . .	44
59	Isolated Surface Porosity Detected at Failure Initiation of 0.25-Inch- Thick GTA-Welded Specimen 7-1 with Fatigue Endurance in the $K_t = 2$ to $K_t = 3$ Range (20 X MAG) . . . . .	46
60	Isolated Subsurface Porosity Detected at Failure Initiation of 0.25-Inch- Thick GTA-Welded Specimen 11-2 with Fatigue Endurance in $K_t = 2$ to $K_t = 3$ Range (20 X MAG) . . . . .	46
61	Failure Initiation Site at a Surface Porosity Cluster in 0.25-Inch-Thick GTA-Welded Specimen 10-3 with Fatigue Endurance Below the $K_t = 3$ Curve (20 X MAG) . . . . .	47
62	Subsurface Porosity Cluster at the Failure Initiation Site in 0.25-Inch- Thick GTA-Welded Specimen 3-3 with Fatigue Endurance Below the $K_t = 3$ Curve (20 X MAG) . . . . .	47
63	Interior Porosity Cluster at the Failure Initiation Site in 0.25-Inch- Thick GTA-Welded Specimen 3-4 with Fatigue Endurance Below the $K_t = 3$ Curve (20 X MAG) . . . . .	48
64	Fatigue Endurance of 0.080-Inch-Thick GTA-Welded Specimen with Minor (About 0.015 Inch) Face and Root Reinforcements . . . . .	48
65	Contour of a Typical Reinforced 0.080-Inch-Thick GTA Weldment . . . . .	49

ILLUSTRATIONS (Continued)

Figure		Page
66	Typical Contour of Reinforced 0.25-Inch-Thick GTA Welds . . . . .	49
67	Fatigue Endurance of Reinforced 0.25-Inch-Thick GTA Welds . . . . .	51
68	Typical Configuration of 0.080-Inch-Thick GTA Welds with 0.010-Inch Underfills . . . . .	52
69	Typical Configuration of 0.080-Inch-Thick GTA Welds with 0.015-Inch Underfill . . . . .	52
70	Fatigue Endurance of 0.080-Inch-Thick GTA Welds with Minor Underfills . .	53
71	Typical Contour of 0.25-Inch-Thick GTA Welds with Minor Underfills . . . . .	54
72	Fatigue Endurance of 0.25-Inch-Thick GTA Welds with Minor Underfills . . .	54
73	Typical Linear (Root) Initiation Site in 0.025-Inch-Thick GTA Specimen with Minor Underfills (20 X MAG) . . . . .	56
74	Typical Contour of 0.080-Inch-Thick GTA Welds with Very Minor Undercuts . . . . .	56
75	Fatigue Endurance of 0.080-Inch-Thick GTA Welds with Minor Undercuts . .	57
76	Typical Contour of 0.25-Inch-Thick GTA Welds with Intentional Undercuts . .	57
77	Contour of 0.25-Inch-Thick GTA Welded Specimen 4-1 with Intentional Undercuts . . . . .	58
78	Fatigue Endurance of 0.25-Inch-Thick GTA Welds with Intentional Minor Undercuts . . . . .	58
79	Fatigue Endurance of 0.080-Inch-Thick GTA Welds with Tungsten Inclusions . . . . .	60
80	Internal Tungsten Inclusion Intentionally Produced in a 0.080-Inch-Thick GTA Weld (20 X MAG) . . . . .	60
81	Surface-Exposed Tungsten Inclusion in 0.080-Inch-Thick GTA Weld (20 X MAG) . . . . .	61
82	Surface View of Tungsten Inclusion in a 0.080-Inch-Thick GTA Weld (20 X MAG) . . . . .	61
83	Typical Contour of 0.25-Inch-Thick GTA Welds Containing Inclusions . . . . .	62
84	Fatigue Endurance of Contoured 0.25-Inch-Thick GTA Welds Containing Tungsten Inclusions . . . . .	62
85	Linear Failure Initiation at the Root of a 0.25-Inch-Thick GTA Weld Containing Tungsten Inclusions (No Inclusions Were Detected on Fracture Surfaces) (20 X MAG) . . . . .	63
86	Typical Contour of 0.080-Inch-Thick GTA Welds with 0.015-Inch Mismatch of Faying Surfaces . . . . .	63
87	Typical Contour of 0.080-Inch-Thick GTA Welds with 0.025-Inch Mismatch of Faying Surfaces . . . . .	63

ILLUSTRATIONS (Continued)

Figure		Page
88	Fatigue Endurance of 0.080-Inch-Thick GTA Welds with Mismatched Faying Surfaces . . . . .	65
89	Typical Failure Initiation Site at the Root of a 0.080-Inch-Thick GTA-Welded Specimen with Mismatched Faying Surfaces . . . . .	66
90	Typical Contour of 0.025-Inch-Thick GTA Weld With 0.010-Inch-Thick Mismatch . . . . .	66
91	Typical Contour of 0.25-Inch-Thick GTA Weld with 0.036-Inch-Mismatch . . . . .	66
92	Fatigue Endurance of .25-Inch-GTA Specimens with Mismatched Faying Surfaces . . . . .	67
93	Typical Linear (Root) Surface Failure Initiation 0.25-Inch-Thick GTA Welds with Mismatched Faying Surfaces . . . . .	67
94	Typical Contour of 0.080-Inch-Thick GTA Weld No. 1 Produced Under Inadequate Shielding Conditions . . . . .	68
95	Typical Contour of 0.080-Inch-Thick GTA Weld No. 2 Produced Under Inadequate Shielding Conditions . . . . .	68
96	Typical Contour of 0.080-Inch-Thick GTA Weld No. 3 Produced Under Inadequate Shielding Conditions . . . . .	68
97	Fatigue Endurance of 0.080-Inch-Thick GTA Weldments Produced Under Inadequate Shielding Conditions . . . . .	70
98	Typical Contour of 0.25-Inch-Thick GTA Welds Produced Under Intentionally Inadequate Shielding Conditions . . . . .	70
99	Fatigue Endurance of a 0.25-Inch-Thick GTA Weldments Produced Under Inadequate Shielding Conditions . . . . .	71
100	Transverse Cracks Detected in 0.25-Inch-Thick GTA Welds No. 3 Produced Under Intentionally Inadequate Shielding Conditions . . . . .	72
101	Failure Initiation Site in Specimen No. 1-2 Containing Transverse Cracks . . . . .	74
102	Fatigue Endurance of GTA-Repaired 0.25-Inch-Thick EB Welds . . . . .	75
103	Agglomeration of Porosity at EB/GTA Weld Interface Caused by Incomplete Removal of Porous EB Weld . . . . .	74
104	Fatigue Endurance of Flawless 0.080-Inch-Thick EB Welds . . . . .	78

ILLUSTRATIONS (Continued)

Figure		Page
105	Typical Surface Failure Initiation Site in Flawless 0.080-Inch-Thick EB Welds . . . . .	79
106	Fatigue Endurance of Flawless 0.25-Inch-Thick EB Welds . . . . .	79
107	Failure Initiation Site in Flawless 0.25-Inch-Thick EB Weld Specimen 2-1 (20X MAG) . . . . .	80
108	Failure Initiation Site at a Linear Cluster of Fine Porosity at the Subsurface of Flawless 0.25-Inch-Thick EB Weld 4-3 (20X MAG) . . . . .	80
109	Fatigue Endurance of Flawless 1.5-Inch-Thick EB Welds . . . . .	81
110	Fatigue Properties of Porosity-Containing 0.080-Inch-Thick EB Welds . . . . .	82
111	Multiple-Fracture Initiation Pattern Detected in Specimen 7-3 (20X MAG) . . . . .	83
112	Fracture Surface of Specimen 2-1 For Which Double-Line Porosity Indications Were Detected by Prior Radiography . . . . .	83
113	Failure Initiation Site in Specimen 13-1 . . . . .	84
114	Failure Initiation Site in Specimen 5-1 . . . . .	84
115	Fatigue Properties of Porosity-Containing 0.25-Inch-Thick EB Weldments . . . . .	84
116	Location of a 0.001-Inch-Diameter Pore on the Fracture Surface of Specimen 17-4 (20X MAG) . . . . .	85
117	Location of a 0.004-Inch-Diameter Pore on the Fracture Surface of Specimen 17-3 (20X MAG) . . . . .	85
118	Failure Initiation of Internal Porosity in Specimen 3-1 (20X MAG) . . . . .	85
119	Subsurface Failure Initiation Site in Specimen 6-1 (20X MAG) . . . . .	85
120	Cluster of Fine Pores Detected at the Subsurface Initiation Site in Specimen 3-2 (20X MAG) . . . . .	87
121	Shallow (Visual) Indication at the Surface-Failure-Initiation Site in Specimen 27-3 (20X MAG) . . . . .	87
122	Surface Pore at the Failure Initiation Site in Specimen 27-2 (20X MAG) . . . . .	87
123	Massive Porosity Encountered at the Failure Initiation Site in Specimen 24-2 (20X MAG) . . . . .	87

ILLUSTRATIONS (Continued)

Figure		Page
124	Fracture Initiation Site at a 0.015-Inch-Diameter Subsurface Pore in Specimen 28-1 (20X MAG) . . . . .	88
125	Fracture Initiation in Specimen 31-1 . . . . .	88
126	Failure Initiation at an Internal Porosity Cluster in Specimen 28-2 . . . . .	88
127	Indications of a Missed Seam Detected in Specimen 12-2 . . . . .	88
128	Large Void at the surface of Specimen 13-2 . . . . .	88
129	Fatigue of Porosity-Containing 1.5-Inch-Thick EB Welds . . . . .	90
130	Failure Initiation Site in 1.5-Inch-Thick EB Welded Specimen 20-2 . . . . .	91
131	Failure Initiation Site in 1.5-Inch-Thick EB Welded Specimen 20-1 . . . . .	91
132	Failure Initiation Site in Porosity-Containing 1.5-Inch-Thick EB Welded Specimen 15-1 . . . . .	92
133	Failure Initiation Site in Porosity-Containing 1.5-Inch-Thick EB Welded Specimen 14-1 . . . . .	93
134	Ultrasonic "C"-Scan Printout of Porosity-Containing 1.5-Inch-Thick EB Welded Specimen 14-1 . . . . .	93
135	Fracture Surface of Porosity-Containing 1.5-Inch-Thick EB Welded Specimen 2-2 . . . . .	94
136	Ultrasonic "C"-Scan Printout of 1.5-Inch-Thick EB Welded Specimen 2-2 . . . . .	94
137	Internal Void in Porous 1.5-Inch-Thick EB Welded Specimen 13-3 . . . . .	95
138	Internal Voids in Porous 1.5-Inch-Thick EB Welded Specimen 18-1 . . . . .	95
139	Extensive Multiple Defects in Porous 1.5-Inch-Thick EB Welded Specimen 13-2 . . . . .	96
140	Ultrasonic "C"-Scan Printout of Porous 1.5-Inch-Thick EB Welded Specimen 13-2 . . . . .	96
141	Acoustic Emission Monitoring System . . . . .	97
142	Monitoring of Failure Initiation and Propagation by Acoustic Emission . . . . .	98
143	Acoustic Emission Data Obtained for Failure Initiation and Propagation in Three Defective Welds . . . . .	99
144	Contour of EB Weldments with 0.016-Inch Mismatch of Faying Surfaces . . . . .	101
145	Contour of EB Weldments with 0.025-Inch-Mismatch of Faying Surfaces . . . . .	101
146	Fatigue Characteristic of 0.25-Inch-Thick EB Welds with Mismatch of Faying Surfaces . . . . .	102
147	Typical Failure Initiation in Mismatched 0.25-Inch-Thick EB Welds in Specimens 4-3 . . . . .	102
148	Fatigue Properties of 0.25-Inch-Thick EB Welds with Intentional Underfills . . . . .	103

ILLUSTRATIONS (Continued)

Figure	Page
149	103
150	105
151	105
152	106
153	106
154	107
155	107
156	108
157	110
158	111
159	112
160	116
161	117
162	118
163	119
164	119
165	119
166	120
167	120
168	121
169	122
170	123
171	123
172	123
173	124

ILLUSTRATIONS (Continued)

Figure	Page
174	Typical Contour of 0.25-Inch-Thick Plasma-Arc Welds Produced Without Filler Wire . . . . . 124
175	Weld Contour of Plasma-Arc Welded Specimen R-1-2 . . . . . 125
176	Fatigue Endurance of Reinforced 0.25-Inch-Thick PAW Weldments . . . . . 125
177	Typical Linear Failure Invitation Encountered in Reinforced 0.25-Inch-Thick PAW Weldments . . . . . 126
178	Typical Weld Contour of Surface - Contaminated 0.25-Inch-Thick Plasma-Arc Weldments . . . . . 127
179	Fatigue Endurance of Surface-Contaminated 0.25-Inch-Thick Plasma-Arc Weldments . . . . . 127
180	Microhardness Measurements on Cross-Sections of Surface-Contaminated PAW Welds . . . . . 128
181	Typical Failure Initiation Site in Surface-Contaminated PAW Weldments . . . . . 128
182	Fatigue Endurance of Flawless 0.25-Inch-Thick GMA Welded Specimens . . . . . 132
183	Failure Initiation Site Not Associated with Porosity in Specimens 1-3 . . . . . 133
184	Failure Initiation at Internal Porosity in Specimen 3-2 . . . . . 133
185	Failure Initiation at a Face Pore in Specimen 3-1 . . . . . 133
186	Fatigue Endurance of 0.25-Inch-Thick GMA Welds with Lack-of-Penetration Defects . . . . . 135
187	0.006-Inch-Thick Lack-of-Penetration Defect in Specimen 6-4 . . . . . 135
188	0.030 to 0.045-Inch-Deep Lack-of-Penetration Defect in Specimen P5-3 . . . . . 135
189	Transverse Contour of Specimen 5-4 . . . . . 136
190	Fatigue Endurance of Porous GMA Welds . . . . . 136
191	0.002-Inch-Diameter Surface Pore at the Failure Initiation Site in Specimen 14-1 . . . . . 137
192	0.008 to 0.010-Inch-Diameter Surface and Subsurface Pores at the Failure Initiation Site in Specimen 14-2 . . . . . 137
193	Internal Cluster of Pores (0.004 to 0.020-Inch-Diameter Range) Detected at Failure Initiation Site in Specimen 4-2 . . . . . 137
194	Fatigue Endurance of .25" EB Weldments . . . . . 146
195	Fatigue Endurance of 0.25-Inch-Thick PAW, GTA and GMA Weldments . . . . . 146
196	Fatigue Endurance of Flawless, Acceptable (in terms of Proposed Spec) and Rejectable 0.080-Inch-Thick and EB and GTA Welds . . . . . 147

## SECTION I

### INTRODUCTION

#### A. BACKGROUND

In the past two decades, the usage of titanium has increased dramatically. Welded titanium offers more efficient light-weight joint design than aluminum alloy systems for many applications in supersonic aircraft.

Welded structures have become a reality in the airframe industry. Major structures have been designed and fabricated in titanium. These include the electron-beam-welded titanium propeller hub structure for the Cheyenne helicopter, the 22-foot-long F-14A wing center-section which contains 70 Ti-6Al-4V electron-beam welds, a similar box welded for the Messerschmitt Mach 2 + MRCA, and Ti-6Al-4V and Ti-6Al-6V-2Sn upper and lower F-14A wing covers which are electron-beam welds to the wing pivot fittings. Melt-through GTA welding of titanium has been developed for use in the sine-wave beams on the vertical fin and conventional GTA welding for joining bulkhead forgings of the new B-1 bomber. Recently, an Air Force program was started on plasma-arc welding (PAW) of B-1 configurations. In engine applications, titanium is used (often in sheet thickness) for casings, in the inner fan ducts, and forward blades. Fusion welding techniques are often considered for such areas. As a result, there is currently considerable interest in using welding to fabricate future aircraft structures and engine parts of titanium.

In the design and fabrication of such parts, the presence of flaws in welds must be taken into account. To evaluate, design, fabricate and inspect these welds, it is necessary to have meaningful guidelines defining defect limits based on engineering data obtained on flawed welded elements tested under representative conditions. To date, design allowables for high integrity, highly stressed welded joints in aerospace structures have been estimated utilizing artificially induced surface defects.

#### B. OBJECTIVES

The primary objective of this program was to determine the effects of typical weld defects encountered in production welding of Ti-6Al-4V titanium alloy on fatigue characteristics of anomalous welds. To achieve the primary objective, techniques had to be developed for reproducible fabrication of weld defects similar to those encountered in production welding. Development of these techniques constituted a secondary objective.

The final objective of the program was the correlation of the generated fatigue data with findings of non-destructive inspections and fractographic evaluations to develop guidelines to be utilized in consideration of proposed specifications.

### C. PROGRAM SCOPE

The program consisted of the following three phases:

● **Phase I.** This study was designed to demonstrate the feasibility of producing typical defects encountered in production welding of Ti-6Al-4V titanium alloy by (intentional) variation of processing parameters, and characterize these defects by commercially available NDI techniques. The types of specimens evaluated in the course of these studies are summarized in Table I.

Table I. Phase I Welding Defect Specimens

Weld Defect	Welding Processes	
	0.080-Inch-Thick Sheet	0.250-Inch-Thick Plate
Porosity	EBW, GTAW	EBW, PAW, GTAW, GMAW
Mismatch	GTAW	—
Underfill	GTAW	—
Surface Contamination	—	EBW, PAW
Lack of Penetration	—	EBW
Reinforcement	—	PAW
Undercut	—	PAW
Bursts	—	EBW
Cracks	EBW, GTAW	EBW, PAW, GMAW
Flawless	EBW, GTAW	EBW, PAW
Inclusions	GTAW	—

● **Phase II.** This was the major effort of the program. It encompassed fabrication of (intentional) weld defects utilizing parameters developed in Phase I and evaluation of their fatigue characteristics in tension-tension ( $R = 0.1$ ) tests. Flawless welds produced by identical welding processes using conventional parameters and base-metal specimens with  $K_I$  stress intensity factors of one, two and three were processed simultaneously to provide baseline data. Phase II was designed to study the weld anomalies shown in Table II.

Table II. Phase II Welding Defect Specimens

Weld Defect	Welding Process		
	0.080-Inch-Thick Sheet	0.025-Inch-Thick Plate	1.500-Inch-Thick Plate
Porosity	EBW, GTAW	GMAW, GTAW, EBW, PAW	EBW
Mismatch	GTAW	GTAW, PAW, EBW	
Underfill	GTAW	GTAW, PAW, EBW	
Surface Contamination	GTAW	GTAW, PAW, EBW	
Lack of Penetration	—	GMAW	EBW
Reinforcement	GTAW	GTAW, PAW	
Undercut	GTAW	GTAW, PAW	
Bursts	—	EBW	EBW
Cracks	GTAW, EBW	GMAW, GTAW, PAW, EBW	
Inclusions	GTAW	GTAW	
Flawless	GTAW, EBW	GMAW, GTAW, PAW, EBW	EBW

In addition, fatigue characteristics of EB welds repaired by GTAW manual and mechanized repair techniques were evaluated.

● Phase III. This phase was designed to analyze fatigue data generated in Phase II as related to pre-test NDI findings, and results of subsequent fractographic studies of failed test specimens. The conclusions of Phase III are summarized in a guideline format to supplement proposed acceptance criteria.

The general procedures utilized in the fabrication and processing of experimental welds, and specific parameters developed for generation of intentional defects (Phase I) are discussed in Sections II and III, respectively. Fatigue characteristics of experimental welds produced by GTA, EB, PA and GMA processes (Phase II) are presented in Sections IV through VII. Proposed acceptance criteria for titanium fusion welds and guidelines relating the findings of this investigation to proposed standards (Phase III) are discussed in Section VIII.

Program results and recommendations pertaining to the utilization of advanced nondestructive inspection (NDI) techniques, some of which are under development, to refine the generated data are summarized in Section IX.

## SECTION II

### EXPERIMENTAL PROCEDURES

#### A. MATERIALS

##### 1. Phase I

The raw materials used in this phase were 0.090-inch-thick Ti-6Al-4V sheet in the annealed condition, and 0.25-inch-thick Ti-6Al-4V plate in the STA (solution treated and aged) condition. Prior to machining, the 0.25-inch-thick plate was heat treated at 1250°F for four hours to obtain an STOA (solution treated and overaged) condition. The 0.090-inch-thick sheet was utilized in the "as-received" (annealed) condition to expedite initiation of the experimental studies, since the condition of the base material was not expected to be a significant factor in parametric studies.

##### 2. Phase II

The materials used in this phase were 0.090-, 0.25- and 1.5-inch-thick Ti-6Al-4V alloy sheet and plate conforming to the requirements of MIL-T-9046. All materials were in the STOA condition which was obtained by the following heat treating method:

- Solution heat treating at 1750°F
- Quenching in air or water
- Aged at 1250°F for four hours and air cooled

The 0.090- and 0.25-inch-thick plates were air quenched. The 1.5-inch-thick plate was water quenched from the solution treating temperature. Data on vendors, heat numbers, chemical analyses, and mechanical properties of material utilized in Phase II are included in Appendix A, Figures A1 through A5.

#### B. PROCESSING OF TEST SPECIMENS

A processing flow chart for all test specimens utilized in this program is shown in Figure 1. Details and/or additional operations involved in the fabrication of each type of test specimen are discussed in subsequent sections.

##### 1. Machining of Weld Blanks (1)

The configurations of the weld blanks utilized in Phases I and II were as follows:

0.090-inch-thick sheet - 8 x 18 inches

---

<sup>1</sup>Numbers in parentheses refer to operations indicated in Figure 1.

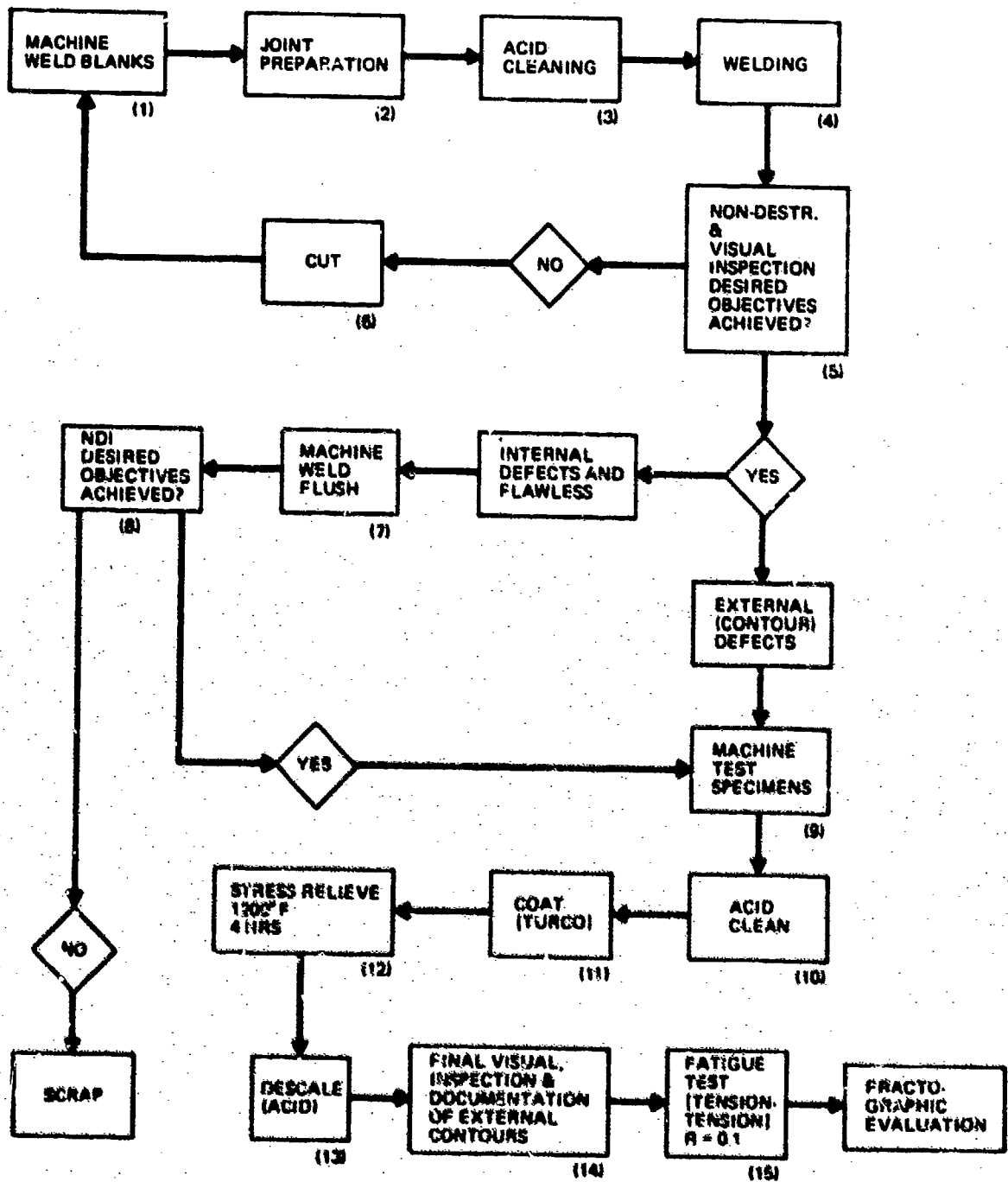


Figure 1. Processing Flow Chart for Weld Defect Specimens

0.25-inch-thick plate - 8 x 12 inch (Phase I)

- 8 x 18 inch (Phase II)

1.5-inch-thick plate - 15-1/2 x 36 inches

The blanks were machined to ascertain alignment of the rolling direction with the longitudinal axis of the (welded) test specimens. Flat surfaces of 0.25-inch thick plate used in Phase II were milled to 0.240 - 0.245 inch thickness.

## 2. Joint Preparation (2)

Square and parallel edges were used in blanks designed for electron-beam welding. Faying surfaces were chamfered to give an included angle of 60 degrees for GTA and GMA welds with 0.060-0.065-inch wide lands; 0.25-inch thick plate used in Phase I was given an included angle of 90 degrees. For manual PAW blanks the included angle was 120 degrees and the land was 0.030-inch. Joint preparation utilized in studies of repair techniques are discussed under specific headings.

## 3. Acid Cleaning (3, 10, 13)

Pre-welding and pre-heat treating cleaning and post-heat treating descaling were carried out in a HF/HNO<sub>3</sub>/H<sub>2</sub>O bath.

## 4. Welding (4)

This discussion pertains to equipment and general procedures applicable to four welding processes utilized in this investigation. Data on variations of process parameters required to produce required anomalies in the weld are presented under specific headings in subsequent sections.

a. Electron-Beam (EB) Welding. This welding operation is accomplished in a vacuum, generally 10<sup>-4</sup> torr, or less. The welding heat is generated at the joint by a stream of high-velocity electrons which, upon impingement on the workpiece, transfers its kinetic energy to the workpiece and heats it up.

The electron-beam gun consists of an electrode, an anode and a focusing coil. Magnetic beam focusing, oscillation and deflection are provided. Welding parameters relating to the gun are:

- Voltage and Current - variation affects penetration in direct proportion.
- Focus - inversely affects penetration by varying power density.
- Welding Speed (up to 100 inches per minute) - distributes power over a given distance in a given time.

The amount of heat which is introduced into a weld joint by the electron-beam may be calculated by the following equation:

$$H = \frac{(V) \times (C) \times 60}{I \times 1000}$$

where H = Heat Input, kilojoules/inch

V = Beam Voltage, kilovolts

C = Beam Current, milliamperes

I = Welding Speed, inches per minute

A keyhole EB welding technique was used in this program. This required that the electron beam first create a hole in the work. As the electron-beam advanced along the joint, a weld was formed by the following three simultaneously occurring effects:

- Metal on the leading side of the hole vaporized and then condensed to form molten metal on the trailing side of the hole
- The molten metal on the leading side of the hole flowed to the trailing side of the hole
- The molten metal thus formed continuously filled the hole and solidified as the electron-beam advanced.

Electron-beam welding for this program was accomplished using a 30-kw Sciaky electron-beam welding unit (Figure 2). This unit has a rectangular 54- x 50- x 54-inch chamber that can be pumped in 5 to 10 minutes, incorporates a 3-axis movement system and has welding speeds of 0- to 100-inches per minute. The electron-beam gun in this unit has the same characteristics as the EB gun used in the large EBW production chambers. This unit is used by both production and development personnel.

b. Plasma-Arc Welding (PAW). Plasma-arc welding is an arc welding process in which heat is produced by a constricted arc between a non-consumable tungsten electrode and a workpiece establishing a non-transferred arc. When an arc is established through a gaseous column separating two electrodes, some of the gas becomes ionized and is called plasma. This plasma, or current-conducting section of the arc, is kept hot by the resistance heating effect of the current passing through it. Thermal ionization is aided by the constriction caused by the constricted orifice. The incoming gas flow causes the plasma to impinge on the workpiece causing melting.

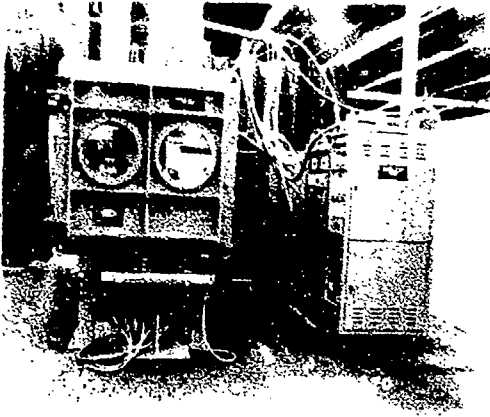


**Figure 2. 30-KW Sciaky Electron-Beam Welding Unit**

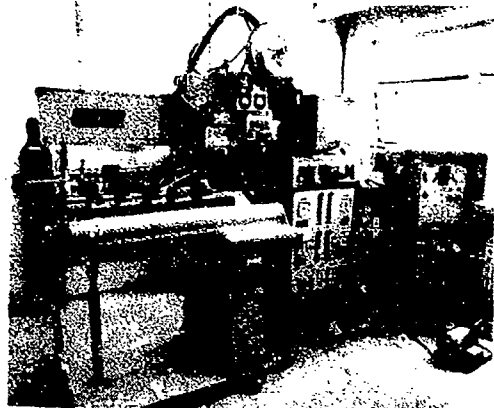


**Figure 3. Automatic Plasma Arc Welding Unit**

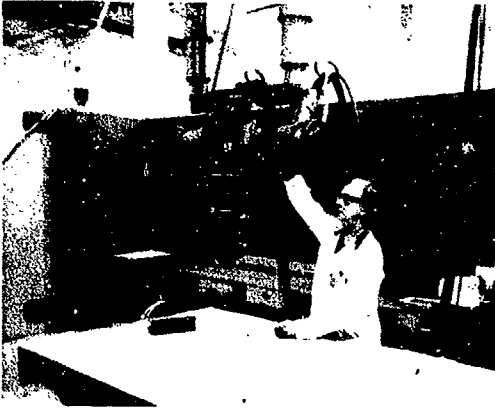


**Figure 4. Radiography Equipment for Inspection of Weld Quality Weldments**

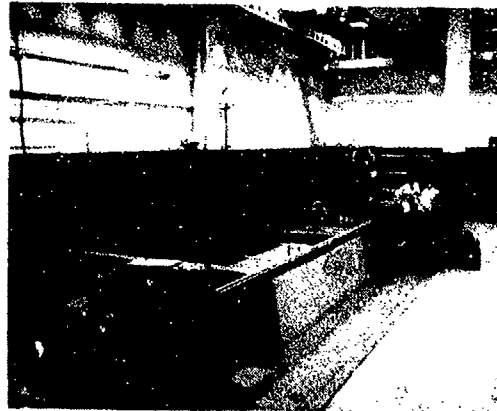


**Figure 5. 36' X 12' X 6' Ultrasonic Inspection Tank**



**Figure 6. Sontag Constant-Amplitude Fatigue Machines and Multipliers**

The plasma-arc column is sufficiently strong to produce a keyhole-type weld. This means that the plasma jet penetrates through the entire thickness of the butt joint, melting the adjacent metal but not expelling it from the weld joint. As the weld progresses, the base metal is melted ahead of the keyhole, flows around it and solidifies behind the keyhole to form a weld bead.

The welding equipment used was a 500-ampere (DC), fully automatic plasma-arc welding unit. The associated controls (shielding gas, backup gas, orifice gas and water flow) as well as sloping-in and sloping-out of the weld current are fully automatic. This equipment is shown in Figure 3.

c. Gas-Tungsten-Arc (GTA) Welding. This process is an arc welding process in which the heat is produced between a non-consumable electrode and the work metal. The electrode, weld puddle, arc and adjacent heat areas of the workpiece are protected from atmospheric contamination by a gaseous shield. This shield is provided by a stream of inert gas.

Gas-tungsten-arc welding was performed utilizing a 600-ampere Sciaky Boom Welder. This equipment is a standard production tool. The unit has an 8-foot longitudinal movement suitable for welding, an 8-foot vertical travel capacity and 360° rotation capability. The last two travel capabilities are used for positioning only. The equipment has a constant-current, automatic-voltage-control system and maintains a given pre-set arc length. Travel speeds range from 0 to 100-ipm, although welding is rarely done above 10 ipm except on very thin gages.

d. Gas-Metal-Arc (GMA) Welding. This is an arc welding process in which the heat for welding is generated by an arc between a consumable electrode and the workpiece. The electrode, a solid bare wire that is continuously fed into the weld area, becomes the filler metal as it is consumed. The electrode, weld puddle, arc and adjacent areas of the base metal are protected from atmospheric contamination by a gaseous shield provided by a stream of gas fed through the electrode holder and a trailing shield.

GMA welding was accomplished using a convertible manual GMA torch in an automatic mode on a Linde SV-1 500-ampere power supply. This torch was hard-mounted on the boom welder used in the GTA welding process. Argon gas was used as the inert shielding gas.

## 5. WELD CHARACTERIZATION (5, 8, 14)

### a. Equipment

The non-destructive examination/weld characterization to which welds were subjected was accomplished using the NDI equipment developed for the production electron-beam welding of aerospace components. Radiographic and ultrasonic inspections were accomplished in the same area. There were two 320Kv-30Ma X-ray units available for use (Figure 4). The radiographs produced by this facility provided 1-percent sensitivity on the material used. Ultrasonic inspection was accomplished in a 3-1/2 x 12 x 6-foot water tank which is also used for production weld inspection (Figure 5).

Dye-penetrant inspection utilized in Phase I was accomplished in an area detached from the above inspection area. This area has the capability of using either fluorescent, penetrant or visible techniques.

### b. Inspection Procedures

The basic purpose of non-destructive inspection was to demonstrate the capability of producing only one type of defect per weld, that is, to ascertain that if a weld required an undercut, underfill or reinforcement-type of defect, it could not have any other type of defect associated with it (e.g., internal porosity).

Weld evaluation for this program was performed at several intervals during the weld production cycle, as follows:

- After initial welding - radiographic inspection. Dye penetrant and metallographic inspections were also used in Phase I.
- After machining of weld - radiographic inspection and ultrasonic inspection (for 1.5-in. thick plate)
- After machining of (contoured) specimen - documentation of weld contours
- After fatigue testing to failure - fractography of failed surfaces.

This intensive nondestructive inspection program made possible the characterization of every weld based on its inspection records. Initial radiographic inspection was applied on a 100-percent basis to all welds to establish the suitability of that weld for future operations and indicated the basic defect or lack of defects. In addition to radiographic inspection in Phase I metallographic samples were also taken, together with selective employment of dye penetrant inspection of the weld surfaces. The metallographic sample allowed the examination of a representative section of the weld for profile evaluation and actual defect demonstration. The application of the dye penetrant as an inspection tool was limited to the crack specimens. The fluid used for this inspection was a water-base titanium-compatible inspection fluid.

A second inspection followed immediately after flush machining of the crown and root of the weld. This radiograph was compared with the initial X-ray film and evaluated for the specific defect. If the weld required a defect which did not allow the

weld bead to be machined flush, this inspection would be the critical test to demonstrate the capability of producing only one type of defect without having any other defect generated as an unwanted by-product.

The application of ultrasonic evaluation at this point was limited. Attempts were made to utilize a water immersion 15-MHz, longitudinal-wave, pulse-echo system on the 0.250-inch thick material. This inspection system is in production use for the examination of electron-beam weldments. The results were unsatisfactory, since the C-Scan was unable to separate the front face of the material from the back face, because of the thinness of the material. Attempts to utilize a shear wave system were somewhat more successful. This method did separate the front face from the back face, but the lack of an available standard with which to calibrate the system limited its effectiveness. Ultrasonic C-Scan techniques were employed to characterize all 1.5-inch-thick specimens.

The third inspection point was limited to welded specimens with contour anomalies such as underfill, mismatch and others. For these specimens, the weld contours were projected on the screen of an optical comparator at 10X magnification and documented by tracing on the graph paper positioned on the screen.

The fourth and final inspection point involved examination of the failed fatigue test coupons and identification of the failure-initiating defect. The failure origin was examined and correlated with available radiographic films and ultrasonic C-scan printouts.

#### 6. Identification of Test Specimen Configurations (9)

The configurations of test specimens used in both phases of this program are shown in Figures A6 to A13 (Appendix A).

To maintain a positive tracking system for each specimen, the following identification system employing up to seven symbols using numbers and letters was devised:

- Symbol 1 identified the material thickness: 8 = 0.080-inch; 9 = 0.090-inch; 4 = 0.250-inch and 15 = 1.500 inches.
- Symbol 2 identified the welding process used; EB = Electron-Beam Welding, PAW = Plasma-Arc Welding, GTAW = Gas-Tungsten-Arc Welding, GMAW = Gas-Metal-Arc Welding
- Symbol 3 identified the contract phase: No number identifies Phase I; 2 identifies work done during Phase II
- Symbol 4 identified the specific weld defect: B = Bursts; I = Tungsten Inclusions; P = Porosity; UC = Undercut; UF = Underfill; MS = Mismatch; R = Reinforcement; SU = Surface Contamination; LP = Lack of Penetration; C = Cracks and F = Flawless

- Symbol 5 identified the condition of the weld bead: X signifies that the weld has not been machined flush; M identifies that the weld bead has been machined flush on top and bottom
- Symbol 6 identified the weld blank number
- Symbol 7 identified the specimen machined from a given blank.

The following is an example of the use of this specimen identification system. Specimen 4-PAW-PM-2-1 means that it is the first specimen of the second 0.250-inch thick plasma-arc welded blank with a porosity-type weld that has been machined flush.

#### 7. Fatigue Tests

Fatigue characteristics were determined in constant-amplitude tension-tension ( $R = 0.1$ ) fatigue tests at frequencies of 1800-cpm and 20-cpm. The Sonntag SF14 and SF-104 testing machines shown in Figure 6 were utilized to test the 0.090 and 0.25-inch-thick specimens. The 1,000,000-pound capacity MTS system shown in Figure 7 was used to test the 1.5-inch thick specimens.



Figure 7. One-Million-Pound MTS Testing Machine

## SECTION III

### DEVELOPMENT OF PARAMETERS FOR INTENTIONAL PRODUCTION OF WELD DEFECTS - PHASE I

#### A. PROCEDURES

Desired defects were produced by variations of conventional processing parameters which could inadvertently occur in production welding. "Salting" or deliberate defect placement was not employed. Blanks utilized in GTA, GMA and PAW processes were chamfered and all blanks were acid-cleaned prior to welding, unless otherwise specified. A summary of all approaches considered in intentional manufacturing of defects is presented below. Detailed data on parameters utilized in these studies are discussed in Subsection B.

##### 1. Porosity

The approaches used were:

- Variation of weld parameters - speed, voltage, amperage
- Lack of sufficient cleaning
- Application of a shop fluid to the faying surfaces, i. e., water-soluble cutting oil, vacuum oil, hydraulic oil, hydrocarbon oil, vacuum grease
- Dry abrasive blast residue
- Acid residue - HF/HNO<sub>3</sub>/H<sub>2</sub>O
- Sawcut edges
- Titanium oxide layer - formed by immersion in HNO<sub>3</sub> solution.

The methods which produced defects in the most reproducible fashion were selected for use in fabricating test specimens.

##### 2. Mismatch

This defect was produced by placing aluminum shims of different thicknesses under one of the two plates to be welded, thereby creating a mismatch.

##### 3. Underfill

The specimens were produced by eliminating the filler wire and/or increasing the welding speed.

#### 4. Surface Contamination

The methods used to obtain this type of defect were:

- Electron-Beam (EB) Welding - applying vacuum grease or vacuum oil on faying surfaces
- Gas-Tungsten-Arc (GTA) and Plasma-Arc Welding (PAW) - varying flow of inert shielding gases.

#### 5. Lack of Penetration

The method used to obtain lack of penetration in EB welds consisted of reducing power to obtain a wider yet less penetrating beam. For GMA welds, this defect was produced by decreasing the amperage and increasing the travel speed.

#### 6. Reinforcement

Reinforcement was produced in PAW and GTA weldments by varying the weld speed and/or use of filler wire, and by increasing the feed rate of the filler wire, respectively.

#### 7. Undercut.

Undercuts were produced in PAW weldments by increasing the orifice gas flow rate, amperage and weld speed. In GTA welds undercuts were produced by increasing the arc amperage on the second pass.

#### 8. Inclusions

Tungsten inclusions were produced in GTA weldments by "TIG Tacking", a technique which allows the electrode to touch the weld puddle.

#### 9. Bursts

Intentional generation of bursts in EB weldments included consideration of the following variables:

- Geometry of weld blanks
- Staggered locking passes
- Weld speed
- Use of copper chills
- Heat input
- Welding on inserts
- Repetitive passes

A successful method for burst generation in 1.5-inch-thick EB weldments was developed based on a hypothesis pertaining to the change in the shape of the molten puddle accompanying the transition from full to partial penetration.

#### 10. Cracks

Attempts to produce cracks involved welding under restrained conditions and/or straining of existing welds by circumferential welding to backup assemblies.

## 11. Base Metal Fatigue Endurance

Fatigue characteristics of 0.080- and 0.25-inch-thick base-metal specimens were evaluated at stress intensity ( $K_t$ ) factors of one (unnotched), two and three. The fatigue endurance of 1.5-inch-thick base-metal specimens was determined only in the unnotched condition. Data obtained are presented in Appendix A, Table A-9. Base-metal fatigue endurance curves at several stress intensity levels served as a basis for evaluating the effect of weld anomalies on fatigue characteristics.

### B. DEMONSTRATION OF THE FEASIBILITY OF GENERATING INTENTIONAL DEFECTS

The following summarizes efforts designed to demonstrate the feasibility of generating intentional defects by simulating variations in parameters which could be inadvertently encountered in production welding. Most of these studies were conducted in Phase I of the program which preceded fabrication and testing of EB, PA, GTA and GMA welded specimens containing internal or external defects. The results of these studies are summarized below. Detailed data pertaining to weld parameters and defect characterization are presented in Appendix A, Tables A-1 through A-8.

#### 1. Porosity

a. Gas-Tungsten-Arc Welding. Porosity was introduced into the weld by two methods: (1) exposure of faying surfaces to shop environment prior to welding and, (2) addition of hydrocarbon oil to the faying surface by wiping, duplicating shop contamination. The weld profile obtained by this process is shown in Figure 8.

Method 1 introduced spaced porosity with an average pore size of 0.007 inch (based on radiographic interpretation). It was not a clustered type of porosity, but spaced linear porosity located predominately on one side of the weld; this was the side exposed to shop air for 48 hours while in the weld fixture. The mating half was radiographically clean.

Method 2 produced spaced porosity located along the outer edges of the weld. This porosity was sized to be 0.007 to 0.020 inch, with an average pore size of 0.015 inch based on radiographic examination. Metallographic examination indicated clusters of extremely fine porosity located throughout the grain and grain boundary similar to Figure 9. Figure 10 illustrates a 0.015 inch pore detected in the 9GTA-PX-2 weld.

b. Gas-Metal-Arc Welding. Porosity in GMA welds could be generated by three methods: (1) exposure to shop environment followed by application of machining oil, (2) grit blasting of faying surfaces, and (3) exposure to shop environment followed by handling without protective gloves. A micrograph of a typical pore generated in GMA weldments is shown in Figure 13.

c. Electron-Beam Welding. - Several techniques were utilized to introduce porosity into electron-beam welded joints. Twenty-one welds, using various techniques, were made to produce porosity-containing welds 4EB-PX 1 through 4EB-PX-21. The successful techniques were: (1) Dry abrasion grit blasting without subsequent acid cleaning of milled/edges, (2) Saw-cut edges - solvent wiped only, no acid cleaning, (3) Variation in weld speed - milled edges, (4) Addition of water-soluble cutting fluid to faying surfaces - milled and saw cut edges, (5) Combinations of items (2), (3), and (4).



**Figure 8. Typical Weld Profile for 0.060 inch-Thick Gas-Tungsten-Arc Porosity Specimen (8X MAG)**

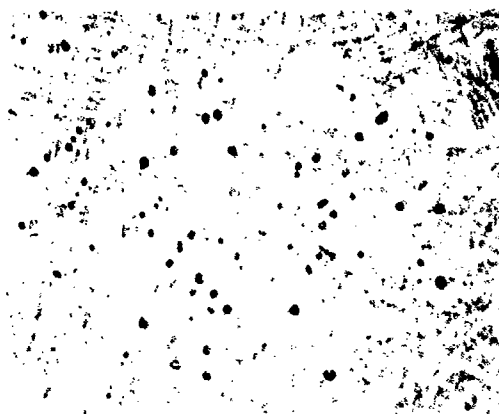


**Figure 9. Photomicrograph of Porosity in SGTA-PX-1 Weld (250X MAG)**



**Figure 10. Cross Section of SGTA-PX-2 Weld Showing 0.015 inch Pore Formed by Hydrocarbon Oil Contamination (10X MAG)**

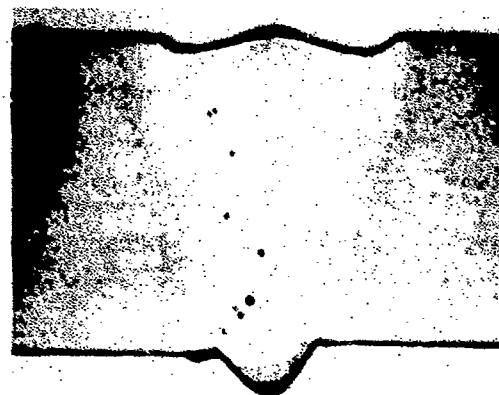


**Figure 11. Weld 4EB-PX-1 One Sided Placement of Porosity, Resulting From Abrasive Grit Blast Residue (10X MAG)**

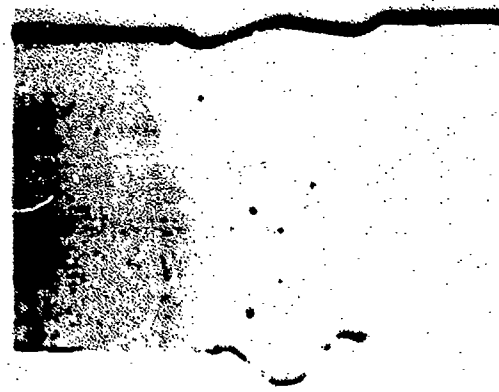


**Figure 12. Weld 4EB-PX-3 Scattered Linear Porosity Throughout the Weld Showing the Effect of Cut Edges Without Acid Cleaning (10X MAG)**



**Figure 13. Cross-Section of a 4GMA-2PX-Type Weld Showing Induced Porosity (10X MAG)**

Dry abrasion grit blasting produced porosity on the side of the weld which had the abrasion grit residue. In this case, aluminum oxide grit was applied to milled surfaces without subsequent acid cleaning. This generated porosity was approximately 0.005 inch in size and linear in nature. This weld is identified as 4EB-PX-1 (Figure 11).

The use of saw-cut edges to introduce porosity was also successful; the porosity generated by this technique was of the scattered-linear type and ranged in size from 0.005 to 0.015 inch. This is demonstrated by Welds 4EB-PX-6 and 9 (Figure 12). Variations in weld speed (Welds 4EB-PX-17 and 19) also produced similar porosity distribution, with the porosity size increasing as the weld speed increased.

The addition of a water-soluble saw cutting oil to the faying surfaces was extremely effective in the generation of porosity. This technique, together with the increase in welding speed and saw cut edges, resulted in the porosity shown in Figures 14 and 15.

Metallurgical sectioning performed on the root side of Weld 4EB-PX-21, polished parallel to the welding direction 0.025 inch into the base metal, revealed a double-track porosity with sizes ranging from less than 0.001 inch in diameter to 0.005 inch in diameter (Figure 16).

d. Plasma-Arc Welding. Porosity was introduced into the weld by applying either hydrocarbon oil or acid to the faying surfaces just prior to welding.

Method 1 introduced linear porosity at the side of the weld to which hydrocarbon oil was applied, as represented by Weld 4PAW-PX-2. This allowed placement of the porosity to either or both sides of the weld. The porosity developed by this technique ranged between 0.005 to 0.020 inch with an average size of 0.010 inch. The distribution was of a continuous linear type.

Method 2, the acid-cleaning residue ( $\text{HF-HNO}_3\text{-H}_2\text{O}$ ), is represented by Weld 4PAW-PX-3. This produced linear type porosity with a size range of 0.003 to 0.010 inch maximum, with an average size of 0.005 inch. Figures 17, 18, and 19 illustrate 4PAW-PX series weld profiles and associated porosity.

## 2. Lack of Penetration

In Phase I, it was necessary to produce this defect in 0.250 inch-thick electron-beam weldments. Two approaches were used: (1) missing seams, and (2) varying the applied voltage, amperage, focus current and weld speed. It was found that the most important variable was focus current. Settings were developed to produce both welds with approximately 50% and 80% penetration. Welds 4EB-LPX-1-2 and -3 represent Method 1 and Welds 4EB-LPX-4 and -5 represent Method 2.

Figures 20 and 21 illustrate the welds produced by the missed seam technique. Figures 22 and 23 illustrate the parameter variation technique. The two defect levels selected were 70% and 90% penetration. The technique selected for Phase II specimen production was that of varying beam power.



**Figure 14. Weld 4EB-PX-18 Porosity Generated by Saw Cut Edges, Insufficient Cleaning and Increased Welding Speed (10X MAG)**



**Figure 15. Weld 4EB-PX-21 Porosity Generated by Addition of Cutting Oil to Milled Edges and Increased Weld Speed in Weld 4EB-PX-21 (10X MAG)**

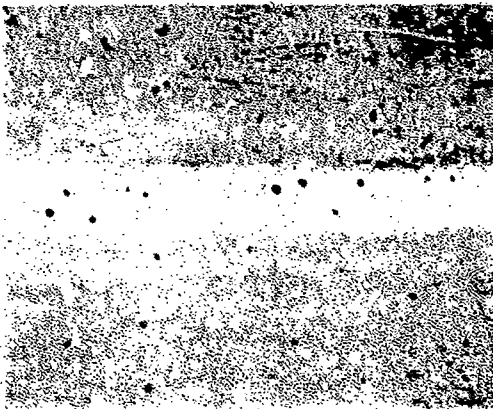


**Figure 16. Plan View of Root Surface Showing EB Weld Porosity (10X MAG)**

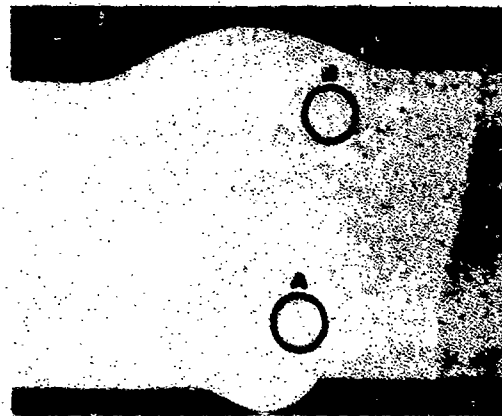


**Figure 17. The Profile of Weld 4-PAW-PX-3. Area A Identifies Location Where Very Fine Porosity Was Detected in Weld 4PAW-PM-2 (Figure 18). Area B Identifies Location Where Porosity Was Detected in 4PAW-PM-3 (Figure 19) (10X MAG)**

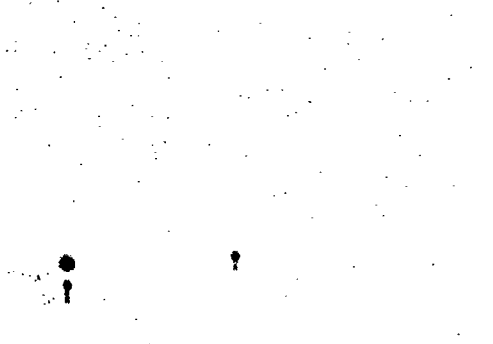


**Figure 18. Weld 4PAW-PM-2. Porosity Located in Area A of Figure 17. The Large Pore Measures 0.0013 Inch in Cross-Section (100X MAG)**

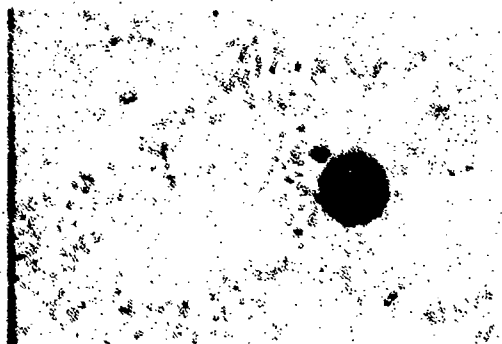


**Figure 19. Weld 4PAW-PM-3. Porosity Located in Area B of Figure 17. The Large Pore Measures 0.006 Inch in Cross-Section (100X MAG)**



**Figure 20. Weld 4EB-LPX-1 Showing Lack of Penetration (8X MAG)**



**Figure 21. Weld 4EB-LPX-3 Showing Lack of Penetration, (8X MAG)**



**Figure 22. Lack of Penetration as Produced by Variations in Beam Power, Weld 4EB-LPX-4 (10X MAG)**



**Figure 23. Lack of Penetration as Produced by Variations in Beam Power, Weld 4EB-LPX-5 (8X MAG)**

### 3. Undercut

In Phase I, this defect was produced in the 0.250 inch plasma-arc weldments. Two approaches were used: (1) elimination of filler wire, and (2) increasing orifice gas flow. The initial approach (eliminating filler wire) produced underfills. The second approach (increasing orifice gas flow from 10cfm to 13cfm and 15cfm, increasing the welding speed and eliminating filler wire) resulted in the generation of two levels of undercut - 0.004 and 0.010 inch. Weld 4PAW-UCX-3 (Figure 24) contained 0.004 inch undercut. Weld 4-PAW-UCX-3 (Figure 25) contained 0.011 inch undercut. Further increases in orifice gas flow resulted in the generation of 0.022-inch-deep undercut (Figure 26). The parameters utilized in production of 0.022-inch-undercut, however, resulted in the generation of additional defects in the first half of the weld.

### 4. Underfill

In Phase I, this defect was produced in the 0.090-inch-thick GTA weldments. The two welds produced (9GTA-UFX-1 and -2) are shown in Figure 27. These weldments were produced by varying the weld travel speed without the use of filler wire. Welds 9GTA-UFX-1 and -2 resulted in underfills of 0.011 and 0.022 inch.

### 5. Inclusions

Several approaches were evaluated for incorporating tungsten into the molten puddle on GTA welding. The initial approach was to introduce tungsten into the weld puddle by tack welding the two plates together in the weld fixture and allowing the electrode to touch the weld puddle, depositing tungsten. The deposit was then covered with weld metal using a single-pass weld. Radiographic examination indicated the tungsten inclusion to be pore-free. However, metallographic sectioning revealed that tungsten sank to the bottom of the weld, resulting in an unusable weld defect, since the inclusion would be removed when the weld bead was machined flush. Several additional attempts were made using two-pass and three-pass weld operations with the tungsten being placed prior to the last pass. Success was finally achieved on a random basis using the two-pass system.

There was no way to predict whether a tungsten inclusion would be located in a usable portion of the weld. The ability to develop defects of different sizes is solely a function of the mass of the tungsten electrode breaking off in the puddle. The tungsten electrodes used were of the 2% thoriated tungsten type with diameters varying from 0.020 to 0.060 inch. Various taper lengths were also used in an effort to generate tungsten inclusions.

Examination of Figure 28, which shows metallurgical cross-sections of a 12-inch-long weld, reveals the random nature of this operation. Seven tungsten deposits were made utilizing the two-pass technique and, in all cases, the tungsten sank towards the bottom of the weld puddle resulting in two useable samples. They had approximately rectangular configurations ranging in size from 0.005 to 0.050 inch.

### 6. Mismatch

This defect was obtained by the addition of shims under one of the two butting plates. Shims of 0.016 and 0.025 inch were used to establish the two defect levels. The fabrication of this specimen utilized acid-cleaned, milled plates. Measurements



Figure 24. Slight Undercut in Weld 4PAW-UCX-3 (6X MAG)



Figure 25. Intermediate-Depth Undercut in Weld 4PAW-UCX-4 (10X MAG)



Figure 26. Extensive Undercut in Weld 4PAW-UCX-5 (10X MAG)

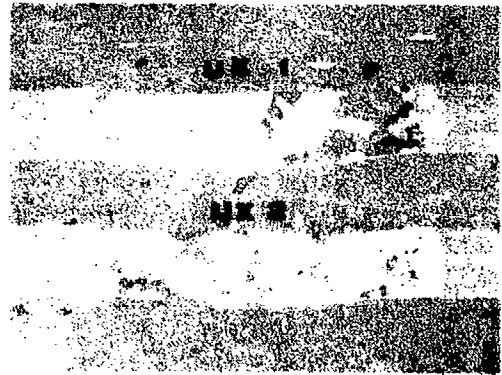


Figure 27. Underfill in Welds 9GTA-UFX-1 and -2 (5.5X MAG)

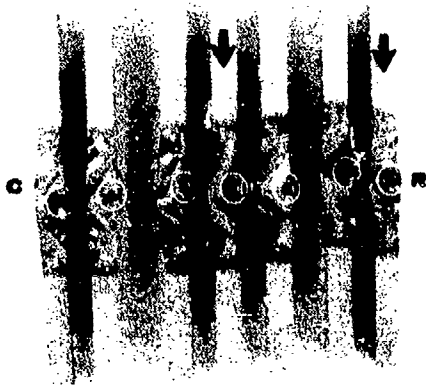


Figure 28. Metallographic Section of a GTA Test Weld Showing Tungsten Inclusions. (2.6X MAG)

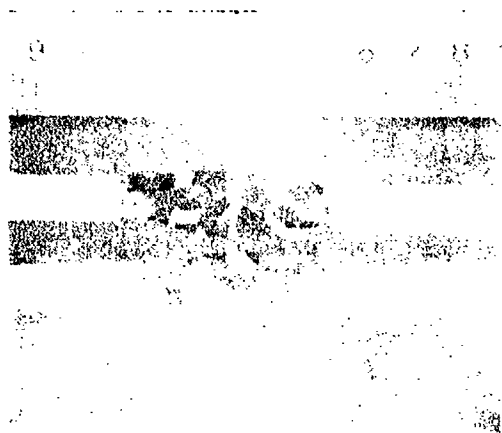


Figure 29. Metallographic Section of Welds 9GTA-M5X-1, 2 Showing the Intended Mismatch (4X MAG)

performed on metallographic sections of 0.080 inch GTA welds (Figure 29) revealed offsets of 0.013 and 0.023 inch for 0.016- and 0.025-inch shims, respectively. Radiographic examination revealed that both welds were pore-free.

## 7. Reinforcement

The concept of reinforcement identifies the weld defect in which the weld bead is left intact and the height of the crown is varied, concurrently changing the angle of departure of the crown from the base metal. The feasibility of intentionally producing this defect was demonstrated on two 0.25-inch PAW specimens which had significant variations in crown height and were free from internal defects.

## 8. Surface Contamination

This defect was produced by two welding processes - electron-beam welding (EBW) and plasma-arc welding (PAW).

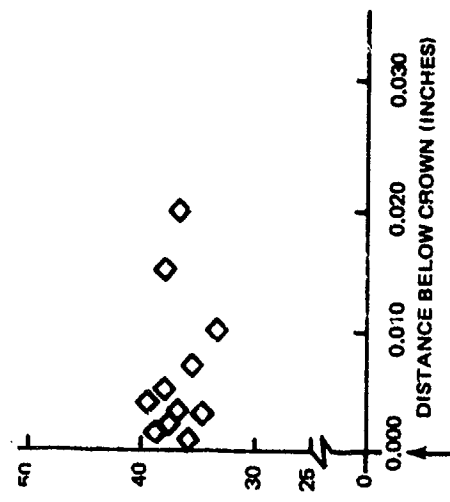
a. Electron-Beam Welding. The approach used in EB welding was to apply vacuum grease (Dow Corning-971V silicon vacuum lubricant) to the faying surfaces of the weld joint (Weld 4EB-SUX-4). Additional samples were also produced using a light coat (4EB-SUX-1) and a heavy coat (4EB-SUX-2) of vacuum oil, and one with hydrocarbon oil (4EB-SUX-3). Hardness readings performed on cross-sections of all four samples revealed no hardness increase attributable to surface contamination. All hardness readings (Figure 30) were taken from the weld crown inward using a standard microhardness testing device with a 100-gram load. Weld 4EB-SUX-4 is shown in Figure 31. No hardness increase was detected in any of the welds examined.

b. Plasma-Arc Welding. Surface contamination in plasma-arc weldments was produced by varying the flow of shielding and orifice gases. Three specimens were fabricated. The first specimen (4PAW-SUX-1) was produced with the flow of all gases, except the orifice gas, being reduced by 75%. The second specimen (4PAW-SUX-2) was produced with the flow of all gases, except the orifice gas, being reduced by 50%. The third specimen (4PAW-SUX-3) was produced with the flow of all gases being normal except the trailing gas shield, which was turned off. These welds are shown in Figures 32, 33 and 34.

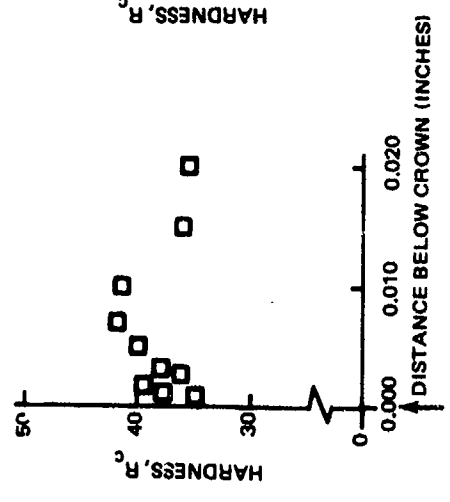
Metallographic examination of each weld revealed a normal microstructure except for Weld 4PAW-SUX-3 which exhibited a surface layer of alpha grains. The microstructures of all three weldments are shown in Figures 35, 36, 37 and 38. Hardness traverses performed on each weld from the weld crown inward revealed a hardness increase only for Weld 4PAW-SUX-3. These hardness traverses are shown in Figure 39. In each case, duplicate traverses were performed to verify the results.

## 9. Cracks

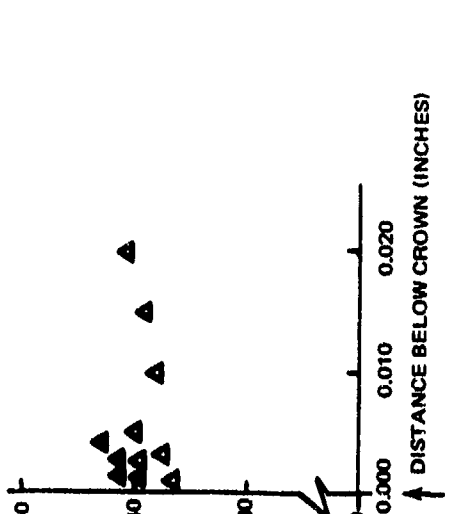
The initial attempts to produce cracks were based on welding blank halves together under high restraint conditions, with sufficient weld passes applied to introduce weld cracking. This restraint condition was developed by welding the blank halves, 19x30x1-3/4, to 2-inch Ti-6Al-4V STA backing plate. Welding of these plates to the backing plates was initially accomplished by manual GTA welding. Weld 4EB-SHX-1 was fabricated this way. Inability to eliminate the preweld butt joint gap



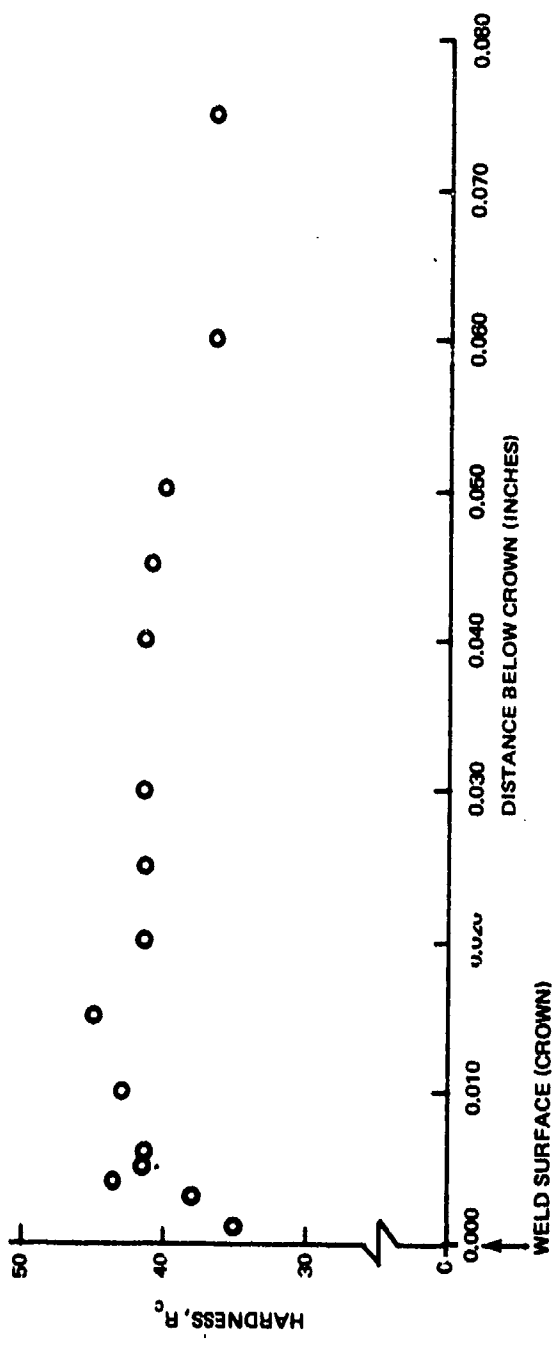
a. SPECIMEN: 4EB-SUX-1, (CONTAMINATED BY LIGHT COAT OF VACUUM OIL)



b. SPECIMEN: 4EB-SUX-2, (CONTAMINATED BY HEAVY COAT OF VACUUM OIL)



c. SPECIMEN: 4EB-SUX-3, (CONTAMINATED BY HYDROCARBON OIL)



d. SPECIMEN: 4EB-SUX-4, (CONTAMINATED BY VACUUM GREASE)

Figure 30. Microhardness Studies on Electron-Beam Welded Surfaces Contamination-Type Specimens.



**Figure 31. Weld 4EB-SUX-4. Microhardness Traces on Weld Cross Section (10X MAG)**

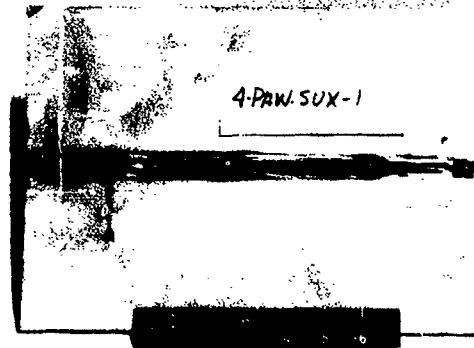


**Figure 32. Weld 4PAW-SUX-1. Surface Contamination Resulting from Gas-Flow-Rate Variation\***

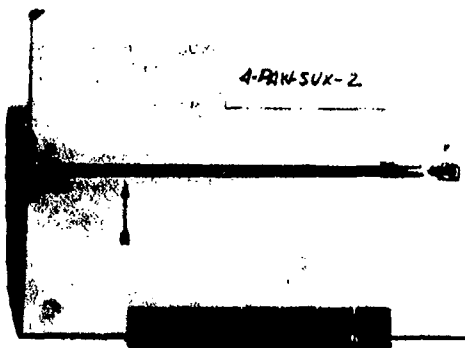


**Figure 33. Weld 4PAW-SUX-2. Surface Contamination Resulting from Gas Flow Rate Variation\***

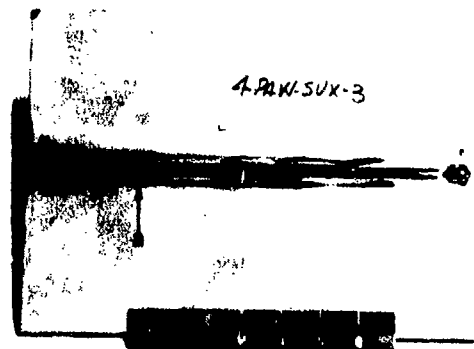


**Figure 34. Weld 4PAW-SUX-3. Surface Contamination Resulting from Gas Flow Rate Variation\***

\*The arrow indicates the location where the metallurgical section was made for the microhardness survey

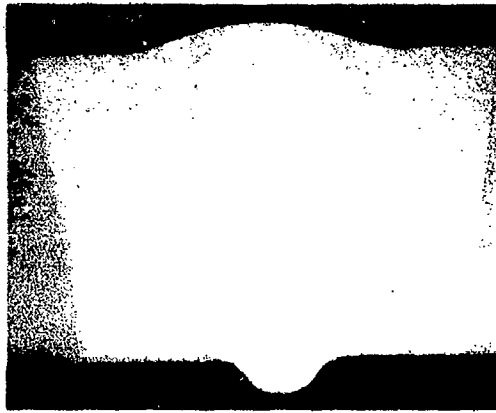


**Figure 35. Cross-Section of Weld 4PAW-SUX-1 (10X MAG)**

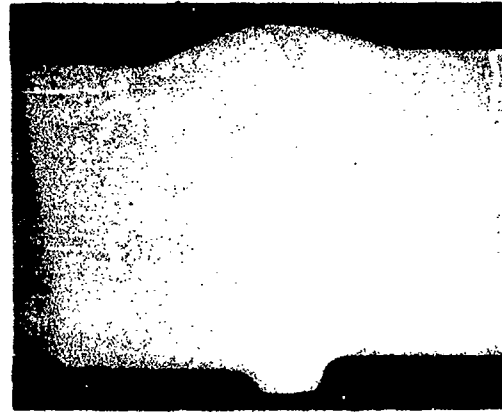


**Figure 36. Cross-Section of Weld 4PAW-SUX-2 (10X MAG)**

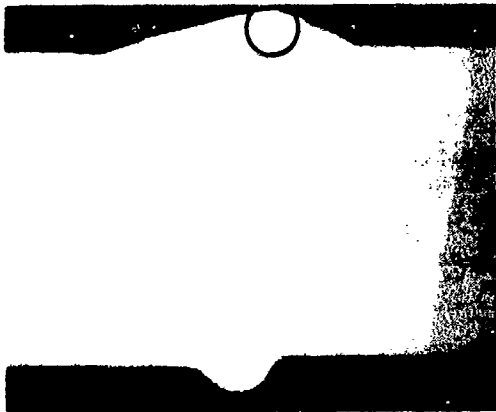


**Figure 37. Cross-Section of Weld 4PAW-SUX-3. The Circled Area Identifies Area Where Hardness Surveys Were Conducted. (10X MAG)**

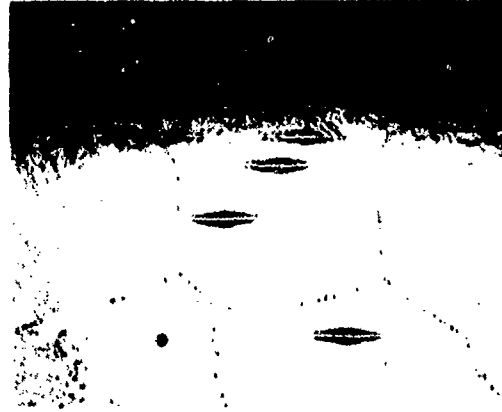


**Figure 38. Weld 4PAW-SUX-3 Hardened Surface Layer and Microhardness Indications. (250X MAG)**

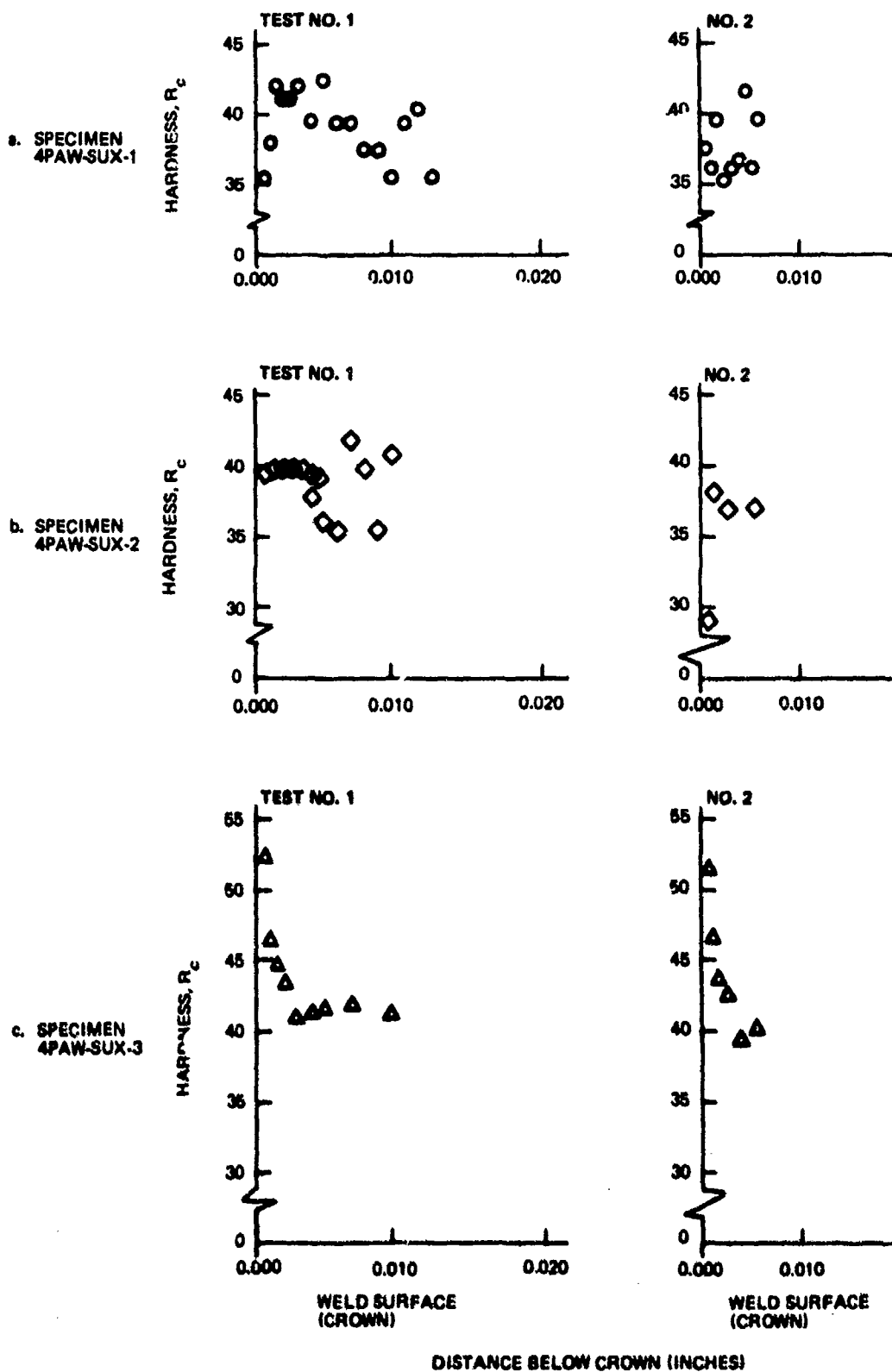


Figure 39. Microhardness Studies on Plasma-Arc Welded Surface Contamination-Type Specimens

necessitated the addition of tooling bolts and a change to EB fillet welding to attach blank halves to the strongback plates. This technique was utilized to produce the remaining specimens (Weld 4EB-CX-2 and 4PAW-CX-1 and 2). Figure 40 illustrates the plate/backing configuration.

Joining of blank halves was performed using a single weld pass without the use of filler wire, with a cool-down to room temperature between each pass. Each new weld pass was applied in the same direction as the previous pass. Both, plasma-arc and electron-beam welding processes were utilized in the initial studies conducted on 0.25-inch-thick plate.

a. Plasma-Arc Welding. Two fully restrained specimens were fabricated (Welds 4PAW-CX-1 and -2). The technique used was one of continually increasing the heat input until the keyhole conditions were obtained. No filler wire was used. Seven passes were applied to Weld 4PAW-CX-1 with a change in the weld direction in the second pass. Dye-penetrant and radiographic inspection performed on this weld between passes (see Appendix A) failed to reveal any crack indications. During the seventh weld pass, the weld metal dropped through the weld joint, resulting in the termination of subsequent welding. The second specimen (Weld 4PAW-CX-2) was subjected to six passes with intermediate NDI (dye penetrant and radiographic) between passes. The weld remained intact after the 6th pass. Results of in-process NDI indicated that no cracks could be produced under these restraint conditions.

b. Electron-Beam Welding. Two fully restrained specimens were produced (Welds 4EB-CX-1 and -2). The technique used was one of repeated weld passes. Weld 4EB-CX-1 was unusable after two weld passes, due to the excessive weld joint gap caused by the existing GTA welds which joined the weld plates to the strongback.

Weld 4EB-CX-2 was subjected to eleven weld passes with intermediate dye penetrant and radiographic inspections. In an effort to minimize weld drop through, the heat input was decreased and the assembly allowed to cool between welding passes. No cracks were detected by in-process NDI. Metallography performed on this weld after completion of the 11th pass revealed a satisfactory microstructure with excessive underfill, but no cracks (Figure 41).

c. Stressing of Existing Root Welds

In the subsequent attempt to generate cracks in Ti-6Al-4V weldments, two halves of a 0.25-inch weld blank were positioned on the backup plate so that the faying surfaces were located directly over the slot machined in the backup plate as shown in Figure 42. A low-penetration, manual PAW pass was made to join the halves. The blank was subsequently welded to the backup plate by circumferential PAW passes on all four sides. The rationale for this approach was based on calculations indicating that considerable multiaxial stresses should be generated in the root weld by circumferential welding. No cracks were detected in the root weld, however, as revealed by subsequent radiographic inspection.

A review of available information on the susceptibility to cracking of Ti-6Al-4V welds indicated that cracking did not occur under any of the restraint conditions utilized in previous or current studies, and that isolated occurrences of cracks were associated with severe contaminating conditions either on welding or subsequent testing. These findings were verified by the results of the present studies. Transverse cracks were detected only on surfaces of GTA welds produced under intentionally contaminating conditions.

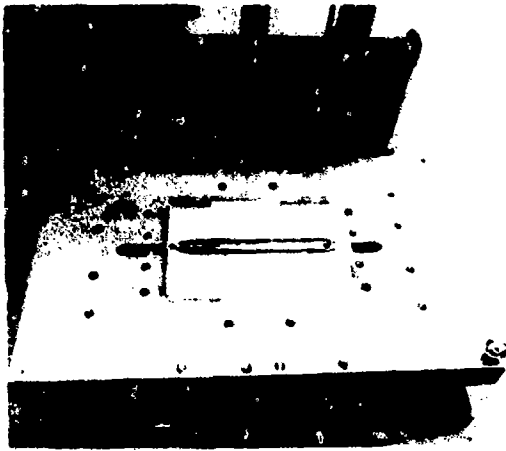


Figure 40. View of Weld Assembly Showing Back Plate and Weld Specimen Used for the Production of Cracks (Weld-4 PAW-C2 is illustrated)

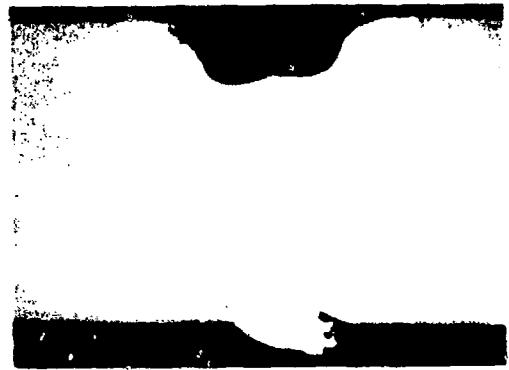


Figure 41. Weld 4EB-CX-2 After the Eleventh Weld Pass (10X MAG)

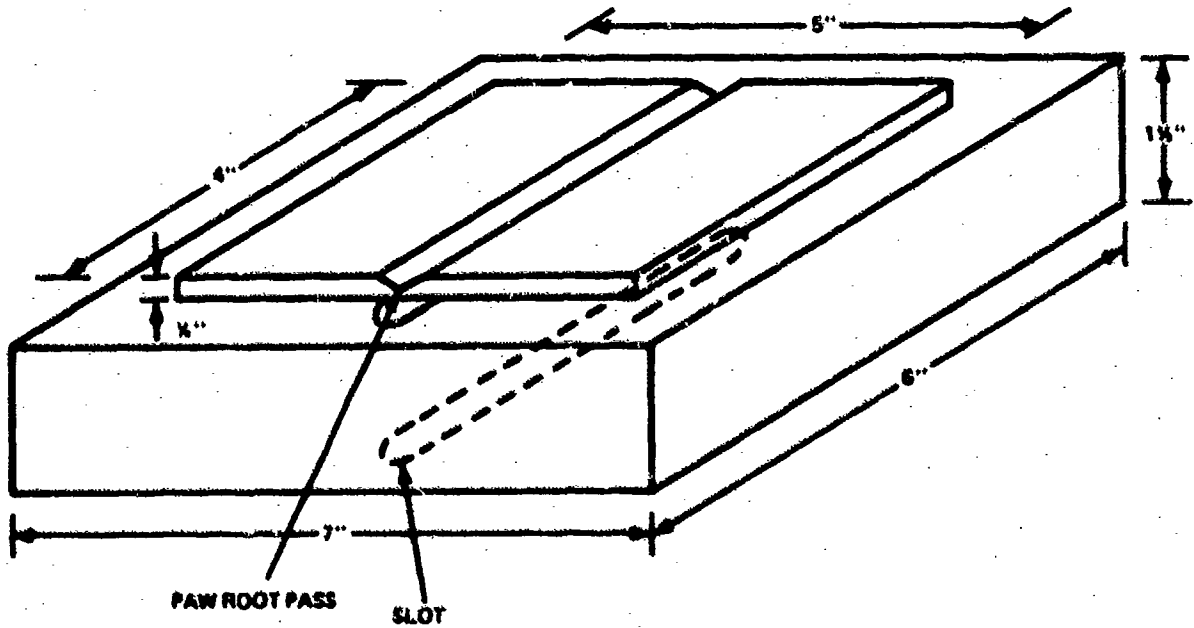


Figure 42. Configuration of Experimental Assembly Utilized in Stressing of Existing Welds

## 10. Bursts

Bursts have been occasionally detected at the terminals of EB welds produced without the use of end tabs. Attempts to produce bursts in experimental configurations in the past resulted in inconsistent results. Although a burst could be occasionally produced by experimental techniques, attempts to reproduce a burst formation by identical parameters were only partially successful. Methods evaluated in the course of initial burst generation studies involved variation of such parameters as weld blank geometry, weld speed, heat input, repeated passes, staggered locking, copper chills and insert molding.

Configuration 1 (Figure 43) was utilized for Welds 4EB-BX-1U through -4U. This geometric design introduced abrupt changes in the electron-beam/base metal interface and allowed intermittent entries and exits of the beam during the operation. All welding was performed in a continuous unidirectional mode. Initial welds and reweld cycles performed on this configuration (varying weld speed and heat input) were unsuccessful. Metallographic examinations performed on segments of each weld between reweld operations verified the lack of burst defects, confirming the radiographic examination results.

Configuration 2 (Figure 44) was utilized for Welds 4EB-BX-1V through -4V. This geometric design introduced similar abrupt changes in the electron-beam/base metal interface as did Configuration 1. The 45-degree angle of departure of the cutout away from the weld line was not as abrupt as on Configuration 1. All welding was performed in a continuous, unidirectional, single-pass mode. Initial welds and reweld cycles performed on this configuration (varying weld speed and heat input) were all unsuccessful. Metallographic examination performed on segments of each weld between reweld operations verified the lack of burst defects, confirming the radiographic examination results.

Configuration 3 (Figure 45) represented a modification of Configuration 1. The number of 90-degree cutouts was reduced in order to increase the amount of restraint exerted on the weld bead. The weld direction was changed to allow welding from the center hole outward using a single-pass mode. Welds 4EB-BX-5U, -6U and -7U were welded using this configuration. Rewelding was not performed on this configuration. Radiographic examination of these welds failed to indicate ~~bursts~~.

Configurations 4 and 5 are shown in Figure 46. In Configuration 4, the cutout was left open and the halves were joined by two EB passes. The first pass was a partial penetration pass and the second was a full-penetration pass. Copper bars were placed alongside the weld to accelerate solidification. These parameters were utilized in fabrication of Weld 4EB-BX-B $\nu$ .

Configuration 5 incorporated a fitted plug of identical thickness material inside the cutout opening. Weld 4EB2-BX-9U was fabricated by the operational sequence used for Weld 4EB-BX-B $\nu$ . Radiographic examination of both welds indicated that no bursts were generated.

Configuration 6 consisted of a straight butt joint produced by a full-length, partial-penetration (0.050-inch deep) locking pass (Weld 4EB2-BX-10) or a full-length, deeper penetration (0.100-inch deep) locking pass (Weld 4EB2-BX-13) followed by a single, full-penetration pass in the same direction. Copper bars were used to accelerate weld chilling and weld restraint formation. Radiographic examination of these welds indicated that no bursts were formed.

Configuration 7 consisted of a straight butt joint produced by intermittent locking passes: 0.050-inch-deep pass for Weld 4EB-2-BX-11 and 0.250-inch-deep pass for Weld 4EB-2-BX-14. These locking passes were followed by a single, full-penetration pass in the same direction. Copper chill bars were utilized to accelerate weld chilling and weld restraint formation. Radiographic examination of both weldments indicated no bursts.

Configuration 8, represented by Weld 4EB-BX-12, was produced by joining halves of the weld blank using a single, full-penetration EBW pass. Two 3/8-inch-diameter by 1/2-inch-high Ti-6Al-4V plugs were placed on the face of the weld in such a way that the centerline of the round plug was perpendicular to the longitudinal axis of the weldment. The assembly was rewelded using the second, full-penetration pass. The objective of this approach was to introduce variations in the cooling rate along the length of the weld. The plugs were then cut off and a cosmetic pass was applied to the face of the weldment. A radiographic examination of the weld did not, however, indicate formation of bursts.

Configuration 9, represented by Weld 4EB2-BX-15, utilized the existing 4EB2-BX-13 plate assembly. Two 3/8-inch-diameter, through-holes were drilled into the weld four inches apart perpendicularly to the longitudinal axis of the weld. Two 3/8-inch-diameter Ti-6Al-4V plugs (one 3/4 inch long and the other 7/8 inch long) were inserted and positioned flush with the upper surface. A single, full-length, full-penetration pass was made along the existing weld and through the centers of inserts. Radiographic examination of this plate indicated that no bursts were generated.

Configuration 10 (Figure 47), represented by Weld 4EB2-BX-16, was a combination of all previous design concepts. It contained offset cutouts with metal plugs welded in place simulating start/stop run-off tabs. The fill-in plugs were 3/4-inch-wide, 1-1/8-inch-long and were equal in thickness to the metal plate. On the underside of the plate, several 1/2-inch-square Ti-6Al-4V bars were located so that the longitudinal axis of the weld was perpendicular to the longitudinal axis of the square bars. These bars, located in five places, simulated the effect of the electron-beam entering and exiting a perpendicular segment of base metal, instantaneously increasing or decreasing the effective thickness of the weld. Welding was accomplished in a single-pass operation. Radiographic examination of this plot indicated that no bursts were generated.

At the conclusion of the Phase I efforts, only three burst defects could be produced (two in 0.250-inch PAW weldments and one in 0.090-inch EB weldments). The bursts occurred in specimens not specifically designed to facilitate burst formation. Their location, however, was similar to that encountered in production welding. The burst defects could not be reproduced utilizing identical configurations and parameters.

Upon conclusion of the initial studies, findings of an independent investigation (Ref. 1) became available which indicated that the formation of burst defects in EB weldments may be related to a change in the configuration of the molten puddle accompanying the transition from a partial to full EB penetration. It was postulated that bursts could be formed on non-uniform solidification of the molten metal in the vicinity of a free interface upon rapid cooling following extinction of the beam. Figure 48 illustrates this hypothesis.

Dimensional characteristics of an experimental weld blank designed to test the validity of this hypothesis are shown in Figure 49. In these blanks, changes in the

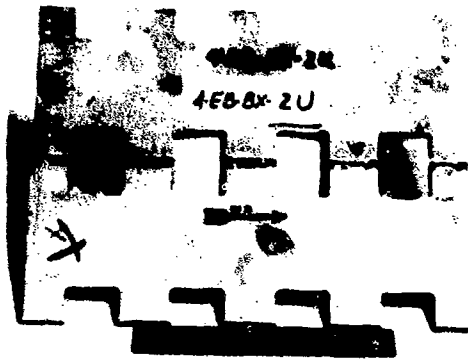


Figure 43. Overall View of Configuration 1 Utilized for Burst Defect Generation (0.7X MAG). Arrow Indicates Weld Direction.

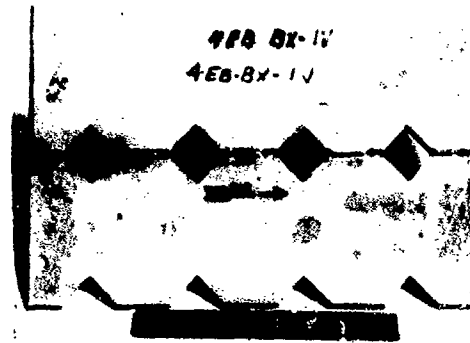


Figure 44. Overall View of Configuration 2 Utilized for Burst Defect Generation. Arrow Indicates Weld Direction (0.7X MAG).

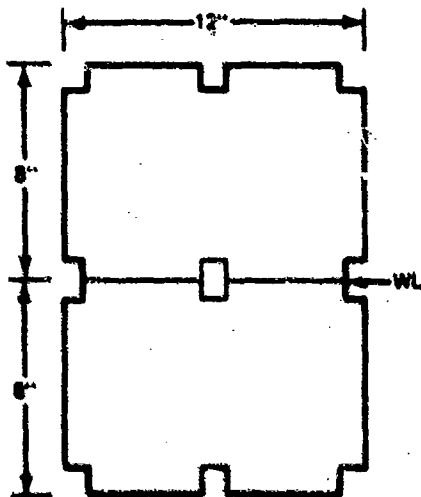


Figure 45. Configuration 3 - Burst Generation

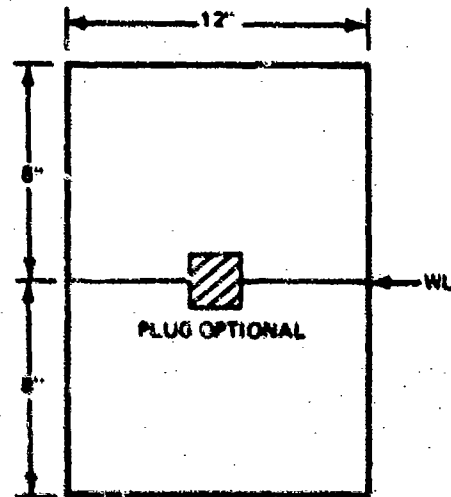
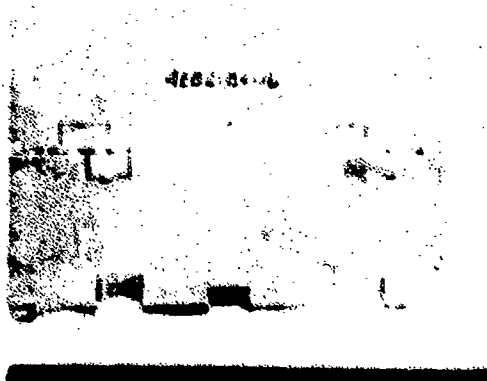
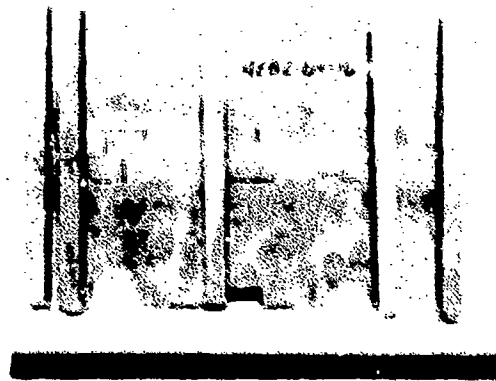


Figure 46. Configurations 4 and D - Burst Generation



a. Top Surface Showing Cutouts Welded in Place



b. Bottom Surface Showing Placement of 1/2-inch Bars (Note Weld Penetration Through Bars)

Figure 47. Weld 4EB2-BX-16

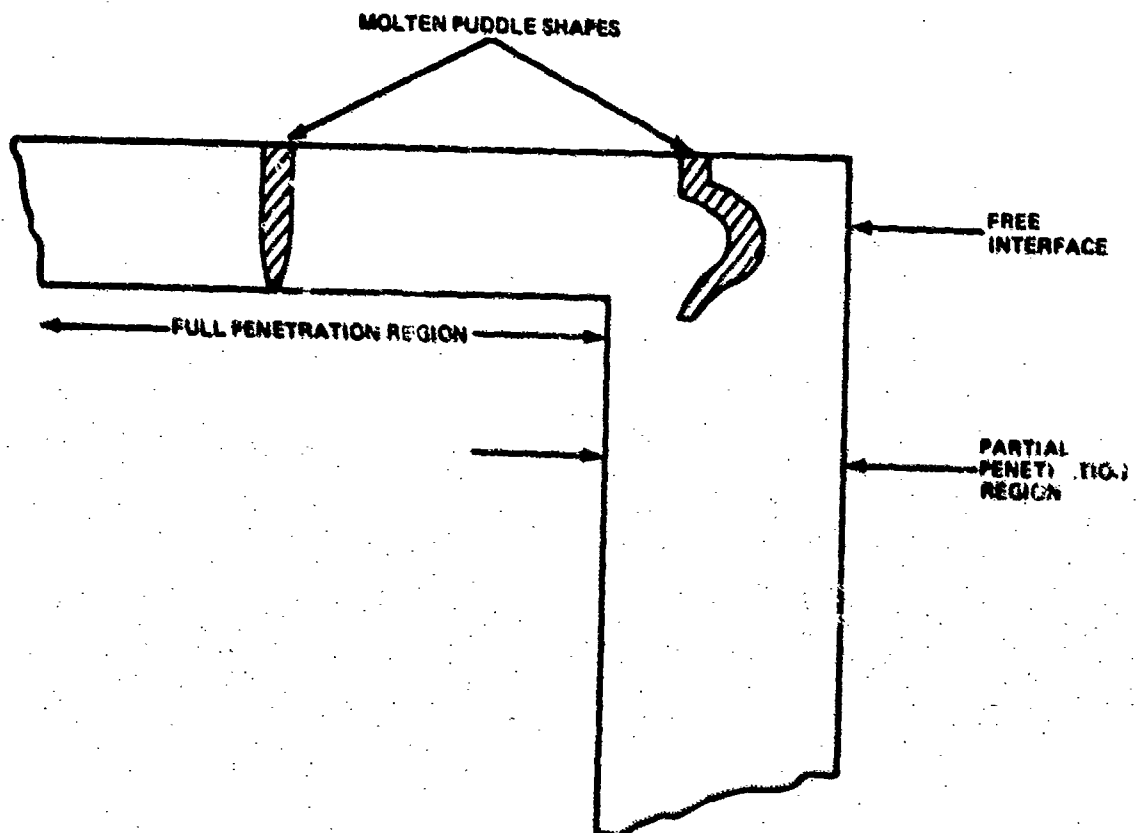
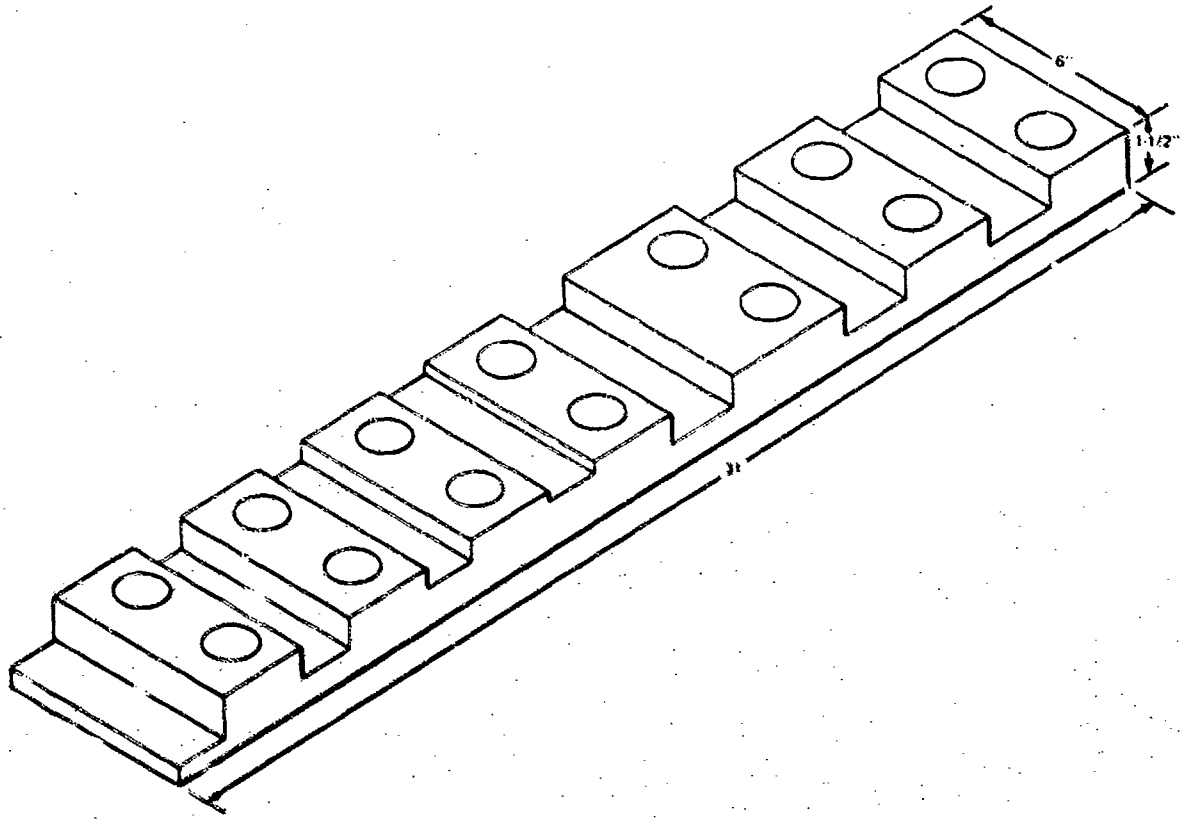
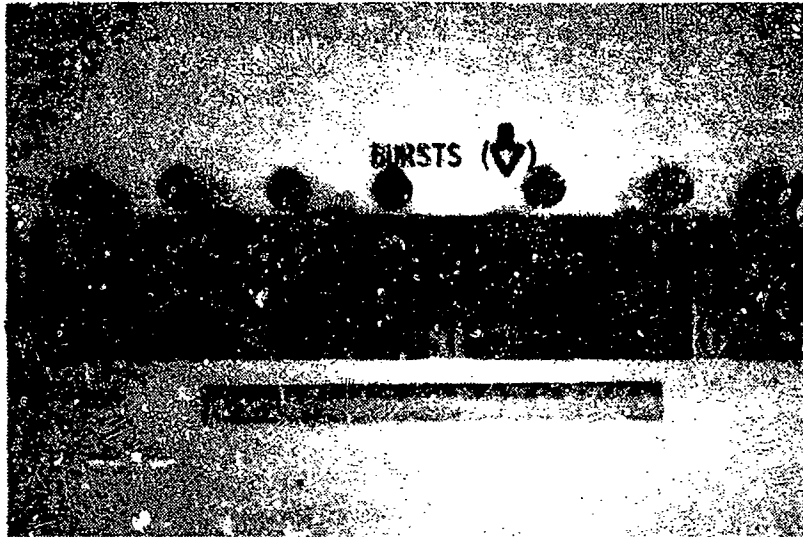


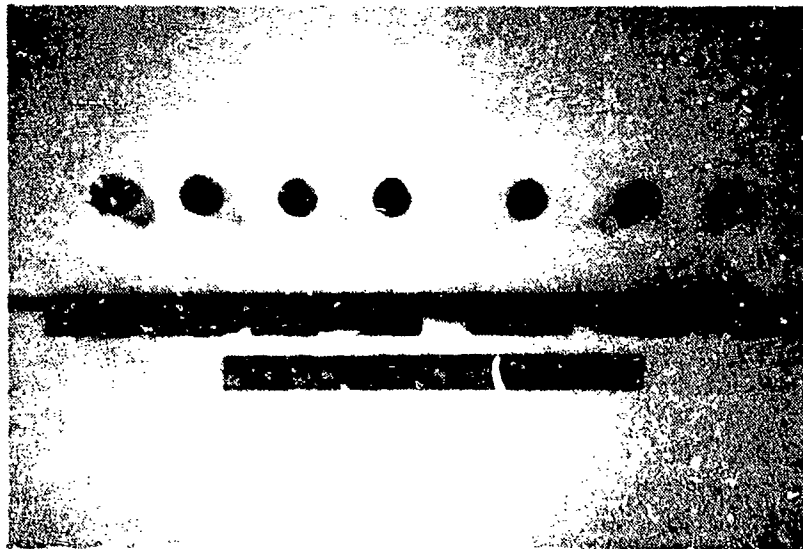
Figure 48. Mechanism of Burst Formation During EB Welding



**Figure 49. Configuration of Experimental Weld Blank to Determine Burst Formation Mechanism During EB Welding**



a. Top View (Arrows indicate location of bursts and the direction of EBW pass)



b. Side View

Figure 30. Contoured Welding Blank Used in Burst-Generation Studies.



a. Top View



b. Side View

Figure 51. Radiographs Showing Indication of Burst (5X MAG)

puddle configurations were to be obtained by varying the thickness of the blank segments. Conditions of rapid cooling were simulated by inserting round slide-fitting plugs into openings of the weld-blank-assembly as shown in Figure 50. It was postulated that as the beam entered the plug, the expansion of the plug would bring it into intimate contact with the surrounding (and much cooler) mass of metal and thus simulate the conditions existing at the extinction of the beam in normal welding practices. The EB welding pass was designed to completely penetrate thinner segments and to obtain 50 percent penetration in full-thickness sections containing plugs. Figure 50 shows the welding assembly and locations of bursts which were successfully generated in five out of seven inserts in 1-1/2-inch-thick plates. Radiographic indications of generated bursts are shown in Figure 51.

#### 11. Flawless Welds

Several fatigue test specimens were machined from radiographically flawless EB welded 0.090 and 0.25-inch-thick blanks, GTA-welded 0.090-inch-thick, and PA welded 0.25-inch-thick blanks. Welding of all blanks was performed using conventional parameters designed for production welding. The machined specimens were stress relieved and tested in tension-tension ( $R=0.1$ ) fatigue to failure at 100 ksi (maximum) stress level. The endurance values obtained were in the 50,000 to 65,000-cycle range and thus were comparable to the corresponding values of the base metal.

## SECTION IV

### FATIGUE ENDURANCE OF GTA WELDMENTS

#### A. INTRODUCTION

This section presents data on fatigue endurance of flawless and (intentionally) defective GTA weldments. The data are presented in the following sequence:

- General fabrication procedure
- Flawless welds
- Porous welds
- Reinforced welds
- Minor underfills
- Minor undercuts
- Tungsten inclusions
- Mismatch
- Inadequate shielding
- Transverse cracks
- GTA-repaired EB welds
- Summary

#### B. GENERAL FABRICATION PROCEDURE

Experimental GTA weldments were manufactured using a Sciaky Welder, HW27 Linde torch equipped with a No. 12 (3/4-inch ID) Lava cup and 3/32-inch thoriated tungsten electrode. The faying surfaces of the weld blanks were machined to provide a 60-degree internal angle and 0.060 to 0.065-inch lands.

#### C. FLAWLESS GTA WELDMENTS

##### 1. 0.080-inch Thick Welds

##### a. Fabrication of Experimental Welds

Radiographically flawless, 0.080-inch-thick welds were produced on one pass at 10 volts, 180-190 amperes, and a travel speed of 14 inches per minute. Ti-6Al-4V filler wire was utilized at a feed rate of 35 inches per minute. Argon was used for torch and trail shielding, and back-up applications at flow rates of 60, 60 and 5 cubic feet per hour, respectively. No radiographic indications were detected in contoured welds and after machining the welds flush with the surface.

##### b. Evaluation of Fatigue Data

Fatigue endurance values obtained are presented in Figure 52. All experimental points were within the upper portion of the  $K_t = 1$  to  $K_t = 2$  range. The specimens tested at 20 cpm failed in the base metal away from the weld (Specimen No's 9-1, 9-2 and 9-3). All specimens tested at 1800 cpm failed in the weld. The subsequent fractographic evaluation revealed failure initiation at the surface of the test specimens (Figure 53). No porosity was detected on any of the fracture surfaces. Data on fatigue endurance values and fractographic findings for individual specimens are listed in Appendix B, Table B-1.

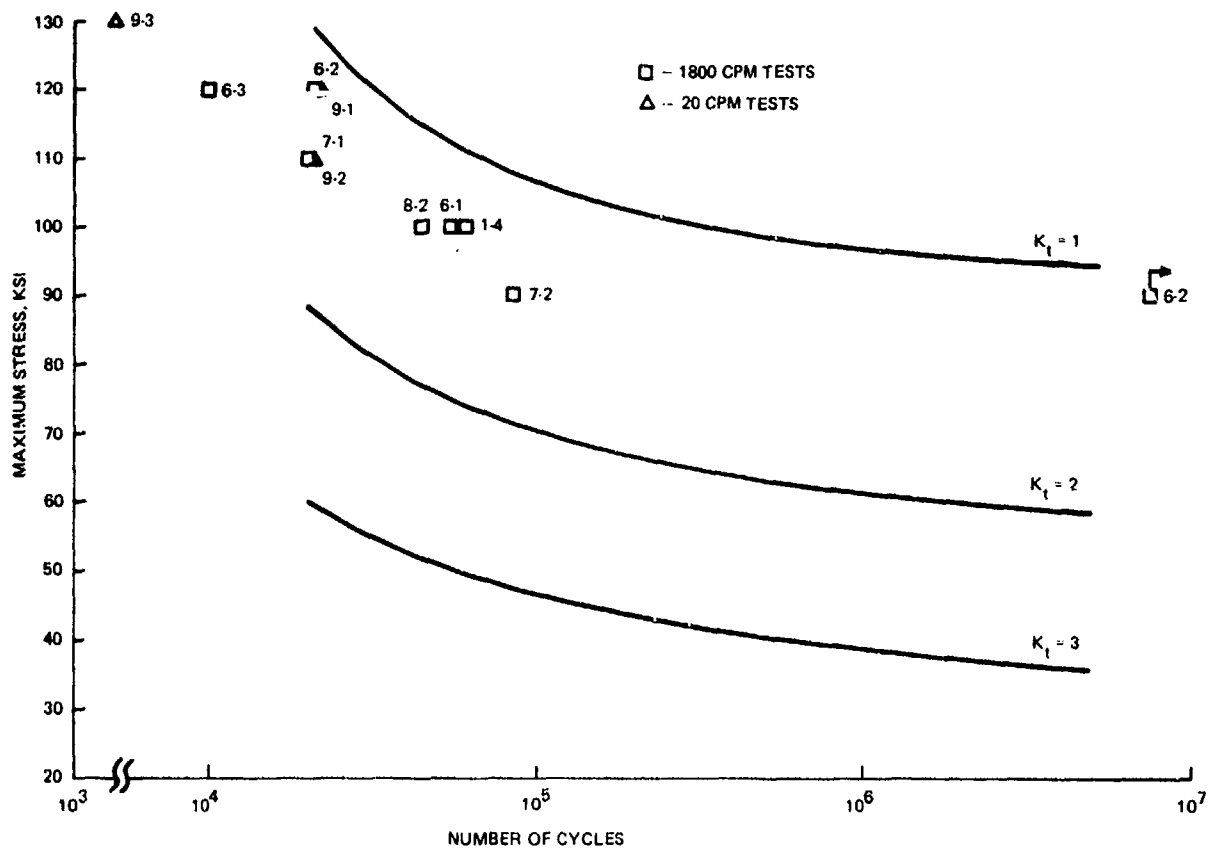


Figure 52. Fatigue Endurance of Flawless 0.080-Inch-Thick GTA-Welded Specimens

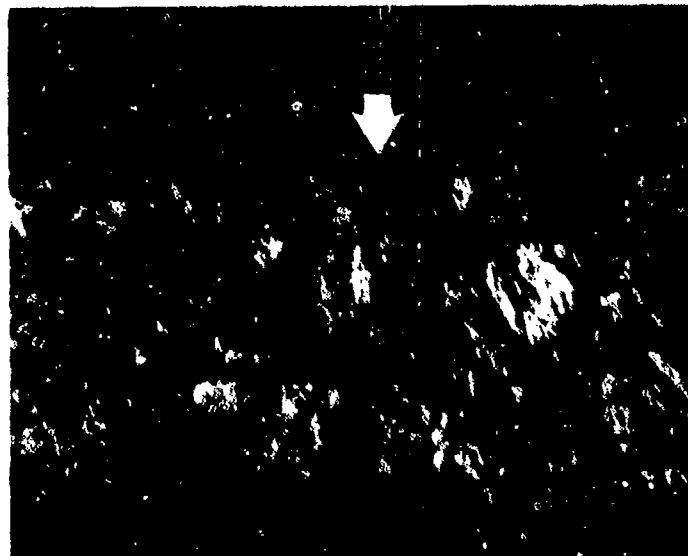


Figure 53. Typical Surface Failure Initiation Site in Flawless 0.080-Inch-Thick GTA Weldment (20 X MAG)

## 2. 0.25-Inch-Thick Welds

### a. Fabrication of Experimental Welds

Radiographically flawless 0.25-inch-thick GTA welds were produced in two passes. Voltage and arc current settings were 13 and 14 volts, and 275 and 250 amperes for the first and second passes, respectively. The carriage travel speed was kept constant in the range of 7.0 to 8.5 inches per minute; the wire feed was 60 inches per minute in both passes. Helium was used for torch and trailing shielding and back-up applications at flow rates of 60, 60 and 10 cubic feet per hour, respectively. No radiographic indications were detected in any of the welds after final machining.

### b. Evaluation of Fatigue Endurance

Experimental fatigue endurance data are plotted in Figure 54. All data points were located in the upper portion of the  $K_t = 1$  to  $K_t = 2$  range, except for specimens 7-3 and 8-4 in which the failure initiation was associated with isolated 0.004-inch pores, 0.080 and 0.10 inch from the surface, respectively. No porosity was detected at other fracture surfaces. In six specimens, the failure initiated in the base metal away from the weld. In the remaining four specimens, failure initiated at either the face or root surfaces of the weldments. Data on fatigue endurance and fractographic findings are listed in Appendix B, Table B-2.

## D. POROUS GTA WELDS

### 1. .080-INCH THICK WELDS

#### a. Fabrication of Experimental Welds

The parameters utilized in fabricating of 0.080-inch-thick porous welds were identical to those utilized in production of radiographically flawless GTA welds except that the machined and cleaned blanks were exposed for two to three weeks to a shop environment and faying surfaces were intentionally contaminated to simulate handling without protective equipment. Several porosity containing specimens were also obtained from blanks intended for production of radiographically flawless specimens. The prefix "F" is used to identify these specimens.

#### b. Evaluation of Fatigue Data

Fatigue data on experimental welds are plotted in Figure 55. It is evident that data points are widely scattered in the  $K_t = 1$  to  $K_t = 3$  range except for Specimen 9-4 whose endurance fell below the  $K_t = 3$  curve. The exceptionally low endurance value obtained for this specimen was caused by a cluster of pores, 0.015 to 0.020-inch in diameter. Many data points in the middle and upper portions of the  $K_t = 1$  to  $K_t = 2$  range were associated with failure initiations at isolated porosity in the range of 0.005 to 0.010 inch located 0.020 to 0.030 inch from the surface (Specimen 4-3, F8-4, F7-4, F8-1, 9-4). Figure 56 shows a failure initiation associated with a 0.007-inch internal pore in Specimen F7-4.

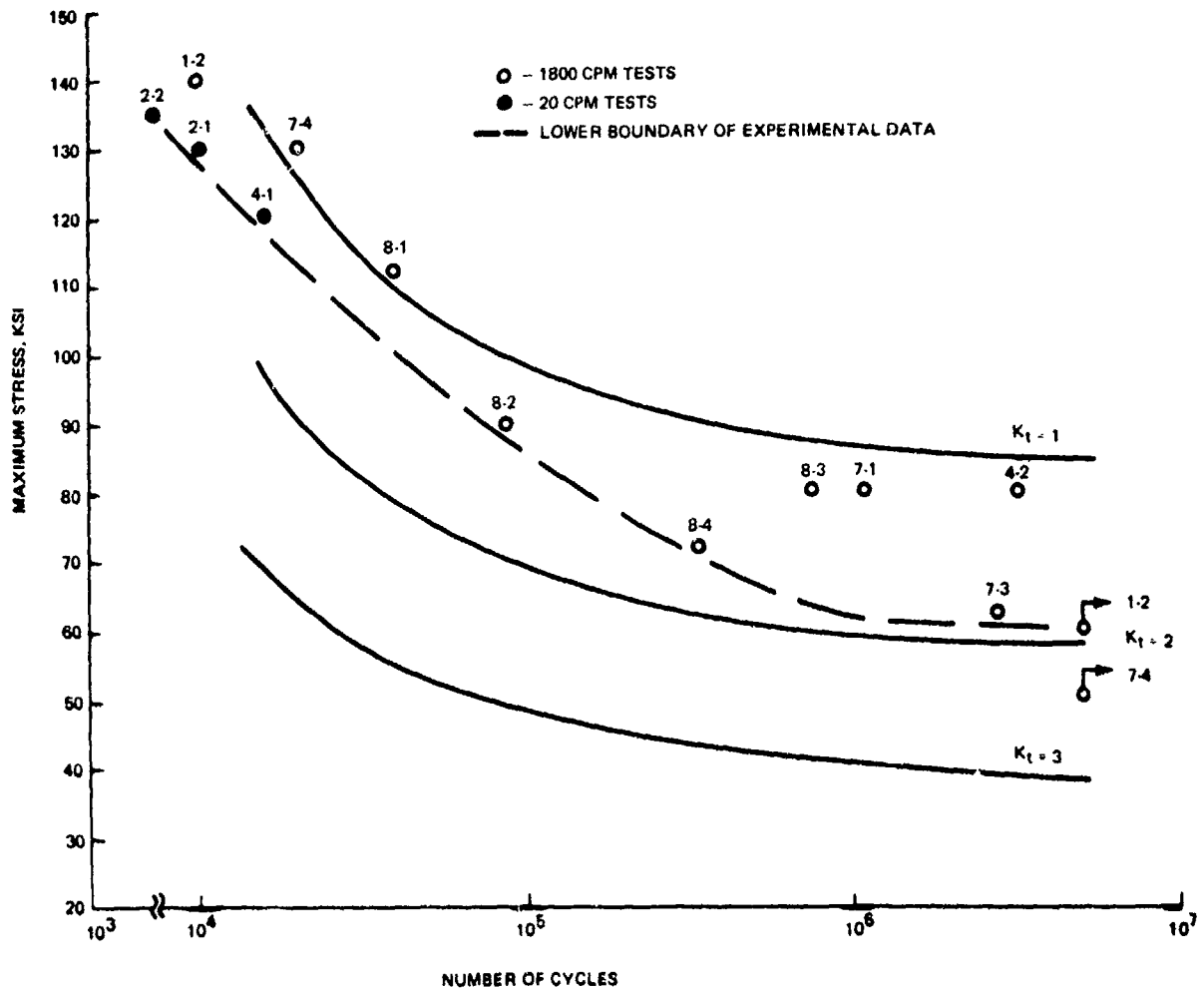


Figure 54. Fatigue Endurance of Flawless 0.25-Inch-Thick GTA Welds

Attempts to correlate fractographic findings with fatigue endurance data contained in the  $K_t = 2$  to  $K_t = 3$  range, and the lower portion of  $K_t = 1$  to  $K_t = 2$  range were only partially successful. Most of the test specimens with fatigue endurance values in this range contained porosity in the order of 0.020 to 0.030 inch in diameter (about one-third of the specimen's thickness  $\sim T/3$ ). The presence of coarse pores led to frequent multiple failure initiations and interaction of several fatigue zones, both of which made it difficult to correlate the data. Results of pre-test radiography, fatigue endurance and fractographic findings are presented in Appendix B, Table B-3.

## 2. 0.25-INCH-THICK-WELDS

### a. Fabrication of Experimental Welds

Porosity-containing 0.25-inch-thick GTA welds were produced by omitting the conventional cleaning cycle on blanks prior to welding. In addition, this group included several specimens which, although welded using parameters designed to produce flawless welds, did contain porosity detectable by pre-test radiography. The prefix "F" was used to identify these samples.

### b. Evaluation of Fatigue Data

Experimental fatigue data are plotted in Figure 57. Three "F" specimens had fatigue endurance in the range expected for flawless specimens. Isolated porosity

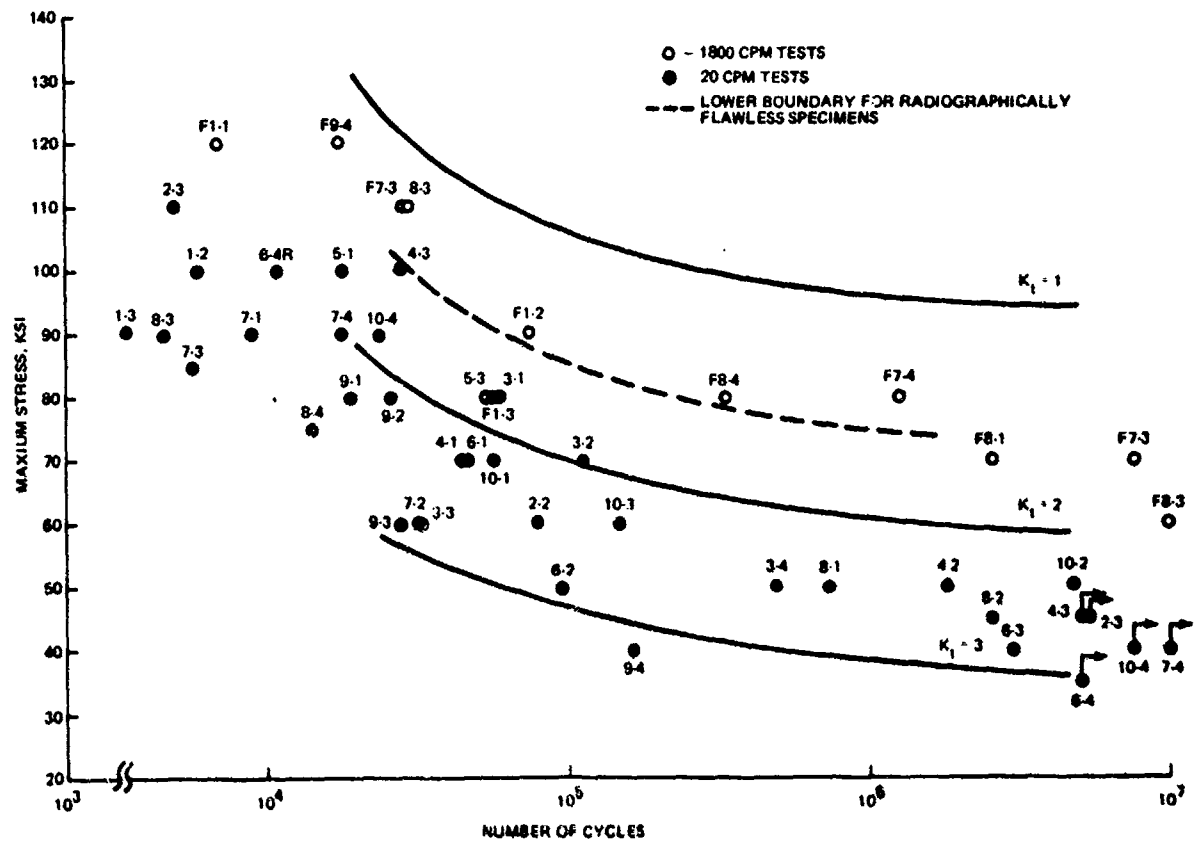


Figure 55. Fatigue Endurance of Porous .080-inch-Thick GTA Weldments

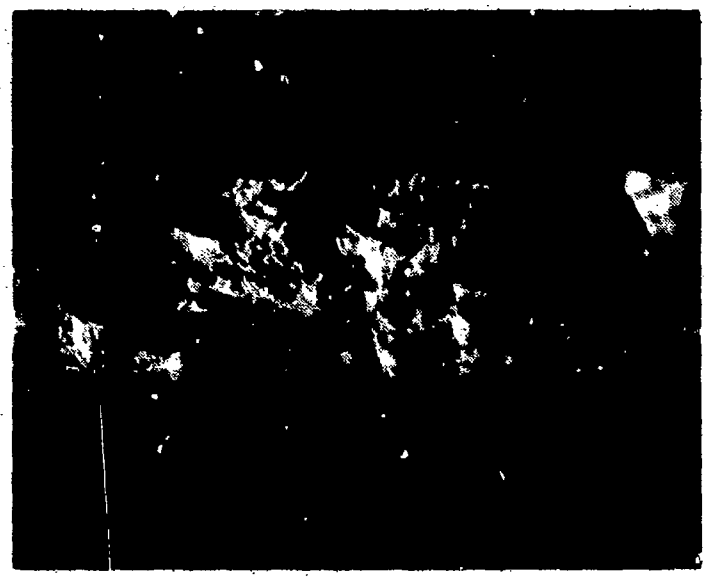


Figure 56. 0.007-inch Pore at Failure Initiation Site in Specimen F7-4 (20 X MAG)

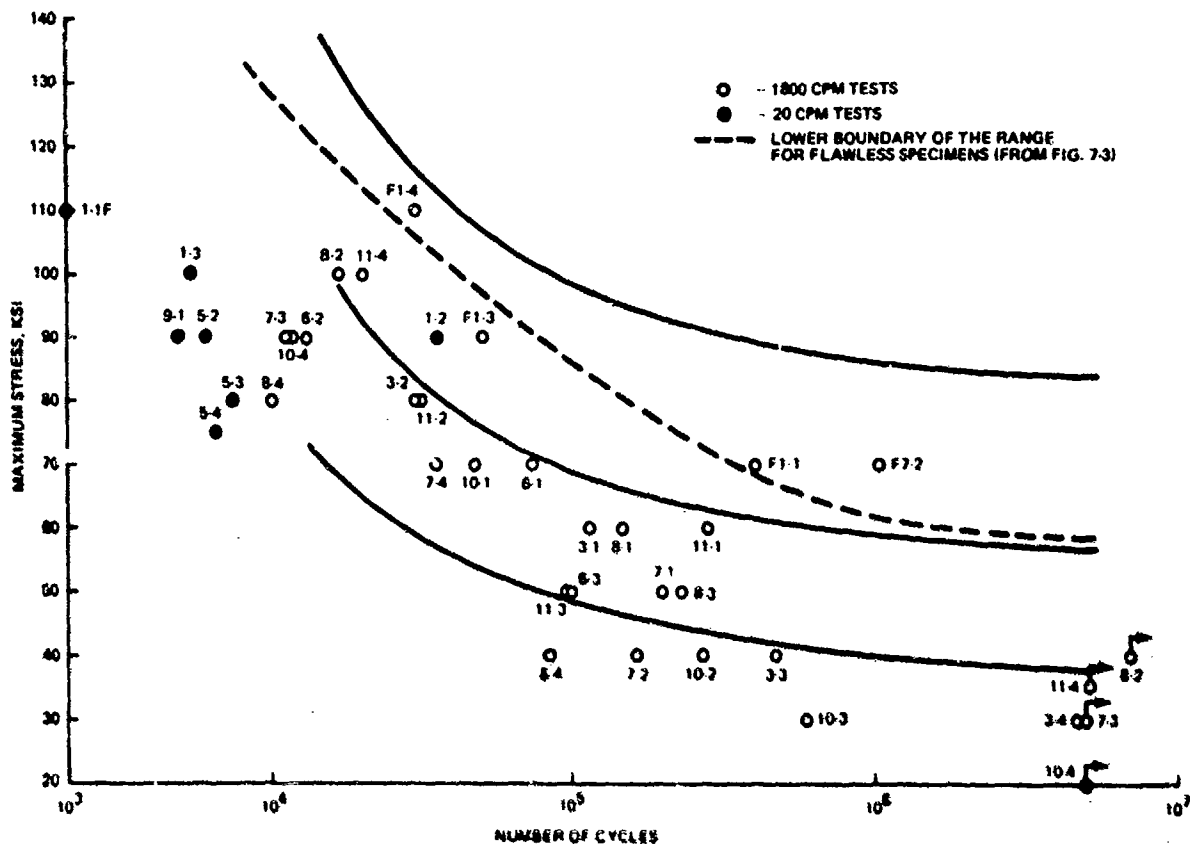


Figure 57. Fatigue Endurance of 0.25-inch-Thick GTA Welds Containing Porosity



Figure 58. Multiple Failure Initiation Encountered in 0.25-inch-Thick Porous GTA Specimens with Fatigue Endurance in the  $K_1 = 2$  to  $K_1 = 3$  Range (20X MAG)

detected in these specimens ranged from 0.005 to 0.020 inch, and its distance from the surface was in the range of 0.040 to 0.110 inch (Specimens F1-1, F1-4 and F7-2). In specimen F1-3, which exhibited endurance slightly below this range, the failure initiated at a 0.004-inch pore at the subsurface of the specimen. Of the three other specimens with endurance values between the lower boundary of the flawless range and the  $K_t = 2$  curve, Specimen 1-2 failed in the base metal; in Specimen 11-4, failure initiated at an isolated 0.025-inch pore 0.090 inch from the surface. Multiple failure initiations in Specimen 8-2 were associated with 0.010 to 0.020-inch pores dispersed in the interior of the weld.

Failures in specimens with fatigue endurance values in the  $K_t = 2$  to  $K_t = 3$  range were associated typically with 0.010 to 0.035 inch porosity scattered throughout the thickness of the specimens which caused multiple failure initiations (Figure 58), and isolated surface or subsurface porosity, as shown in Figures 59 and 60, respectively.

Failure initiation sites in specimens with fatigue endurance values below the  $K_t = 3$  curve were associated with surface, subsurface or interior porosity clusters as shown in Figures 61 through 63, respectively. Radiographic, fatigue endurance, and fractographic data for 0.25-inch-thick porous GTA welds are summarized in Appendix B, Table B-4.

## **E. REINFORCED GTA WELDS**

### **1. 0.080-INCH THICK WELDS**

#### **a. Fabrication of Experimental Welds**

Reinforcement contours were obtained by increasing the feed rate of the filler wire from 38 to 42 inches per minute. The remaining parameters were identical to those utilized in conventional welding. Contours of weldments were recorded by tracing images projected on the screen of an optical comparator at 10X magnification. A typical weld contour recorded by this technique is shown in Figure 65. The height and width of the face and root reinforcements were 0.015/0.30 and 0.015/0.20 inch, respectively. Pre-test radiography showed that the welds were free of internal defects.

#### **b. Evaluation of Fatigue Data**

Fatigue endurance values for the experimental welds are plotted in Figure 64. All points were located between the lower boundary of the band expected for flawless machined specimens (dotted curve) and the  $K_t = 2$  curve. The failure initiated in all specimens at the root of the weld as shown in Figure 65, except for Specimen 1-2, in which the failure initiated at a 0.002-inch pore at the mid-section of the test specimen.

### **2. 0.25-INCH-THICK WELDS**

#### **a. Fabrication of Experimental Welds**

Reinforcement contours were obtained by increasing the feed rate of the filler wire on the second pass from 60 to 70 inches per minute. The remaining parameters were identical to those utilized in conventional welding. Contours of weldments were recorded by tracing images projected onto the screen of an optical comparator at 10X magnification. A typical weld contour recorded by this technique is shown in

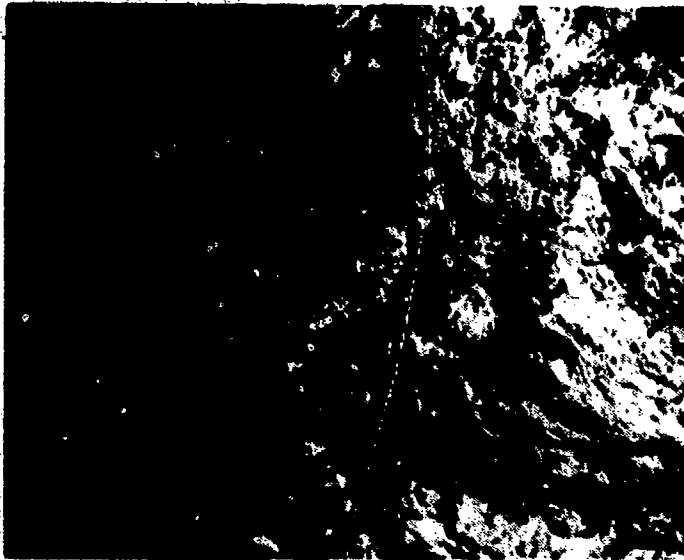


**Figure 58. Isolated Surface Porosity Detected at Failure Initiation of 0.25-Inch-Thick GTA-Welded Specimen 7-1 with Fatigue Endurance in the  $K_t = 2$  to  $K_t = 3$  Range (20X MAG)**

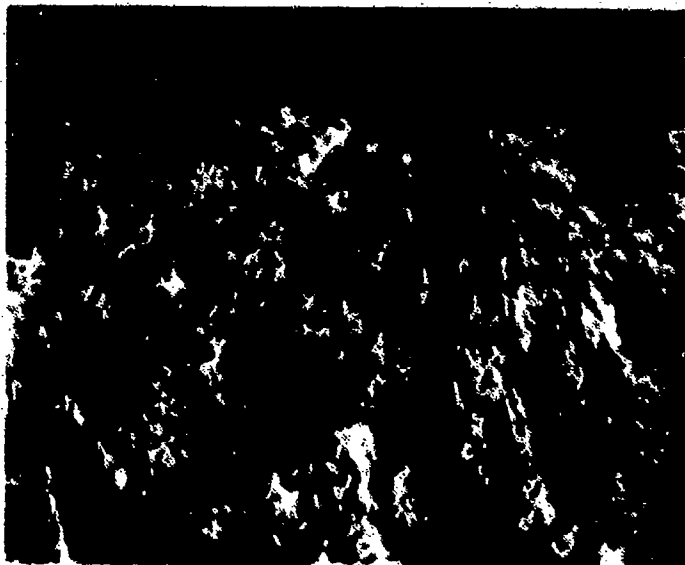


**Figure 59. Isolated Subsurface Porosity Detected at Failure Initiation of 0.25-Inch-Thick GTA-Welded Specimen 11-2 With Fatigue Endurance in  $K_t = 2$  to  $K_t = 3$  Range (20X MAG)**

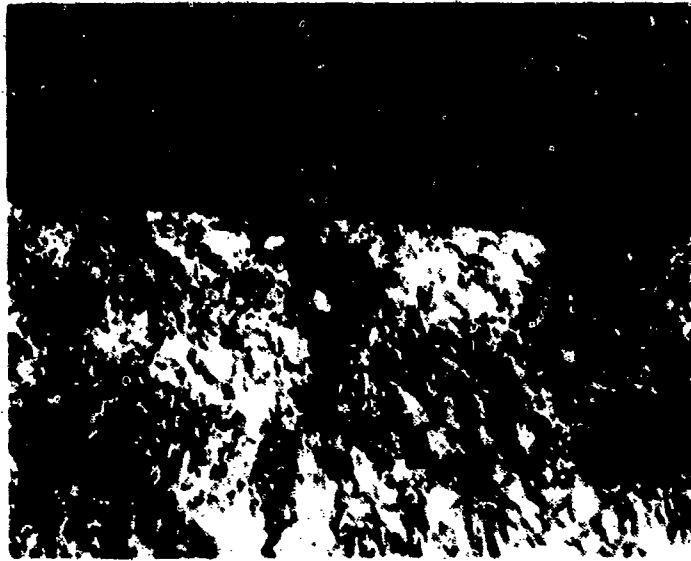


**Figure 61. Failure Initiation Site at a Surface Porosity Cluster in 0.25-Inch-Thick GTA-Welded Specimen 10-3 With Fatigue Endurance Below the  $K_t = 3$  Curve (20X MAG)**

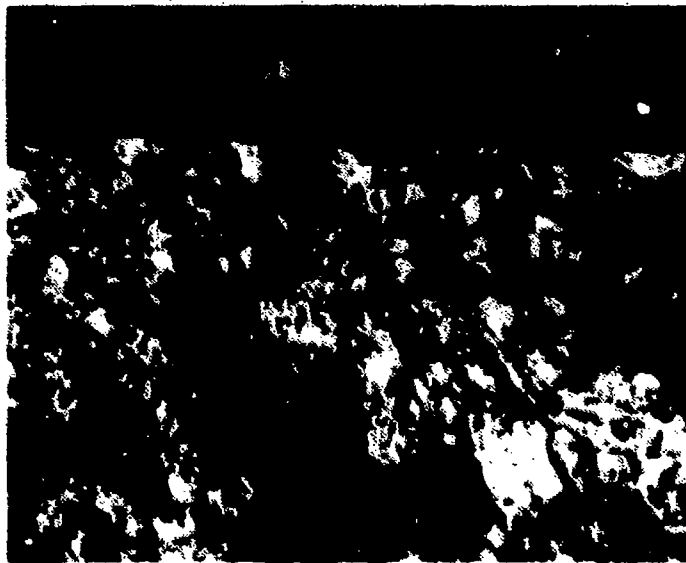


**Figure 62. Subsurface Porosity Cluster at the Failure Initiation Site in 0.25-Inch-Thick GTA-Welded Specimen 3-3 With Fatigue Endurance Below the  $K_t = 3$  Curve (20X MAG)**

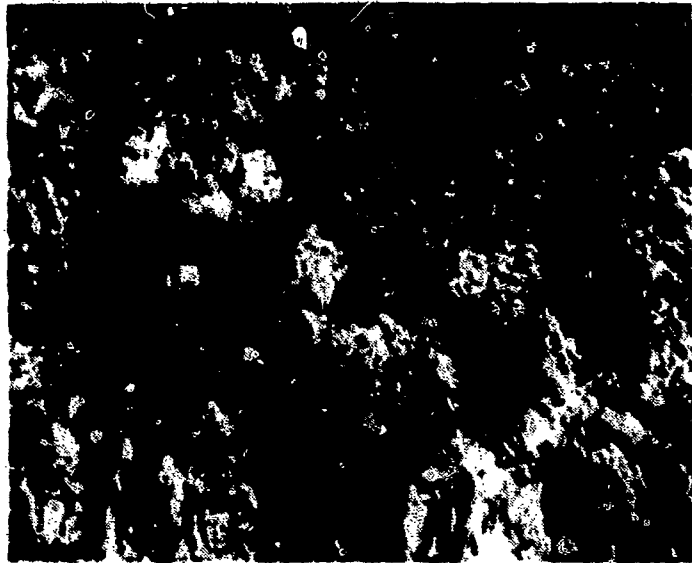


Figure 63. Interior Porosity Cluster at the Failure Initiation Site in 2.25-Inch-Thick GTA-Welded Specimen 3-4 With Fatigue Endurance Below the  $K_t = 3$  Curve (20X MAG)

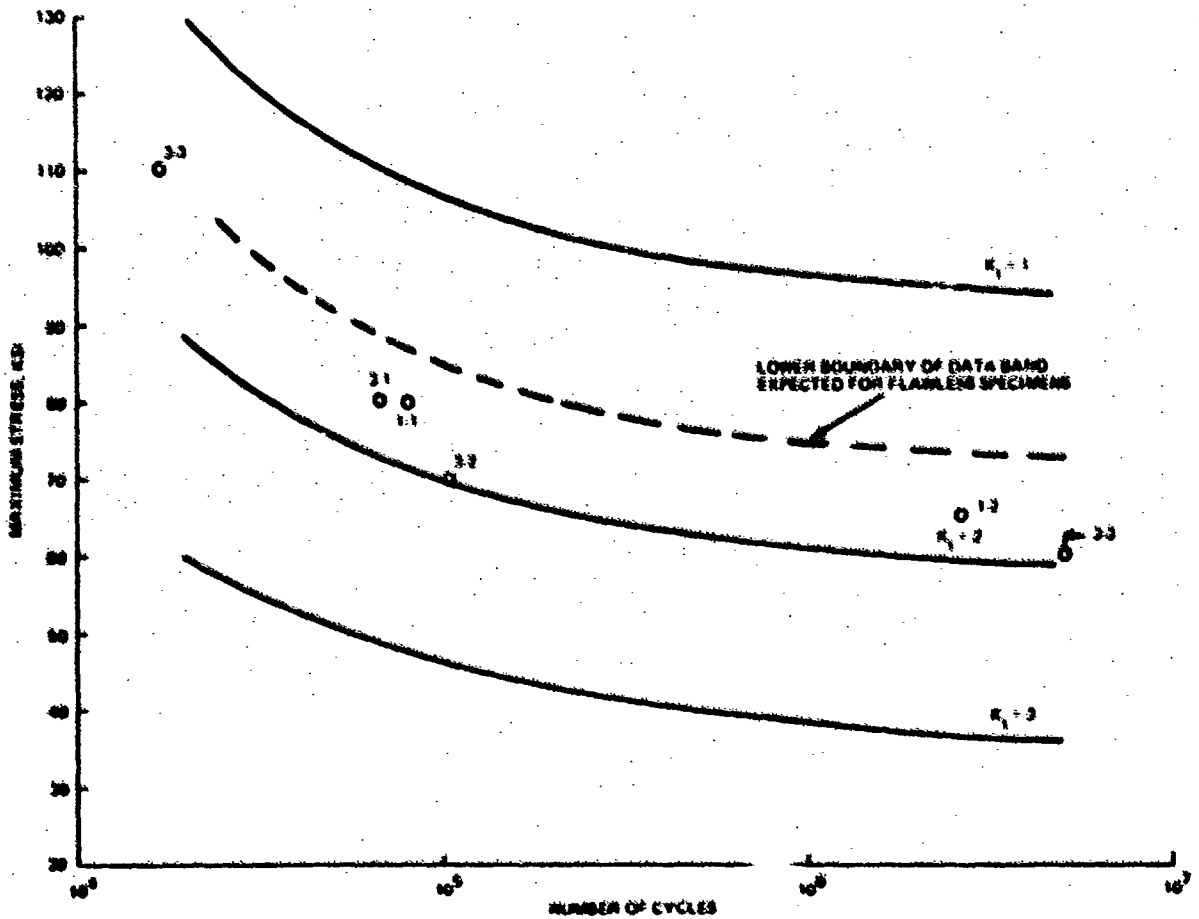


Figure 64. Fatigue Endurances of 0.080-Inch-Thick GTA-Welded Specimens with Minor (About 0.015 Inch) Faw and Root Reinforcements

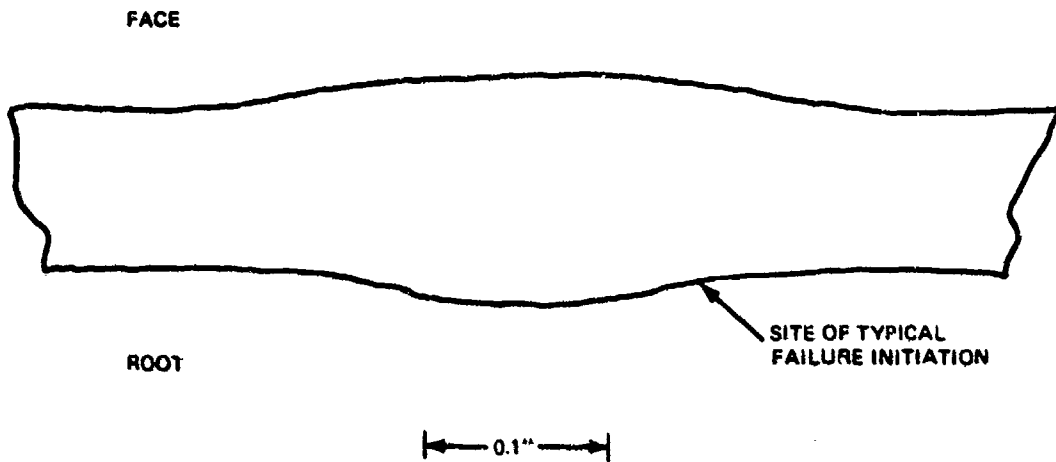


Figure 65. Contour of a Typical Reinforced 0.080-Inch-Thick GTA Weldment

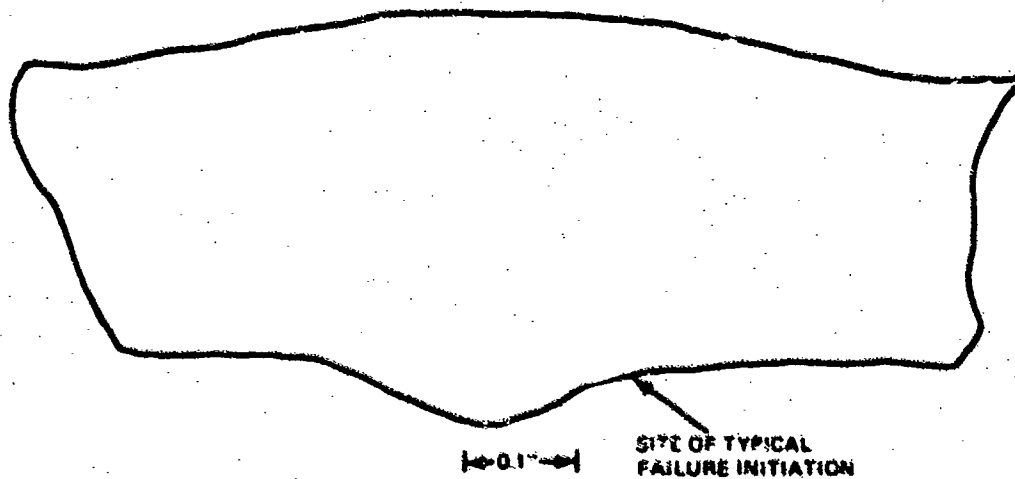


Figure 66. Typical Contour of Reinforced 0.25-Inch-Thick GTA Welds

Figure 66. The height and width of the face and root reinforcements were 0.055/0.75 and 0.050/0.25 inch, respectively. Pre-test radiography had shown that the welds were free of internal defects.

b. Evaluation of Fatigue Data

Fatigue endurance values for experimental welds are plotted in Figure 67. Although the data are limited, it is evident that fatigue endurance of these welds is comparable to that of the base metal at the  $K_t = 3$  level. Failure initiated in all specimens at the root of the weld in locations designated in Figure 66

F. MINOR UNDERFILLS

1. .080-INCH-THICK WELDS

a. Fabrication of Experimental Welds

Minor underfills were obtained in 0.080-inch-thick GTA weldments by lowering the current from 205 to 170 amperes and decreasing the filler wire feed rate on the second pass from 35 to 10 inches per minute for Blanks 2 and 3 and to 5 inches per minute for Blanks 5 and 6. Typical contours of minor underfills obtained by these techniques are shown in Figures 68 and 69. These contours were documented by tracing the images on the viewing screen at 10X magnification. The depth and width of underfill for both types of welds were 0.010/0.35 and 0.015/0.35 inch, respectively. Pretest radiography detected underfills in all specimens. All welds were free of internal defects.

b. Evaluation of Fatigue Data

Fatigue endurance data for experimental welds are plotted in Figure 70. Although two of the specimens with 0.010 inch underfill exceeded the  $5 \times 10^6$ -cycle endurance limit in the stress range expected for flawless machined specimens, the majority of the remaining data points were in the region between the flawless range and the  $K_t = 2$  curve. The scatter of experimental data and the limited number of data points in the high-cycle region of the plot did not permit drawing of definite conclusions as to the effects of 0.005-inch depth variation in shallow underfills on fatigue characteristics. Failure initiated in all specimens at radii of underfills, except for Specimen 3-2 in which a secondary failure initiation was detected at a 0.004-inch-diameter pore in the interior of the specimen.

2. 0.25-INCH-THICK WELDS

a. Fabrication of Experimental Welds

Minor underfills were produced in 0.25-inch-thick GTA welds by decreasing the filler wire feed rate on the second pass from 60 to 10 inches per minute. A typical contour of welds produced by these techniques is shown in Figure 71. The width of this underfill was 0.8 inch and its depth varied from 0.005 to 0.015 inch. The width of the root reinforcement was in the 0.25 to 0.30-inch range and its height was 0.050 inch. Pre-test radiography identified underfills in all specimens. There were no indications of internal defects.

b. Evaluation of Fatigue Data

Fatigue endurance data for experimental welds are plotted in Figure 72. It is evident that all data points were located in the lower portion of the  $K_t = 1$  to  $K_t = 2$

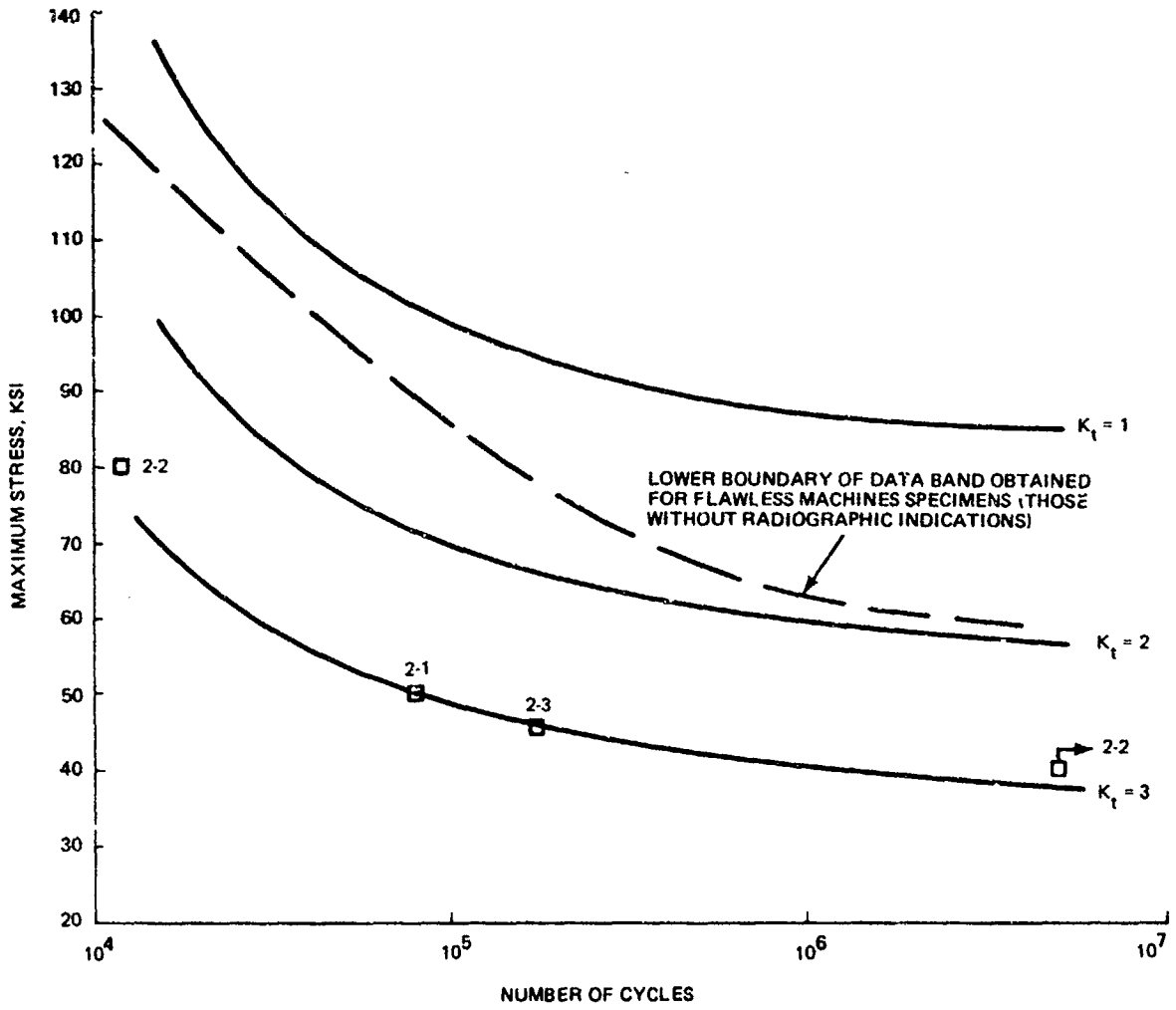
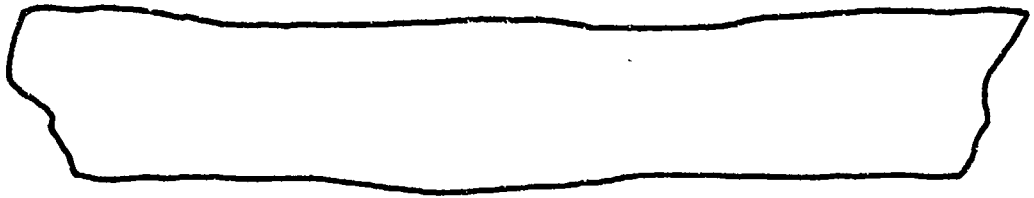


Figure 67. Fatigue Endurance of Reinforced 0.25-Inch-Thick GTA Welds



|—0.1"—|

**Figure 68. Typical Configuration of 0.080-Inch-Thick GTA Welds with 0.010-Inch Underfills**



|—0.1"—|

**Figure 69. Typical Configuration of 0.080-Inch-Thick GTA Welds with 0.015-Inch Underfill**

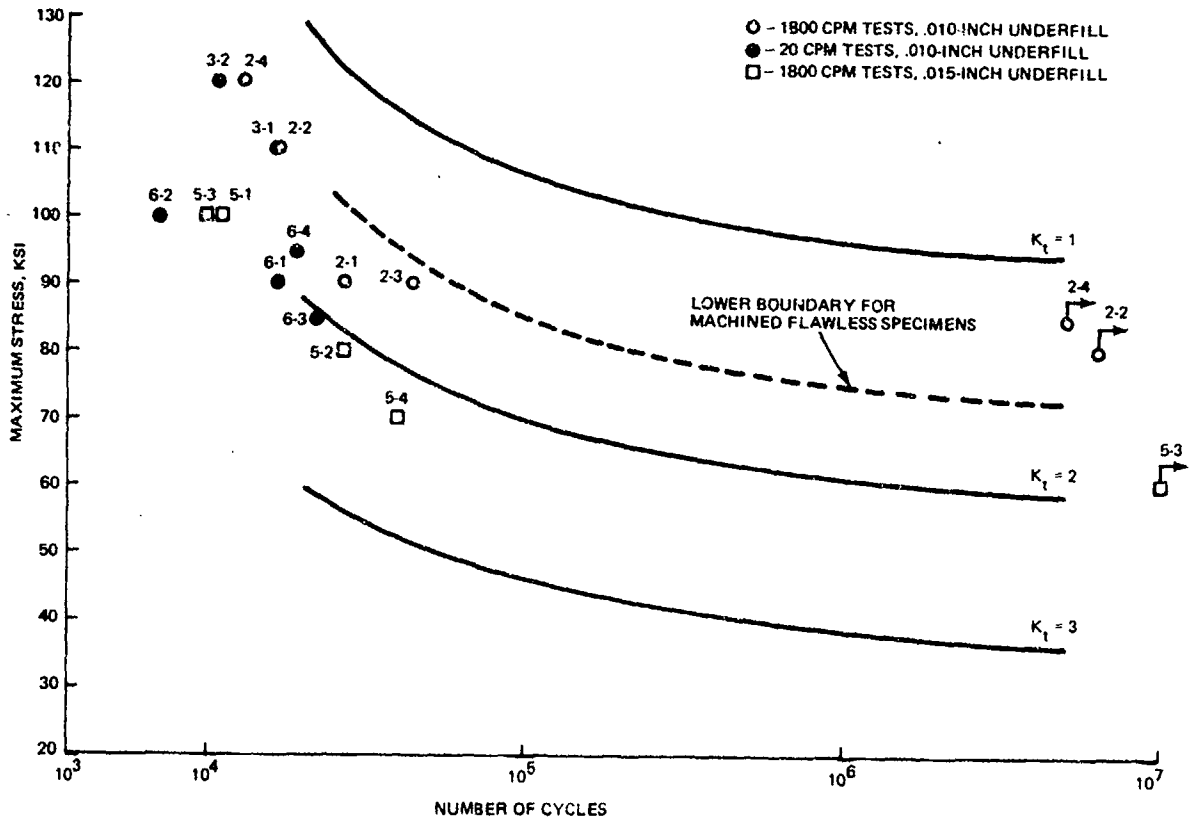


Figure 70. Fatigue Endurance of 0.080-Inch-Thick GTA Welds With Minor Underfills

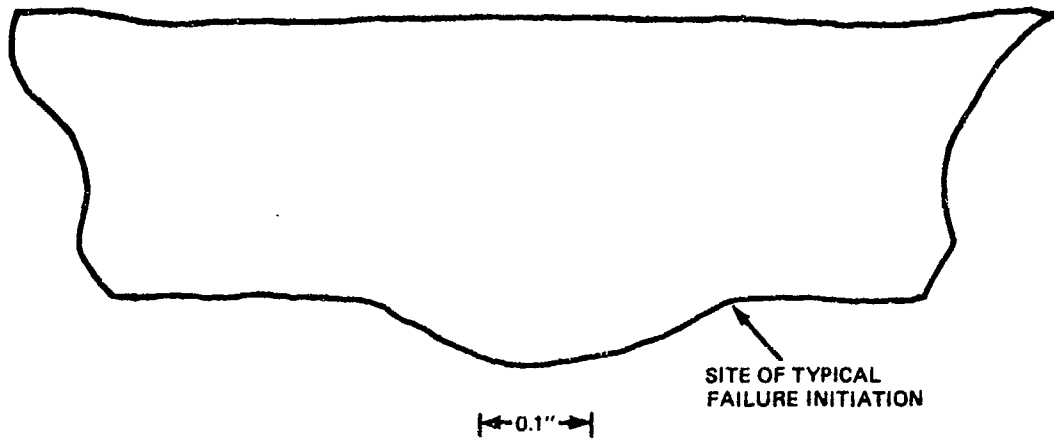


Figure 71. Typical Contour of 0.25-Inch-Thick GTA Welds with Minor Underfills

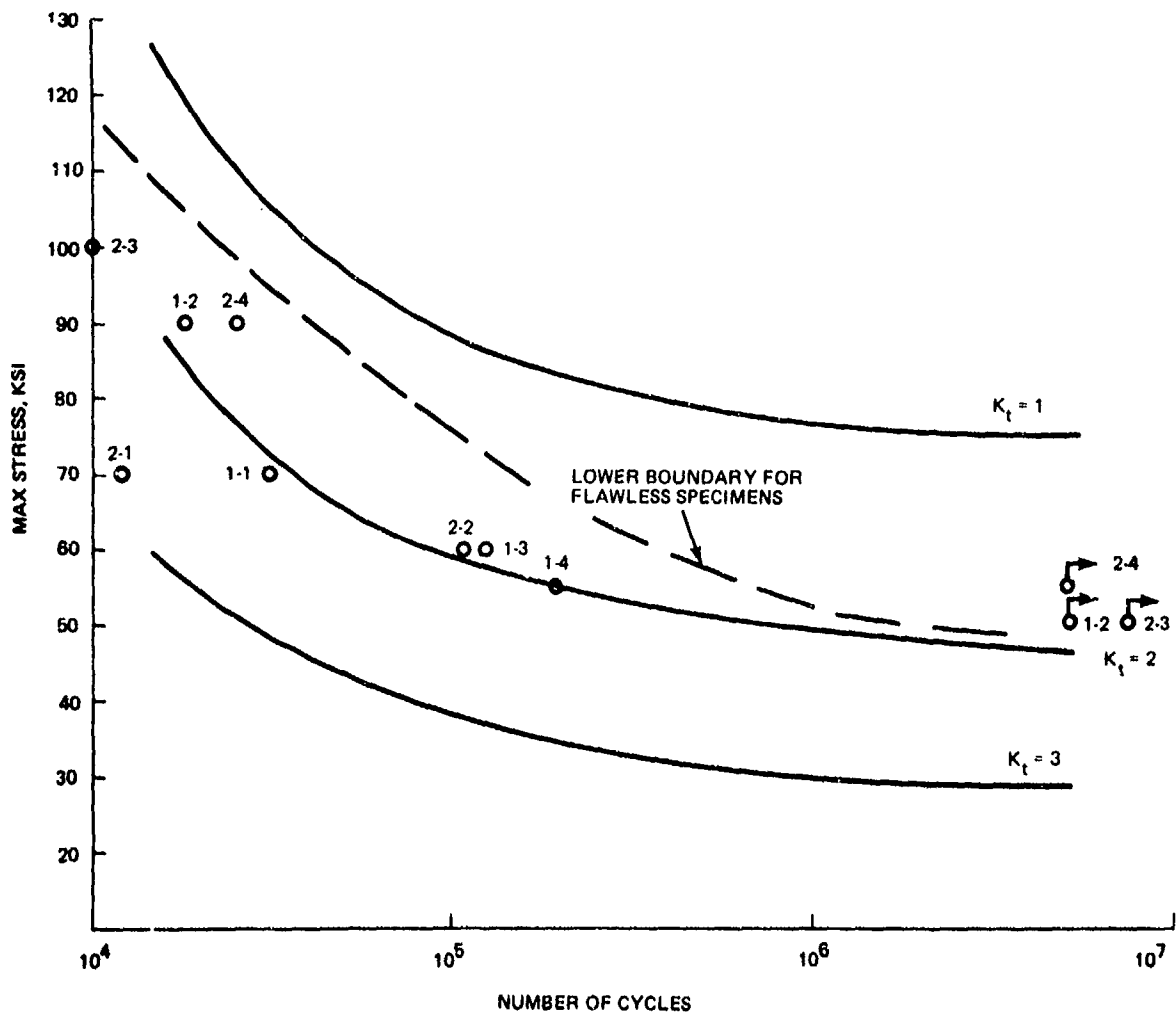


Figure 72. Fatigue Endurance of 0.25-Inch-Thick GTA Welds With Minor Underfills

range, except for Specimen 2-1. In all weldments, the failures initiated at the root of the weld as shown in Figure 71. A typical linear failure initiation along radii of the root reinforcement is shown in Figure 73.

## G. MINOR UNDERCUT, 0.080-INCH-THICK WELDS

### a. Fabrication of Experimental Welds

Very shallow (about 0.005 inch deep) undercuts could be produced by lowering the wire feed rate from 35 to 20 inches per minute. The contour of a typical weld produced by this technique is shown in Figure 74. It is evident that in addition to producing shallow face undercuts, a 0.015-inch-high and approximately 0.25-inch-wide reinforcement was produced at the root side of the weld. Pre-test radiography failed to reveal indications of external or internal defects.

### b. Evaluation of Fatigue Data

Fatigue endurance data for experimental welds are plotted in Figure 75. All points fell within the  $K_t = 1$  to  $K_t = 2$  range for the base material, and most of them were in close proximity to the lower boundary for machined flawless specimens. Fractography failed to indicate the reason for the somewhat lower fatigue endurance exhibited by Specimen 11-1. The failure initiated at either face undercuts or root reinforcement radii. There was no apparent correlation between the location of failure initiation sites and fatigue characteristics.

## 1. 0.25-INCH-THICK WELDS

### a. Fabrication of Experimental Welds

Undercuts were produced in 0.25-inch-thick GTA welds by increasing the torch travel speed on the second pass from 8 to 14 inches per minute and simultaneously increasing the arc current from 250 to 300 amperes. Figure 76 shows a typical weld contour obtained by these techniques. The only exception was Specimen 4-1 whose contour is shown in Figure 77. The presence of undercuts was verified by pre-test radiography; no internal defects were indicated. The depth of a typical undercut shown in Figure 76 was 0.010 inch and its width was 0.125 inch. Corresponding values for Specimen 4-1 were 0.020 and 0.125 inch. The height of a typical root crown was 0.050 inch and its width 0.25 inch. Corresponding values for Specimen 4-1 were 0.090 inch and 0.40 inch.

### 2. Evaluation of Fatigue Data

Fatigue endurance values for experimental welds are plotted in Figure 78. All data points were in close proximity to the  $K_t = 3$  curve. Deviation of the weld contour in Specimen 4-1 from that of a typical weld did not result in a significant decrease in its fatigue endurance. Failure initiated in all specimens at the root of the weld in locations indicated in Figure 76. In Specimen 4-1, a secondary initiation site was also detected at one of the face undercuts.

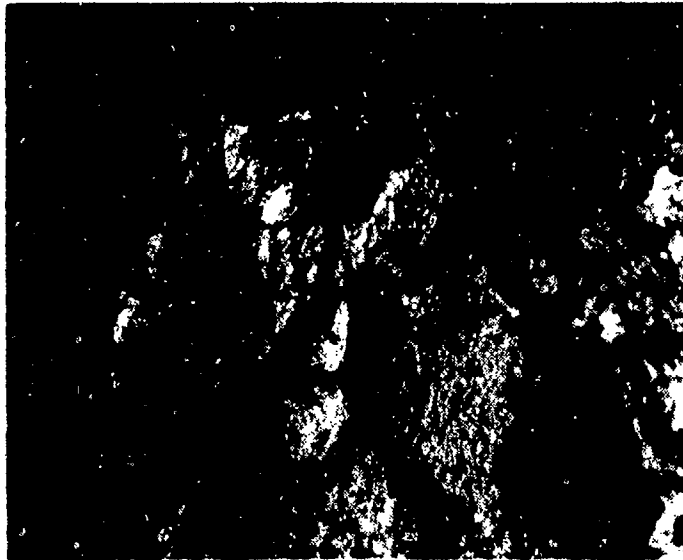


**Figure 73. Typical Linear (Root) Initiation Site in 0.25-Inch-Thick GTA Specimen with Minor Underfills (20X MAG)**

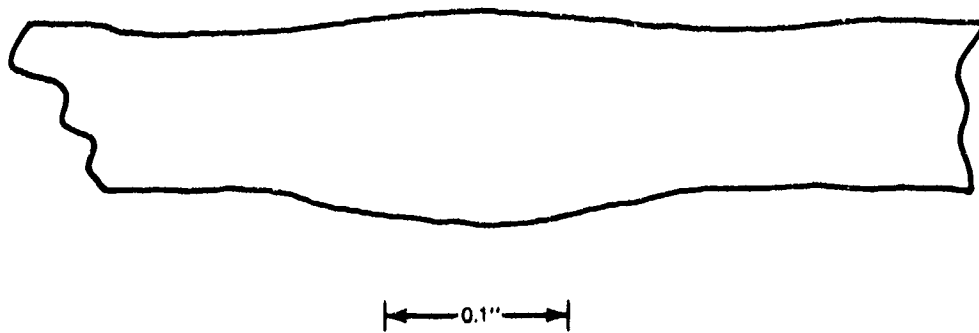


**Figure 74. Typical Contour of 0.080-Inch-Thick GTA Welds with Very Minor Undercuts**

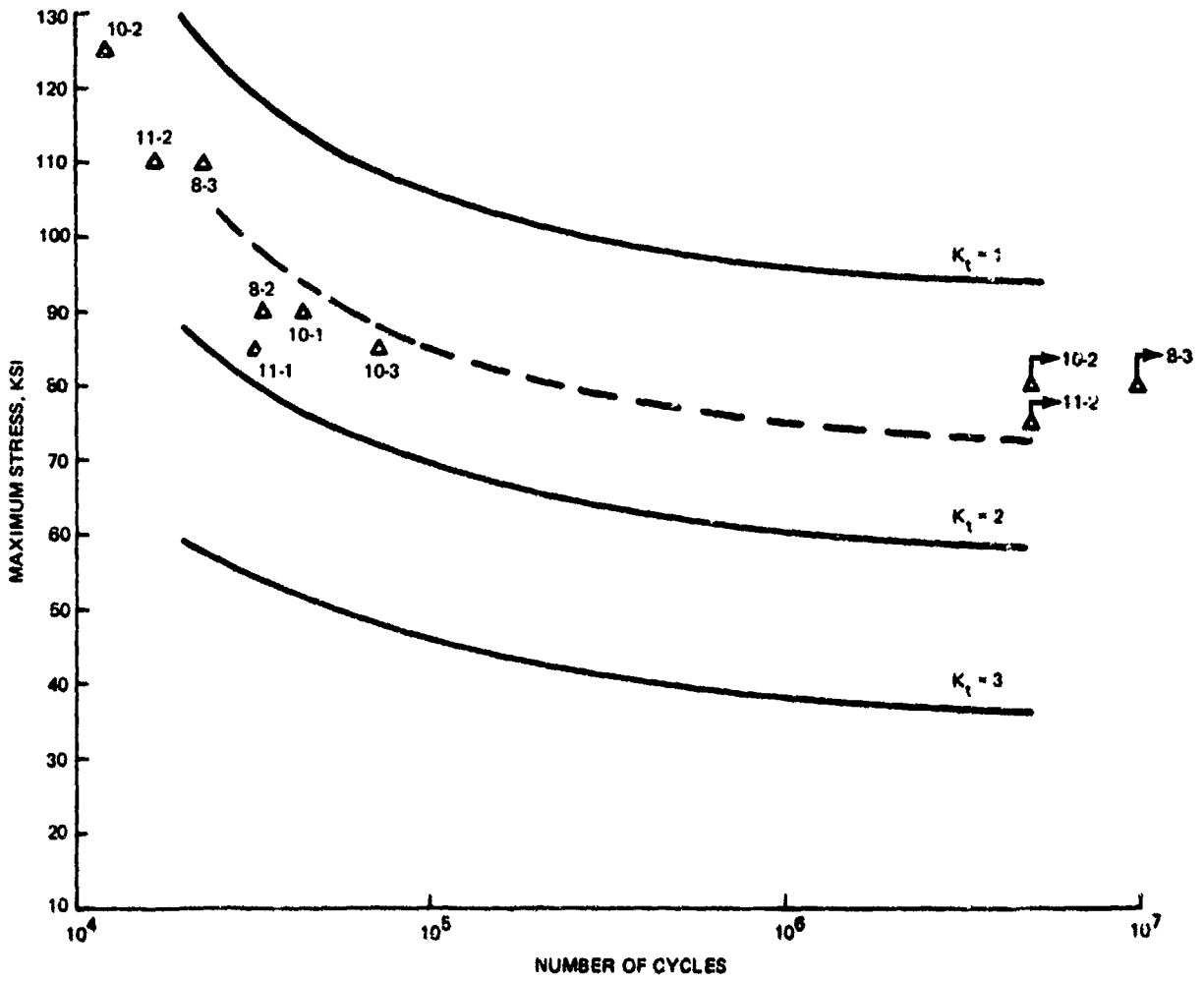


Figure 75. Fatigue Endurance of 0.080-Inch-Thick GTA Welds With Minor Undercuts

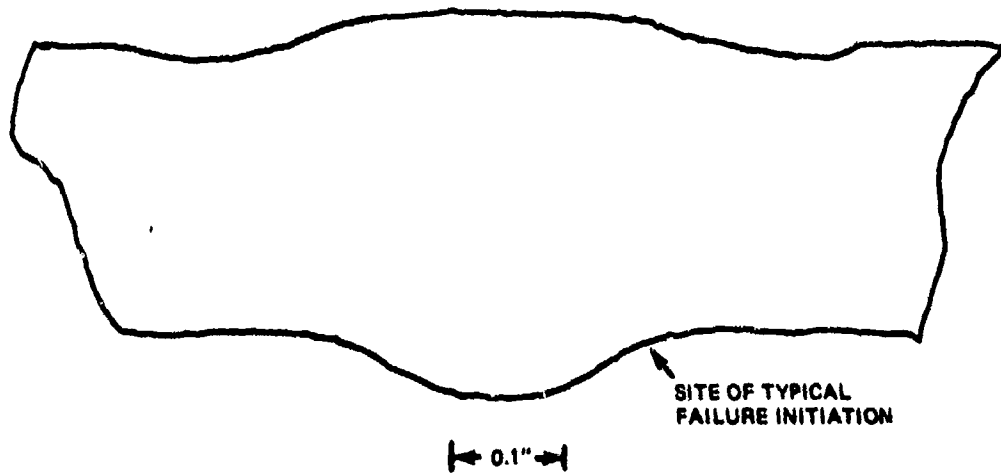


Figure 76. Typical Contour of 0.25-Inch-Thick GTA Welds with Intentional Undercuts

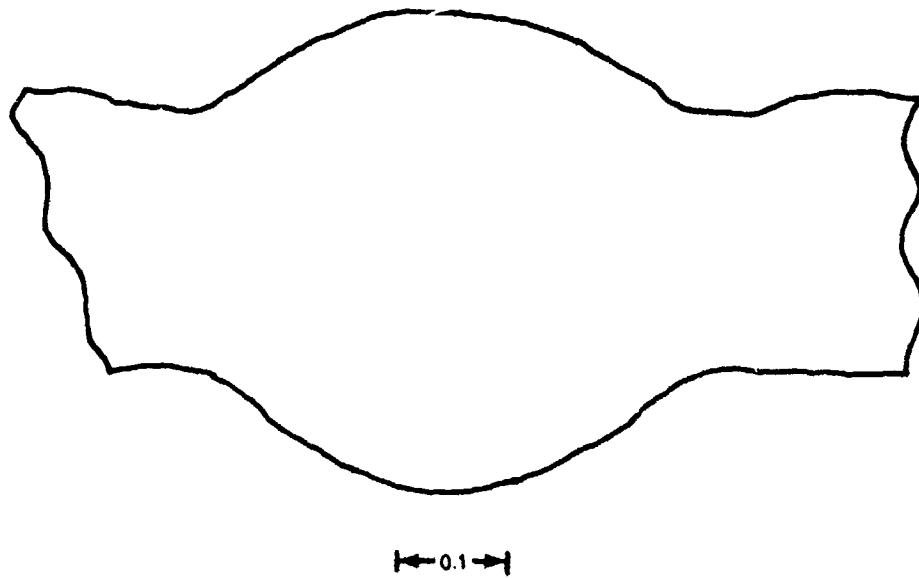


Figure 77. Contour of 0.25-Inch-Thick GTA Welded Specimen 4-1 with Intentional Undercuts

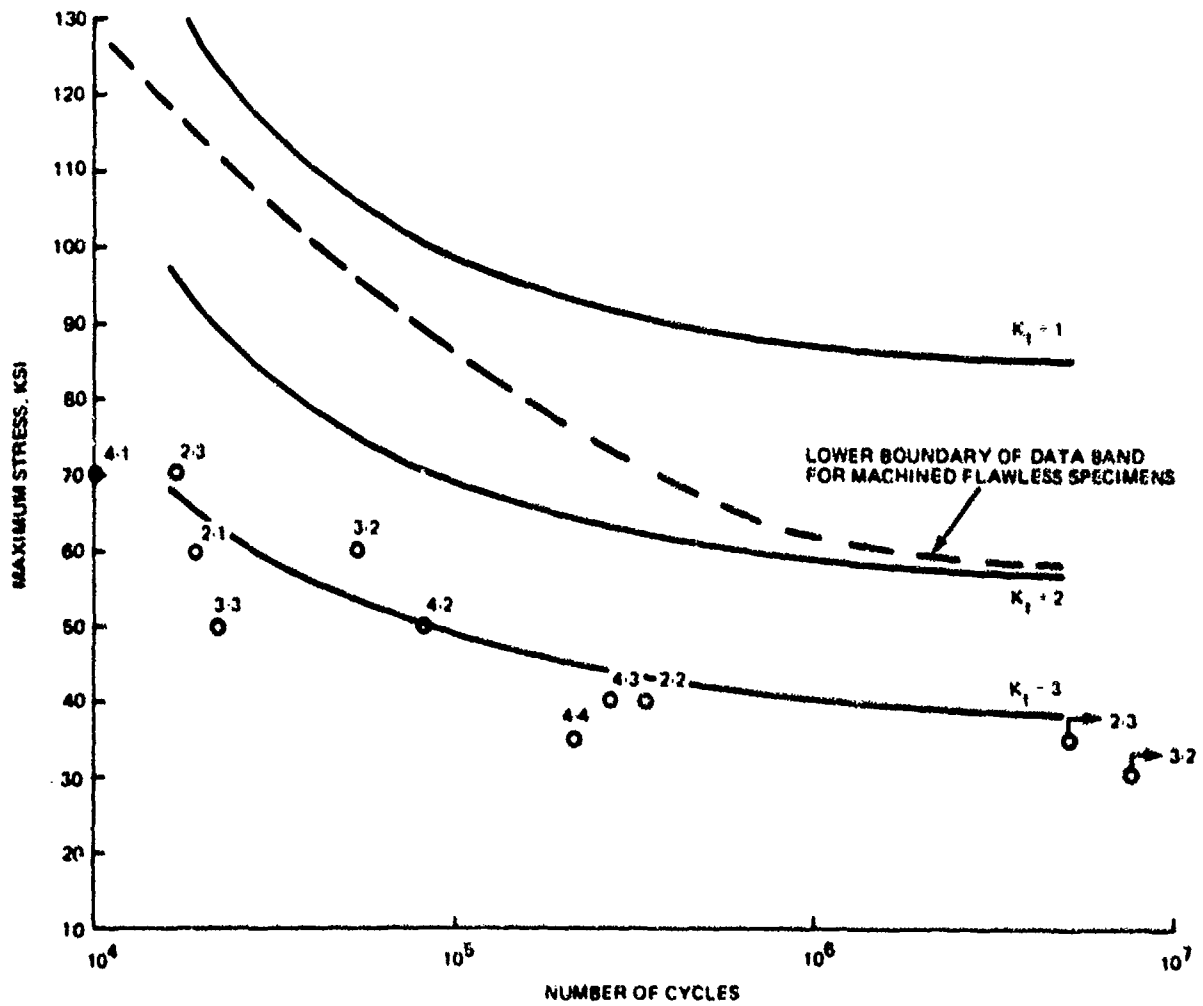


Figure 78. Fatigue Endurance of 0.25-Inch-Thick GTA Welds With Intentional Minor Undercuts

## H. TUNGSTEN INCLUSIONS IN GTA WELDS

### 1. Fabrication of Experimental Welds

Welds containing tungsten inclusions were prepared in three passes. The first was a mechanized, shallow root pass without the use of filler wire. The second was a manual pass in the course of which tungsten inclusions were melted in. The third was a final, mechanized pass utilizing filler wire. Contours of 0.080-inch-thick welds were machined flush with the base metal and the presence of tungsten was confirmed in all welds by pre-test radiography. Data on radiographic findings are included in Appendix B, Table B-5.

### 2. Evaluation of Fatigue Data

#### a. 0.080-Inch-Thick Welds

Fatigue endurance data for experimental welds are plotted in Figure 79. Also shown are  $K_t = 1, 2,$  and  $3$  curves for the base metal. It is evident that the data fall into two distinct groups: (1) Specimens 6-1, -2 and -3 with fatigue endurance values slightly below the lower boundary of the data band for machined flawless specimens, and (2) Specimens 4-1, -2 and -3 and 5-1 and -2 in the proximity of the  $K_t = 3$  curve. Fractographic evaluation of failed surfaces in the first group of specimens established the presence of internal inclusions as shown in Figure 80. In specimens with fatigue endurance in the proximity of the  $K_t = 3$  curve, tungsten inclusions were exposed to the surface as shown in Figures 81 and 82. Approximate dimensions of inclusions, as determined by measurements or radiographic films, varied from 0.100 x 0.050 inch to 0.025 x 0.015 inch in the first group and from 0.150 x 0.100 inch to 0.050 x 0.055 inch for the second group of specimens. No correlations between inclusion size variation and fatigue endurance were readily detectable. Data on pre-test radiographic evaluations, fatigue endurance and fractographic studies are included in Appendix B, Table B-5.

#### b. 0.25-Inch-Thick GTA Welds

A typical contour of 0.25-inch-thick GTA welds prepared in the course of this study is shown in Figure 83. Fatigue endurance values of these specimens are plotted in Figure 84. The data points fell in close proximity to the  $K_t = 3$  curve and were thus comparable to those of the 0.25-inch-thick GTA welds with minor reinforcements as shown in Figure 67. In all welds, the failure initiated at the root in locations designated in Figure 83. Examination of fractured surfaces failed to detect the presence of inclusions. Accordingly, it appears that the weld contour was the limiting factor as far as fatigue endurance is concerned. Figure 85 shows a typical linear failure initiation which occurred at the root of the weld.

## I. MISMATCH

### 1. Fabrication of Experimental Welds

Welds with intentionally mismatched faying surfaces, were produced by inserting 0.015 or 0.025-inch-thick shims under one of the welding blank halves to be joined. Representative profiles of welds obtained by these techniques were documented using images on optical comparators at 10X magnification (see Figures 86 and 87).

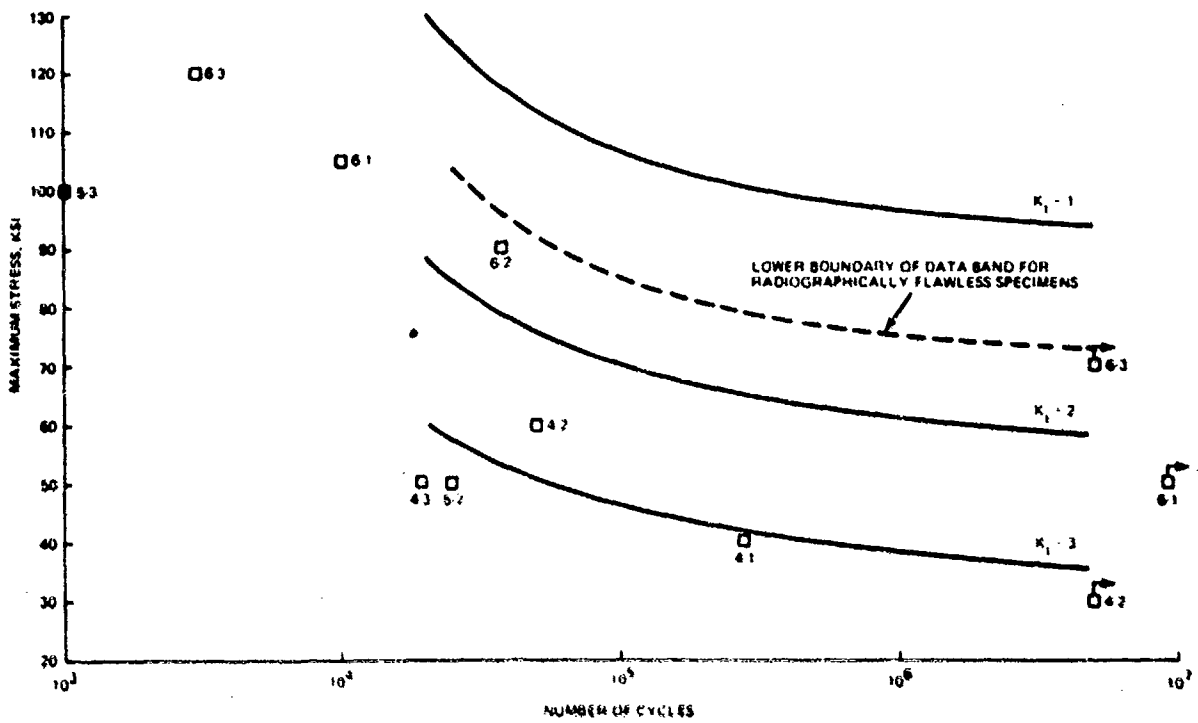


Figure 78. Fatigue Endurance of 0.080-Inch-Thick GTA Welds with Tungsten Inclusions



Figure 80. Internal Tungsten Inclusion Intentionally Produced in a 0.080-Inch-Thick GTA Weld (20X MAG)



**Figure 81. Surface-Exposed Tungsten Inclusion in 0.080-Inch-Thick GTA Weld (20X MAG)**



**Figure 82. Surface View of a Tungsten Inclusion in a 0.080-Inch-Thick GTA Weld (20X MAG)**

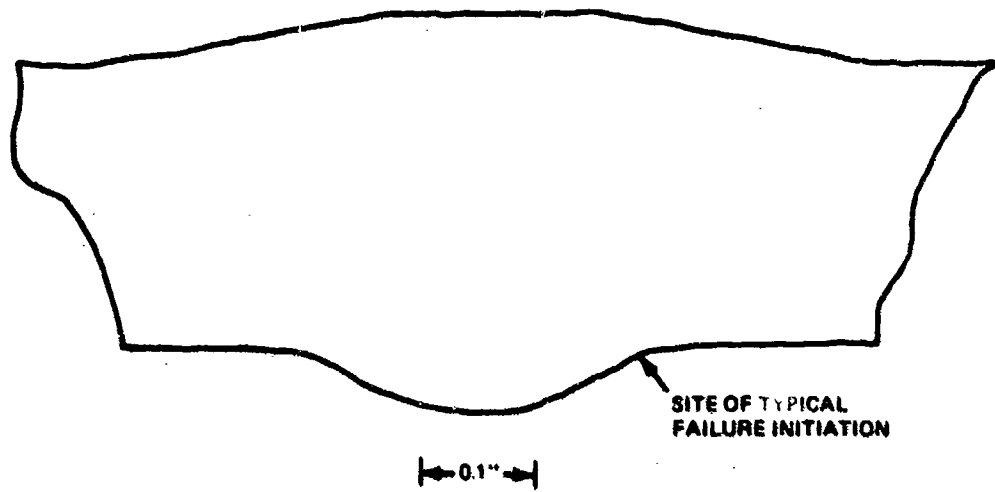


Figure 83. Typical Contour of 0.25-Inch-Thick GTA Welds Containing Inclusions

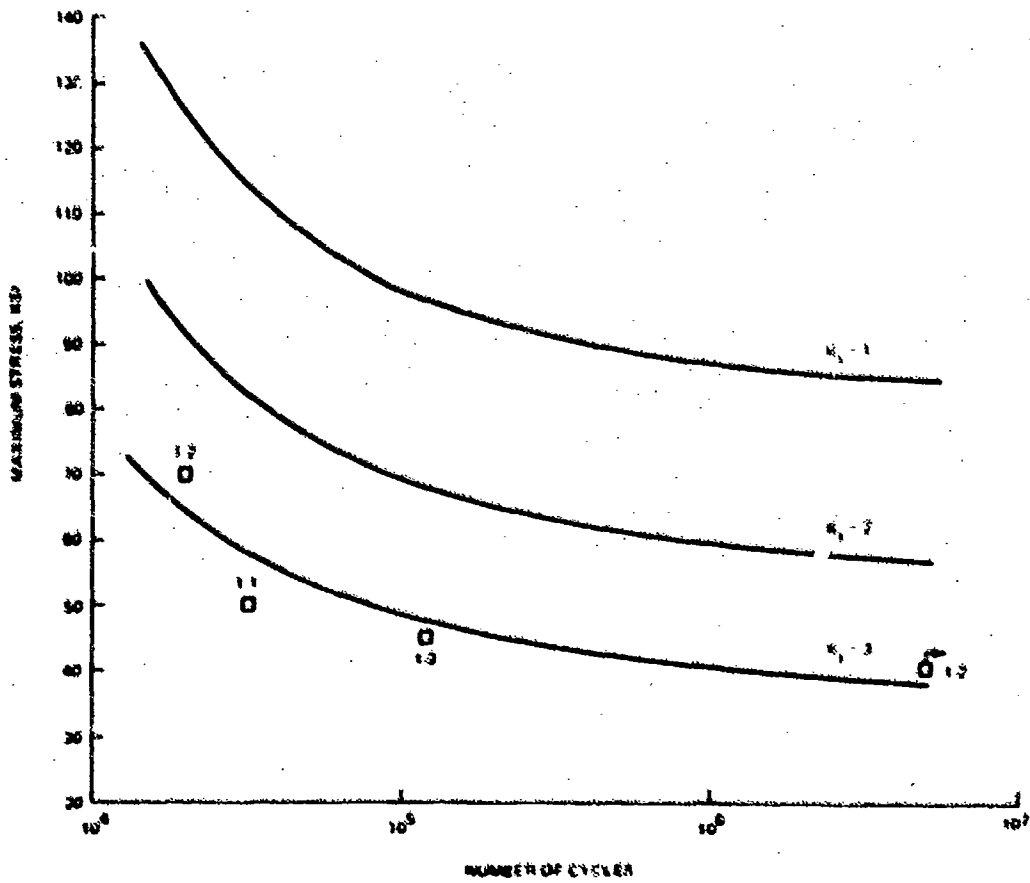
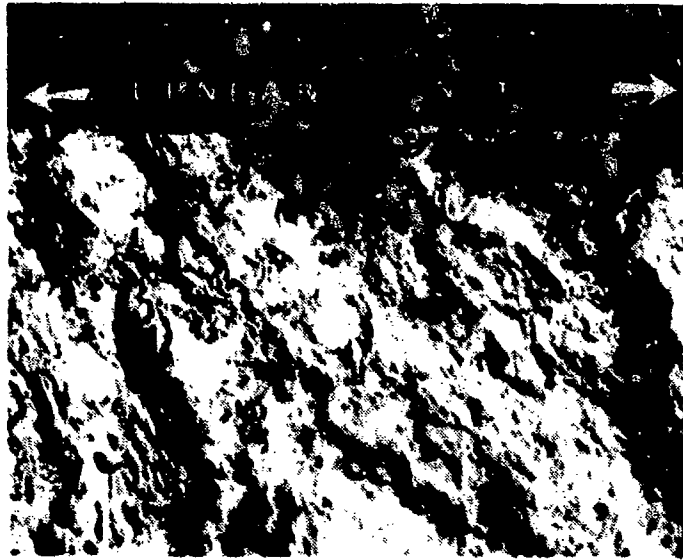
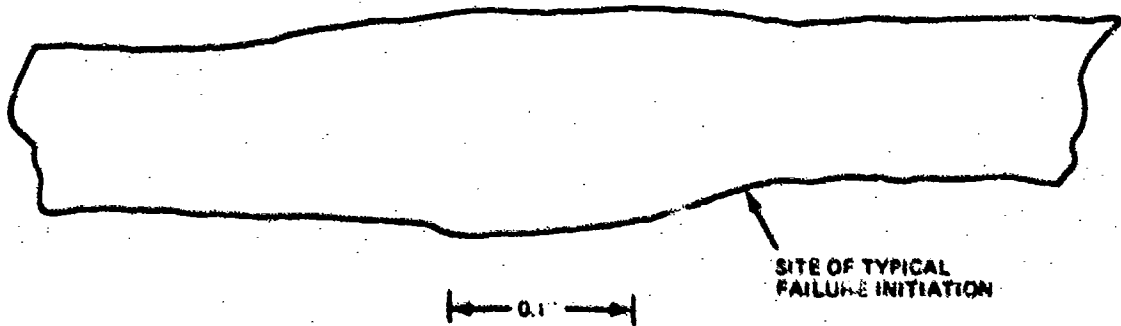


Figure 84. Fatigue Endurance of Contoured 0.25-Inch-Thick DTA Welds Containing Tungsten Inclusions



**Figure 85. Linear Failure Initiation at the Root of a 0.25-Inch-Thick GTA Weld Containing Tungsten Inclusions (No Inclusions were detected on Fracture Surfaces) (20X MAG)**



**Figure 86. Typical Contour of 0.080-Inch-Thick GTA Welds With 0.015-Inch Mismatch of Faying Surfaces**

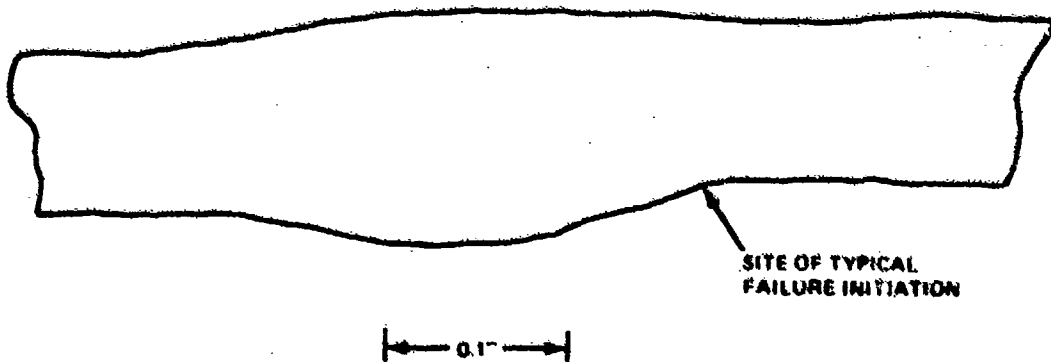


**Figure 87. Typical Contour of 0.080-Inch-Thick GTA Welds With 0.025-Inch Mismatch of Faying Surfaces**

Pre-test radiography showed that the reduced sections of test specimens were free of internal defects.

b. Evaluation of Fatigue Data

Fatigue endurance results for experimental welds are plotted in Figure 88. No significant variations were apparent in the fatigue endurance of specimens with 0.015-inch mismatch (Specimen 1-1, -2 and -3) and 0.025-inch mismatch (Specimen 4-1, 5-1, -2, -3, and -4). All data points fell in the  $K_t = 2$  to  $K_t = 3$  range. Failures initiated in all specimens at the root of the weld in locations indicated in Figures 85 and 86. Figure 89 illustrates a typical failure initiation site at the root of the weld.

2. MISMATCHED - 0.25-INCH-THICK WELDS

a. Fabrication of Experimental Welds

Welds with intentionally mismatched faying surfaces were produced by inserting 0.010 and 0.036-inch-thick shims under one of the halves of the welding blank to be joined. Typical profiles of welds produced by these techniques were recorded by tracing their images on an optical comparator at 10X magnification (see Figures 90 and 91).

b. Evaluation of Fatigue Data

Fatigue endurance data for experimental welds are plotted in Figure 92. A significant difference could be detected in the fatigue characteristics of specimens with 0.010-inch mismatch which were located above the  $K_t = 3$  curve and of specimens with 0.036-inch mismatch for which data points fell below the  $K_t = 3$  curve. Failure initiated in all specimens at the root of the weld in locations indicated in Figures 90 and 91. Figure 93 illustrates a typical linear failure initiation detected in mismatch-type welds. No porosity was detected in any of the failure surfaces except in Specimen 3-1 in which an isolated 0.003-inch pore was detected in the interior. The failure initiation was not related to this pore.

J. GTA WELDS PRODUCED UNDER INTENTIONALLY INADEQUATE SHIELDING CONDITIONS

1. .080-INCH-THICK WELDS

a. Fabrication of Experimental Welds

Three experimental welds were produced utilizing the following deviations from conventional shielding parameters: Weld No. 1. The flow of torch shielding gas (argon) was reduced from 60 to 30 cubic feet per hour and the trailing shield was completely eliminated; Weld No. 2. This weld was produced in two passes; in the first pass, the flow of torch shielding gas was reduced from 60 to 30 cubic feet per hour and the trailing shield was completely eliminated; and Weld No. 3. This weld was produced in three passes; the flow of trailing shield gas (argon) varied from 20 cubic feet per hour to none to 60 cubic feet per hour in the first, second and third passes, respectively. Typical contours of specimens machined from these welds are shown in Figures 94, 95 and 96. These contours were recorded utilizing optical comparator images at 10X magnification. Pre-test radiography indicated no internal defects in any of the specimens. The color of the weld beads produced under inadequate shielding condition varied from light or medium blue to gray.

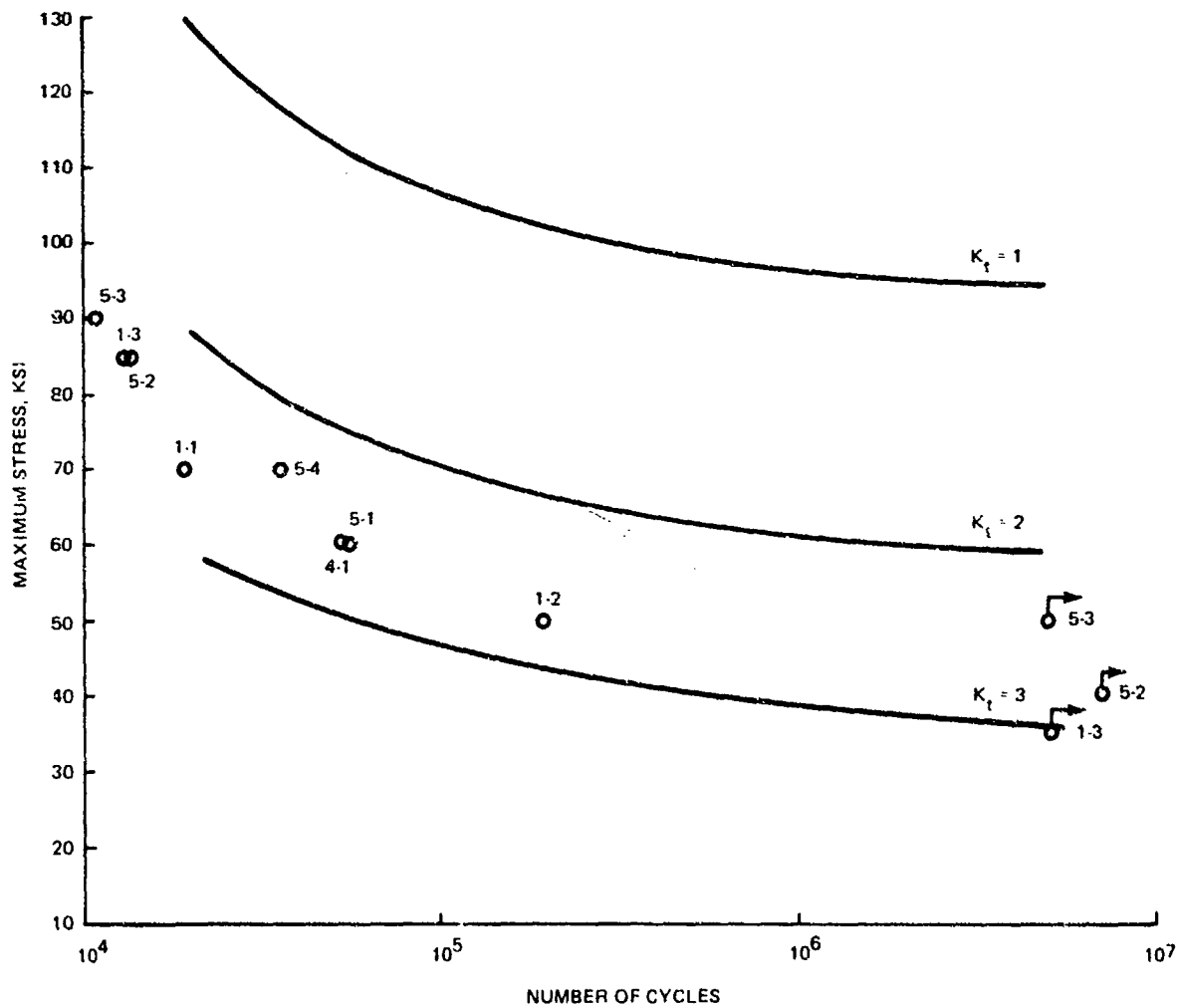
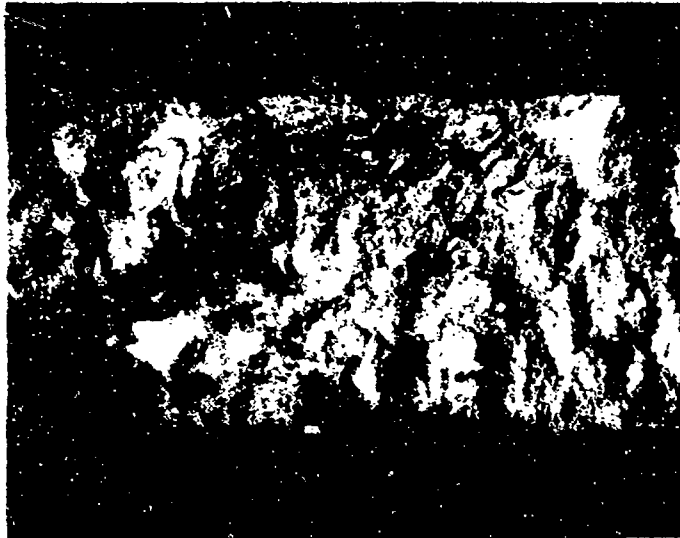
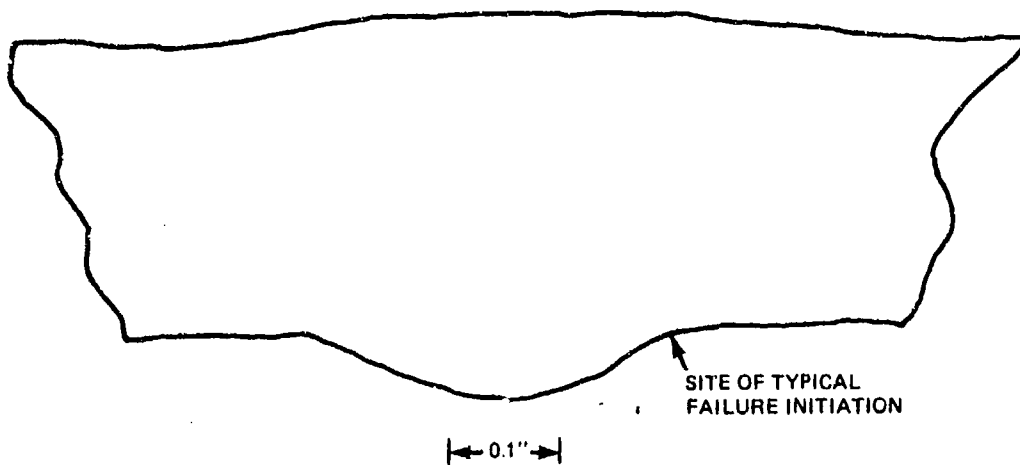


Figure 88. Fatigue Endurance of 0.080-Inch-Thick GTA Welds With Mismatched Faying Surfaces



**Figure 89. Typical Failure Initiation Site at the Root of a 0.080-Inch-Thick GTA-Welded Specimen With Mismatched Faying Surfaces (20X MAG)**



**Figure 90. Typical Contour of 0.025-Inch-Thick GTA Weld With 0.010-Inch Mismatch**

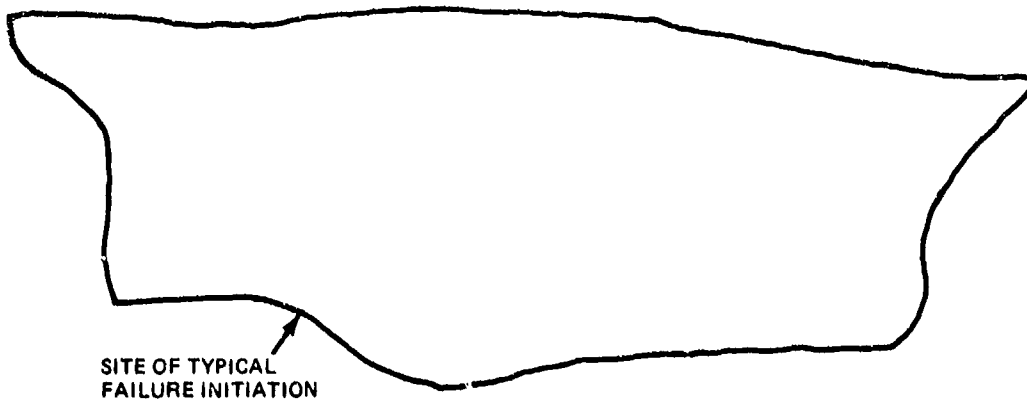


**Figure 91. Typical Contour of 0.25-Inch-Thick GTA Weld With 0.036-Inch Mismatch**

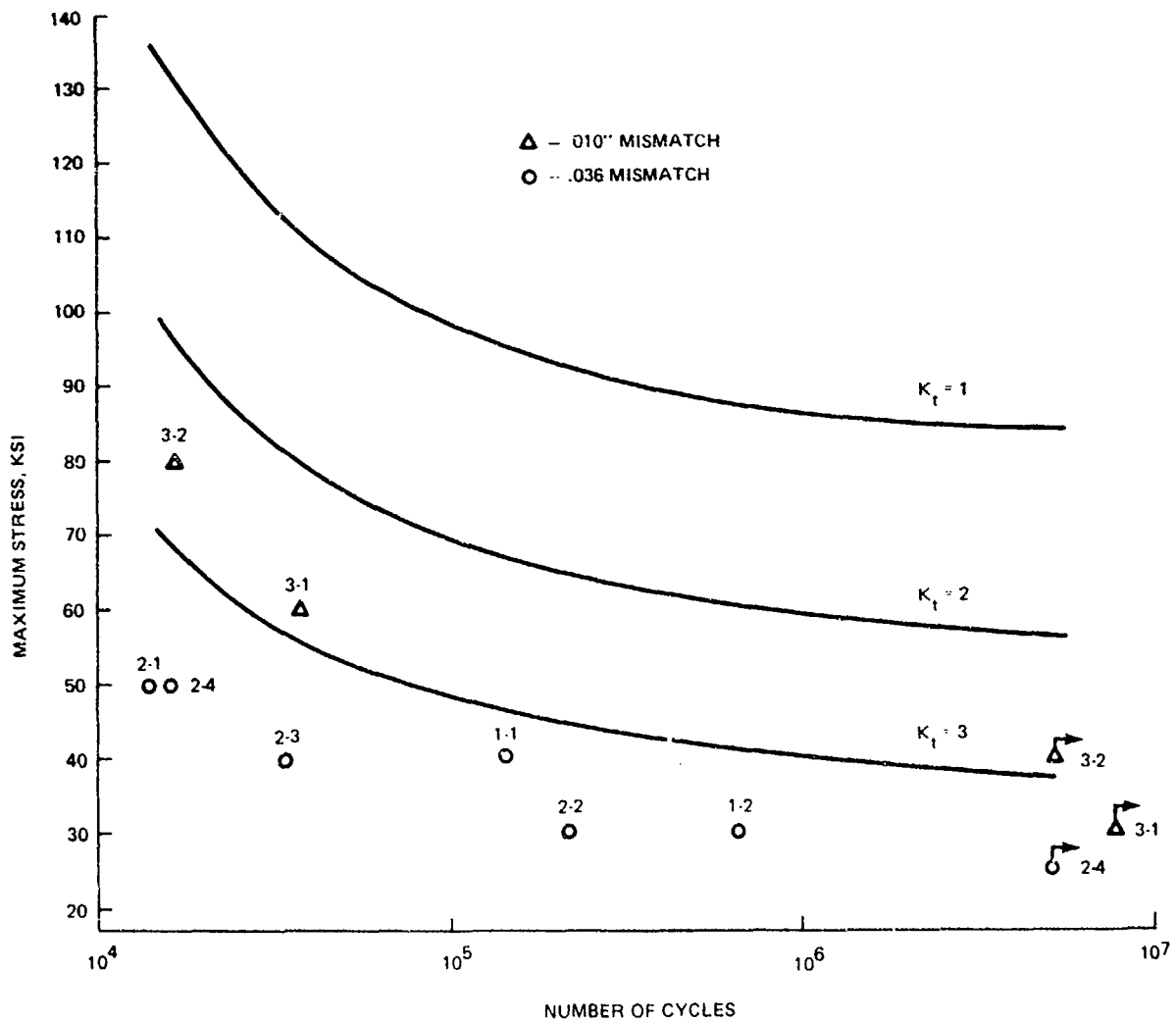
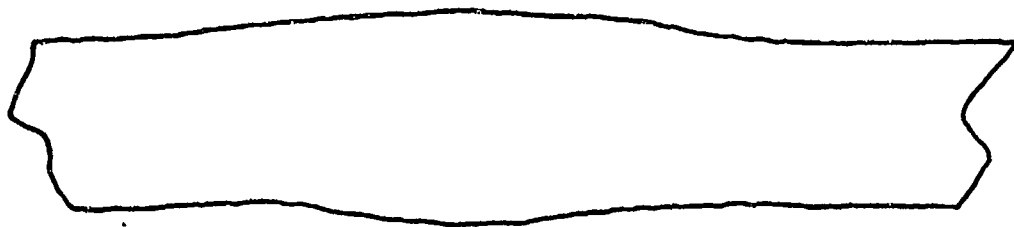


Figure 92. Fatigue Endurance of .25-Inch GTA Specimens With Mismatched Faying Surfaces

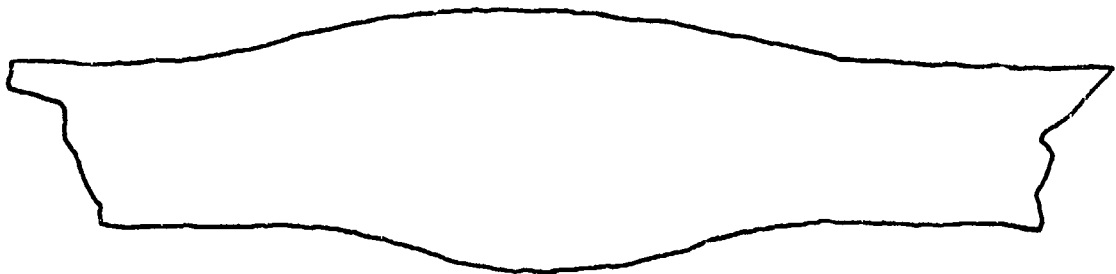


Figure 93. Typical Linear (Root) Surface Failure Initiation in 0.25-Inch-Thick GTA Welds with Mismatched Faying Surfaces (20X MAG)



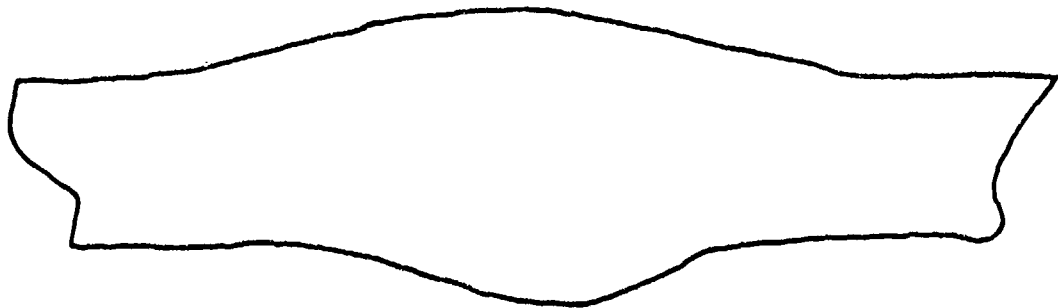
← 0.1" →

**Figure 94. Typical Contour of 0.080-Inch-Thick GTA Weld No. 1 Produced Under Inadequate Shielding Conditions**



← 0.1" →

**Figure 95. Typical Contour of 0.080-Inch-Thick GTA Weld No. 2 Produced Under Inadequate Shielding Conditions**



← 0.1" →

**Figure 96. Typical Contour of 0.080-Inch-Thick GTA Weld No. 3 Produced Under Inadequate Shielding Conditions**

## b. Evaluation of Fatigue Data

Fatigue endurance data for specimens machined from experimental welds are plotted in Figure 97. All data points fell either at the lower boundary of the data band for machined flawless weldments or were located between this boundary and the  $K_t = 2$  curve. The values obtained were very close to those obtained for specimens welded by conventional processes (see Figure 64). Since microhardness surveys indicated no significant hardness deviations within the weld, it appears that variation of the shielding parameters did not result in significant contamination of the weldments.

### 2. 0.25-INCH-THICK WELDS

#### a. Fabrication of Experimental Welds

The experimental welds were produced by eliminating (on the second pass) the trailing shield (helium) flow in welding blanks No. 1, 3 and 4, and by reducing helium flow from 60 to 5 cubic feet per hour in welding Blank No. 2. The remaining parameters were identical to those utilized in conventional welding. A typical contour of specimens produced by these techniques is shown in Figure 98. Pre-test radiography indicated no defects in specimens machined from Blanks No. 1, 2 and 4. Blank No. 3 was shown to have several transverse cracks; specimens machined from this blank will be discussed in Paragraph K. The color of the weldments produced without the trailing shield varied from light and medium blue to gray. A reduction of the trailing shield gas flow from 60 to 5 cubic feet per hour resulted in discoloration (gray) of both ends of the weldment.

#### b. Evaluation of Fatigue Data

Fatigue endurance data are plotted in Figure 99. The data points fell either at the  $K_t = 3$  curve or in the lower portion of the  $K_t = 2$  to  $K_t = 3$  range and were thus comparable to the fatigue characteristics of specimens with minor reinforcements produced by conventional welding techniques, that is, without intentional contamination (see Figure 67). The failure initiated in all specimens at the root in locations indicated in Figure 98. In Specimen No. 2-4, a secondary failure initiation was detected at a 0.004-inch-diameter pore 0.025 inch from the surface.

### K. 0.25-INCH-THICK GTA WELDS CONTAINING TRANSVERSE CRACKS

#### 1. Fabrication of Experimental Welds

As described in Section III, attempts to initiate cracks by welding under conditions of severe restraints were not successful. Transverse cracks were detected, however, in Weld No. 3 produced under intentionally inadequate shielding conditions, as described in Paragraph I. The visual indications of these cracks are shown in Figure 100. The presence of cracks was confirmed by pre-test radiography. Specimens 1-1 and 1-2 were machined from Weld No. 3 so as to include transverse cracks in the test section of one specimen. Specimen 1-3 was machined from that portion of the weld which did not exhibit any visual or radiographic indications. Contours of the specimens were left intact in the course of machining.

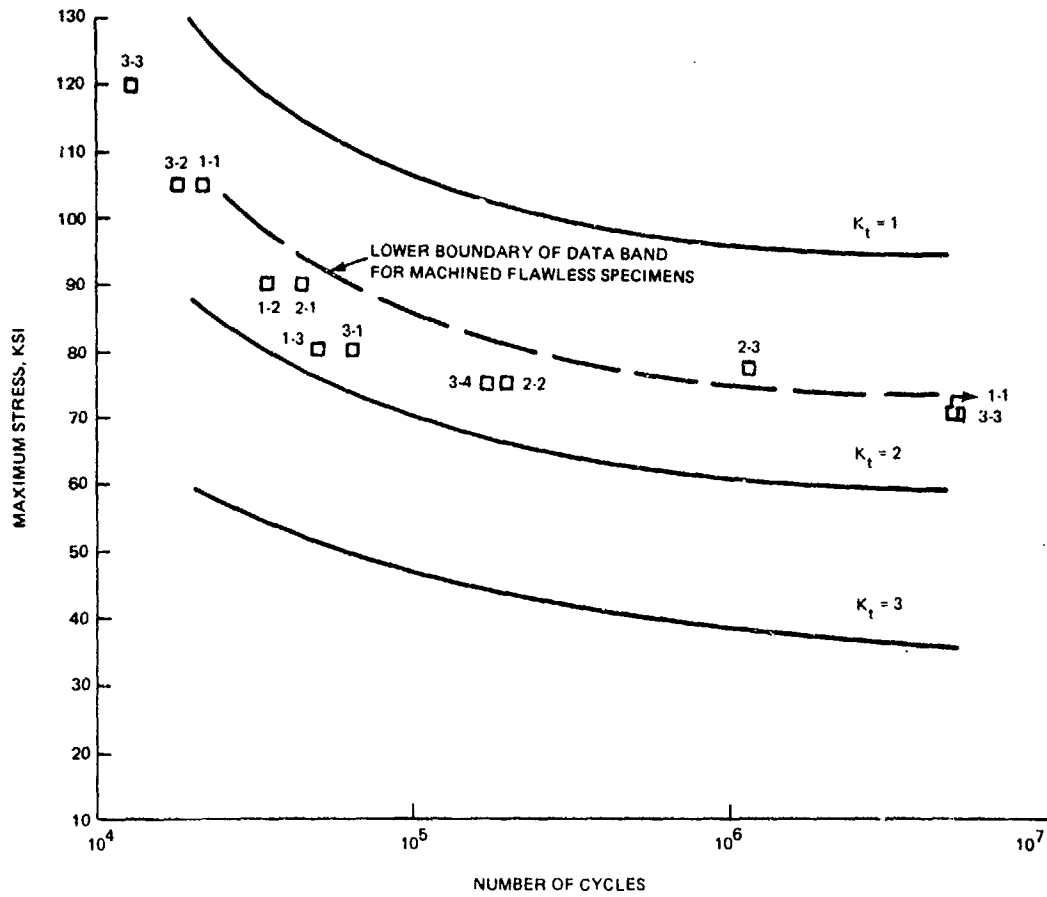


Figure 97. Fatigue Endurance of 0.080-Inch-Thick GTA Weldments Produced Under Inadequate Shielding Conditions

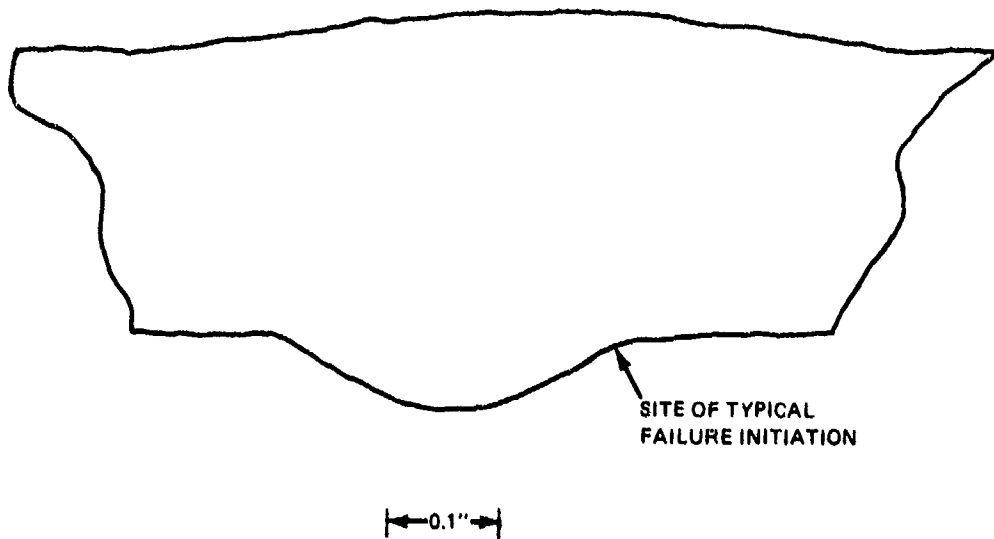


Figure 98. Typical Contour of 0.25-Inch-Thick GTA Welds Produced Under Intentionally Inadequate Shielding Conditions

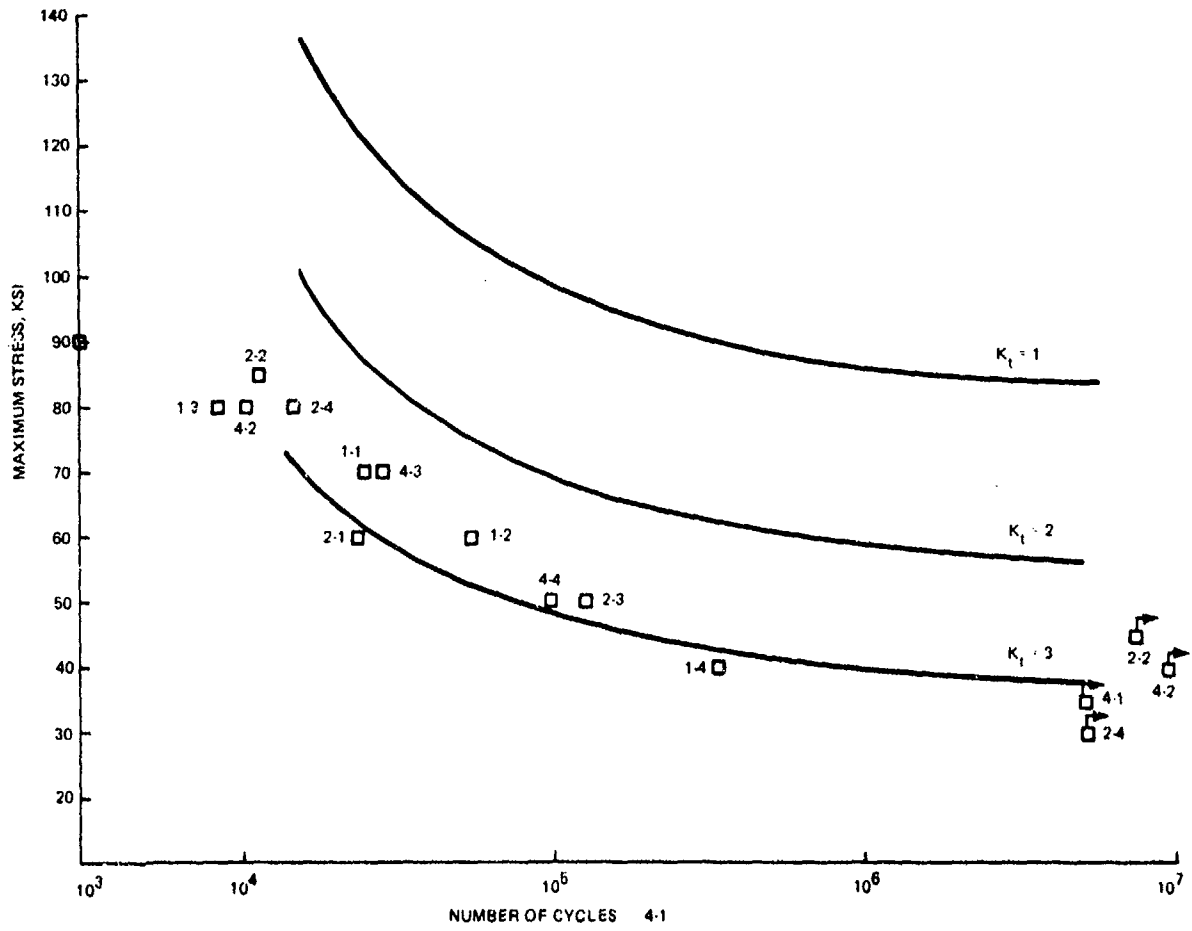
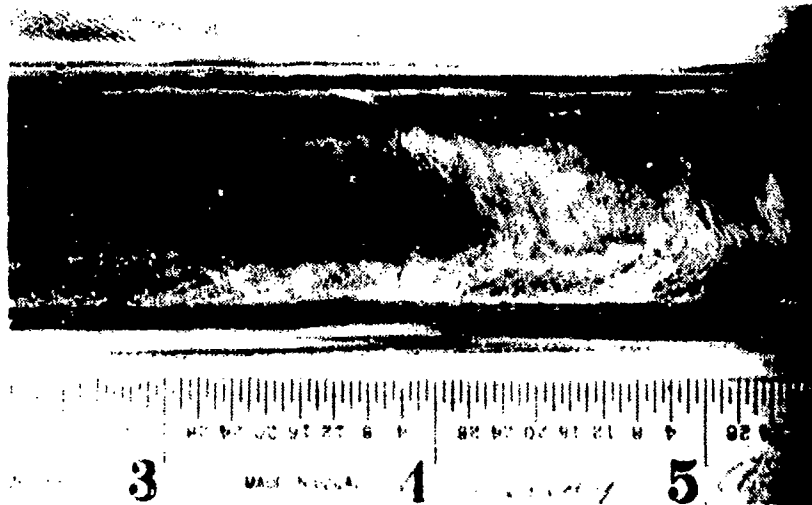
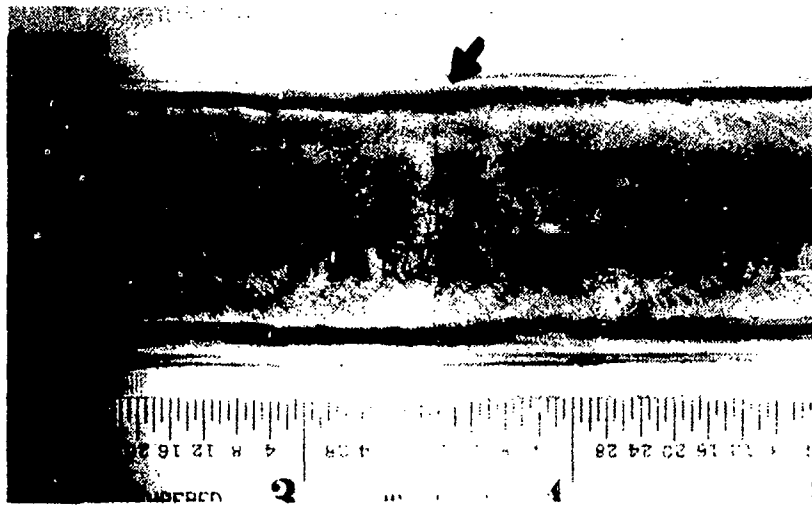


Figure 99. Fatigue Endurance of 0.25-Inch-Thick GTA Weldments Produced Under Inadequate Shielding Conditions



**Figure 100. Transverse Cracks Detected in 0.25-Inch-Thick GTA-Weld No. 3 Produced under Intentionally Inadequate Shielding Conditions (Arrow Indicates a Typical Failure Initiation Site.)**

The oxygen content of the weld metal was found to be 2514-ppm and 1390-ppm for Specimens 1-1 and 1-2, respectively. Corresponding values for nitrogen were found to be 1731-ppm and 114-ppm for Specimens 1-1 and 1-2, respectively. A micro-hardness survey conducted on the transverse section of Specimen 1-1 indicated that the hardness of the metal deposited during the second pass was in the 39 to 43.5 Rc range, that is, significantly higher than that of the metal deposited on the first pass.

## 2. Evaluation of Fatigue Data

All data points fell below the  $K_t = 3$  curve. In Specimens 1-1 and 1-2, failure initiated at the transverse cracks on the face of the weld in the locations shown in Figures 100 and 101.

## L. GTA-REPAIRED 0.25-INCH-THICK ELECTRON-BEAM WELDS

### 1. Fabrication of Experimental Welds

The face portions of EB welds containing external imperfections were machined to remove weld metal down to one half of the original weld thickness and rewelded by both manual and mechanized GTA techniques utilizing four and two passes, respectively. Filler wire was utilized in both repair processes. After repair welding, both the face and root of the weld were machined flush with the surface. Radiography of the repaired welds indicated that all welds were free of internal defects.

### 2. Evaluation of Fatigue Data

Fatigue data for repaired weldments are plotted in Figure 102. There is no significant difference in fatigue endurance of welds repaired by manual and mechanized GTA welding techniques. All data points fell into the lower portion of the  $K_t = 1$  to  $K_t = 2$  range. Fractographic examination established that in all but one case (Specimen 2-3), failure initiated on the root side or EB-welded surface of the weld, and in all cases, isolated pores in the 0.001 to 0.002-inch range were detected at the initiation sites. In Specimen 2-3, failure initiated at an isolated 0.003-inch pore 0.020 inch from the rootside surface. An interesting observation was made in the course of preliminary studies designed to establish suitable repair parameters: a porosity-containing EB weld was machined to remove about three-fourths of the weld metal, rewelded using mechanized GTA techniques, and tested at 80 ksi (maximum) stress level. The specimen failed at 3,000 cycles. Fractographic examination of the failed surfaces detected very fine (less than 0.001 inch) porosity throughout the remaining portion of the EB weld. A considerable agglomeration of porosity occurred, however, at the EB/GTA weld interface as shown in Figure 103. This finding suggests that caution should be exercised when attempting to apply the GTA welding process to repairs of internal porosity in EB welds, since fine porosity which may remain in the weld and may not be detected on pre-repair radiography, can agglomerate at the interface between the original and repair welds, and cause a significant decrease in fatigue endurance.



**Figure 101. Failure Initiation Site in Specimen No. 1-2  
Containing Transverse Cracks (20X MAG)**

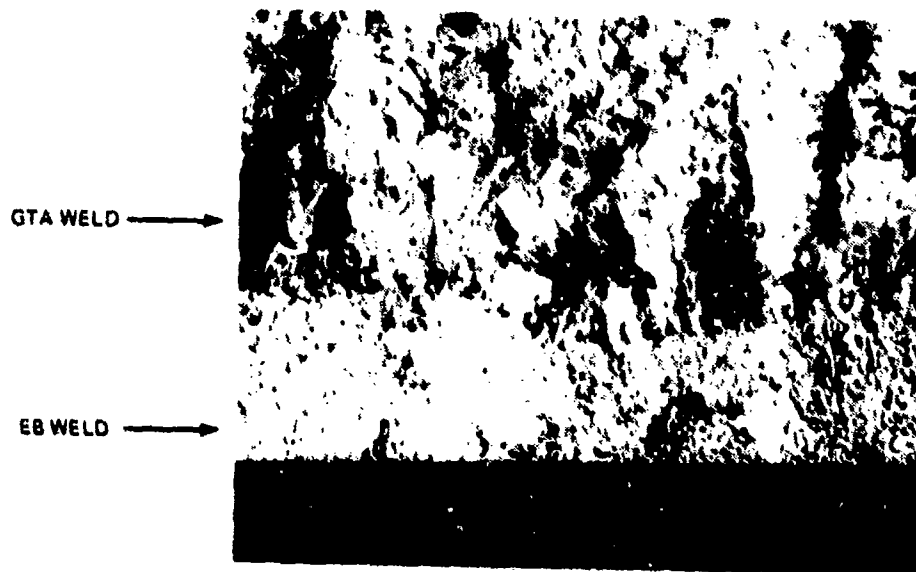


**Figure 103. Agglomeration of Porosity at EB/GTA Weld  
Interface Caused by Incomplete Removal of  
Porous EB Weld (20X MAG)**

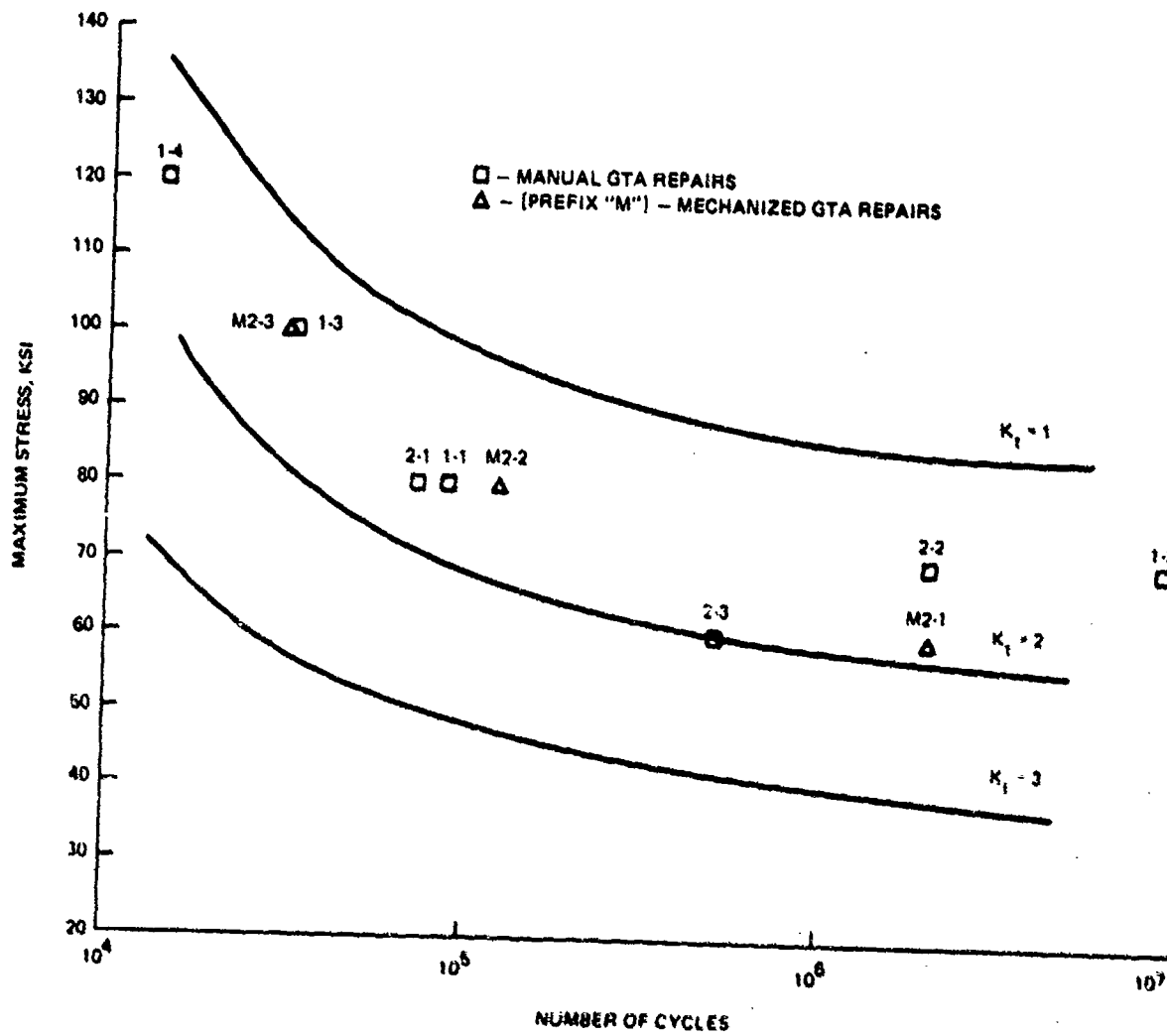


Figure 102. Fatigue Endurance of GTA-Repaired 0.25-Inch-Thick EB Welds

## M. SUMMARY

Fatigue endurance limits ( $10^6$  cycles) for transverse 0.080- and 0.25-inch-thick weldments were estimated to be 75 ksi and 62 ksi, respectively.

Porous 0.080-inch-thick weldments with fatigue endurance in  $K_t=1$  to  $K_t=2$  range exhibited, typically, failure initiation at isolated pores, .005 inch to .010 inch in diameter and 0.020 inch to 0.030 inch from the surface. Multiple failure initiation sites were frequently encountered in  $K_t=2$  to  $K_t=3$  range. Fatigue endurance data below the  $K_t=3$  range were associated with failure initiations at porosity clusters.

Porous 0.25-inch-thick welds with isolated internal porosity in the range of 0.005 to 0.020 inch in diameter exhibited fatigue endurance comparable to flawless specimens. Some initiation sites in the lower portion of the  $K_t=1$  to  $K_t=2$  range were associated with fine subsurface porosity rather than coarser pores in the interior. Frequent multiple-initiation sites were encountered in the  $K_t=2$  to  $K_t=3$  range. Below the  $K_t=3$  range, the failure initiation sites were, typically, associated with porosity clusters.

Fatigue data points for 0.080-inch-thick welds with minor face- and root-reinforcements was in the lower portion of the  $K_t=1$  to  $K_t=2$  range. 0.25-inch-thick weldments with minor face- and root-reinforcements exhibited fatigue endurance in the  $K_t=3$  range.

Minor underfills in 0.080- and 0.25-inch-thick weldments resulted in fatigue endurance in the range between the lower boundary of the flawless data band and  $K_t=2$  graph. Failure in 0.25-inch-thick specimens initiated at the root reinforcements. 0.080-inch-thick weldments with minor undercuts exhibited fatigue endurance in the proximity of the lower boundary for flawless specimens. Data points for 0.25-inch-thick weldments with similar defects were in a proximity of the  $K_t=3$  curve, and failures initiated at the root reinforcements.

Fatigue endurance of 0.080-inch-thick welds with internal tungsten inclusions was slightly below the data band for flawless specimens; inclusions exposed to the surface lowered fatigue endurance to the  $K_t=3$  range. 0.25-inch-thick welds with internal inclusions exhibited fatigue endurance in the  $K_t=3$  range; however, the failure initiated in all specimens at the contour of the weld.

Mismatch of faying surfaces resulted in drastic lowering of fatigue endurance in both 0.080- and 0.25-inch-thick weldments.

Weldments produced under inadequate shielding conditions exhibited considerable variations in fatigue endurance depending on the extent of (intentional) shielding deficiencies. Extensive deficiencies resulted in a substantial pickup of contaminants and formation of cracks.

Fatigue endurance of EB welds repaired by GTA techniques was in the lower portion of the  $K_t=1$  to  $K_t=2$  range.

## SECTION V

### FATIGUE CHARACTERISTICS OF ELECTRON BEAM (EB) WELDMENTS PHASE II

#### A. INTRODUCTION

This section presents data on fatigue endurance of flawless and (intentionally) defective EB weldments. The data are presented in the following sequence:

- Flawless welds
- Porous welds
- Mismatched welds
- Underfills
- Surface contamination
- Lack of penetration
- Bursts
- Summary

#### B. FLAWLESS WELDS

##### 1. Fabrication of Experimental Weldments (0.080 and 0.25-inch-Thick)

Flawless EB welds were produced to generate baseline data for use in evaluating defective welds. The welds were made in accordance with standard production techniques. Both root and face contours were machined flush with the base metal. Pretest radiography revealed no internal defects in any of the specimens.

##### 2. Fatigue Endurance of 0.080-Inch-Thick Flawless Welds

Experimental fatigue endurance values are plotted in Figure 104. Since the  $K_t=1$  curve was constructed based on average values obtained for the base metal, the scatter of data for flawless welds appears to be within the range expected for the parent material. Five of the specimens (3-2, 3-3, 1-3, 2-2 and 5-2) failed in the base metal. In some of the ten specimens which failed in the weld, fine (0.001 to 0.002-inch-diameter) isolated pores were detected at the initiation sites. Fatigue endurance and fractographic data are listed in Appendix B Table B-6. Figure 105 shows a typical surface failure initiation site encountered in flawless 0.080-inch-thick EB welded specimens.

##### 3. Fatigue Endurance of 0.25-Inch-Thick Flawless Welds

Data for flawless 0.25-inch-thick EB welded specimens are superimposed on  $K_t$  curves for the base metal in Figure 106. Fatigue endurance of three of the specimens (2-2, 2-4 and 3-1) which failed in the base metal was in close proximity to the  $K_t=1$  curve. In all specimens which failed in the weld, fine (0.001-0.004 inch) porosity was detected at the initiation site. Of the five specimens containing internal

## SECTION V

### FATIGUE CHARACTERISTICS OF ELECTRON BEAM (EB) WELDMENTS PHASE II

#### A. INTRODUCTION

This section presents data on fatigue endurance of flawless and (intentionally) defective EB weldments. The data are presented in the following sequence:

- Flawless welds
- Porous welds
- Mismatched welds
- Underfills
- Surface contamination
- Lack of penetration
- Bursts
- Summary

#### B. FLAWLESS WEILDS

##### 1. Fabrication of Experimental Weldments (0.080 and 0.25-Inch-Thick)

Flawless EB welds were produced to generate baseline data for use in evaluating defective welds. The welds were made in accordance with standard production techniques. Both root and face contours were machined flush with the base metal. Pretest radiography revealed no internal defects in any of the specimens.

##### 2. Fatigue Endurance of 0.080-Inch-Thick Flawless Welds

Experimental fatigue endurance values are plotted in Figure 104. Since the  $K_t=1$  curve was constructed based on average values obtained for the base metal, the scatter of data for flawless welds appears to be within the range expected for the parent material. Five of the specimens (3-2, 3-3, 1-3, 2-2 and 5-2) failed in the base metal. In some of the ten specimens which failed in the weld, fine (0.001 to 0.002-inch-diameter) isolated pores were detected at the initiation sites. Fatigue endurance and fractographic data are listed in Appendix B Table B-6. Figure 105 shows a typical surface failure initiation site encountered in flawless 0.080-inch-thick EB welded specimens.

##### 3. Fatigue Endurance of 0.25-Inch-Thick Flawless Welds

Data for flawless 0.25-inch-thick EB welded specimens are superimposed on  $K_t$  curves for the base metal in Figure 106. Fatigue endurance of three of the specimens (2-2, 2-4 and 3-1) which failed in the base metal was in close proximity to the  $K_t=1$  curve. In all specimens which failed in the weld, fine (0.001-0.004 inch) porosity was detected at the initiation site. Of the five specimens containing internal

porosity, three specimens (1-2, 2-1 and 3-2) were located within the normal scattering range from the  $K_t=1$  curve. The remaining two specimens (2-3 and 3-4) exhibited somewhat lower endurance values, although the size and location of internal porosity found in these two specimens did not deviate appreciably from those found in the first three samples. Fatigue endurance of specimens containing minor subsurface porosity (4-1, 3-3 and 4-4) were also somewhat below the expected scatter range for base metal values. Fine (0.001-inch diameter) pores were found throughout the fracture surface of Specimen 4-2.

Figure 107 shows an internal failure initiation site detected in Specimen 2-1. Figure 108 illustrates a subsurface failure initiation found in Specimen 4-3. Data on fatigue endurance and fractographic evaluations are listed in Appendix B Table B-7.

#### 4. Radiographically and Ultrasonically Flawless 1.5-Inch-Thick EB Welds

##### a. Fabrication of Experimental Welds.

The blank assembly halves were joined by an EB welding pass using a beam voltage of 55 kv, a beam current of 350 milliamp. and a gun travel speed of 40 ipm. This welding pass was preceded by a locking pass (beam voltage - 30 kv, beam current - 40 milliamp. and gun travel speed - 40 ipm) and followed by a cosmetic pass (beam voltage - 30 kv, beam current - 100 milliamp. and gun travel speed - 30 ipm). Radiographic examination of contoured welds and subsequent radiographic and ultrasonic examinations of welds machined flush with the base metal surfaces did not reveal any indications of defects.

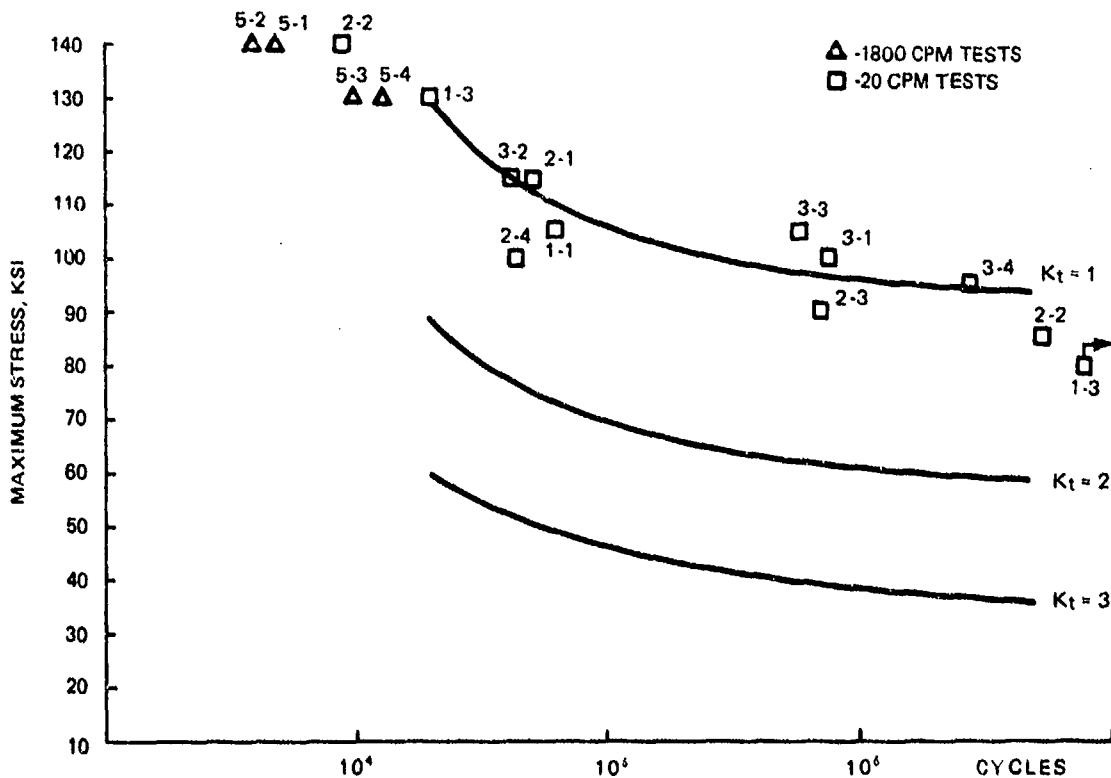


Figure 104. Fatigue Endurance of Flawless 0.080-Inch-Thick EB Welds



Figure 105. Typical Surface Failure Initiation Site in Flawless 0.080-Inch-Thick EB Welds (20 X MAG)

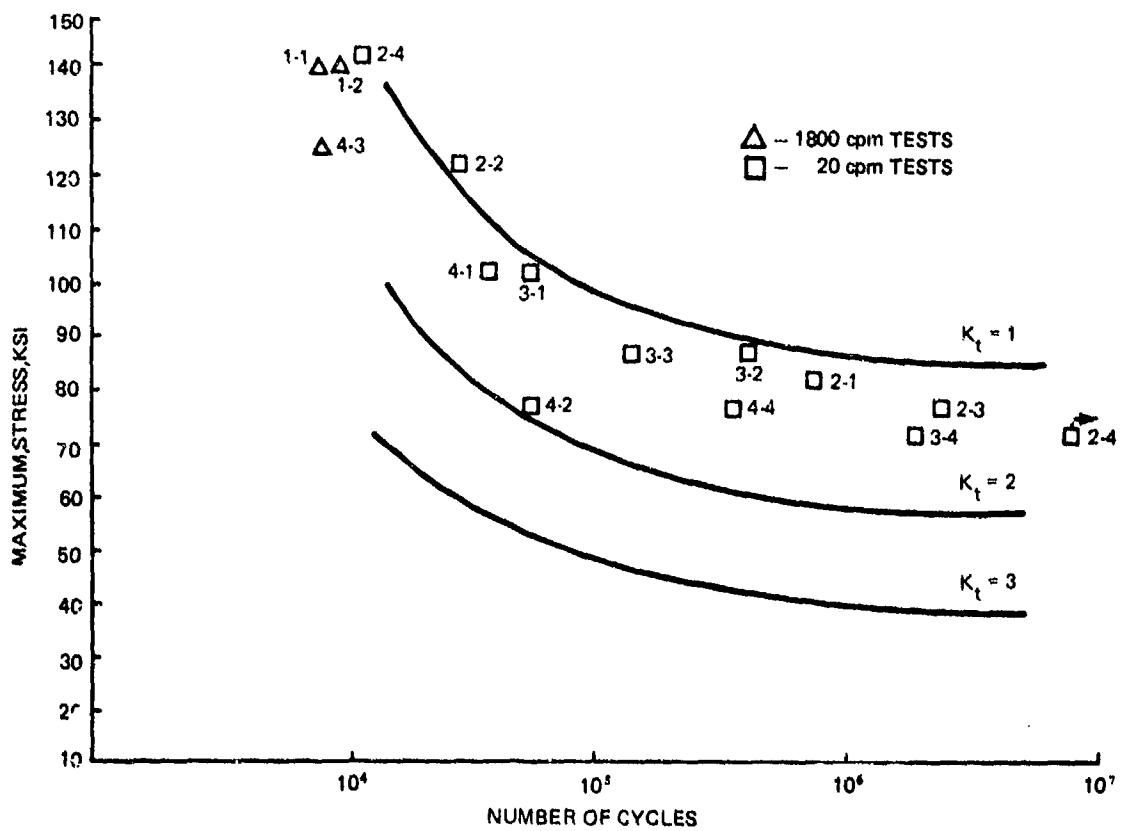


Figure 106. Fatigue Endurance of Flawless 0.25-Inch-Thick EB Welds

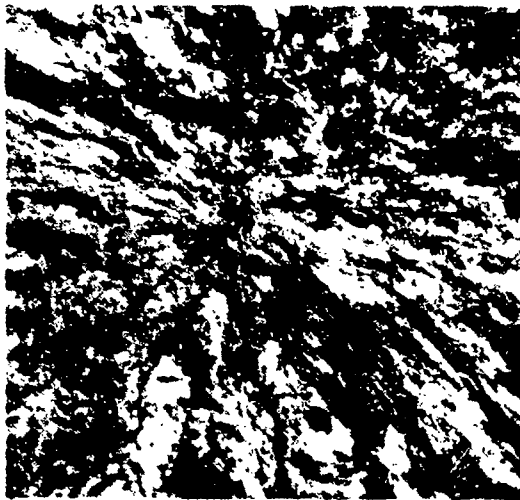


Figure 107. Failure Initiation Site in Flawless 0.25-Inch-Thick EB Weld Specimen 2-1 (20X MAG)

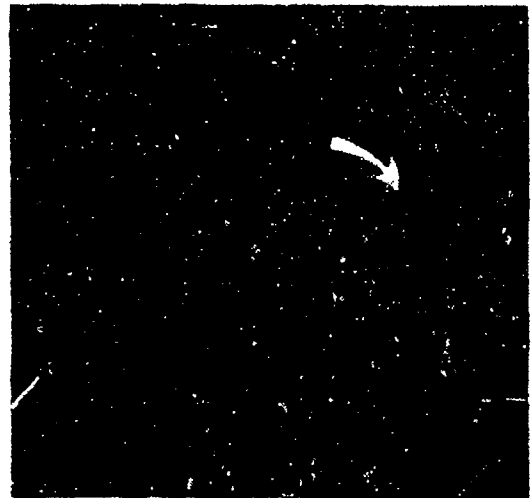


Figure 108. Failure Initiation Site at a Linear Cluster of Fine Porosity at the Subsurface of Flawless 0.25 Inch-Thick EB Weld 4-3 (20X MAG)

#### b. Evaluation of Fatigue Data

Fatigue endurance data for flawless 1.5-inch-thick EB welds are plotted in Figure 109. The  $K_t = 1$  curve indicates the fatigue endurance of 1.5-inch-thick unnotched base-metal specimens. All the experimental data points were in close proximity to the  $K_t = 1$  curve. A few isolated pores in the 0.002 to 0.006-inch range were detected on fracture surfaces. Failure initiated in Specimen 4-2 at a 0.006-inch pore, 0.040-inch from the surface.

#### C. POROSITY-CONTAINING WELDS

Porosity was produced in electron-beam weldments through intentional contamination of faying surfaces by extensive exposure to the following:

- Shop environment
- Acid residues simulating inadequate rinsing on pre-weld cleaning cycle
- Oil films to simulate total elimination of the pre-weld cleaning cycle
- Other techniques designed to simulate deficiencies in pre-weld preparation which could be inadvertently encountered in welding practices.

Detailed data pertaining to the intentional contamination techniques utilized, pre-weld radiographic and ultrasonic findings, fatigue tests and subsequent fractography of failed surface are presented in Appendix B Tables B8 and B9. The complete reproduction of desired defects could not be established, however, for a given type of contamination technique or for the entire length of the weld produced by a given method. Both face and root contours were machined flush with the surface and specimens were stress relieved before being subjected to tension - tension fatigue tests.

## 1. 0.080-Inch-Thick Welds

Experimental data on the fatigue characteristics of porosity-containing welds are superimposed on  $K_t = 1, = 2$  and  $= 3$  plots for 0.080-inch-thick base metal in Figure 110. Conclusions based on analyses of experimental data are as follows:

- There are no apparent deviations of data obtained in 20-cpm and 1800-cpm tests.
- Multiple-fracture initiation pattern was predominant above 100 ksi (Line A-A in Figure 110). In this region, no consistent relationship was apparent between the size and location of the weld defects and weld fatigue endurance. A typical multiple-fracture initiation is shown in Figure 111.
- Line B-B of Figure 110 separates the region containing experimental fatigue data on specimens for the majority of which single or double linear indications were indicated by pre-test radiography (RT). In the case of single linear RT indications, heavy concentrations of fine (about 0.001-inch diameter) porosity were detected in the face-side portion of the weld by fractographic analysis. For double-line RT indications, in addition to the fine porosity adjacent to the face of the weld, somewhat lighter concentrations of larger (0.002 to 0.003-inch-diameter) porosity were detected at the root-

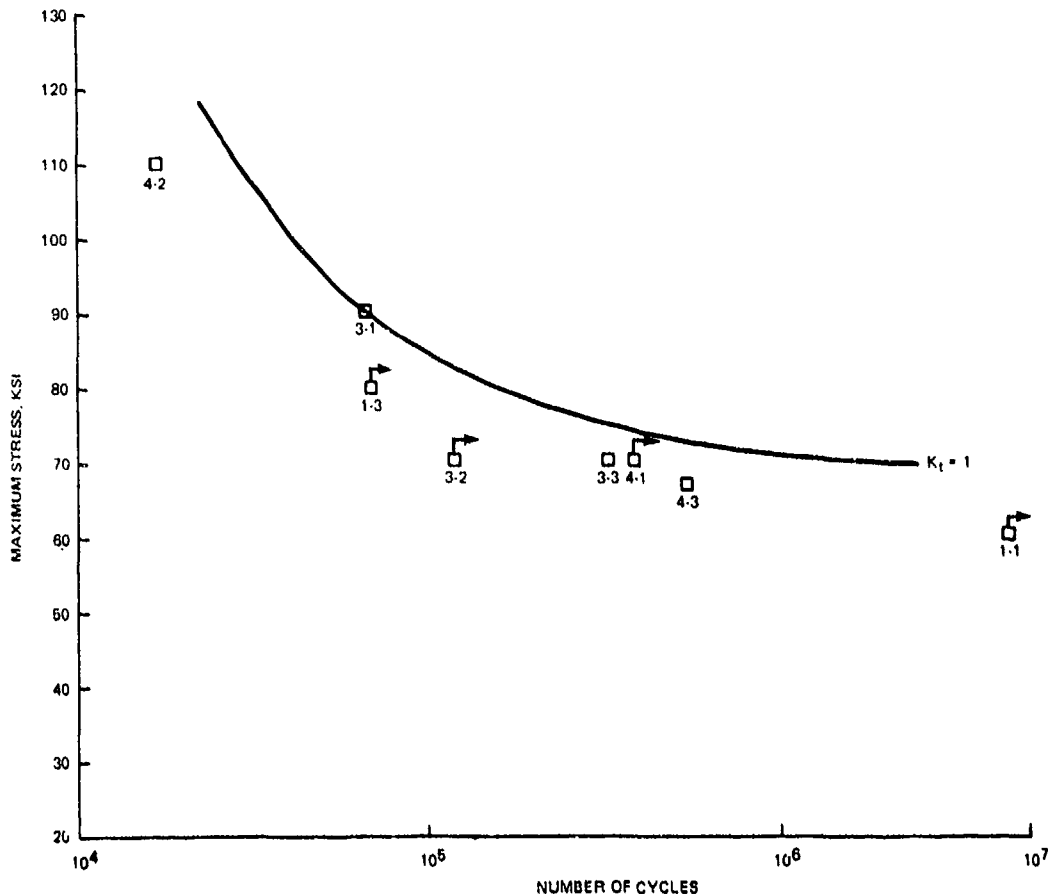


Figure 109. Fatigue Endurance of Flawless 1.5-Inch-Thick EB Welds

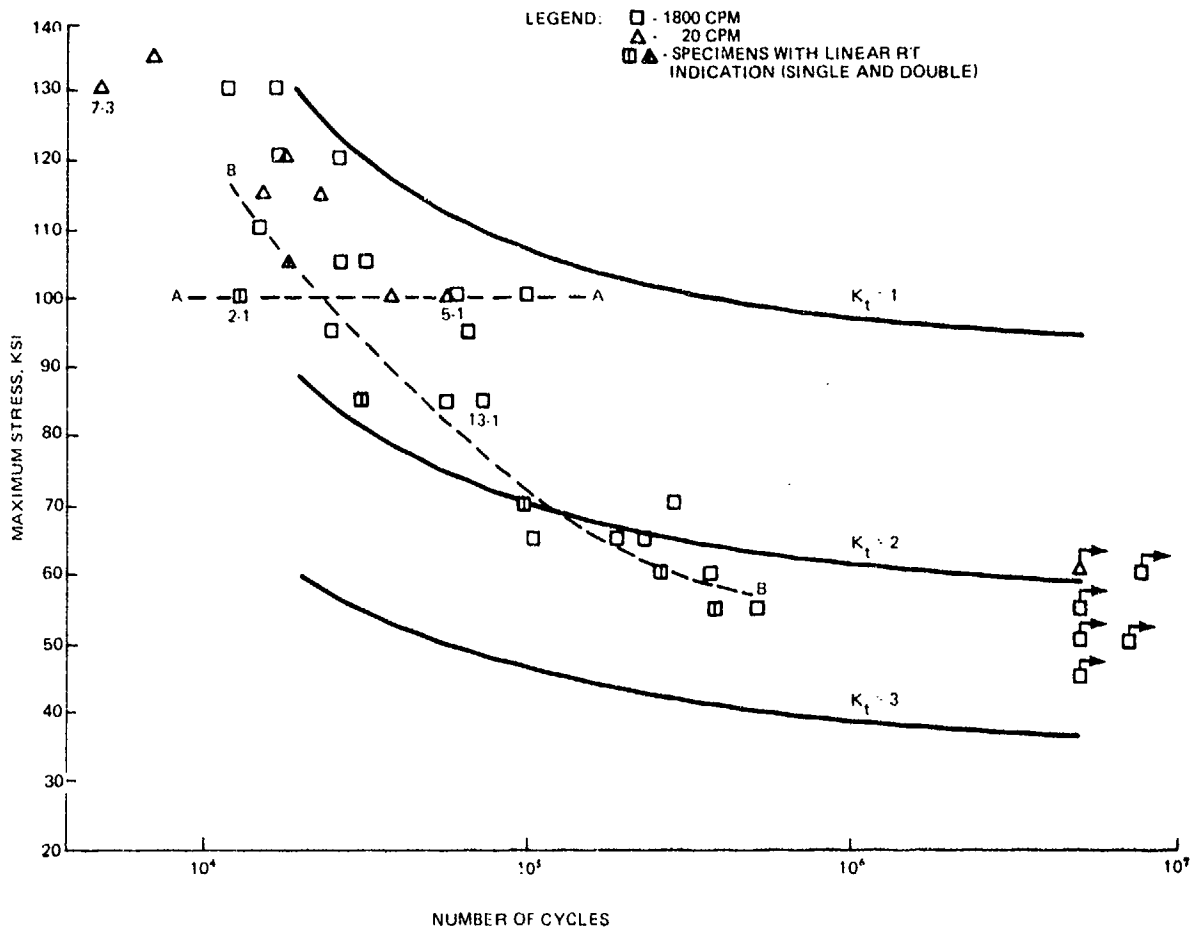


Figure 110. Fatigue Properties of Porosity-Containing 0.080-Inch-Thick EB Welds

side of the weld cross-section. Figure 112 shows the fracture surface of a specimen for which double-line RT indications were obtained during pre-test radiography. A heavy concentration of fine porosity is readily detectable in the face-side (top) portion of the weld. Definition of larger porosity in the root-side portion of the weld was somewhat more difficult due to focusing complications related to contour variations.

- For the majority of points located to the right of Line B-B of Figure 110, minor scattered 0.003-0.008-inch porosity was indicated by radiography. Examination of fracture surfaces confirmed radiographic findings. In addition, presence of finer 0.001 to 0.002-inch-diameter porosity was detected. From specimens containing scattered porosity and exhibiting well-defined failure initiation sites, samples were selected for analysis by the method developed by Lindh and Peshak(2) which assigns  $K_t$  factors based on their size and distance from the surface. In Specimen 13-1, for example, failure occurred at a 0.002-inch-diameter pore as shown in Figure 113. The distance from the center of the pore to the surface was also 0.002 inch. Thus, the ratio of the radius to the distance from the surface ( $r/h$ ) was 0.5. For this ratio, Reference 2 estimates the value of  $K_t$  to be approximately 6. This value could not be verified by experimental data.

On the other hand, the  $r/h$  ratio for Specimen 5-1 shown in Figure 114 was calculated to be 0.17 and the corresponding  $K_t$  value to be approximately 2. In this case, the calculated value of  $K_t$  provides a reasonable approximation for the experimental value. It should be noted that the location of the initiation site in Specimen 5-1 is more closely related to the configurations of photoelastic models utilized in Reference 2.

## 2. 0.25-Inch-Thick Welds

Data on porous 0.25-inch-thick EB welds are superimposed on  $K_t$  curves for the base metal in Figure 115. In addition to specimens with definite radiographic indications, some specimens without RT defects were tested to verify that flawless specimens machined from porosity-induced blanks were comparable to flawless specimens produced by standard techniques, i. e., without intentional contamination of faying surfaces. These specimens are identified with an "X" prefix. Both face and root contours of all specimens were machined flush with the surface.

### a. Fatigue Endurance of Specimens Without Radiographic (RT) Indications

Of seven specimens without pre-test RT indications, three (3-3X, 6-1X and 17-2X) failed in the base metal and in the remaining four (13-3X, 17-1X, 17-3X and 17-4X) failure initiated at isolated microporosity (0.001 to 0.004-inch in diameter) as shown in Figures 116 and 117. The endurance values obtained were comparable to those of flawless specimens produced by conventional techniques (Figure 106).

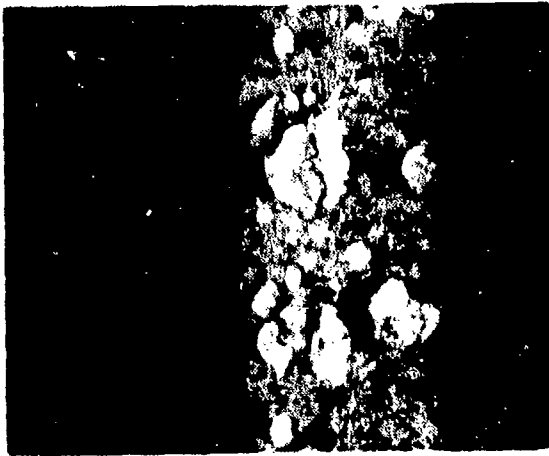


Figure 111. Multiple-Fracture Initiation Pattern Detected in Specimen 7-3 (20X MAG)

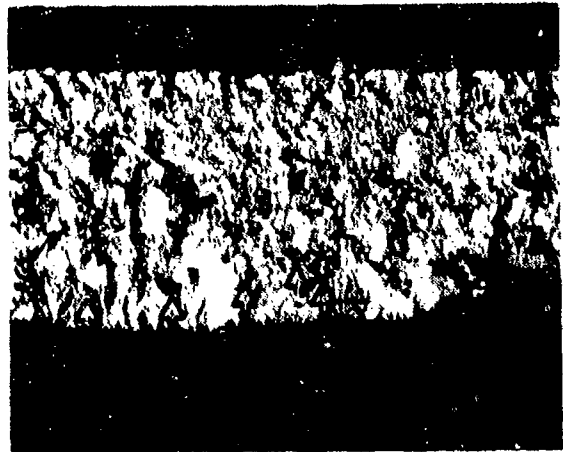
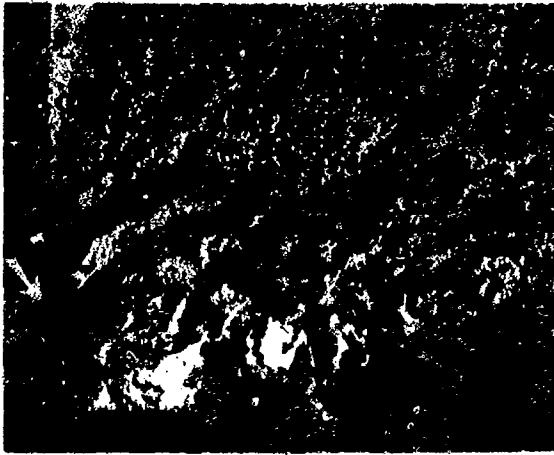
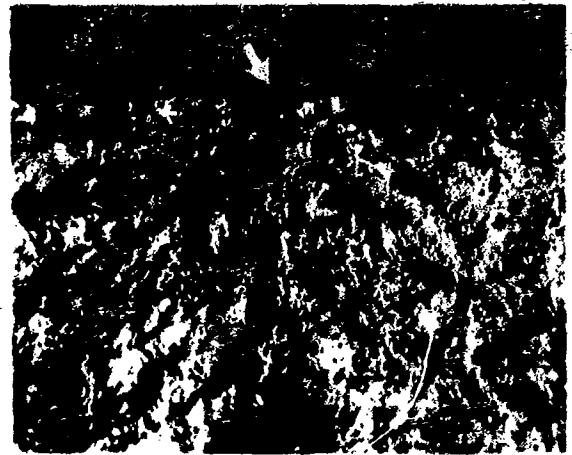


Figure 112. Fracture Surface of Specimen 2-1 For Which Double-Line Porosity Indications Were Detected by Prior Radiography





**Figure 116. Location of a 0.001-Inch-Diameter Pore On the Fracture Surface of Specimen 17-4 (20X MAG)**



**Figure 117. Location of a 0.004-Inch-Diameter Pore On the Fracture Surface of Specimen 17-3 (20X MAG)**

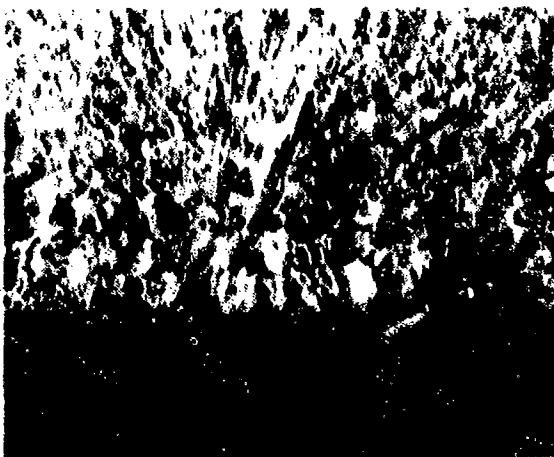


**Figure 118. Failure Initiation at Internal Porosity in Specimen 3-1 (20X MAG)**

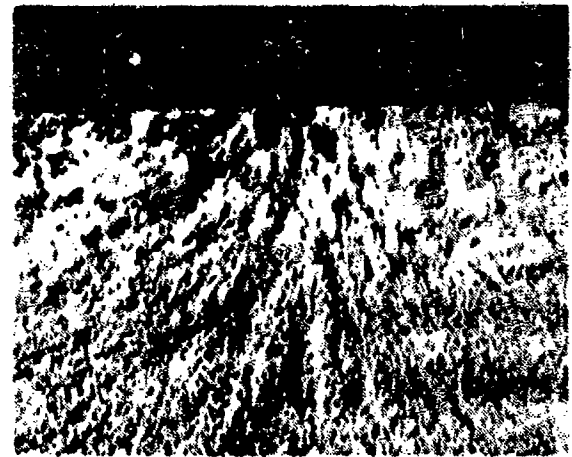


**Figure 119. Subsurface Failure Initiation Site in Specimen 6-1 (20X MAG)**

b. Fatigue Endurance of Specimens with Indications of Linear (0.003 to 0.005 Inch) Porosity.

Fatigue endurance data on specimens with linear porosity indications (and no other defects) were located in the upper portion of the  $K_t=1$  to  $K_t=2$  range and were thus generally comparable to flawless specimens. Specimens 3-1, 6-1, 6-2 and 6-3 were included in this group. Specimens 3-1, 6-3 and 6-2 contained internal porosity at which failure initiated as shown in Figure 118. Figure 119 shows two 0.003-inch subsurface (0.001 to 0.010 inch from the surface) pores at which fracture initiated in Specimen 6-1.

c. Fatigue Endurance of Specimens with Scattered 0.003 to 0.005-Inch Porosity.

The endurance values of the two specimens included in this group (3-2 and 31-4) were in the proximity of the  $K_t=2$  curve. A cluster of 0.002 to 0.003-inch pores was detected at the subsurface of Specimen 3-2 as shown in Figure 120. Fractography of Specimen 31-4 indicated a multiple failure initiation pattern.

d. Visual Surface Indications

Visual surface indications were detected in Specimens 27-2, 27-3 and 27-4 in addition to the fine linear porosity detected by radiography. These visual indications were the remaining portions of surface porosity partially removed during machining as shown in Figures 121 and 122. A shallow remaining contour detected in Specimen 27-3 reduced the endurance value only moderately; a deep surface pore, on the other hand, led to a very significant decrease in fatigue endurance in Specimens 27-2 and 27-4.

e. Fatigue Endurance of Specimens with Double-Row or Double-Line Porosity Indications

Specimens with double-row or double-line porosity indications (Specimens 24-1, 24-2 and 29-1) exhibited massive porosity and an unpredictable failure initiation pattern. Fatigue endurance values for these specimens were in the  $K_t = 2$  to  $K_t = 3$  range. Figure 123 illustrates massive porosity detected at the failure initiation site in Specimen 24-2.

f. Fatigue Endurance of Specimens Containing Pores Greater Than 0.010 Inch In Diameter

The specimens in this group (21-1, 21-2, 21-3, 24-4, 28-1, 28-2, 31-1 and 31-2) did not exhibit any uniform failure initiation pattern or fatigue endurance characteristic that could be correlated with the size of detected pores. In Specimen 28-1, for instance, the failure initiation site was definitely associated with a subsurface 0.020-inch pore (Figure 124). In Specimen 31-1 (Figure 125), on the other hand, the failure initiated at a partially removed 0.005-inch surface pore rather than at the 0.020-inch pore in the interior. The topography of the region surrounding the larger pore was definitely of the overload type. In Specimen 28-2, the failure initiated at the extensive interior cluster shown in Figure 126 rather than at the internal 0.020 to 0.025-inch pores indicated by radiography.

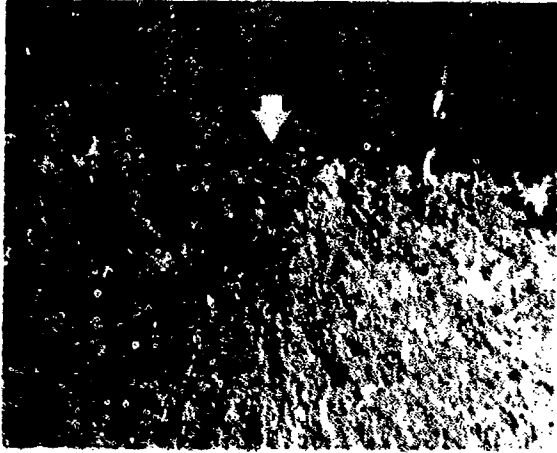


**Figure 120.** Cluster of Fine Pores Detected at the Subsurface Initiation Site in Specimen 3-2 (20X MAG)

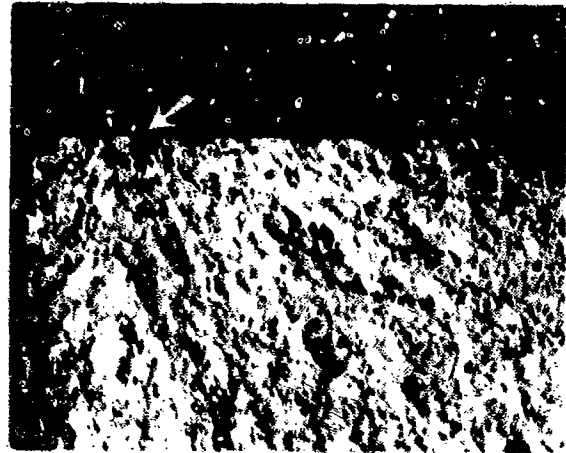


**Figure 121.** Shallow (Visual) Indication at the Surface-Failure-Initiation Site in Specimen 27-3 (20X MAG)

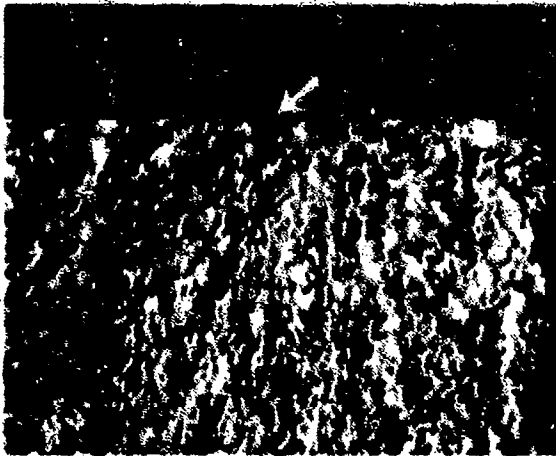


**Figure 122.** Surface Pore at the Failure Initiation Site in Specimen 27-2 (20X MAG)

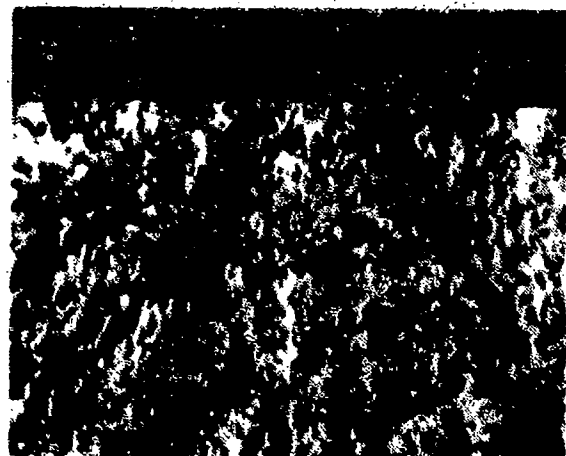


**Figure 123.** Massive Porosity Encountered At the Failure Initiation Site in Specimen 24-2 (20X MAG)

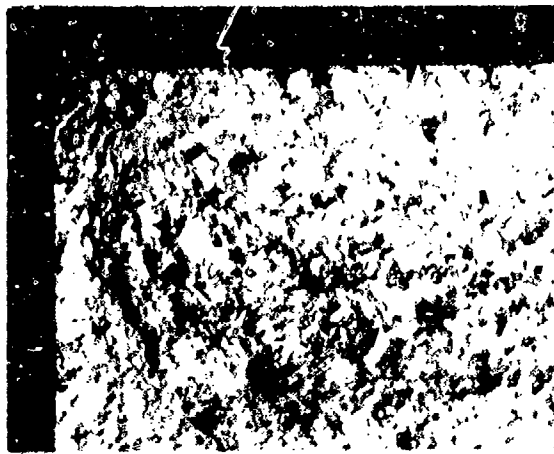


Figure 124. Fracture Initiation Site at a 0.015 Inch-Diameter Subsurface Pore in Specimen 28-1 (20X MAG)

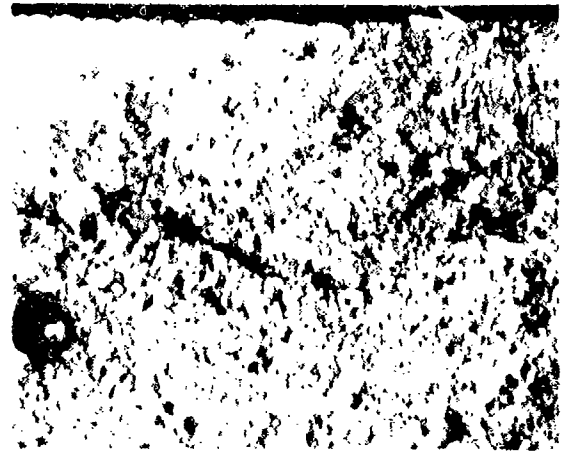


Figure 125. Fracture Initiation (Arrow) in Specimen 31-1 (20X MAG)

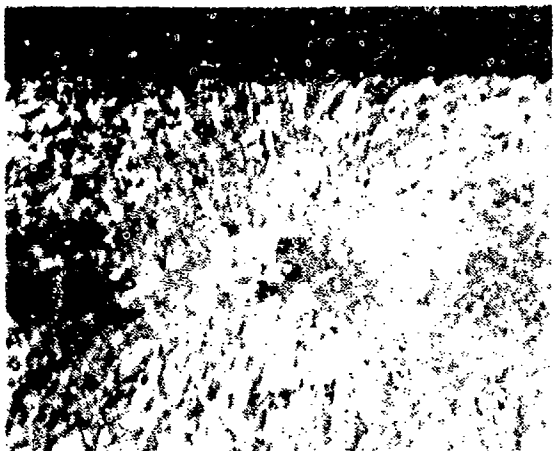


Figure 126. Fatigue Initiation at an Internal Porosity Cluster in Specimen 28-2 (20X MAG)

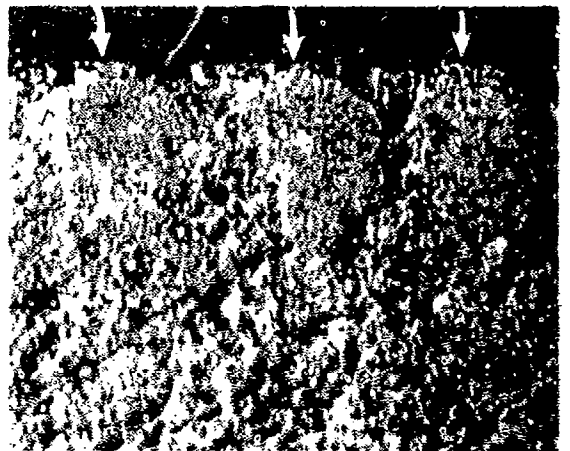


Figure 127. Indications of a Missed Seam Detected in Specimen 12-2 (20X MAG)

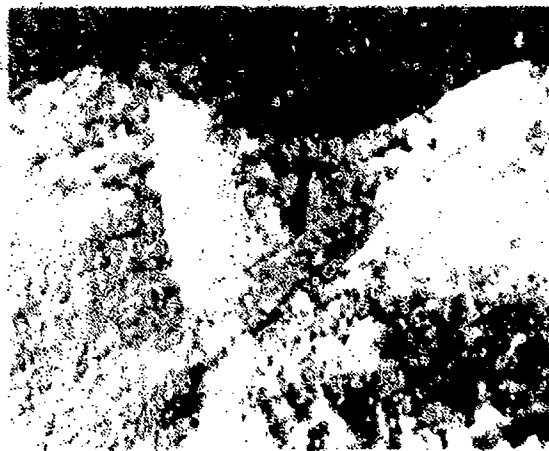


Figure 128. Large Void at the Surface of Specimen 13-2 (20X MAG)

### g. Fatigue Endurance of Specimens with Missed Seams and Large Surface Voids

Missed seams and surface voids indicated by RT in Specimens 12-2 and 13-2, respectively, and verified by subsequent fractography are shown in Figures 127 and 128. Both defects resulted in a severe degradation of fatigue endurance as shown in Figure 115.

### 3. 1.5-Inch-Thick Welds

#### a. Fabrication of Experimental Welds

As stated in the previous sections, internal porosity was to be induced in experimental welds by intentional contamination of faying surfaces to simulate conditions of inadequate cleaning which could inadvertently occur in production. In most cases, weldments produced by these techniques contained segments without radiographic indications from which specimens could be machined to verify that experimental techniques utilized did not lead to reduction of fatigue endurance in absence of internal porosity. In the case of 1.5-inch-thick weldments, however, techniques utilized in inducing porosity in 0.080 and 0.25-inch-thick welds failed to produce detectable radiographic indications. One possible reason for this could be vaporization of impurities due to the high heat input required to obtain full penetration in a 1.5-inch-thick joint and removal of impurities in the vacuum environment which was facilitated by the reduced speed of the gun travel. In subsequent attempts to induce porosity, additional contaminants were added to the cutting oil which was applied to faying surfaces prior to welding. Utilization of one of these contaminants (G1 powder), did result in generation of large voids in 1.5-inch-thick EB weldments. Radiographic and ultrasonic measurements taken on the machined face surface revealed considerable variations in size and configuration of included voids.

#### b. Evaluation of Fatigue Data

Fatigue endurance data for experimental welds are plotted in Figure 129. The solid line refers to the fatigue endurance of unnotched base-metal and specimens machined from 1.5-inch-thick flawless welds (whose data points were in close proximity to the  $K_t = 1$  curve.) The two dotted reference lines (RL1 and RL2) were drawn to separate data regions for specimens with distinctly different defect characteristics.

Specimens 20-2 and 15-2, with fatigue endurance in the  $K_t = 1$  to RL1 range, exhibited no radiographic indications except for one 0.015-inch pore indication in Specimen 20-2. Ultrasonic measurements indicated the presence of some porosity in Specimen 15-2 about 1/2-inch from the face surface to the full thickness. Fractographic evaluation detected some 0.002- to 0.003-inch porosity throughout the cross-section of both specimens. In both specimens, the failure initiated at the surface. In Specimen 15-2 the failure initiation was associated with 0.001-inch scattered porosity. In Specimen 20-2 the initiation site was associated with surface and subsurface porosity in the 0.004 to 0.008-inch range. As discussed in para. A, which deals with fatigue characteristics of flawless specimens produced by conventional welding techniques, data points for these specimens were in close proximity to the  $K_t = 1$  curve. The considerable deviation of data points for Specimens 20-2 and 15-2 from the  $K_t = 1$  curve suggests the possibility of contamination of the weld metal. Accordingly, a comparison of the fatigue endurance of porous 1.5-inch-thick EB welds to that of the

base metal may not be fully justified. Figure 130 shows the failure initiation site in Specimen 20-2. Specimens 2-1, 14-1, 15-1, 20-1 and 2-2 exhibited fatigue endurance in the range between Reference Lines 1 and 2 (Figure 129).

The fracture surface for Specimen 20-1 is shown in Figure 131. The failure initiated at the face-side surface of the weld. Pre-test radiography of this specimen failed to reveal the presence of internal defects. Ultrasonic "C" scan indicated a void 5/8-inch from the face and subsequent fractography showed this indication to be a 0.015-inch pore at the specified location. Additional porosity in the 0.005 to 0.015-inch range, however, located within 0.050-inch from the face, was not detected. Porosity in the 0.004 to 0.010-inch range was detected by fractography at the initiation site.

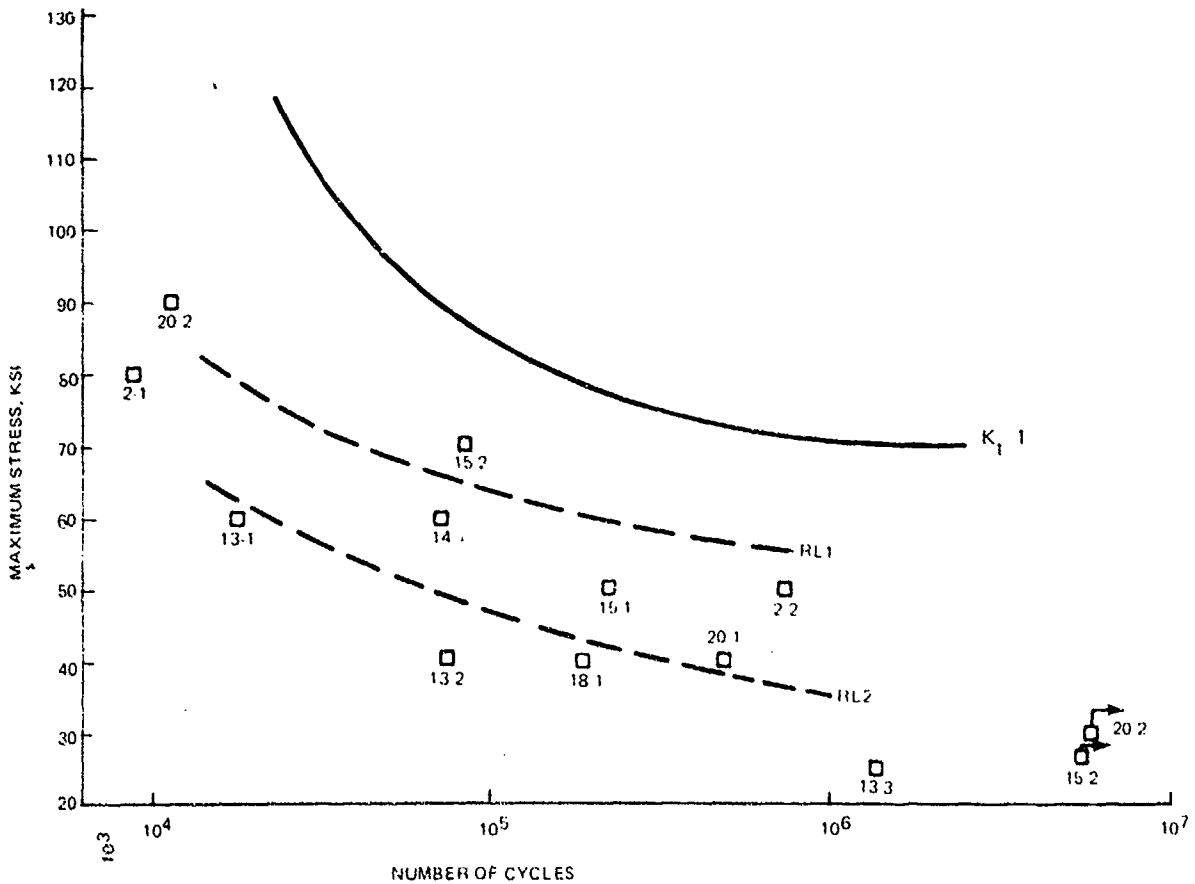
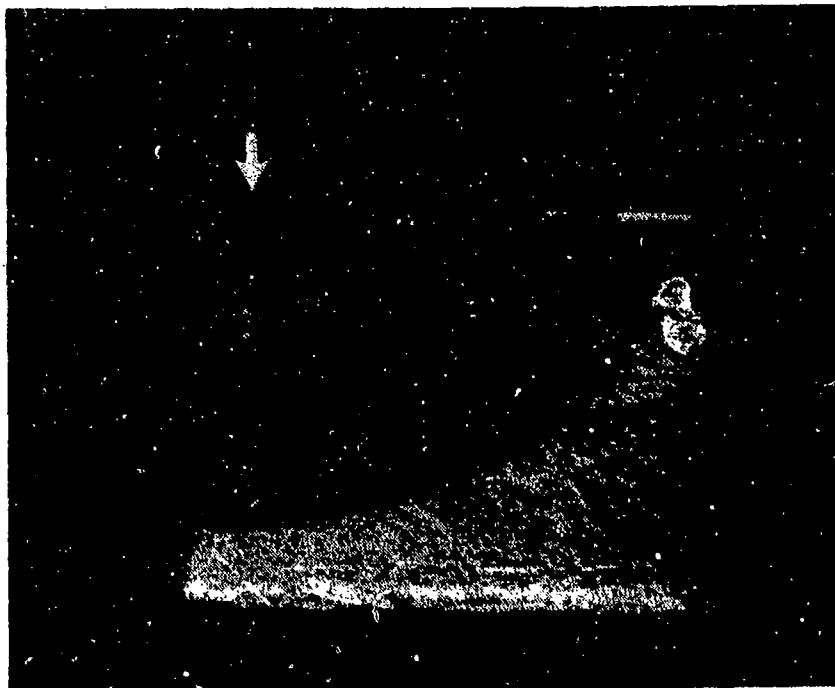


Figure 129. Fatigue Endurance of Porosity-Containing 1.5-Inch-Thick EB Welds



**Figure 130. Failure Initiation Site in 1.5-Inch-Thick EB-Welded Specimen 20-2 (1.5X MAG)**



**Figure 131. Failure Initiation Site in 1.5-Inch-Thick EB-Welded Specimen 20-1 (1.5X MAG)**

In Specimen 15-1, the failure initiated at a 0.115 x 0.050-inch void approximately 5/16-inch from the face surface as shown in Figure 132. The presence of this void was detected by both pretest radiography and ultrasonic "C" scan inspection.

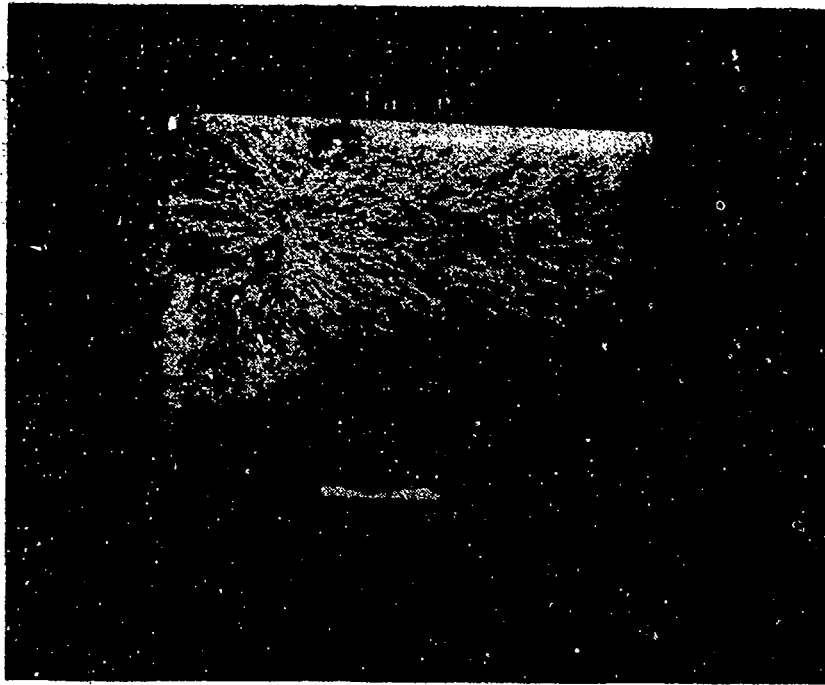
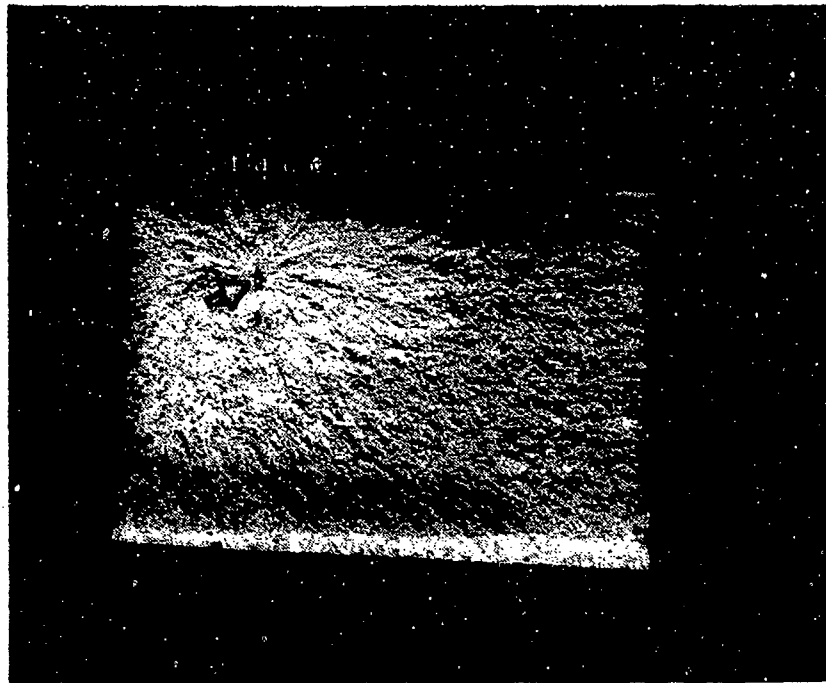
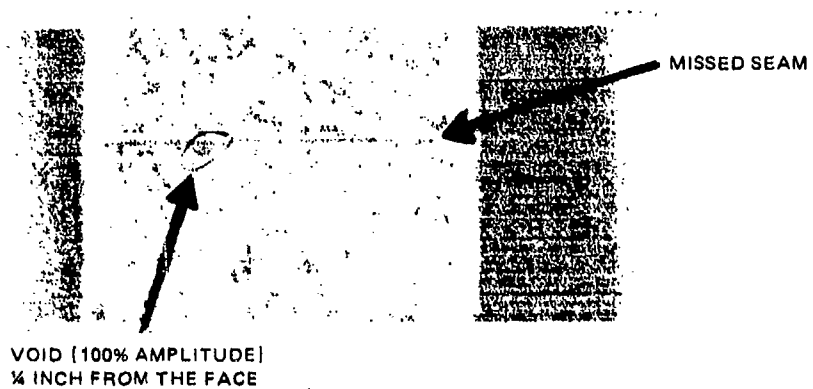


Figure 132. Failure Initiation Site in Porosity-Containing 1.5-Inch-Thick EB-Welded Specimen 15-1 (1.5 x MAG)

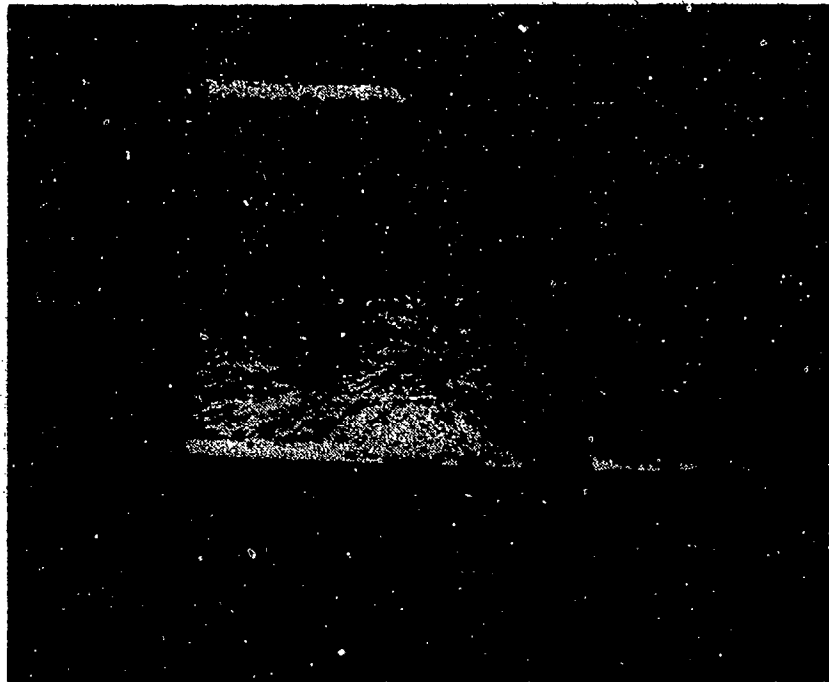
Figure 133 shows the fracture surface of Specimen 14-1, where the failure initiated at a cluster of two voids (0.040 x 0.110-inch and 0.030 x 0.030-inch, 0.080-inch apart). Pretest radiography identified these defects as 0.050- and 0.025-inch voids and also reported (linear) indications of a missed seam. Figure 134 shows an ultrasonic "C" scan printout for Specimen 14-1 which identifies the location of the cluster and the presence of a missed seam. Fractography indicated that the lack of penetration (due to a missed seam) was in the 0.010 to 0.020-inch range. There were only a few secondary failure initiation sites associated with this lack of penetration. Figure 135 illustrates voids that are 0.140 to 0.180-inch-long and 0.090 to 0.100-inch-wide detected at failure initiation sites in Specimens 2-1 and 2-2. The second smaller void shown in Figure 135 was located outside the failure initiation site. Pretest radiography identified the internal defects as two voids with a resultant (total) length of 0.150-inch.



**Figure 133.** Failure Initiation Site in Porosity-Containing 1.5-Inch-Thick EB-Welded Specimen 14-1 (1.5x MAG)



**Figure 134.** Ultrasonic "C"-Scan Printout of Porosity-Containing 1.5-Inch-Thick EB-Welded Specimen 14-1



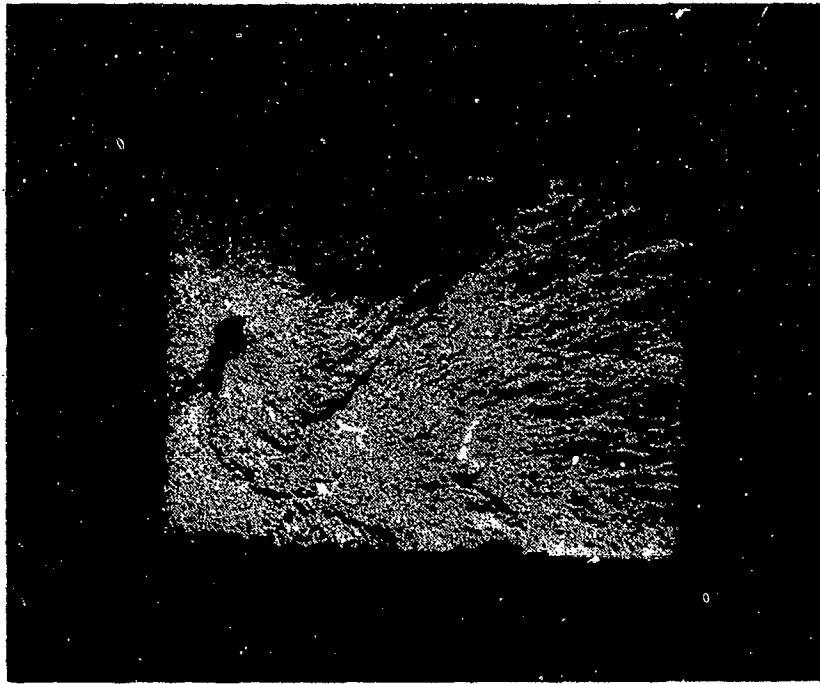
**Figure 135. Fracture Surface of Porosity-Containing 1.5-Inch-Thick EB-Welded Specimen 2-2 (1.5x MAG)**

Figure 136 shows the ultrasonic "C" scan printout for Specimen 2-2 in the one-inch to full thickness range. The defects were identified as a large void located one to 1-1/8 inch from the face (upper edge of the macrograph).

Figures 137 through 139 illustrate the type of internal defects encountered in specimens which exhibited even lower fatigue values (data points below the RL2 Line). The presence of defects was correctly predicted by both the pre-test radiographic and ultrasonic tests. All these defects were sites of failure initiation. In Specimen 13-2 (Figure 139), which contained several extensive internal defects, the failure initiated at an edge void. Figure 140 shows the ultrasonic "C"-scan printout for Specimen 13-2 in the 1/2 to 1-inch focusing range.



**Figure 136. Ultrasonic "C"-Scan Printout of 1.5-Inch-Thick EB-Welded Specimen 2-2 (Arrow indicates location of a void indication)**



**Figure 137. Internal Void in Porous 1.5-Inch-Thick EB-Welded Specimen 13-3  
(1.5X MAG)**

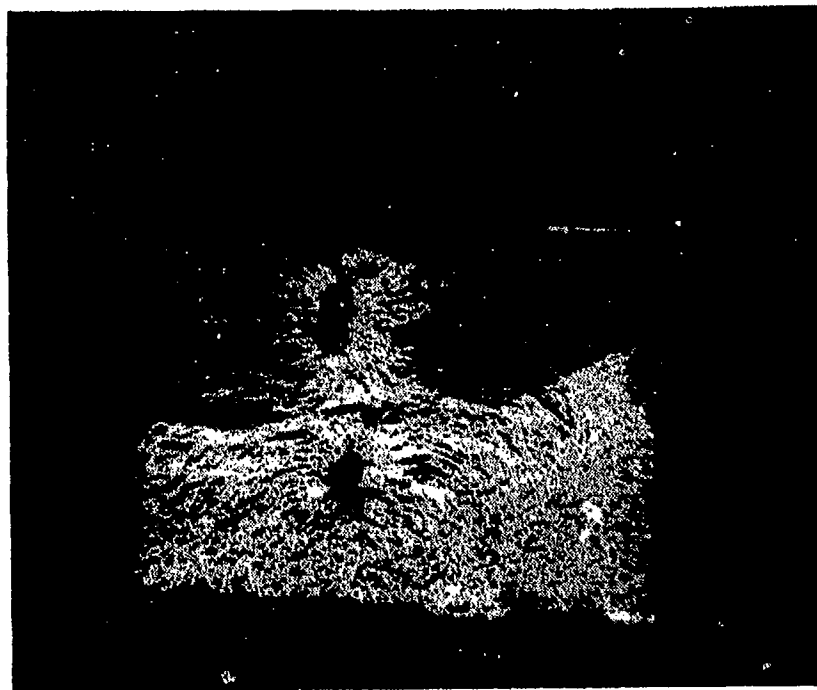


**Figure 138. Internal Voids in Porous 1.5-Inch-Thick EB-Welded Specimen 18-1 |  
1.5X MAG)**

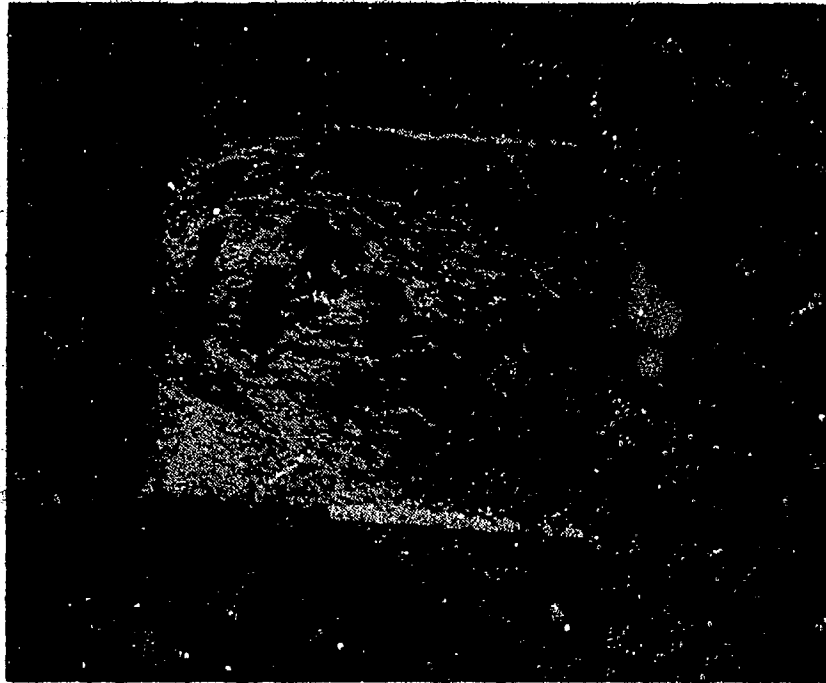


**Figure 139.** Extensive Multiple Defects in Porous 1.5-Inch-Thick EB-Welded Specimen 13-2 (1.5x MAG)



**Figure 140.** Ultrasonic "C"-Scan Printout of Porous 1.5-Inch-Thick EB-Welded Specimen 13-2

### **c. Acoustic Emission Monitoring**

Several welded titanium specimens were monitored with an advanced acoustic emission monitoring system (Figure 141) which eliminated noise interference from pumps and fixtures. The purpose of monitoring these specimens was to determine the cycle at which crack initiation occurred and to see if a correlation between acoustic emission events and crack propagation rates would be feasible. The computerized, complex electronic system was also utilized to locate the source of the acoustic emission signals.

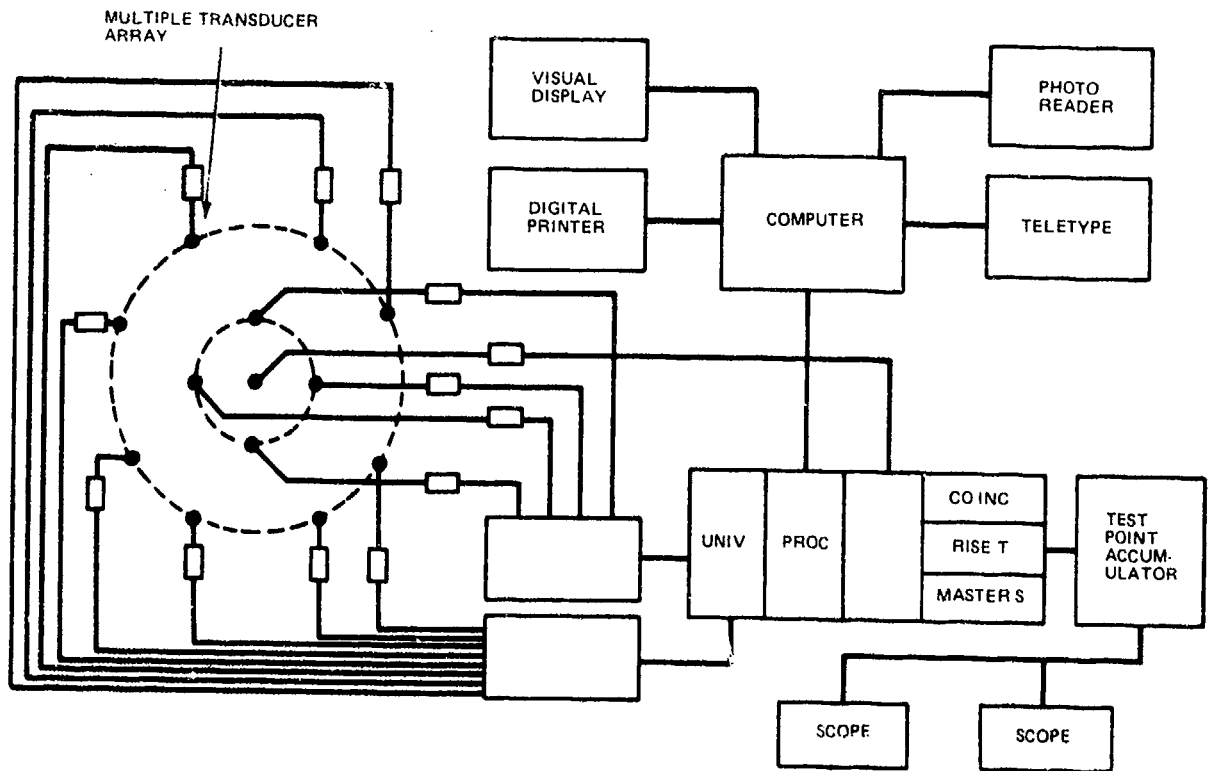


Figure 141. Acoustic Emission Monitoring System

Three specimens identified as P-14-1, P 14-2 and P 18-1 were evaluated. These specimens were monitored as shown in Figure 142 using transducers arranged for "master-slave" and "coincidence" discrimination techniques. The two techniques combined with electronic acoustic emission signal modifications allowed only signals from the cracking area to be detected. The following table shows the cycle at which crack initiation was detected.

Specimen No.	Fatigue Life (cycles)	Crack Initiation (cycles)
P 14-1	71,400	64,000
P 14-2	5,880	5,240
P 18-1	165,700	64,400

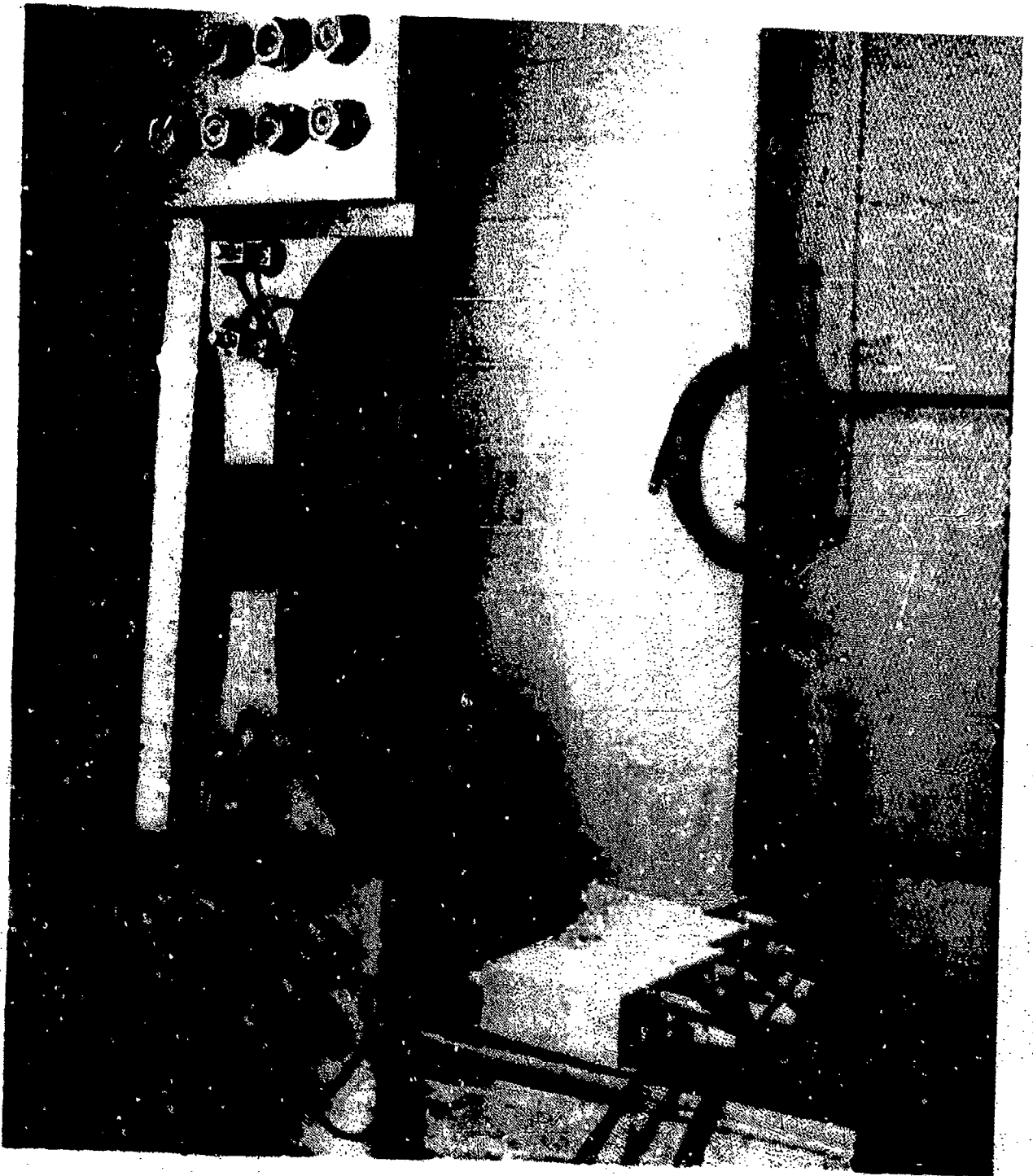
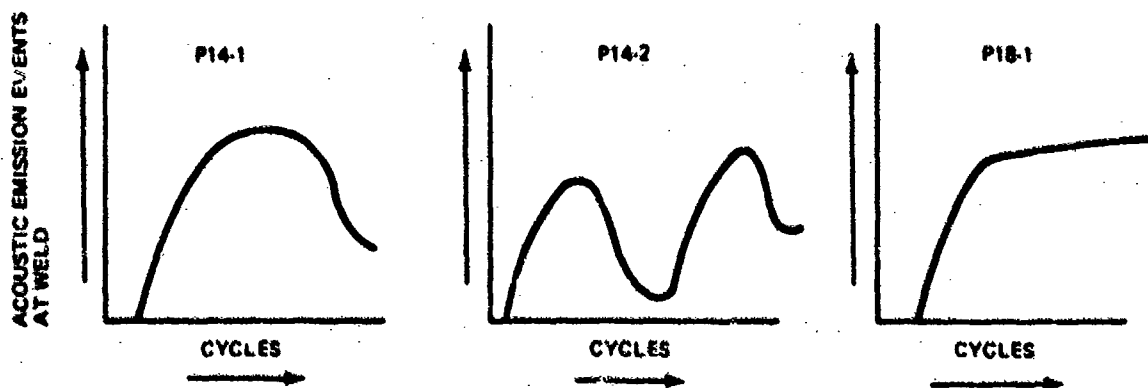


Figure 142. Monitoring of Failure Initiation and Propagation by Acoustic Emission

Examination of the acoustic emission signal distribution during testing of each specimen showed that the rates of emission were not always constant once initiation had begun. Acoustic emission rates for samples tested on the lower part of the S/N curve (Specimens P14-1 and P14-2) showed a fast initial rate which slowed down gradually prior to final failure. The specimen monitored at a higher stress (P18-1) showed a constant rate of emission after crack initiation. Figure 143 indicates data obtained for these specimens. These data indicate that mechanisms for acoustic emission generation differ for different parts of the S/N curve. This is consistent with present theories concerning crack initiation and propagation at various stress levels. Tests performed more recently on production steel parts tend to confirm the P14-1 and P14-2 curves.

Final correlation of the acoustic emission signal rate to the crack propagation rate has yet to be determined. Initial tests have determined that a consistent pattern does emerge when samples of similar stress levels are monitored with acoustic emission. Studies should be continued which would quantify the acoustic emission events to the  $da/dn$  ratio. These studies should be conducted on both micro and macro-levels. The micro-approach would attempt to correlate the individual metal-lurgical fatigue striations with the acoustic emission events during each cycle. The macro-program would quantify the crack growth over a number of cycles using advanced NDI techniques. The relative growth of the crack would be measured and correlated to the acoustic emission events. In either case, these studies can only be continued with acoustic emission monitoring systems that have appropriate noise discrimination techniques for accurate flaw detection and location.



NOTE: SPECIMEN P14-2 HAD TWO INITIATION SITES WHICH APPARENTLY BEGAN AT DIFFERENT TIMES; HENCE, TWO DISTINCT CURVES.

Figure 143. Acoustic Emission Data Obtained for Failure Initiation and Propagation in Three Defective Welds

## D. MISMATCH - .25-INCH-WELDS

### 1. Fabrication of Test Specimens

Mismatched joints were produced by utilizing 0.016 and 0.025-inch shims under one of the faying surfaces. The blanks were cleaned and welded using conventional EB welding parameters. Pre-test radiography revealed no defect indications in any of the specimens. The specimens were tested in the as-welded condition (no machining). Figures 144 and 145 shown actual images obtained on an optical comparator for both levels of mismatch.

### 2. Fatigue Tests

In Figure 146, the experimental data obtained are superimposed on  $K_t=1$ ,  $=2$  and  $=3$  curves for the base metal. It is evident that these specimens exhibited very low endurance values; however, there were no significant variations in data obtained for 0.016 and 0.025-inch mismatch

Fractographic evaluation of fracture surfaces revealed that failure initiation occurred at random at either the root or face of the weld. Figure 147 shows a typical failure initiation site encountered in mismatched specimens. The test data for mismatched EB weldments are summarized in Appendix B, Table B-10.

## E. INTENTIONAL UNDERFILL, 0.25-INCH-THICK WELDS

### 1. Fabrication of Experimental Weldments

Underfill defects were produced in experimental weldments by inserting shims between faying surfaces at outer edges of welding blanks. A description of the shims utilized in welding various blanks is included in Appendix B-11. This table also lists fatigue test results for various underfill configurations.

### 2. Fatigue Test Results

Fatigue test data are plotted in Figure 148. These data were analyzed to determine the correlation between endurance values and width-to-depth (W/D) ratios determined on actual weld contours utilizing optical comparator images at 10X magnification. For W/D ratios above 2.4, no definite correlations could be determined between fatigue endurance values and specific W/D ratios (dotted band in Figure 148). A definite lowering of fatigue endurance was evident, however, at W/D ratios in the 1.4 to 1.6 range and below.

Two of the specimens failed at the root. In these specimens, the weld metal penetrated below the lower surface of the joint forming a narrow reinforcement type contour with sharp radii which caused failure initiation at this site.

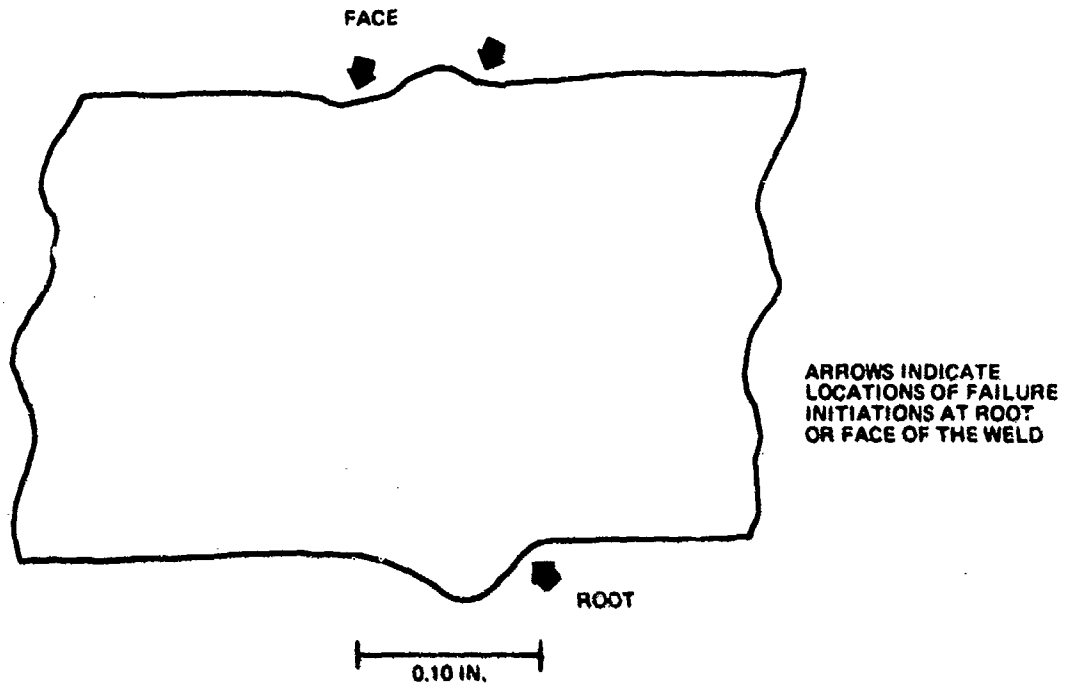


Figure 144. Contour of EB Weldments With 0.016-Inch Mismatch of Faying Surfaces

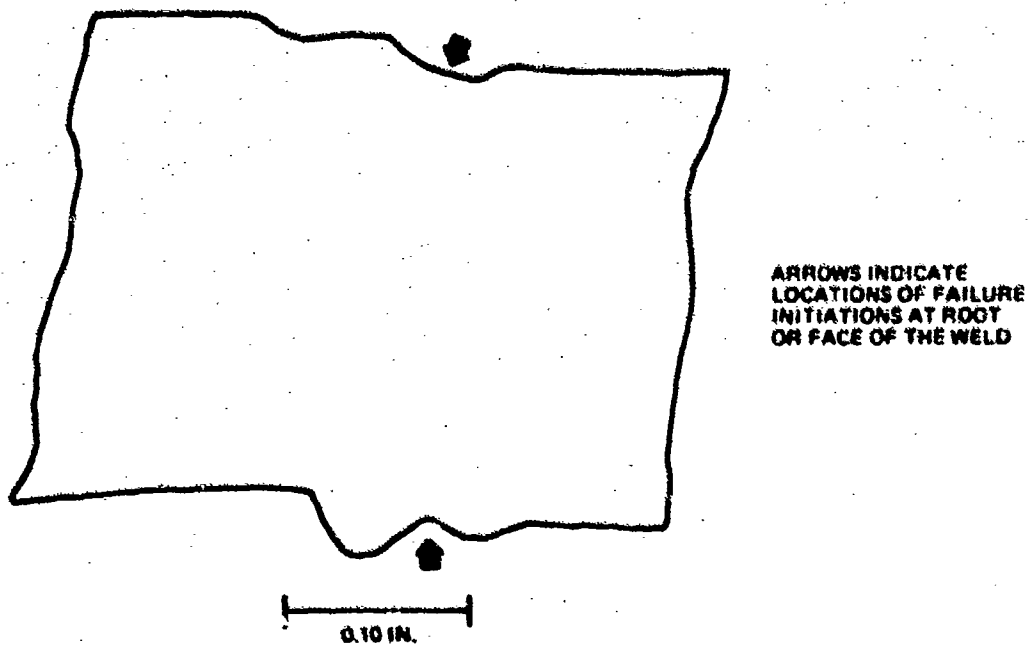


Figure 145. Contour of EB Weldments With 0.025-Inch Mismatch of Faying Surfaces

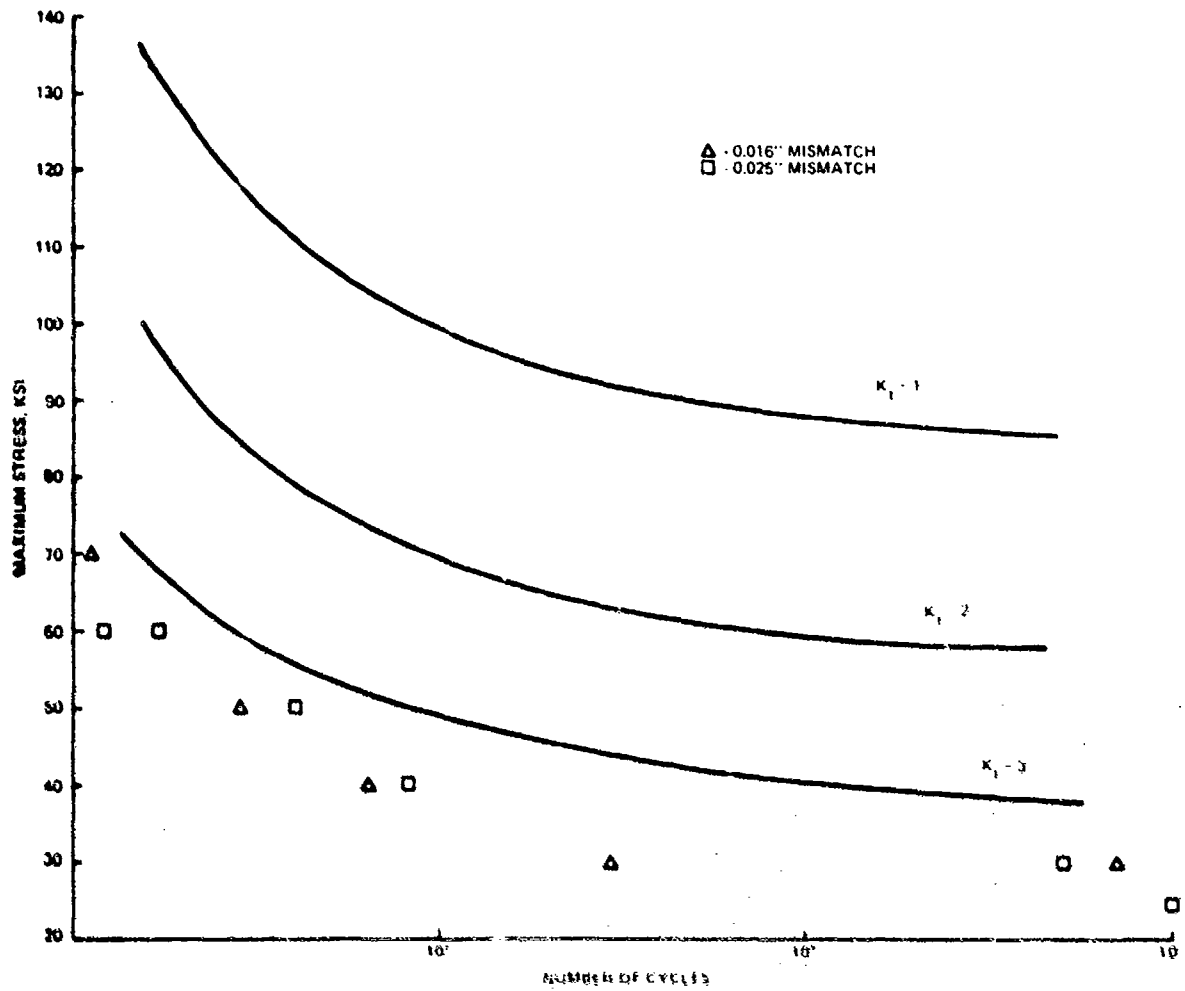


Figure 146. Fatigue Characteristics of 0.25-Inch-Thick EB Welds With Mismatch of Faying Surfaces

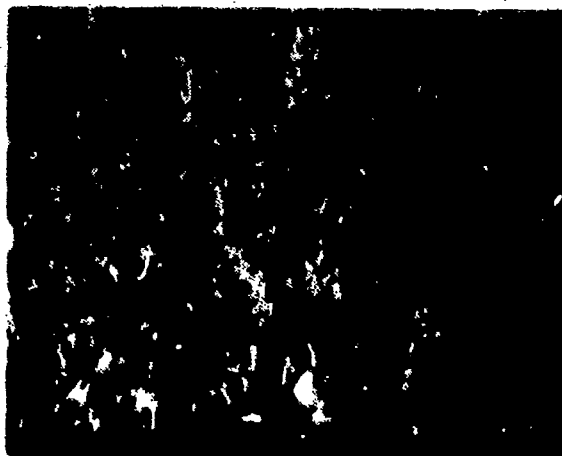


Figure 147. Typical Failure Initiation in Mismatched 0.25-Inch-Thick EB Welds in Specimen 4-3 (20X MAG)

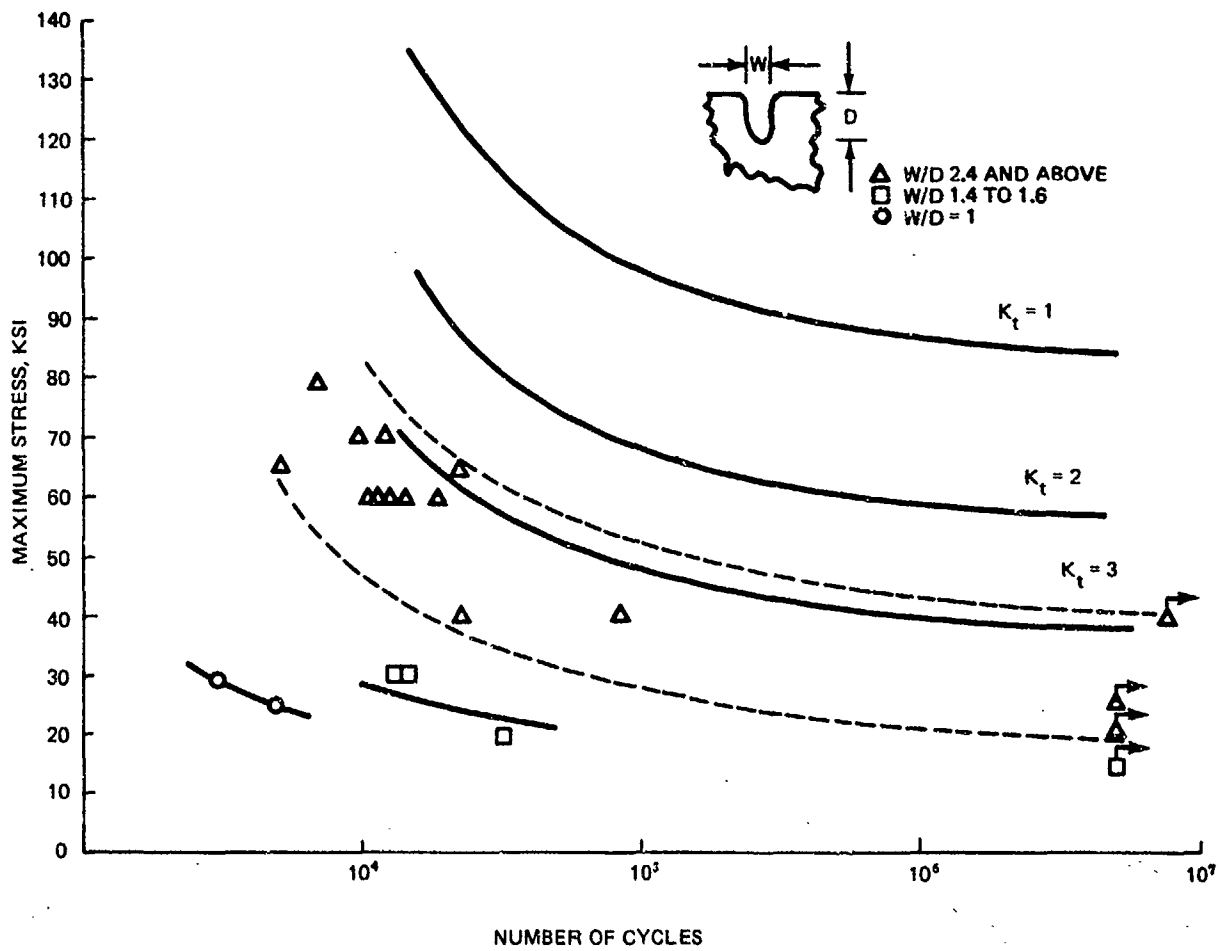


Figure 148. Fatigue Properties of 0.25-Inch-Thick EB Welds With Intentional Underfills



Figure 149. Typical Linear Failure Initiation Site Encountered In Intentional EB Underfills (20X MAG)

Width and depth measurements taken on each underfill configuration are included in Appendix B, Table B-11. Figure 149 shows a typical failure initiation at the radius of an underfill.

## F. SURFACE CONTAMINATION - 0.25-INCH-THICK WELDS

### 1. Fabrication of Experimental Weldments

After conventional acid cleaning, faying surfaces were wiped with a cloth wetted with Mobil SB12FOB4420EM vacuum oil. All other operating parameters were identical to those utilized in conventional welding. Both root and face surfaces of the weld were left intact, that is, in the as-welded condition. Pre-test radiography indicated all specimens to be free from internal defects.

### 2. Evaluation of Fatigue Test Results

The generated data are plotted in Figure 150. Since the obtained endurance values are in close proximity to the  $K_t=3$  curve, they are comparable to values expected for conventional weldments tested without prior machining of weld contours. A typical contour of weldments produced in the course of these studies is shown in Figure 151.

The results of a microhardness survey conducted on cross-sections of contaminated welds are shown in Figure 152. No significant microhardness variations were detected.

Fractographic analysis detected fine, scattered 0.001-inch porosity in one of the specimens (Figure 153). Numerical data on fatigue endurance values and results of fractographic evaluations are presented in Appendix B, Table B-12.

## G. LACK OF PENETRATION - 1.5-INCH-THICK WELDMENTS

### 1. Fabrication of Experimental Welds.

Two levels of lack-of-penetration were obtained by decreasing the beam, voltage and beam current settings and increasing travel speed on the final weld pass (which followed the locking pass.) Minor and extensive lack-of-penetration levels were obtained by decreasing the 55kv and 300 milliamp. settings utilized in conventional manufacturing to 45kv - 275 milliamp. and 40 kv -250 milliamp, respectively. In addition, travel speed was increased in both cases from 40 to 45-ipm. Incomplete fusion was detected by both, radiographic and ultrasonic "C" - scan techniques.

### 2. Evaluation of Fatigue Data

Fractographic examination showed that the zone of incomplete fusion was 0.44-inch-wide (average value) in Specimens 4-1, 4-2 and 4-3 (Figure 154), and in the 0.010 to 0.020-inch range in Specimens 1-1, 1-2, and 1-3 (Figure 155). Both types of specimens exhibited a drastic lowering of fatigue endurance as shown in Figure 156. The effect of variation in the extent of the lack-of-penetration appeared to be minor, however.

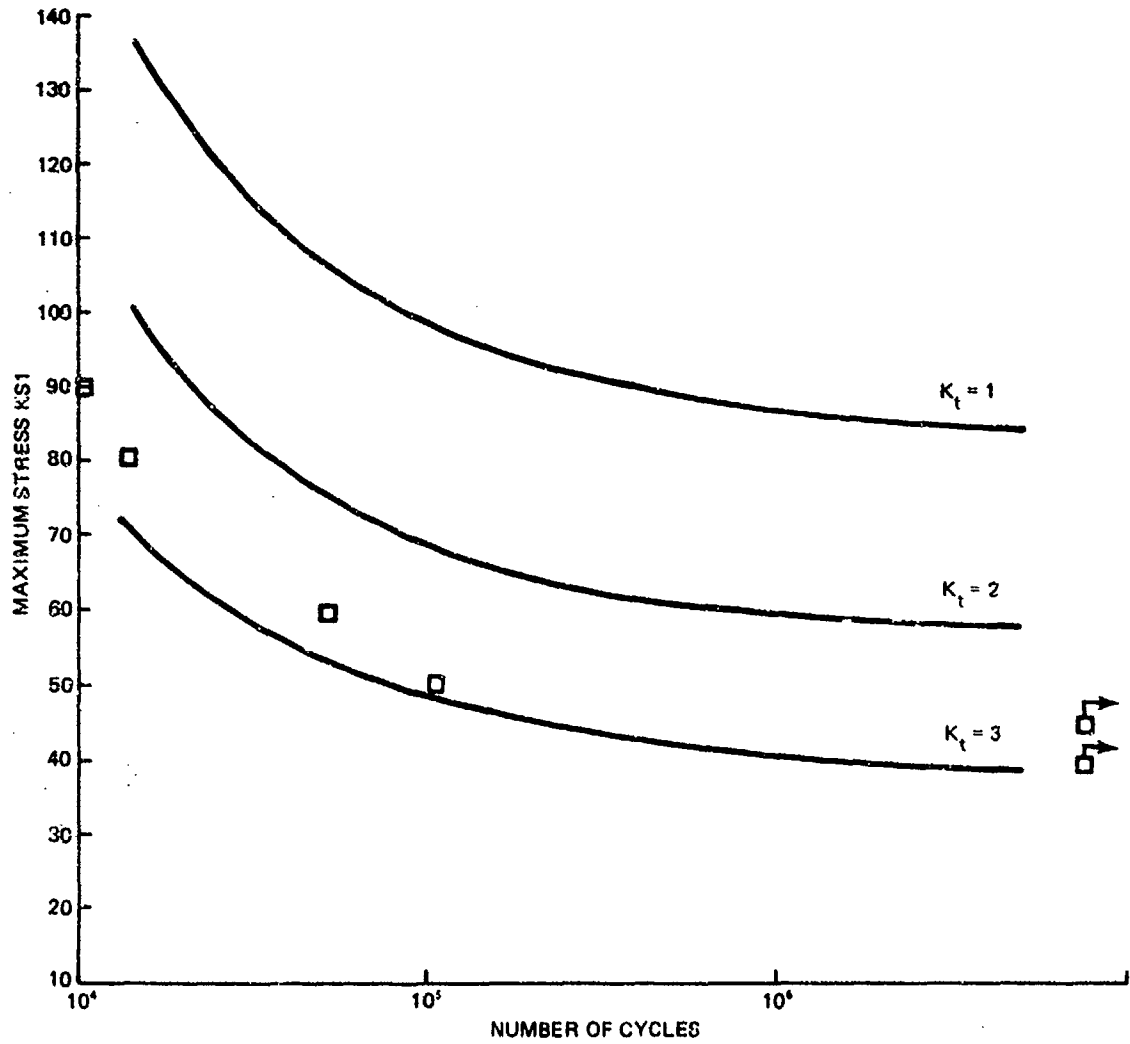


Figure 150. Fatigue Endurance of Surface Contaminated 0.25-Inch-Thick EB Welds

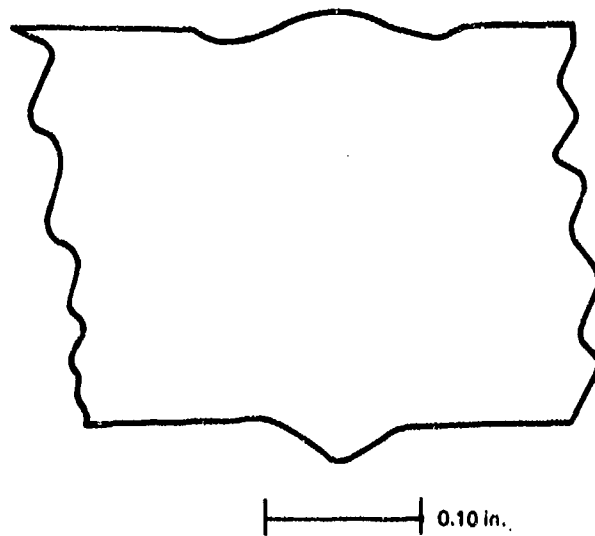


Figure 151. Typical Contour of Surface-Contaminated 0.25-Inch-Thick EB Weldments

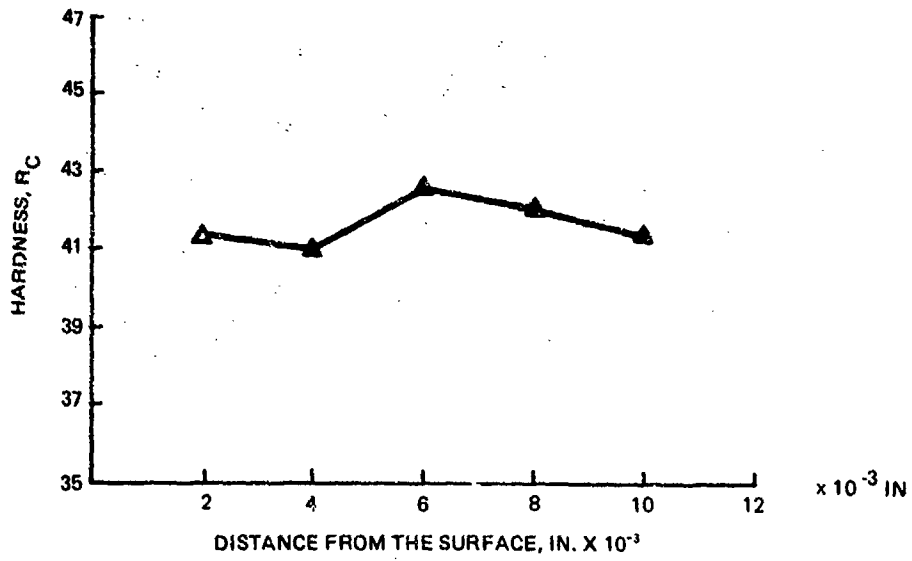


Figure 152. Micro Hardness Survey on Cross-Sections of Surface Contaminated EB Welds

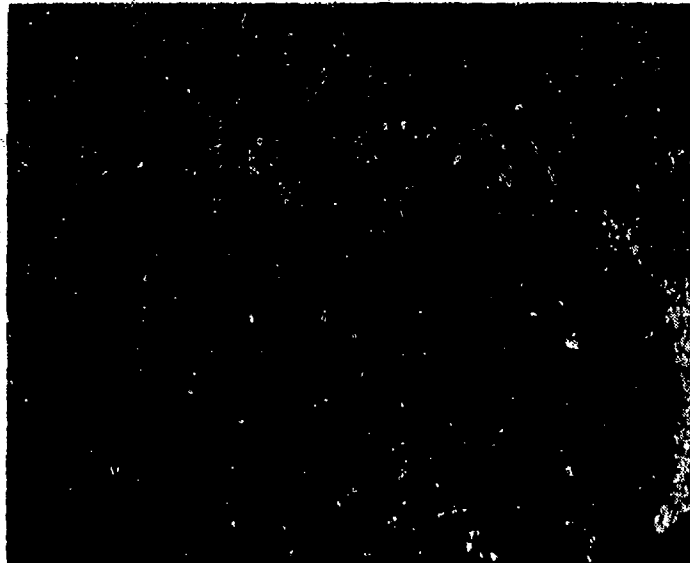
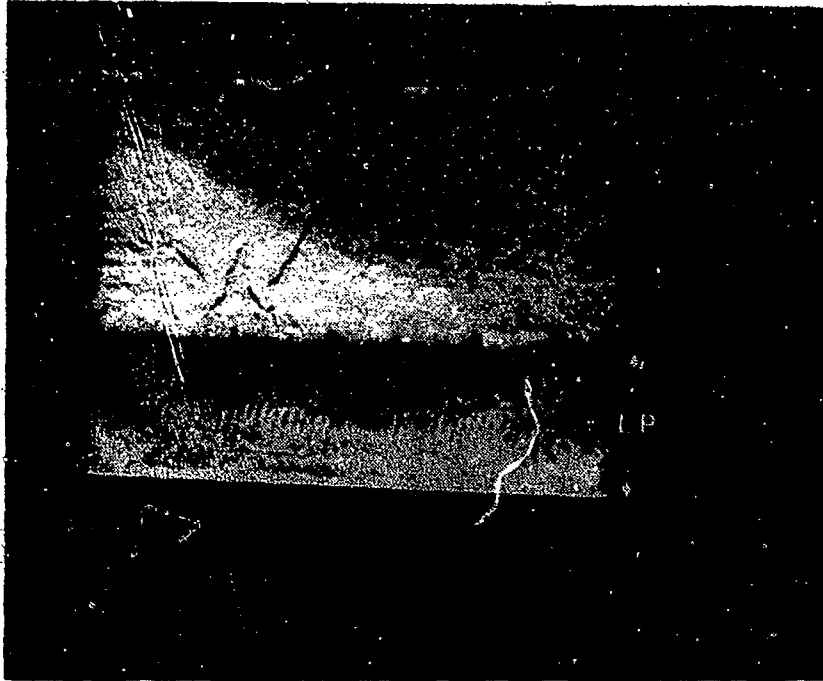
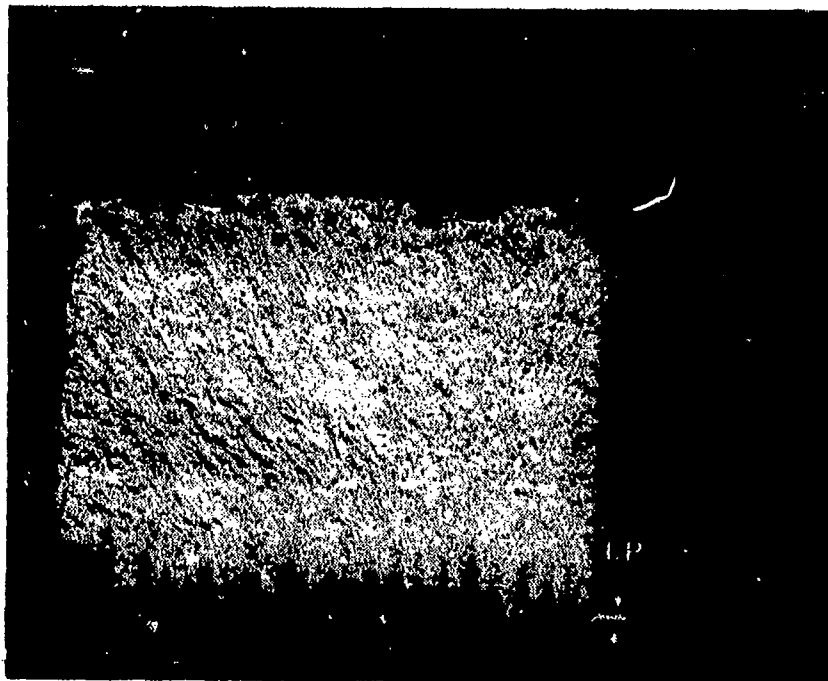


Figure 153. Typical (Linear) Surface Failure Initiation in Surface Contaminated Weldments



**Figure 154. Typical Lack-of-Penetration Defect in 1.5-Inch-Thick EB Welds 4-1, 4-2 and 4-3 (1.5X MAG)**



**Figure 155. Typical Lack-of-Penetration Defects in Specimens 1-1, 1-2 and 1-3 (1.5X MAG)**

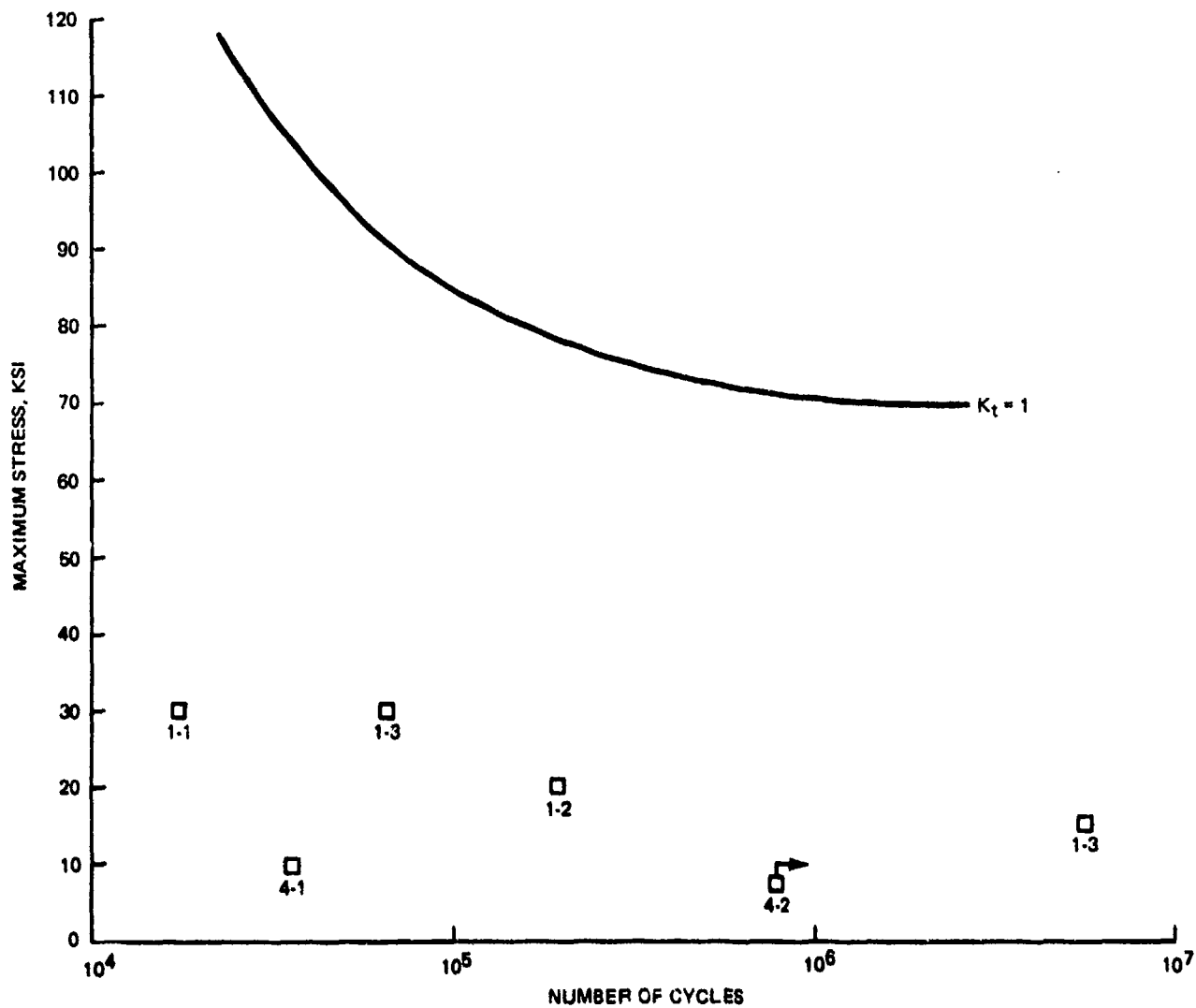


Figure 156. Fatigue Endurance of 1.5-Inch-Thick EB Welds with Lack-of-Penetration Defects

## H. FATIGUE ENDURANCE OF EB WELDMENTS CONTAINING BURSTS

### 1. Fabrication of Experimental Welds

Experimental welds containing (intentional) bursts were produced utilizing a weld blank assembly especially designed to induce a change in the shape of the molten puddle and to simulate rapid cooling conditions existing after extinction of the beam. Considerations involved in design of the experimental weld assembly have been discussed in details in Section 3.

Cylindrical inserts, 1.5 inches in both length and diameter, containing intentionally induced bursts were removed from the weld and radiographically inspected. The bursts were found to extend from a point 1/4 inch to 3/8 inch from the periphery of the insert - 0.175 to 0.300 inch toward the center of the weld (top view). In depth, the bursts extended to 0.400-0.500 inch from the (face) subsurface.

Difficulties were encountered in attempts to incorporate burst-containing inserts into test panels: radiography of circumferential welds revealed extensive defects. The presence of these defects was attributed to the fact that no conventional start- and end tabs could be utilized in circumferential welding. Attempts to repair weldments by rewelding from both sides using less penetrating beams were not successful.

Intermittent machining operations to remove contours of circumferential beams prior to NDI evaluations decreased thickness of test panels and thus exposed some bursts to the surface.

Subsequently the inserts were removed from the test panel and remachined to rectangular shapes. These modifications permitted the utilization of straight welds and conventional "start" and "stop" tabs. The final radiographic and ultrasonic examinations verified presence of original bursts in test specimens.

### 2. Evaluation of Fatigue Data

Experimental data for 1.5 inch thick EB weldments containing intentional bursts are plotted in Figure 157. It is evident that presence of bursts led in all cases to a drastic reduction of fatigue characteristics.

Figures 158 and 159 illustrate typical failure initiation sites detected by subsequent fractography. Of the five specimens tested, only specimen No. 3 contained an interior burst; bursts in other specimens were exposed to the surface and contained some foreign residues. Although all bursts reduced drastically fatigue endurance of weldments, the specimen with an internal burst (No. 3) compared favorably to those containing surface-exposed bursts.

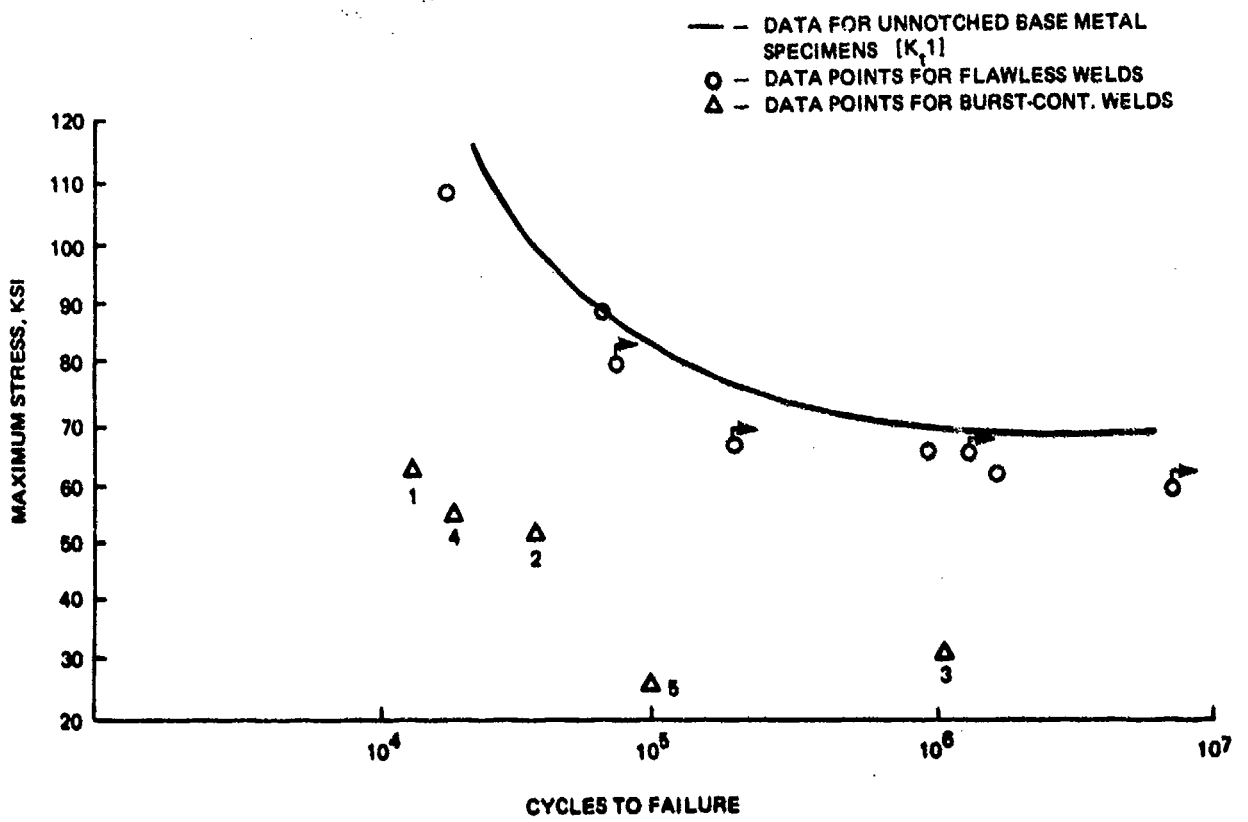
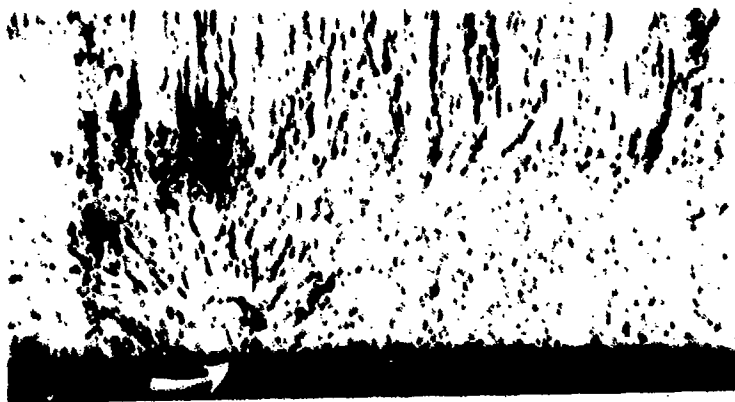
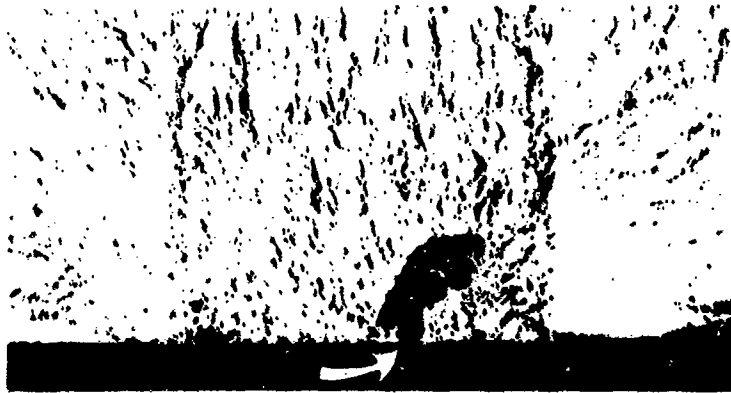


Fig. 157 Fatigue Endurance of 1.5-Inch-Thick EB Welds Containing Bursts



**Fig. 158** Burst Indications Detected in B-3 Weld by (1) Metallography (Top, 2.5 X Magn.), (2) Ultrasonic C Scan (Middle, 2.5 X Magn. of the Printout), and (3) Radiography (Actual Size)



**Fig. 150** Fracture Surfaces in Specimens B-1 (Top) and B-4 (Bottom) Showing Fracture Initiations (Arrows) at Surface-Connected Bursts. Magn. 2.5 X

## I. SUMMARY

Fatigue endurance limits [ $10^6$  cycles] for machined flawless EB weldments were determined to be: 80 ksi for 0.080 inch-thick welds, 70 ksi for 0.25-inch-thick welds and 65 ksi for 1.5-inch-thick welds. For porosity-containing 0.080-inch-thick welds, no significant deviations were apparent in test data generated in 20 cpm and 1800 cpm tests. Above 100 ksi level, no consistent relationship between the fatigue endurance and size and location of porosity was apparent. At lower stress levels, specimens with linear radiographic indications exhibited lower fatigue endurance caused by heavy concentrations of fine porosity. Validity of predicting fatigue endurance of specimens with isolated internal porosity based on its size and distance from the surface could not be verified by experimental data.

For 0.25-inch-thick weldments, some specimens were machined from flawless portions of the welds designed to induce porosity. Fatigue endurance of these specimens was comparable to that of flawless welded specimens produced by conventional techniques. Fine linear porosity did not produce significant lowering of fatigue endurance in 0.25-inch-thick weldments. Clusters of fine porosity and surface-connected pores resulted in a significant lowering of fatigue endurance, especially for pore diameters in excess of 0.010 inch. Large surface voids and missed seams resulted in a drastic lowering of fatigue endurance.

Techniques utilized in generation of intentional porosity in 1.5-inch-thick weldments may have resulted in contamination of the weld metal, as indicated by fatigue characteristics of specimens machined from flawless portions of these weldments. Fatigue endurance of porous 1.5-inch weldments was related to the number and size of internal voids. Burst-containing welds exhibited drastic reduction in fatigue properties. Feasibility of utilizing acoustic emission monitoring in studies of failure initiation and propagation was established.

Mismatch of faying surfaces in 0.25 inch joint resulted in drastic lowering of fatigue endurance. Data were generated on fatigue properties of 0.25 inch weldments for various depth/width ratios of underfills. Intentional contamination of faying surfaces with vacuum oil did not result in a significant lowering of fatigue endurance of weldments. Lack-of-penetration defects in 1.5-inch weldments resulted in a drastic decrease in fatigue endurance.

SECTION VI  
FATIGUE ENDURANCE OF MECHANIZED PLASMA-ARC WELDED  
(PAW) 0.25-INCH-THICK WELDMENTS  
PHASE II

A. INTRODUCTION

This section presents data on fatigue endurance of flawless and (intentionally) defective PAW weldments. The data are presented in the following sequence:

- Flawless welds
- Porous welds
- Mismatch
- Underfills and undercuts
- Reinforced welds
- Surface-contaminated welds
- Summary

B. FLAWLESS WELDS

1. Fabrication Procedure

Flawless PAW weldments were prepared by joining blanks with squared straight-butt faying surfaces that had been cleaned by conventional acid techniques and also wiped with MEK solvent. Argon was used as the orifice gas in both shielding and backup operations. Radiography was performed on as-welded joints and after the face and root contours were machined flush with the surface. In both instances, all specimens were free of RT indications.

2. Evaluation of Fatigue Data

Fatigue endurance data are plotted in Figure 160. The data points were distributed along a smooth curve with a minimum of scatter and an indicated  $10^6$  cycle endurance limit at approximately 78 ksi. Four of the specimens (1-1, 2-2, 2-4 and 3-2) failed in the base metal. Of the eight specimens which failed in the weld, failure initiated on the surface in one of the specimens (1-2) with no porosity in the immediate vicinity, and at a 0.002-inch pore, 0.070 inch from the surface in another specimen (3-3). Failure initiation sites in the remaining six specimens were associated with a linear arrangement of isolated 0.001 to 0.003-inch pores 0.020 to 0.030 inch from the face-side of the weld (Figure 161). Since about an 0.012-inch layer was removed while machining the weld contours flush with the surface, it was estimated that this line of isolated pores was originally located 0.035 to 0.045 inch from the face of the weldment. It is interesting to note that although the size and concentration of pores in specimens with intentionally induced porosity (Paragraph B) were increased, the basic linear arrangement and the distance from the (face-side) surface remained essentially the same. A typical linear arrangement of pores detected in flawless, plasma-arc welded specimens is shown in Figure 161. Data on fatigue endurance values and results of fractographic evaluations are presented in Appendix B, Table B-13.

## C. POROUS WELDS

### 1. Fabrication Procedure

Techniques utilized to intentionally induce porosity included swabbing faying surfaces with 35% HNO<sub>3</sub> - 5% HF solution, swabbing oil on one side of the butt joint, long-time exposure to shop environment and simulated handling without protective gloves, or a combination of these factors. Other process variables were identical to those used in welding the flawless specimens. Contamination techniques utilized for each blank are listed in Appendix B, Table B-14.

### 2. Evaluation of Fatigue Data

Fatigue endurance data are plotted in Figure 162. All but three of the experimental data points fell within a rather narrow band. Two values above this band

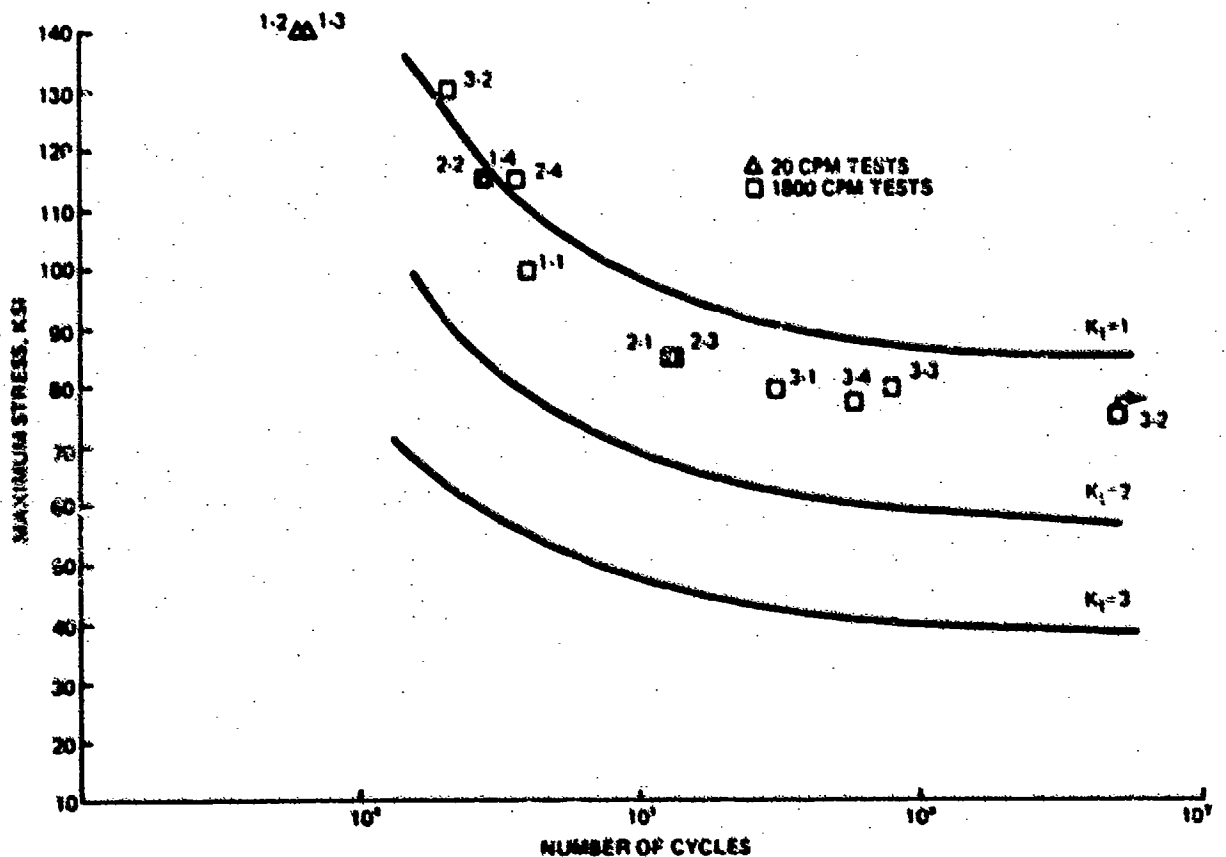


Figure 160. Fatigue Endurance of Flawless PAW Weldments



Figure 161. Typical Linear Arrangement of Isolated Pores Detected in Some Flawless PAW Specimens (20 X MAG)

(3-F and 4-F) were for specimens without pre-test RT indications. The sample below the lower boundary of the band (7-3) had a six-pore cluster in the immediate vicinity of the (edge) surface.

All specimens with pre-test RT indications had one common feature - a linear porosity band at the face-side surface which was detected by radiographic and fractographic analyses. The width of this band varied from 0.010 to 0.030 inch; the median value was 0.020 inch. The distance of this band from the face-side surface of the test specimen varied from 0.010 to 0.040 inch (probably a function on the amount of material removed in machining weld contours flush with the surface). In all specimens, the failure initiated in one or several pores contained in this band, except specimen 7-4 in which the failure initiated at a surface pore at the root-side of the weld. Pre-test radiography described this band as linear porosity on the upper edge of the weld. The size of pores indicated in RT data corresponded closely to actual measurements taken in the course of fractographic analyses. A typical distribution of pores within the porosity band is shown in Figures 163 and 164. In machining the reduced sections of some test specimens, pores contained in the band were brought into the immediate vicinity of the (edge) surface of the specimens. The fatigue endurance values of these specimens were in the lower portion of the data band shown in Figure 162 (for example, Specimens 5-2, 5-3 and 8-4). In Specimen 7-3, the surface-proximity effect was aggravated by the clustering arrangement of pores. Detailed data on the results of fatigue endurance tests and fractographic studies are incorporated in Appendix B, Table B-14.

#### D. MISMATCH

##### 1. Fabrication Procedure

Mismatch defects in PAW weldments were produced by positioning 0.016 and 0.025-inch shims under one of the blank halves to be joined. The parameters used in welding of mismatched plates were identical to those used for the flawless specimens. Specimens machined from blanks representing two levels of mismatch were positioned

on an optical comparator and their exact contour was traced at 10X magnification utilizing graphpaper superimposed on the viewing screen. Typical contours illustrating two levels of mismatch obtained are shown in Figures 165 and 166. Pre-test radiography indicated that all specimens were free from internal defects.

## 2. Evaluation of Fatigue Data

Experimental data on fatigue endurance of specimens representing two levels of mismatch are superimposed on  $K_t$  curves for the base material in Figure 167. It is evident that in both cases the values were either in close proximity to the  $K_t = 3$  curve or below it. Most data obtained for the 0.025-inch mismatch were from 5 to 10 ksi below corresponding values for the 0.016-inch mismatch. Fractographic evaluation of failure surfaces revealed linear initiation sites at the roots of the welds in locations indicated in Figures 165 and 166. A typical linear initiation site encountered in mismatched specimens is shown in Figure 168. Fatigue endurance data are summarized in Table B-15, Appendix B

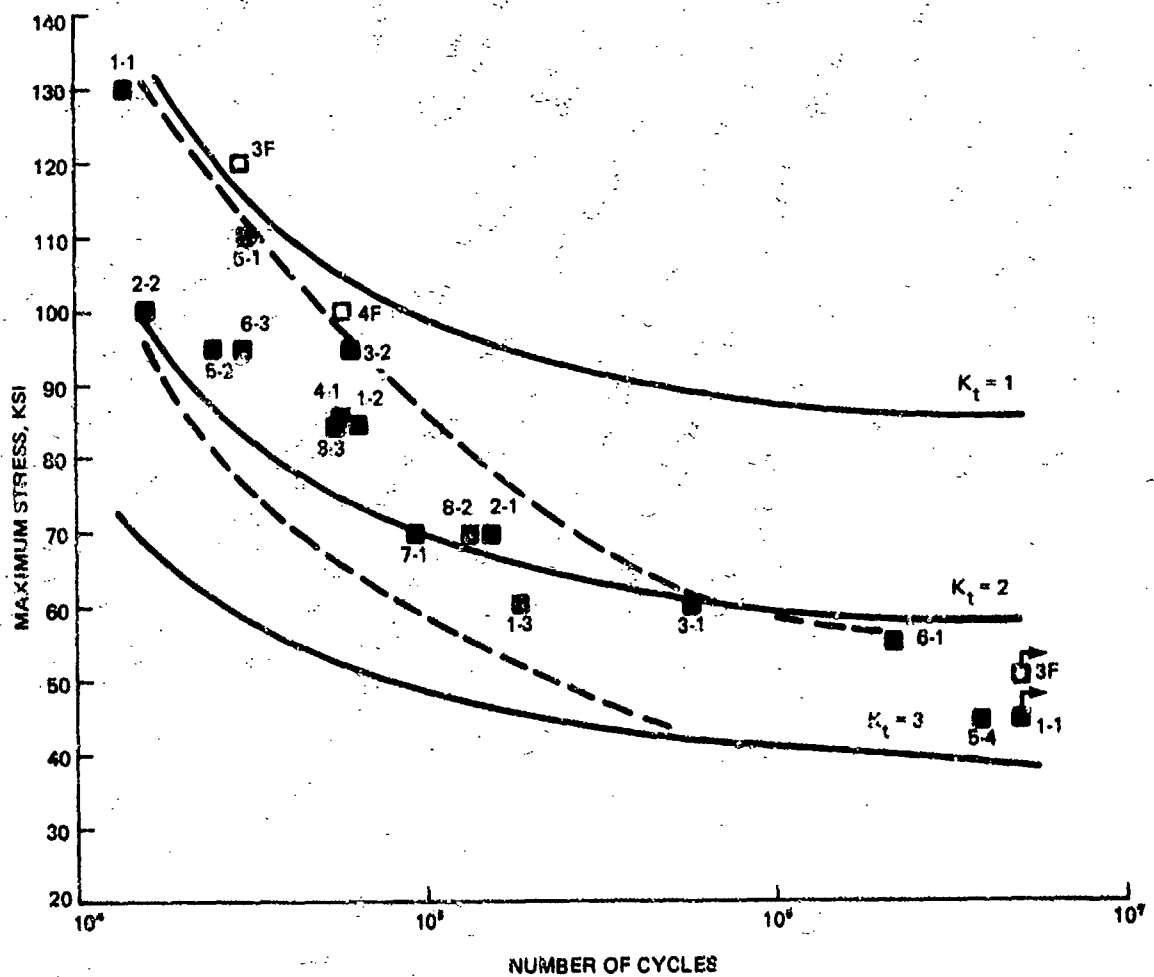


Figure 162. Fatigue Endurance of Porous 0.25-Inch-Thick Welds Produced by Mechanized PAW Techniques

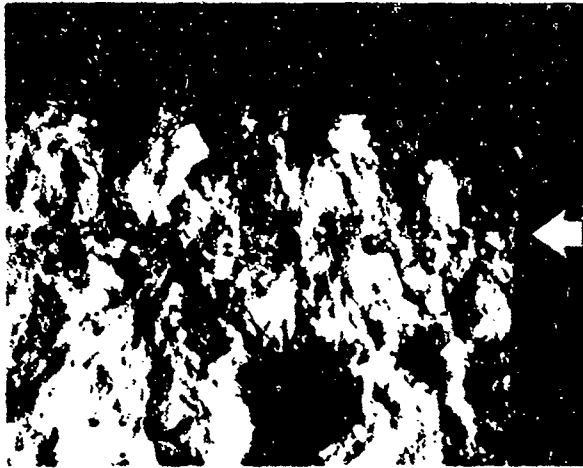


Figure 163. Typical Porosity Band Encountered in PAW Weld Specimen 2-2 with Intentionally Generated Porosity (20X MAG)

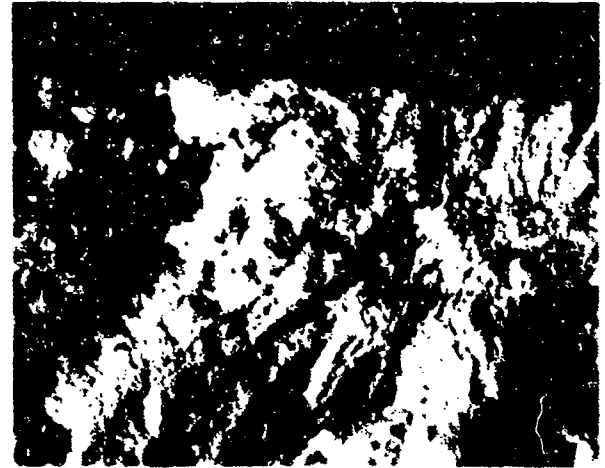
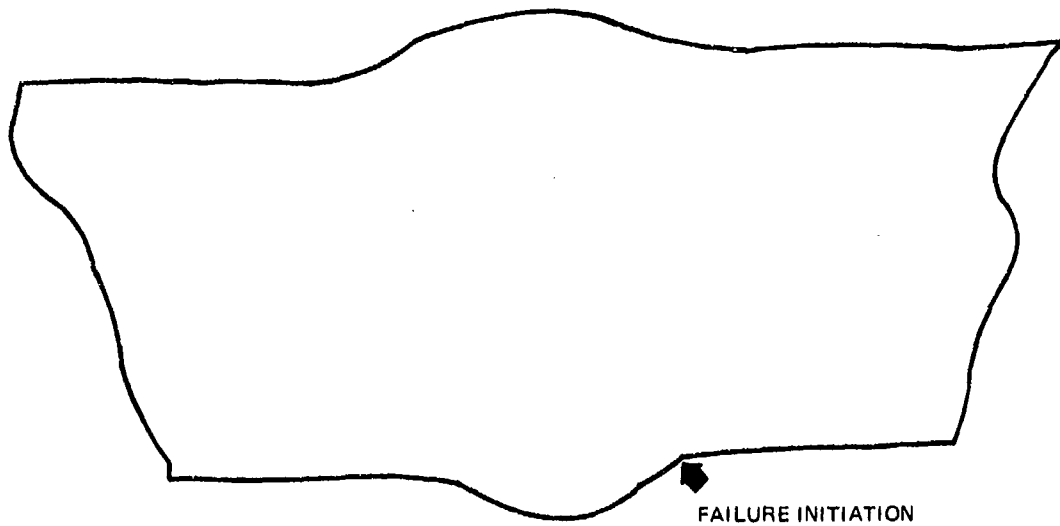


Figure 164. Porosity Band Detected in Specimen 4 PAW-P-1-2 (20X MAG)



0.10 IN.

Figure 165. Typical Contour of PAW Test Specimen with 0.016-Inch Mismatch

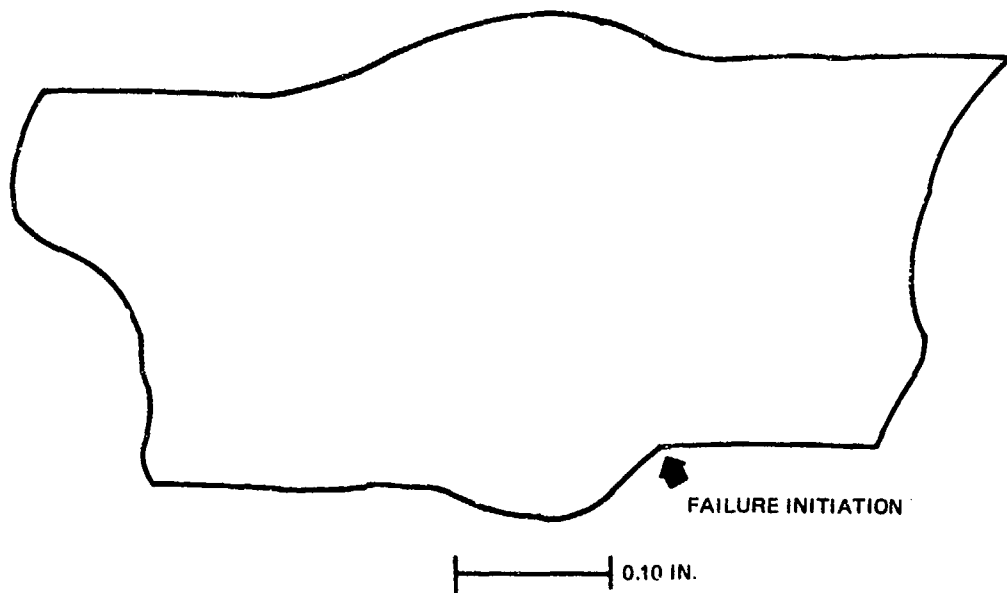


Figure 166. Typical Contour of PAW Test Specimen with 0.025-Inch Mismatch

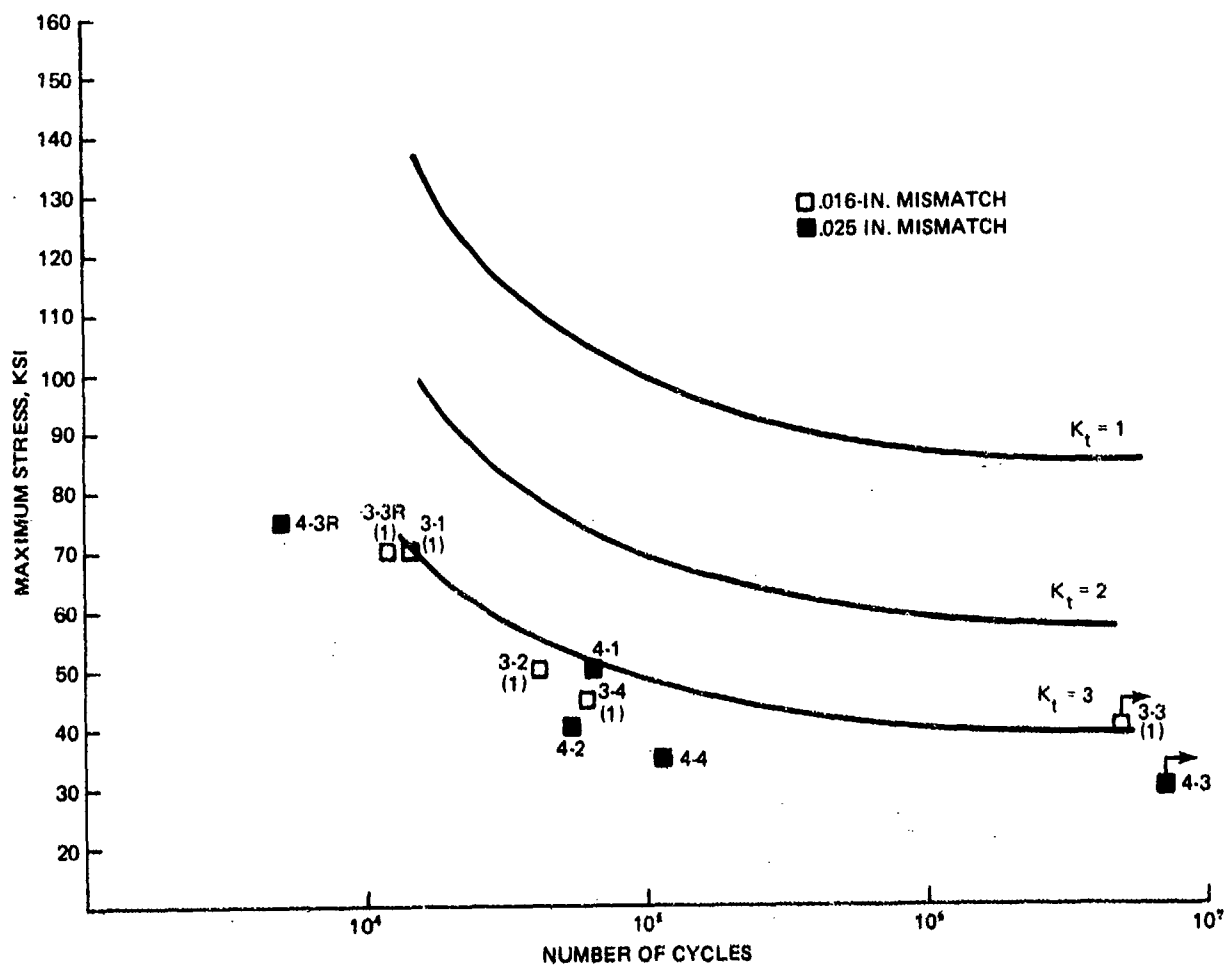


Figure 167. Fatigue Endurance of 0.25-Inch-Thick PAW Welds with Mismatched Faying Surfaces

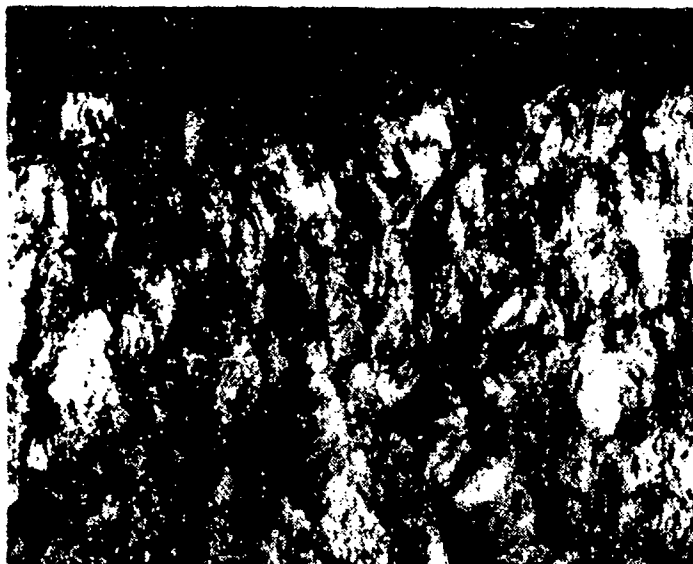


Figure 168. Typical Linear Failure Initiation Site Encountered in Mismatched 0.25-Inch-Thick PAW Welds (20X MAG)

## E. WELDS WITH UNDERFILL AND UNDERCUT DEFECTS

### 1. Fabrication Procedure

During fabrication of (intentional) underfill and undercut defect specimens, the current was increased from 235 amperes (used in manufacturing of flawless welds) to 260 and 300 amperes, respectively, and the slope gas flow was increased from 10 cfh to 11 and 13 cfh, respectively. Utilizing this approach, shallow underfills in the 0.005 to 0.010 inch-deep and 0.13 to 0.17-inch-wide ranges, and undercuts with depths and widths in the 0.005 to 0.015-inch and 0.050 to 0.150 inch ranges, respectively, could be produced. Both shallow underfill and shallow undercut defects were associated, however, with crowns at the root of the weld. The height, width and approximate radius of curvature of these crowns were in the 0.020 to 0.030-inch, 0.125 to 0.150-inch, and 0.125 to 0.140-inch ranges, respectively. A typical configuration of a shallow undercut obtained by these techniques is shown in Figure 169. Pre-test radiography detected no internal defects, and indications of external defects were detected only in some of the undercut configurations.

### 2. Evaluation of Fatigue Data

Experimental fatigue data are plotted in Figure 170. It is evident that fatigue characteristics of PAW weldments with shallow underfill or undercut defects are generally in the lower portion of the  $K_t = 1$  to  $K_t = 2$  range. Fractographic analysis of failed surfaces indicated, however, that in most of the underfill-type specimens and in many of the undercut-type test coupons, the failure initiated not at the face of the weld but at the crown created at the root of the weldments. A typical failure initiation site at the root of the weld is shown in Figure 171. A typical location of the (root) failure initiation with respect to the contour of the weld is shown in Figure 169. Attempts to correlate small differences in the radii of curvature at the (root) initiation sites with the fatigue endurance values obtained did not produce consistent results. Figure 172 shows a failure initiation in the surface undercut in Specimen UC 1-2. Data on fatigue endurance, defect characteristics and fractographic findings are listed in Appendix B, Table B-16.

## F. REINFORCED WELDS

### 1. Fabrication Procedure

Weldments were fabricated utilizing normal production welding parameters. Two levels of reinforcement were obtained by welding blanks with and without the use of Ti-6Al-4V filler wire. Typical weld contours produced by these techniques are shown in Figures 173, 174 and 175. Pre-test radiography did not reveal any internal or contour defects in any of the specimens.

### 2. Evaluation of Fatigue Data

The experimental data representing both levels of reinforcement are shown in Figure 176. These plots show that for specimens produced without the use of filler wire, the fatigue endurance values obtained are in the lower portion of the  $K_t = 1$  to  $K_t = 2$  range. These findings are attributable to the shallow contours of the face and root reinforcements (Specimens 2-1 through 2-4). On the other hand, specimens 1-1 through 1-4, which were welded with filler wire, had more pronounced reinforcement contours on the face and root of the weld (Figure 173). And except

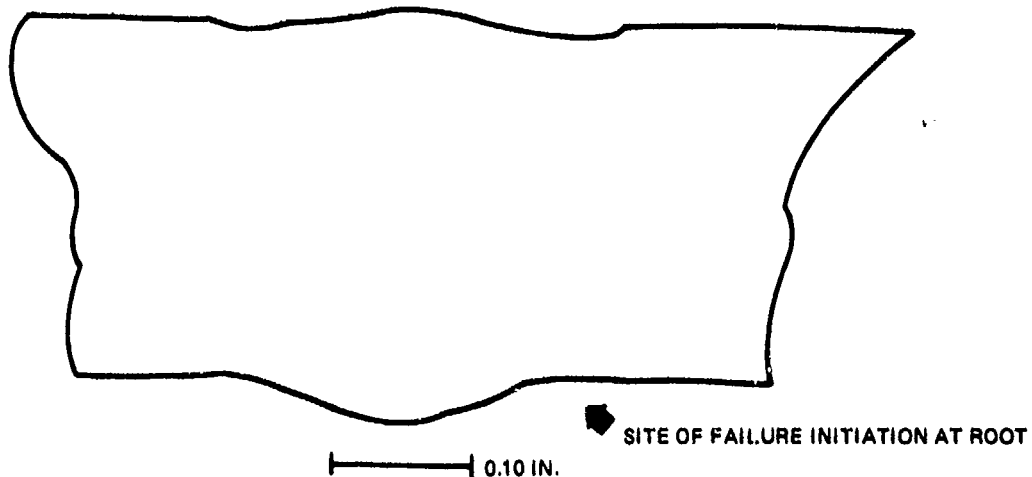


Figure 169. Contour of 0.25-inch-Thick PAW Weld with Shallow Undercut Defect (Specimen UC2-3)

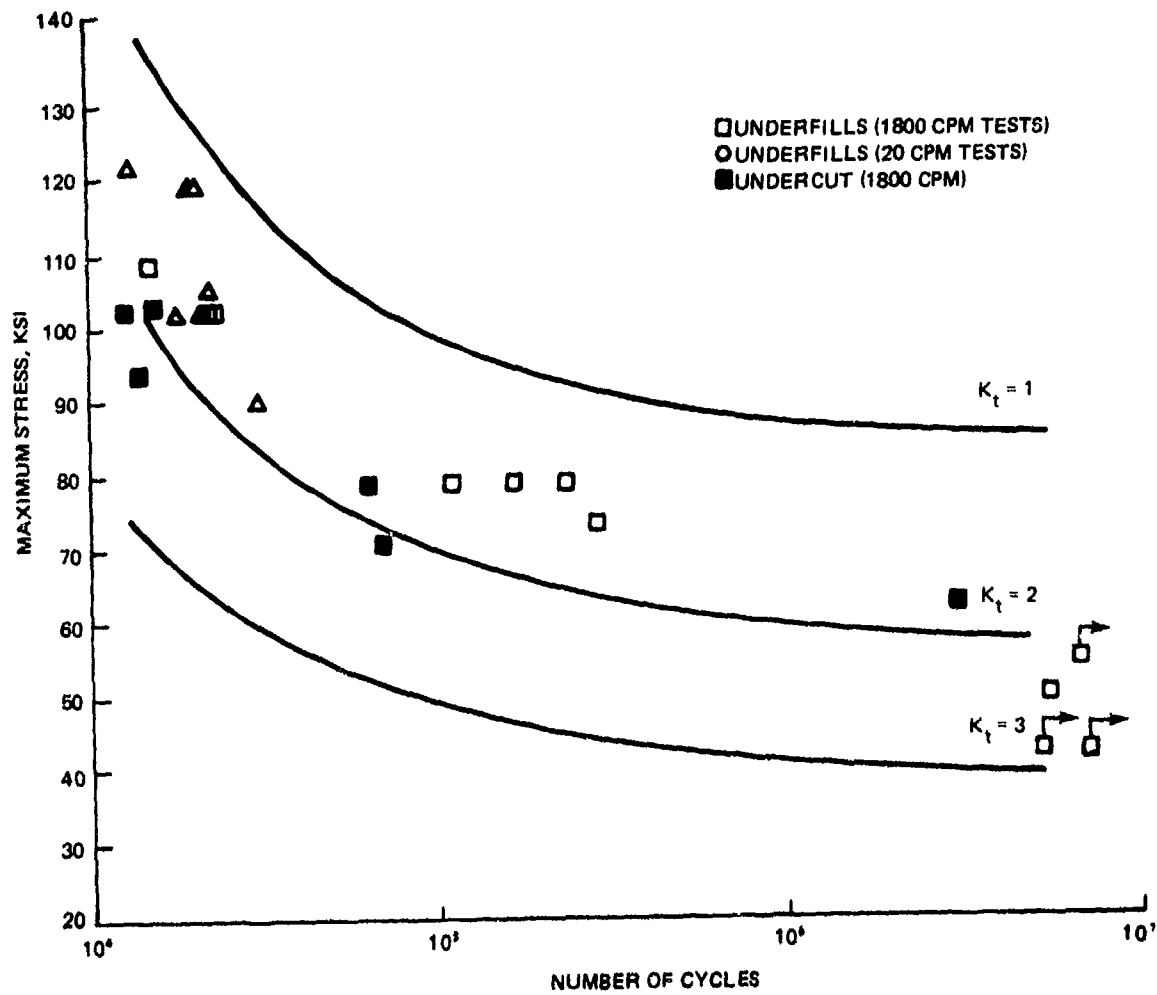


Figure 170. Fatigue Endurance of 0.25-Inch-Thick PAW Weldments with Minor Underfill and Undercut Defects

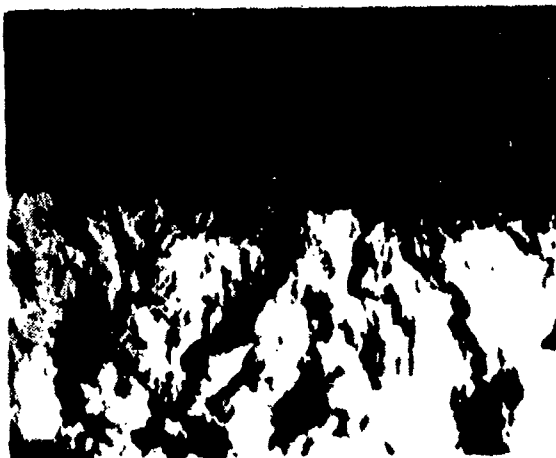


Figure 171. Typical Linear Failure Initiation at the Root Encountered in 0.25-Inch-Thick PAW Specimens with Minor Underfills and Undercuts (20X MAG)

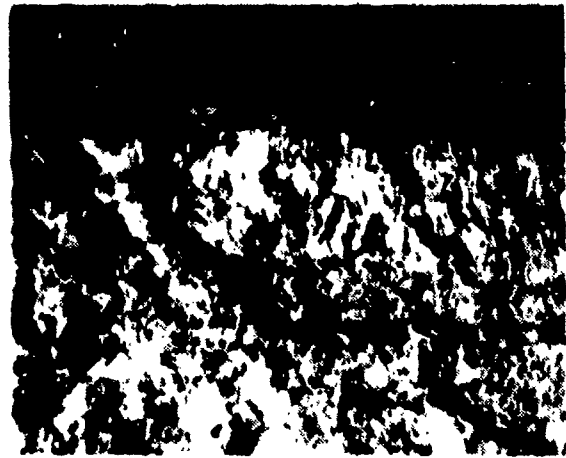
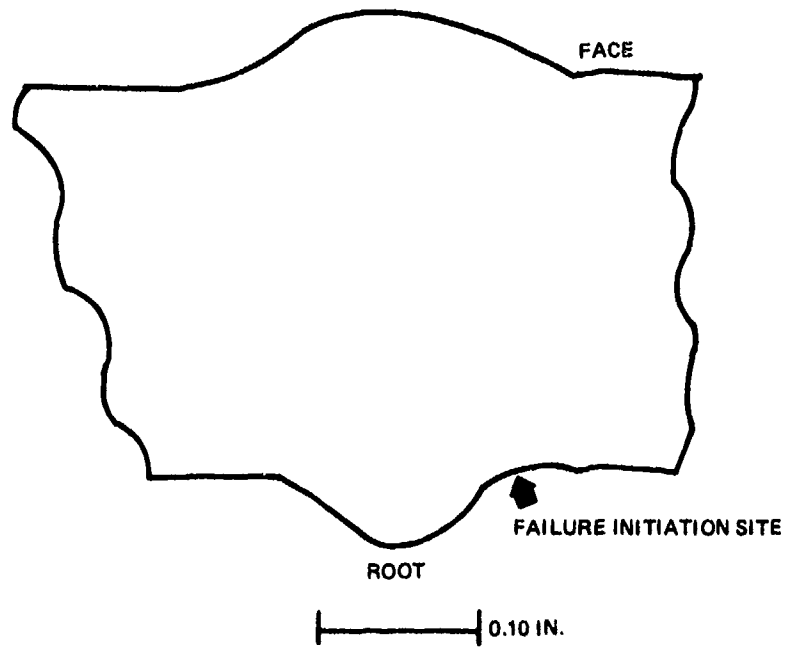
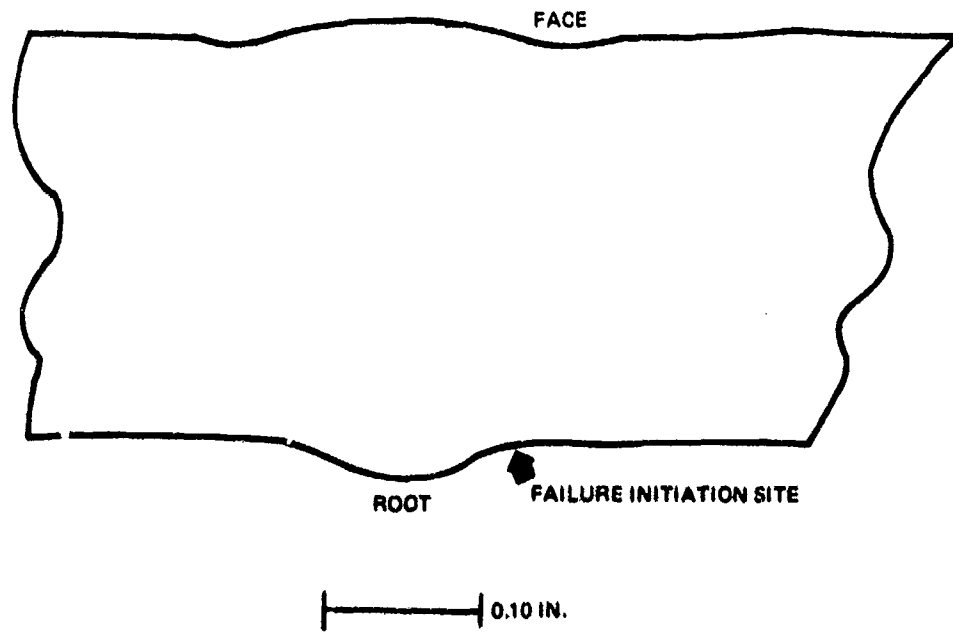


Figure 172. Failure Initiation Site at Surface Undercut in Specimen UC 1-2 (20X MAG)



**Figure 173. Typical Contour of 0.25-Inch-Thick Plasma-Arc Welds Produced Using Filler Wire.**



**Figure 174. Typical Contour of 0.25-Inch-Thick Plasma-Arc Welds Produced Without Filler Wire.**

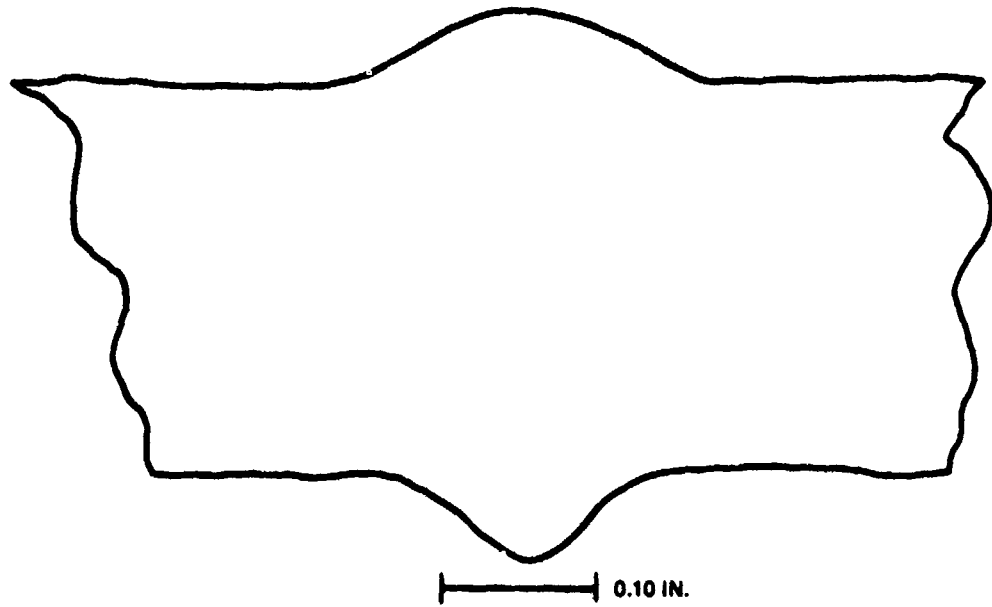


Figure 175. Weld Contour of Plasma-Arc Welded Specimen R-1-2

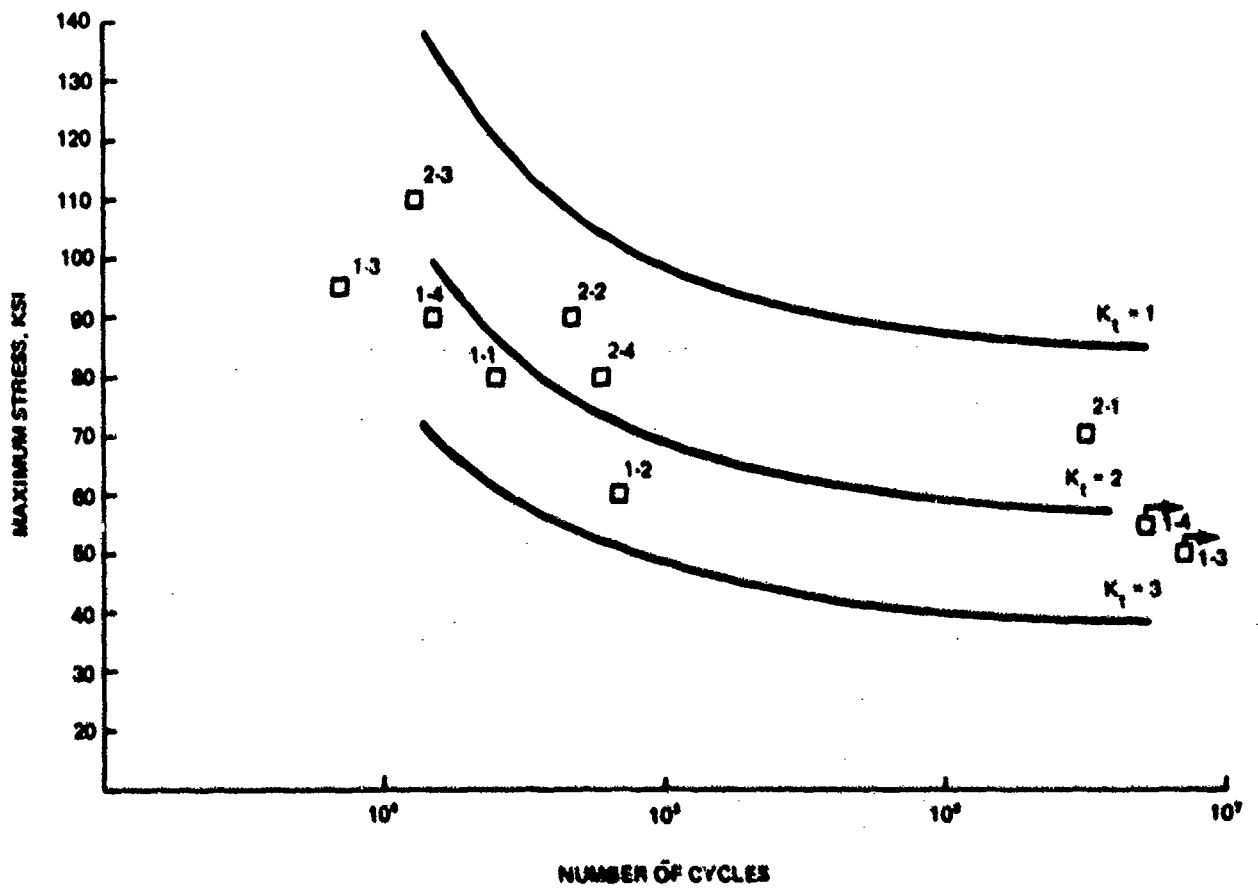


Figure 176. Fatigue Endurance of Reinforced 0.25-inch-Thick PAW Weldments

for Specimen 1-2, their fatigue endurance data were located in the upper portion of the  $K_t = 2$  to  $K_t = 3$  range. The contour of Specimen 1-2 (Figure 175) exhibited a narrower and more protruding root reinforcement which led to a noticeable lowering in fatigue endurance. All specimens failed at the root of the weldments as shown in Figures 173 and 174. A nondescript linear failure initiation detected in all specimens is illustrated in Figure 177. Fatigue endurance data are summarized in Appendix B, Table B-17.

## G. SURFACE-CONTAMINATED WELDS

### 1. Fabrication Procedure

Surface contamination was produced by reducing or eliminating the flow of protective trail-shield and/or torch-shield gases. Detailed data on the flow rate variations of protective gases are included in Appendix B, Table B-18. The weld blanks were processed by conventional cleaning techniques. Pre-test radiography did not indicate the presence of internal defects in any of the specimens. The specimens were tested in the as-welded condition, that is, without machining the face and root contours flush with the surface. A typical weld contour of the test specimens is shown in Figure 178. Discolorations were clearly detectable on all surfaces of weldments.

### 2. Evaluation of Fatigue Data

Experimental fatigue endurance data are presented in Figure 179. All data fell within the  $K_t = 2$  to  $K_t = 3$  range and were equivalent to those for the reinforced specimens with comparable weld contours shown in Figures 173 and 174. Microhardness readings taken on cross-sections of the experimental weldments failed to detect extensive hardness variations in the vicinity of the weld surface (see Figure 180). Failure initiated at the root of the weldments as shown in Figure 178, except for Specimens SU -1-2 and 2-4, which failed at the face crown. A typical failure initiation detected at fracture surfaces is shown in Figure 181. Data on contamination methods utilized and fatigue endurance of specimens are presented in Appendix B, Table B-18.

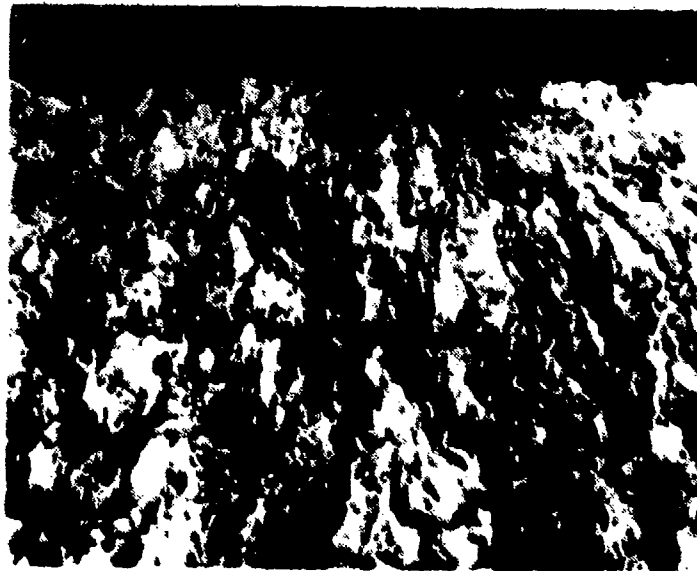
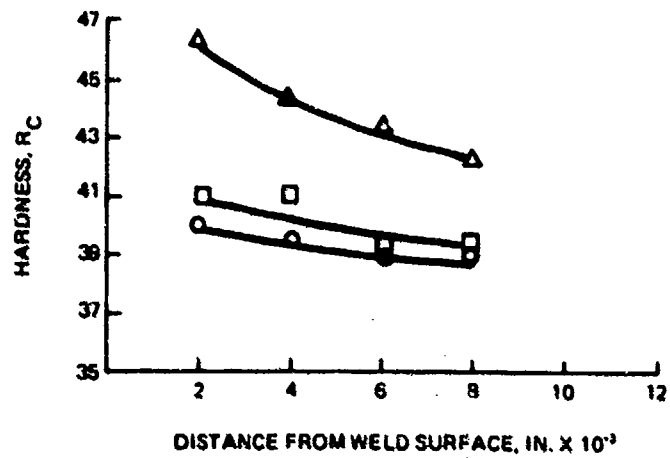
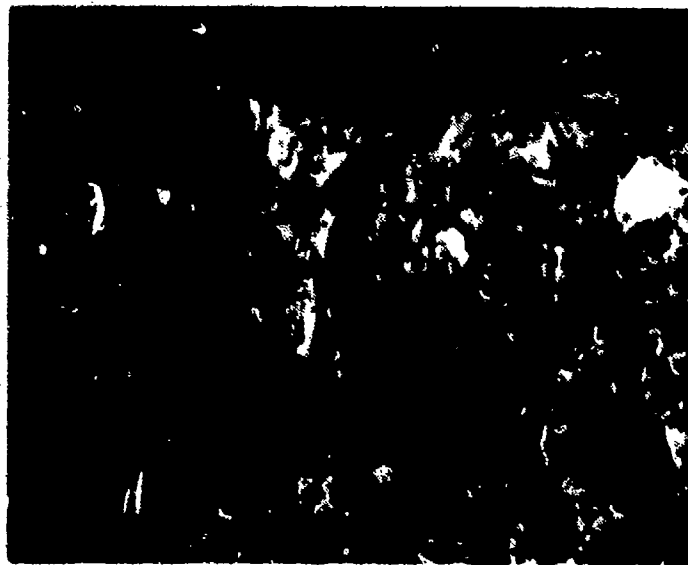


Figure 177. Typical Linear Failure Initiation Encountered in Reinforced 0.25-Inch-Thick PAW Weldments (20X MAG)





**Figure 180. Microhardness Measurements on Cross-Sections of Surface-Contaminated PAW Welds**



**Figure 181. Typical Failure Initiation Site in Surface-Contaminated PAW Weldments (20X MAG)**

## H. SUMMARY

Fatigue endurance limit ( $10^6$  cycles) for machined flawless 0.25 inch-thick PAW welds was determined to be 75 ksi.

All porosity-containing welds exhibited one common feature-linear arrangement of pores about 0.040 inch from the (original) face of weldments. Location of pores with respect to (edge) surfaces of test specimens had a detectable effect on fatigue endurance. Specimens machined from flawless portions of weldments designed to induce porosity exhibited fatigue characteristics comparable to those of flawless specimens produced by standard techniques.

Mismatched welds exhibited a drastic reduction in fatigue endurance. Data points for welds designed to produce minor undercut and underfills were in the lower portion of the  $K_t=1$  to  $K_t=2$  range. In most of these specimens, however, the failure initiated at the root of the weldments. Fatigue endurance data were generated for two levels of (face) reinforcements. Variations in shielding parameters failed to produce detectable variations of fatigue characteristics.

## SECTION VII

### FATIGUE CHARACTERISTICS OF 0.25-INCH-THICK GAS-METAL-ARC (GMA) WELDMENTS - PHASE II

#### A. INTRODUCTION

This section presents data on fatigue characteristics of flawless and (intentionally) defective GMA welds. The data are presented in the following sequence:

- Weld preparation
- Flawless welds
- Welds with undercuts and lack-of-penetration defects
- Porous weldments
- Summary

#### B. WELDMENT PREPARATION

Experimental GMA welds were fabricated utilizing a Linde Type SVI-500 power source, Solaky welding boom, and Linde Sigma Type ST-5 welding torch. Faying surfaces were machined to provide 90-degree included angles and 0.060 to 0.065-inch lands. Argon gas was used for torch and trailing shielding.

#### C. FLAWLESS WELDS

##### 1. Fabrication Procedure

Blanks intended for fabrication of flawless welds were cleaned by conventional processes and scraped prior to welding. Each joint was completed in two passes. After joining, the welds were radiographed and, if found free of defects, face and root contours were machined flush with the surface. Partially machined blanks were again radiographed and, if found acceptable, were machined into transverse weld specimens.

##### 2. Evaluation of Fatigue Data

Data generated in tension-tension ( $R=0.1$ ) fatigue tests are plotted in Figure 182. The values obtained at higher stress levels (100 ksi and above) are within the normal range of scatter around the  $K_t=1$  curve. At the low stress/high cycle region, however, considerable lowering of fatigue endurance is apparent. Specimen 1-2 failed in the base metal. Of the specimens which failed in the weld, failure sites were not associated with porosity in Specimens 1-3 and 4-1; in all remaining specimens, isolated pores 0.001 to 0.002-inch in diameter were found at failure initiations. Specimen 3-1, which had failure initiation at a 0.002-inch surface pore, exhibited abnormally low fatigue endurance. Figures 183, 184 and 185 illustrate three modes of failure initiation in flawless GTA welds. The results of fatigue tests and fractographic evaluations are summarized in Appendix B, Table B-19.

## D. WELDS WITH UNDERCUT AND LACK-OF-PENETRATION DEFECTS

### 1. Fabrication Procedure

Efforts to produce lack-of-penetration defects in experimental GMA weldments were based on a 1/16 -inch increase in the distance from faying surfaces to the contact tube containing the electrode. Although the desired defects could be produced, these techniques resulted also in the generation of pronounced undercuts on the face of the weld and in many instances the failure initiated at undercuts rather than lack-of-penetration defects.

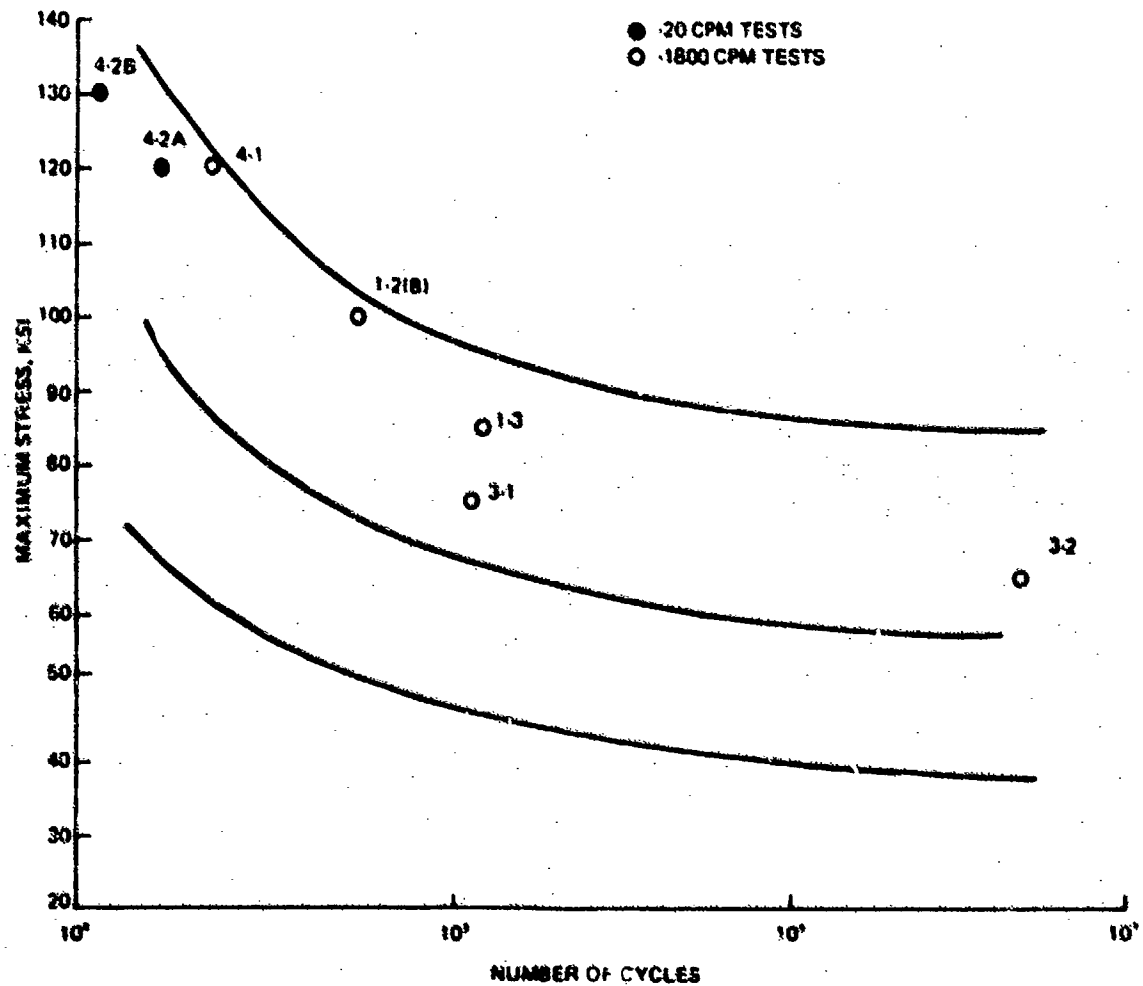
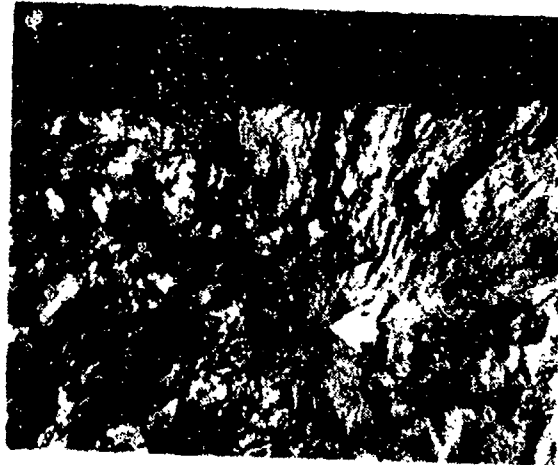


Figure 182. Fatigue Endurance of Flawless 0.25-Inch-Thick GMA Welded Specimens



**Figure 183. Failure Initiation Site Not Associated with Porosity in Specimen 1-3 (20X MAG)**



**Figure 184. Failure Initiation at Internal Porosity in Specimen 3-2 (20X MAG)**

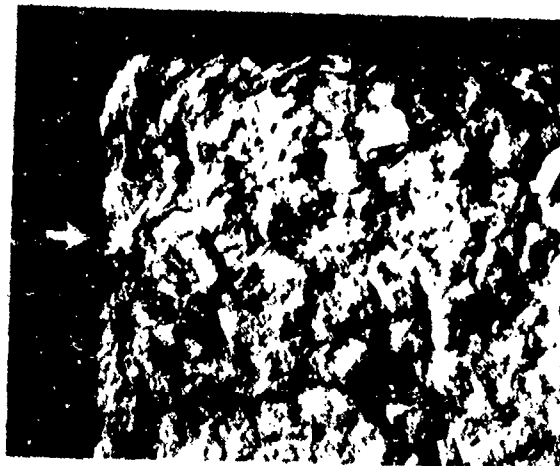


**Figure 185. Failure Initiation at a Face Pore in Specimen 3-1 (20X MAG)**

## 2. Evaluation of Fatigue Data

The results of fatigue tests are plotted in Figure 186. The data obtained fell within a narrow band below the  $K_t=3$  curve. The depth of the lack-of-penetration defects ranged from 0.006 inch in Specimen 6-4 (Figure 187) to 0.050 inch in Specimen 6-1. A lack-of-penetration defect with depth varying from 0.030 to 0.045 inch detected on the surface of Specimen P5-3 is shown in Figure 188; alignment of porosity along the boundary of the defect was also noticed. Width and depth dimensions of the undercut were in the range of 0.002 to 0.049 inch and 0.040 to 0.125 inch, respectively. Figure 189 shows the transverse contour of Specimen 5-4. Data on fatigue endurance and fractographic findings are listed in Appendix B, Table B20.

## E. FATIGUE ENDURANCE OF POROSITY-CONTAINING WELDS

### 1. Fabrication Procedure

The faying surfaces of blanks were contaminated either by No. 10 oil, handling without protective gloves, grit blasting, exposure to shop environment for long periods, or a combination of these factors. Other processing parameters were identical to those utilized in conventional GMA welding.

### 2. Evaluation of Fatigue Data

Fatigue endurance data are plotted in Figure 190. Analysis of the data indicated that, although some evidence of dependence of fatigue endurance on porosity size could be established in the  $10^5 - 10^6$  cycle range (Figures 191, 192 and 193), this trend could not be verified by fractographic data on other experimental specimens. One possible reason for this lack of correlation could be that the heavy concentration of porosity at the root portion of the weld and the fairly uniform size of the majority of the pores caused multiple failure initiations. Overlapping crack propagation zones made it very difficult to determine the primary initiation site. The results of fatigue endurance tests and fractographic evaluations are summarized in Appendix B, Table B21.

## F. SUMMARY

Fatigue endurance limit [ $10^6$  cycles] for machined flawless specimens was estimated to be 65 ksi. Lack-of-penetration and undercut defects reduced fatigue endurance of weldments to  $K_t=3$  range. Although dependence of fatigue endurance on the size of (subsurface) porosity was evident in the  $10^5$  cycle to  $10^6$  cycle range, this trend could not be verified for specimens tested at higher stress levels due to a frequent occurrence of multiple-failure-initiations.

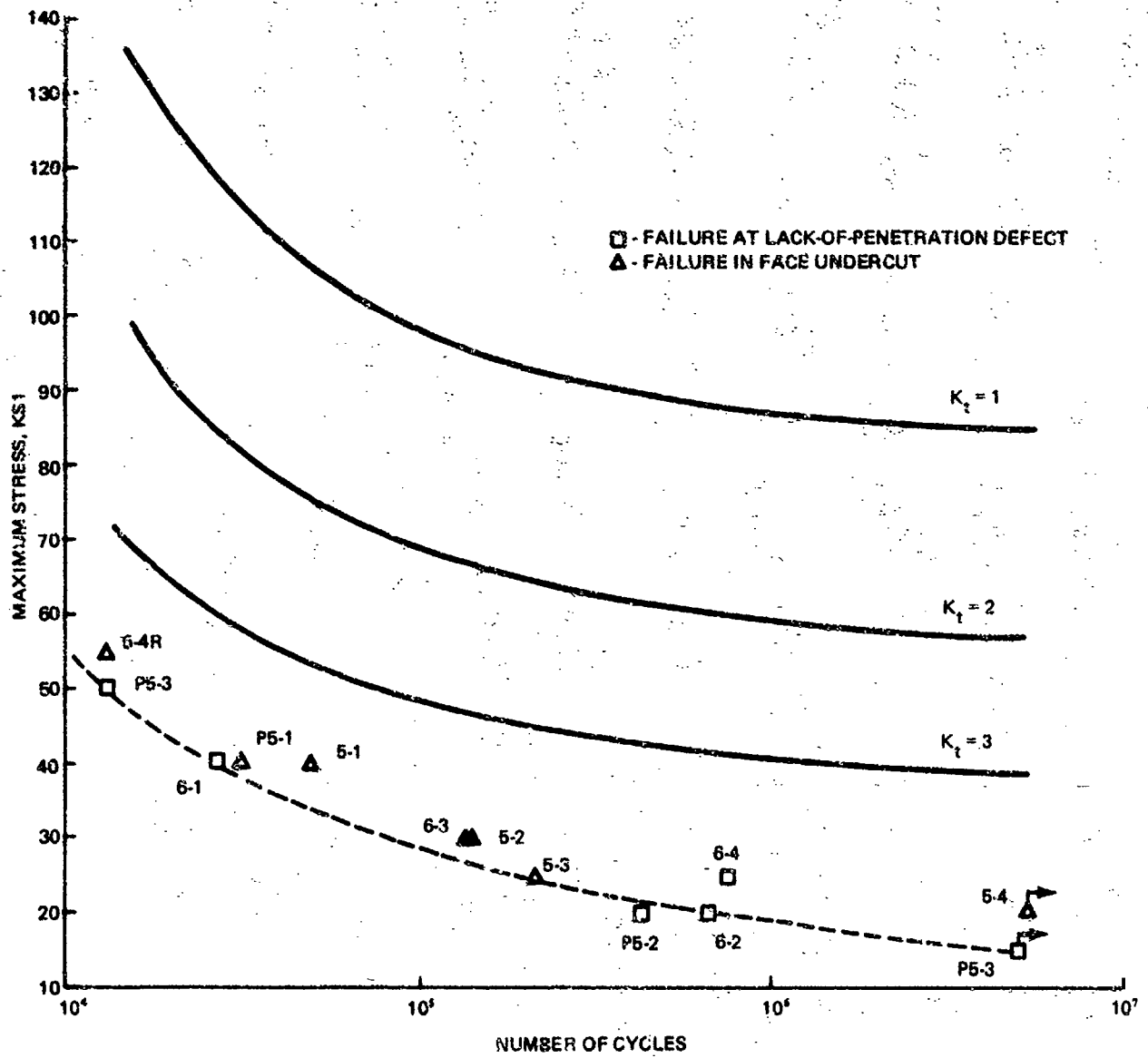


Figure 186. Fatigue Endurance of 0.25 Inch-Thick GMA Welds with Lack-of-Penetration Defects

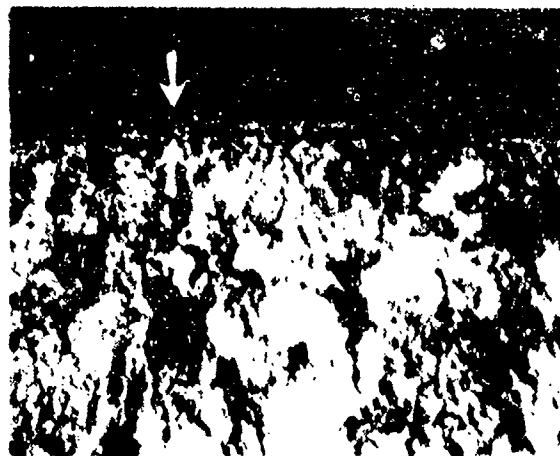


Figure 187. 0.006-Inch-Deep Lack-of-Penetration Defect in Specimen 6-4 (20X MAG)

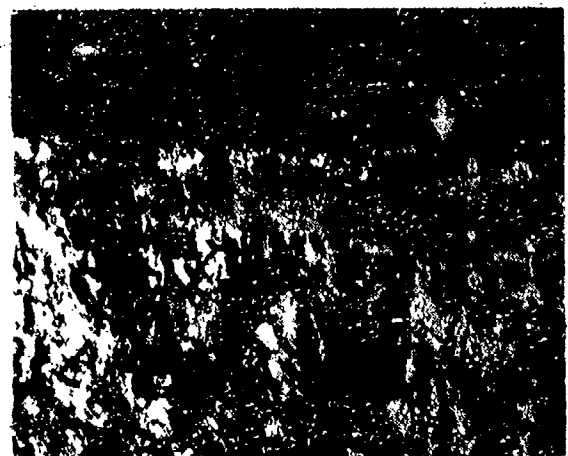
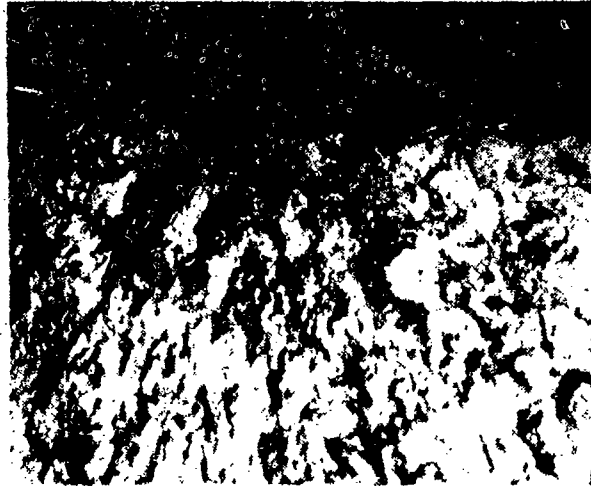
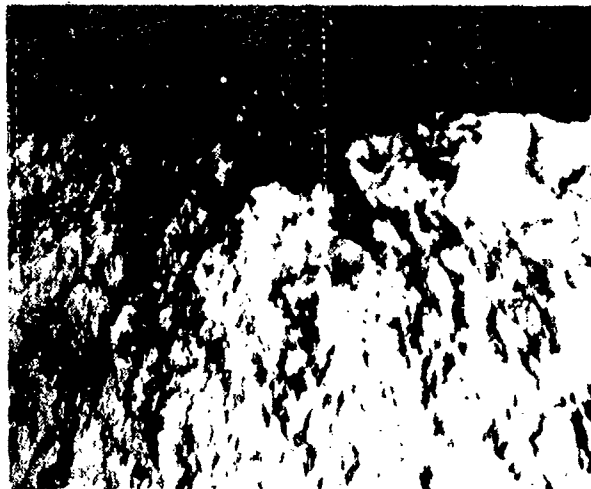


Figure 188. 0.030 to 0.045-Inch-Deep Lack-of-Penetration Defect in Specimen P5-3 (20X MAG)





**Figure 191.** 0.002-Inch-Diameter Surface Pore at the Failure Initiation Site in Specimen 14-1 (20X MAG)



**Figure 192.** 0.008 to 0.010-Inch-Diameter Surface and Sub-surface Pores at the Failure Initiation Site in Specimen 14-2 (20X MAG)

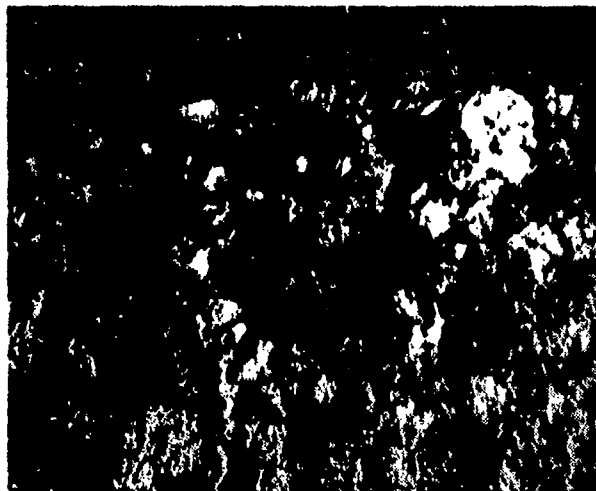


**Figure 193.** Internal Cluster of Pores (0.004 to 0.020-Inch-Diameter Range) Detected at Failure Initiation Site in Specimen 4-2 (20X MAG)

## SECTION VIII

### CRITERIA FOR ACCEPTANCE OF TITANIUM FUSION WELDS

#### A. SCOPE

The proposed acceptance criteria or standards for titanium fusion welds are based not only on the results of this program, but also on Grumman Specifications GSS 6204, "Fusion Welding of Titanium and Titanium Alloys," GSS 6205, "Electron Beam Welding of Titanium and Titanium Alloys," and North American Rockwell Specification STO107LA0017, "Fusion Welding, Titanium." Guidelines for the proposed acceptance standards, which are described in Paragraph C, relate specific data generated in the course of the Exploratory Weld Quality Definition Program to the requirements of proposed specifications and provide supporting data that should be considered by approving agencies and in granting possible requests for deviation.

#### B. PROPOSED ACCEPTANCE STANDARDS FOR TITANIUM FUSION WELDS

##### 1. Visual Inspection

###### a. Discoloration

- PAW, GTA and GMA Welds. The weld bead and adjacent base metal shall have a bright silver to light-straw appearance. A blue-gray or gray discoloration or the presence of loose scale shall be cause for rejection.
- EB Welds. Discoloration due to EB Welding in accordance with approved specifications is acceptable.

b. Incomplete Penetration/Fusion. All welds will show evidence of complete (100-percent) penetration. Incomplete fusion and missed seams shall not be permitted.

c. Weld Contours - Reinforcement, Underfill and Undercut. The depth of underfill and undercut shall not exceed the post-weld machining allowances specified on engineering drawings. For welds which are not to be machined, maximum depth of underfills and undercuts, maximum heights of reinforcement and minimum allowable contour radii must be specified on engineering drawings.

d. Mismatch. Maximum mismatch of ten percent of the thickness of the thinnest member or 0.030-inch (whichever is less) will be acceptable in joints with gradually blended contours.

e. Cracks. The presence of cracks in the weld or adjacent base metal is a cause for rejection.

f. Surface Inclusions and Porosity. The following requirements will apply to surface inclusions and porosity detected in the course of macroscopic and/or liquid penetrant examinations:

- Surface inclusions are not acceptable.
- Linear porosity is not acceptable (for definition of linear porosity, see Paragraph 2e).

- Maximum allowables for pore size and total porosity area specified for internal porosity in Paragraph 2 will be reduced by 50 percent.
- Porosity with sharp terminations is not acceptable.

## 2. Nondestructive Inspection

a. Cracks, Lack of Penetration and Lack of Fusion. Indications of cracks, lack of penetration and lack of fusion will be a cause for rejection.

b. Inclusions. Surface inclusions and inclusions with sharp terminations will be a cause for rejection. Internal inclusions with rounded contours will be acceptable subject to limitations specified for internal porosity in Paragraph 2c.

c. Internal Porosity. Acceptance criteria pertaining to internal porosity occurring in EB weldments and welds produced by other fusion processes (PAW, GTA and GMA) are presented separately because of the significant differences in size and distribution of porosity which occurs in these weldments.

- EB Welds. Two or more adjacent pores other than those aligned (see Paragraph 2c) shall be treated as one pore (excluding the space between them) when the spacing between them is less than three times the greatest dimension of the smaller adjacent pore. The maximum pore diameter shall not exceed  $0.1T$  or  $0.050$  inch, whichever is less ( $T$  is defined as the final thickness of the weld joint after all phases of processing).
- PAW, GTA and GMA Welds. Two or more adjacent pores other than those aligned shall be treated as one pore (excluding the space between them) when the spacing between them is less than four times the average diameter of the smallest adjacent pore. The maximum pore diameter shall not exceed  $1/3T$  or  $0.040$  inch, whichever is less ( $T$  is defined as the final thickness of the weld joint after all phases of processing at the location of porosity to be evaluated).

### d. Total Porosity Area

- EB Welds. The sum of the areas of all pores within one inch of the weld shall not exceed  $0.025T$  square inch or  $0.0125$  square inch, whichever is less.
- PAW, GTA and GMA Welds. The sum of the areas of all pores within one inch of the weld shall not exceed  $0.05T$  square inch or  $0.006$  square inch, whichever is less. Pores having diameters of  $0.01T$  or  $0.01$  inch, whichever is less, are not to be considered in determining the total porosity area.

### e. Aligned Porosity

- EB Welds. Aligned porosity is defined as a group of five or more individual pores within one inch of the weld whose radiographic images are intersected by a straight line (regardless of orientation within the weld). The distance between the adjacent pores being considered shall be less than four times the longest dimension of the smaller adjacent pore. The allowable limits are  $0.01T$  square inch or  $0.006$  square inch, whichever is less.

- PAW, GTA and GMA Welds. Aligned porosity is defined as five or more pores falling on a straight line and within one linear inch of the weld. Linear porosity will be a cause for rejection if the distance between adjacent pores is less than six times the largest dimension of the smaller adjacent pore.

### C. GUIDELINES FOR PROPOSED ACCEPTANCE STANDARDS FOR TITANIUM FUSION WELDS

This section summarizes data generated in the course of the Exploratory Weld Quality Program that pertain to the proposed acceptance standards presented in Paragraph B. The results of radiographic analyses of representative specimens containing internal porosity for compliance with proposed standards are also presented. The information is presented in a sequence that will facilitate correlation of the supporting data with the proposed specifications.

#### 1. Visual Inspection

##### a. Discoloration

- GTA and PAW Weldments. In the Exploratory Weld Quality Definition (WQD) Program welds were produced by the GTA process in 0.080- and 0.25-inch-thick blanks under intentionally inadequate shielding conditions obtained by varying of the flow rates of the torch and trailing shield gases. The welds were tested in tension-tension ( $R = 0.1$ ) fatigue with the weld contours intact.

Although the 0.080-inch-thick welds had a light-to-medium blue to gray appearance, their fatigue endurance was comparable to welds with similar contours produced by conventional techniques. The estimated values for  $10^5$  and  $10^6$  -cycle endurance limits were 75 and 68 ksi, respectively. A microhardness survey of transverse sections of the weld failed to detect hardness anomalies. GTA weldments (0.025 inch thick) with gray discoloration also exhibited fatigue endurance comparable to that for welds with similar contours produced by conventional techniques, and neither the oxygen/nitrogen content of the weld metal nor the microhardness survey indicated any appreciable anomalies. However, specimens having only a slightly different bluish tinge exhibited a pronounced susceptibility to cracking due a significant pickup of contaminants (2514 ppm oxygen and 1731 ppm nitrogen). The microhardness measurements indicated that the hardness of the contaminated weld was in the range of 39-44  $R_C$ , compared to 33-36  $R_C$  in the base metal. Yellowish discolorations intentionally produced in PAW weldments failed to yield detectable variations in fatigue and hardness characteristics.

- EB Welds. Slight yellowish discolorations intentionally produced in 0.25-inch-thick EB welds by contaminating the faying surfaces within vacuum oil failed to result in significant changes in either the fatigue endurance or hardness of the weld.

b. Incomplete Penetration/Fusion. GMA welds (0.25-inch thick) with intentional lack-of-penetration in the 0.006- to 0.050-inch range exhibited a drastic lowering of fatigue endurance. All data points were below the  $K_t = 3$  curve for the base metal. EB welds (1.5-inch-thick) with lack-of-penetration in the 0.010 to 0.44-inch range also exhibited a drastic lowering in fatigue characteristics. The effect of variations in the extent of the lack-of-penetration defect, however, appeared to be minor.

### c. Weld Contours

- **Reinforcement.** Intentional reinforcements were produced by GTA welding on 0.080-inch-thick butt welds and by GTA and PAW welding on 0.025-inch-thick butt welds. Reinforcements on 0.080-inch-thick GTA welds were typically 0.015-inch high and 0.30-inch wide at the face and .015-inch high and 0.20-inch wide at the root. The typical contour of these weldments is illustrated in Section IV, Figure 65. The fatigue endurance properties of these specimens were approximately 10 ksi below the lower boundary of the data band for flawless welds with weld contours machined flush with the base metal.  $10^5$  and  $10^6$  -cycle endurance limits for these weldments were estimated to be 70 and 60 ksi, respectively.

Reinforcements on 0.25-inch-thick GTA welds were typically 0.055-inch in height and 0.75-inch in width on the face of the weldment. The corresponding values of the root crown were 0.05-inch and 0.25-inch. A typical contour of these weldments is illustrated in section IV, Figure 66. Fatigue properties of these weldments were significantly below those of welds with contours machined flush with the surface and comparable to those of the base metal at the  $K_t=3$  stress intensity level.

Reinforcements on 0.25-inch thick PAW weldments were of two types: (1) those with (face) reinforcements in the range of up to 0.015 inch in height and 0.20 - 0.30-inch in width, and root reinforcements in the range of 0.005 - 0.015-inch in height and 0.01 - 0.12 inch in width; and (2) those with face reinforcements in the range of 0.040-0.045 inch in height and 0.20 to 0.25-inch in width. The contours of typical weldments of each type are illustrated in Section VI, Figure 173 and 174. Fatigue endurance of the first type of reinforcements was in the lower half of the  $K_t=1$  to  $K_t=2$  range and the data points were (on the average) only five to seven ksi below the lower boundary of the data band for flawless machined weldments. Data points for the second type fell in the upper half of the  $K_t=2$  to  $K_t=3$  range, and the  $10^6$  cycle endurance limit was estimated to be in the 55 to 60-ksi range.

- **Underfill.** Intentional underfills were produced in 0.080-inch-thick GTA welds and 0.25-inch-thick EB, GTA and PAW weldments. Underfills produced in 0.080-inch-thick GTA welds were 0.010 to 0.015 inch deep and 0.35 inch wide. Their typical contours are shown in Section IV, Figures 68 and 69. Face and root contours were left intact in the course of machining the test specimens. Fatigue endurance data were scattered; the  $10^5$  cycle endurance limit was estimated to be in the 65 to 85-ksi range. Production of intentional underfill in 0.25-inch-thick GTA welds also resulted in generation of root reinforcements. The typical contour of these weldments is shown in Section IV, Figure 70. The width of the underfills was 0.8 inch and the depth varied from 0.005 to 0.015 inch. The height of a typical root reinforcement was 0.050 inch and the width was in the 0.25 to 0.30-inch range. The failure initiated in all specimens at root reinforcements. The  $10^5$  cycle and  $10^6$  cycle endurance limits for these welds were estimated to be 60 ksi and 50 ksi, respectively.

Attempts to produce intentional underfills by PAW techniques also resulted in root reinforcements. The depth of underfills ranged from 0.005 to 0.010 inch and the width ranged from 0.13 to 0.17 inch. The height of the root reinforcement crown was in the 0.020 to 0.030-inch range, and its width was in the 0.125 to 0.150-inch range. In all specimens, the failure initiated at root reinforcements. The endurance limit for these specimens ( $10^6$  cycles) was estimated to be 70 ksi.

In 0.25-inch-thick EB welds, the depth of intentional underfills, ranged from 0.025 to 0.100-inch. All underfills resulted in a drastic lowering of fatigue endurance. Progressive deterioration of fatigue characteristics was noted as the width/depth ratio decreased. A detailed discussion of contour dimensions and endurance characteristics is incorporated in Section V.

- Undercuts. Intentional undercuts were produced in 0.080-inch-thick GTA welds and 0.25-inch-thick GTA and PAW weldments.

In 0.080-inch-thick GTA welds, shallow undercuts about 0.005-inch deep could be produced by decreasing the feed rate of the filler wire. In addition to shallow undercuts, however, 0.015-inch-high and 0.25-inch-wide reinforcement crowns were detected at the roots of the weldments.

Failure initiation sites were detected at both surfaces of the experimental welds. Fatigue endurance data obtained for these specimens was generally within five to ten ksi of the lower boundary of the data band for machined flawless specimens. The typical weld contour of these weldments is illustrated in Section IV, Figure 73.

The depth of the undercuts produced in 0.25-inch-thick welds by GTA techniques varied from 0.010 to 0.020-inch and the width was 0.125-inch. The change in parameters designed to produce undercuts also resulted in the creation of root reinforcement crowns in the range of 0.050 to 0.090-inch in width. The typical contours of these weldments are illustrated in Section IV, Figure 75. Most fatigue endurance data points were within 10 ksi of the  $K_t = 3$  curve for the base metal for which the  $10^6$  cycle endurance limit was approximately 40 ksi. Fractographic evaluation revealed that all failure initiation sites were at the root reinforcement.

Undercuts produced in 0.25-inch-thick PAW weldments were in the range of 0.006 to 0.025-inch in depth and 0.050 to 0.150-inch in width. The height and width of the root reinforcements were in the range of 0.020 to 0.030-inch and 0.125-inch, respectively. The fatigue data points for these weldments were in close proximity to the  $K_t = 2$  curve for the base metal for which the  $10^6$  cycle endurance limit was indicated to be 60 ksi. Fractography indicated failure initiation sites at both face and root-sides of the weld.

d. Mismatch. Intentional mismatches of the faying surfaces were produced in 0.080-inch-thick GTA butt welds and 0.25-inch-thick GTA, EB and PAW butt welds. All weldments were fatigue tested with the face and root contours intact.

Experimental 0.080-inch-thick GTA butt welds were produced with 0.015-inch (about 19 percent) and 0.025-inch (about 31 percent) mismatch. Typical contours of the weldments are illustrated in Section IV, Figure 85. Data points for both types of specimens fell between the  $K_t = 2$  and  $K_t = 3$  curves for the base metal with an estimated  $10^6$  cycle endurance limit of 40 to 45 ksi. In all specimens, failure initiated at the root-side of the weldment.

Experimental 0.25-inch-thick GTA butt welds were produced with 0.010-inch (about 4 percent) and 0.036-inch (about 14 percent) mismatch. Typical contours for both types of weldments are illustrated in Section IV, Figures 90 and 91. Data points for specimens with 0.010-inch mismatch fell between the  $K_t = 2$  and  $K_t = 3$  curves for the base metal with an estimated  $10^6$  cycle endurance limit of 40 ksi. Data points for specimens with 0.036-inch mismatch fell below the  $K_t = 3$  curve for the base metal with an estimated  $10^6$  cycle endurance limit of approximately 30 ksi. In all specimens, failure initiated at the root reinforcement, the presence of which probably aggravated the effect of the mismatch.

Experimental 0.25-inch-thick EB weldments were produced with 0.016-inch (about 6.5 percent) and 0.025-inch (about 10 percent) mismatch. Typical contours of both types of weldments are illustrated in Section V. Both types of specimens exhibited fatigue endurance values below the  $K_t = 3$  curve for the base metal with an estimated  $10^6$  cycle endurance limit of 30 ksi. In all specimens, the failure initiated at unusually sharp undercuts adjacent to the shallow face and root reinforcements which apparently aggravated the effect of the mismatch.

Experimental 0.25-inch-thick PAW weldments were produced with 0.01-inch (about 4 percent) and 0.025-inch (about 10 percent) mismatch. Typical contours of both types of weldments are illustrated in Section VI, Figures 144 and 145. The fatigue endurance data points for both types of specimens fell on or below the  $K_t = 3$  curve for the base metal with an estimated  $10^6$  cycle endurance limit of approximately 30 ksi. As with the 0.25-inch-thick GTA weldments, failure in these specimens initiated at root reinforcements.

In summary, the low fatigue values of mismatched specimens appeared not to be due primarily to mismatches but rather to the change in characteristics of weld contours produced in joining mismatched faying surfaces. The removal of weld contours to allow for a gradual blending can be expected to improve significantly the fatigue characteristics of these weldments. Accordingly, the requirements of limiting the mismatch to 10 percent of the thickness of the thinnest member or 0.030-inch (whichever is less) appears to be satisfactory provided that the acceptance criteria include the requirement for gradual blending of mismatched contours.

e. Cracks. Ti-6Al-4V titanium alloy is a "forgiving" alloy. Various methods of intentional restraints failed to induce cracking. The only cracks detected on the surface of experimental weldments were associated with severe surface contamination intentionally produced by eliminating torch shielding in the GTA welding process. The presence of cracks was verified by subsequent radiography. All cracks ran transversely to the direction of the weld pass and were thus in a parallel alignment with the direction of stress application on subsequent fatigue tests. As discussed in Section IV, the existing cracks served as failure initiation sites and crack-containing specimens exhibited very low fatigue endurance.

f. Surface Inclusions and Porosity. Results indicate that the fatigue endurance of porosity-containing welds is definitely related to the proximity of pores to the surface. In some instances, fractography revealed that the failure initiation site was associated with a small pore at the surface rather than with much larger pores in the interior of the weld. Although limited data generated during the course of this program precluded the possibility of establishing definite mathematical relationships between fatigue endurance and the size and location of porosity, it appeared to be mandatory to recommend a reduction in allowable limits for surface-connected porosity.

Future studies designed to evaluate the effectiveness of surface-treating processes (for example, shot peening) in improving fatigue endurance of welds containing surface pores may eliminate the need for this reduction in allowable limits.

The recommendation for the rejection of surface-connected inclusions is based on the results of fractographic analyses which revealed crevices at the (tungsten) inclusion/weld metal interface. Residues detected in some of these crevices indicated that they were present in the weld prior to fatigue testing.

## 2. Nondestructive Inspection

a. Cracks, Lack of Penetration and Lack of Fusion. (See discussion in Subsection 1c).

b. Internal Inclusions. (See discussion in Subsection 1f)

c. Internal Porosity. To verify the correlation of the acceptance criteria proposed in Paragraph A with the experimental data, radiographic films for 72 0.080- and 0.25-inch-thick welds produced by EB, PAW, GTA and GMA welding processes were evaluated for compliance with proposed specifications. Figure 194 shows that the fatigue endurance of 0.25-inch-thick EB weldments containing internal porosity within the limits of proposed specifications is comparable to that of radiographically flawless specimens.

In Figure 195, experimental data for porosity-containing 0.25-inch-thick welds produced by PAW, GTA and GMA welding processes are superimposed on  $K_t$  curves for the base metal (solid lines) and lower boundaries of the data bands for machined radiographically flawless specimens. It is evident that above 85-ksi level, it is difficult to detect a definite relationship between the radiographic quality of the specimens and fatigue endurance. At lower stress levels, however, this relationship is more pronounced. Most specimens of acceptable radiographic quality exhibited distinctly superior fatigue endurance compared to rejectable specimens tested at the same stress level.

Figure 196 summarizes data on fatigue endurance of 0.080-inch-thick weldments of flawless, acceptable and rejectable radiographic quality produced by EB and GTA welding. As was the case with the data plotted in Figure 195, no definite correlation is apparent for specimens tested at high stress levels (exceeding 100 ksi). Below this level, on the other hand, most specimens with acceptable radiographic characteristics exhibited higher fatigue endurance compared to rejectable specimens tested at the same stress level.

It should be emphasized that considerable relaxation of acceptance criteria for internal porosity may be feasible when sufficient data become available to establish mathematical relationships between the distribution of internal porosity with respect to the weld surfaces and initiation/propagation characteristics of the fatigue failure. Generation of data required in establishing these relationships may be greatly facilitated utilizing acoustic emission monitoring of fatigue specimens (discussed in Section V) and advanced ultrasonic scanning techniques designed to determine precise locations of internal porosity in surface layers of weldments. Both of these methods recently have been shown to have a significant potential in advancing the state-of-the-art of industrial nondestructive inspection.

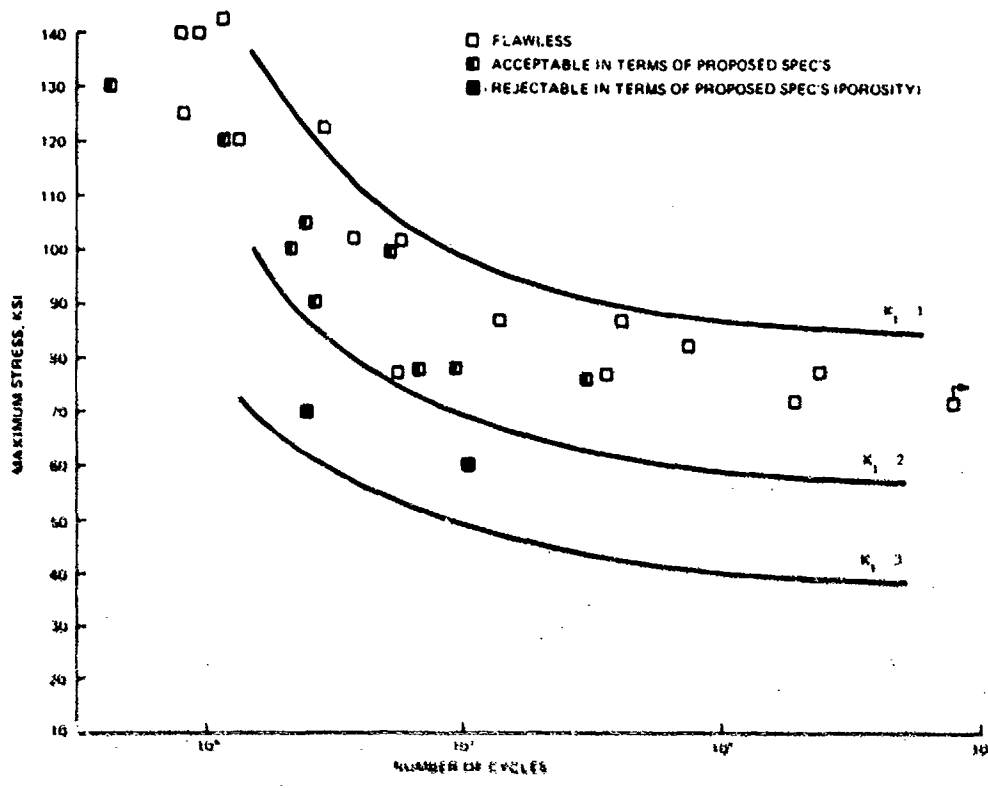


Figure 194. Fatigue Endurance of .25" EB Weldments

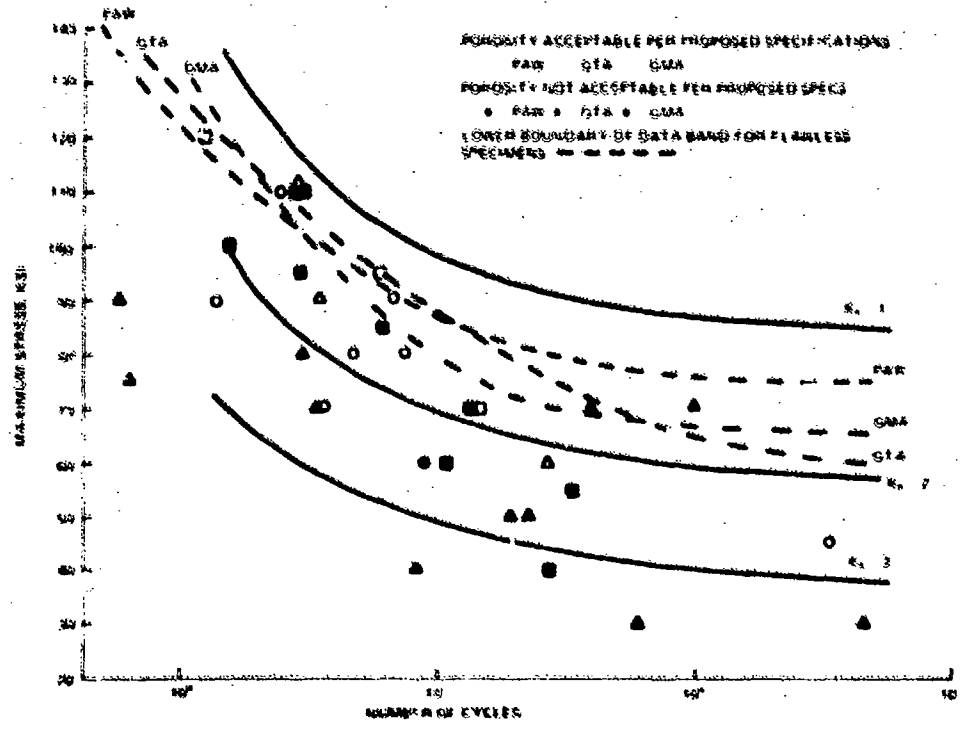


Figure 195. Fatigue Endurance of 0.25-inch-Thick PAW, GTA and GMA Weldments

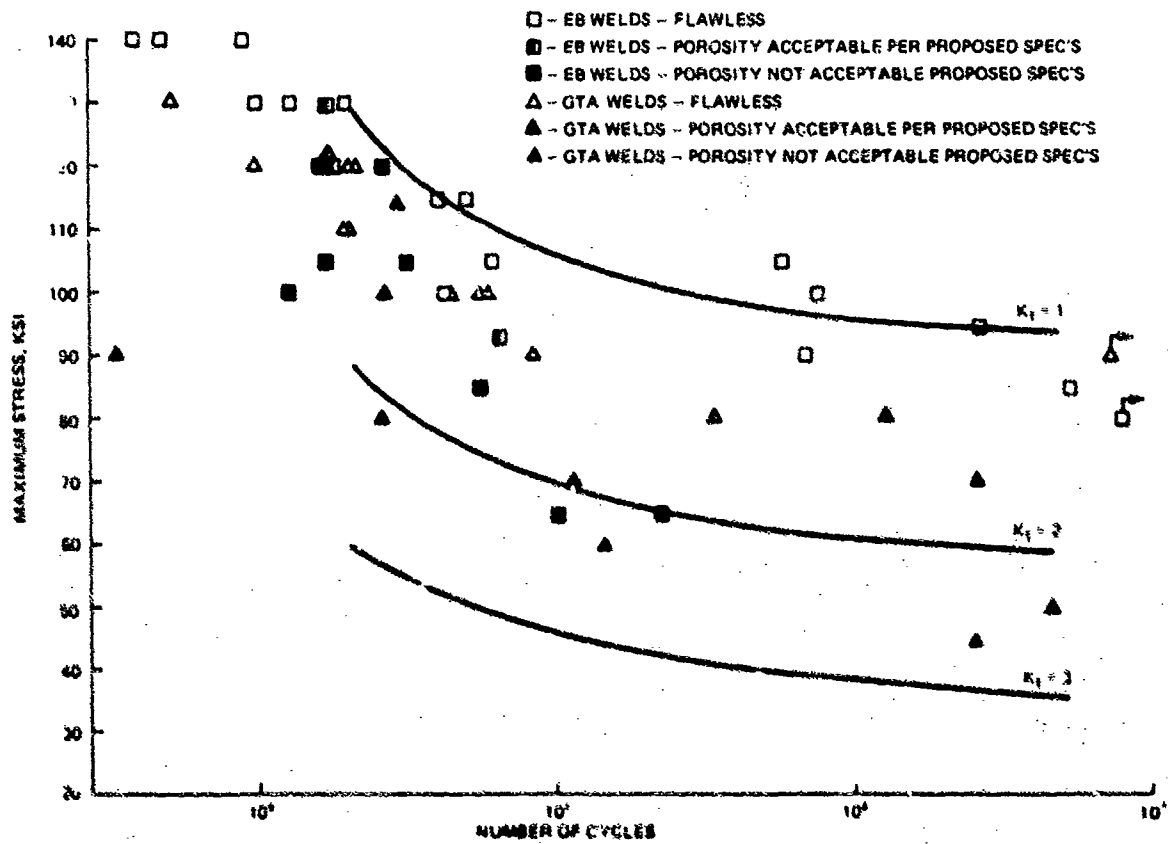


Figure 185. Fatigue Endurance of Flawless, Acceptable (in Terms of Proposed Specification) and Rejectable 0.080-Inch-Thick and EB and GTA Welds

## SECTION IX

### CONCLUSIONS AND RECOMMENDATIONS

#### A. CONCLUSIONS

##### 1. General

- Radiographically flawless weldments having weld contours machined flush with the surface exhibited the following tension-tension ( $R=0.1$ ) fatigue endurance limits at  $10^6$  cycles:

<u>Thick, inch</u>	<u>Welding Process</u>	<u>Fatigue Endur. ksi</u>
0.080	EB	85
0.080	GTA	75
0.25	EB	75
0.25	PA	75
0.25	GMA	65
0.25	GTA	62
1.5	EB	65

- Retention of as-welded contours on GTA and PA weldments will reduce the fatigue endurance limit from 5 to 20 ksi depending on the geometry of the retained contour
- Except for cracks and EB welding bursts, typical defects encountered in production welding can be generated by intentional variation of processing parameters
- Cracks could be detected only in 0.25-inch-thick GTA weldments produced under severely contaminating conditions
- EB welding burst defects can be produced in 1.5-inch-thick plate contoured to meet postulated molten-puddle-shape and cooling conditions existing after extinction of the electron beam
- Differences in the characteristics of defects which may occur in EB weldments and those which may occur in PA, GTA and GMA weldments warrant their separate consideration, especially with regard to formulation of acceptance criteria
- Except for 1.5-inch-thick EB weldments, intentional contamination of faying surfaces to produce internal porosity did not significantly reduce fatigue endurance of specimens machined from radiographically flawless sections of these weldments
- The proposed acceptance/rejection standards for titanium fusion welds can be used to screen out welds having inferior fatigue endurance characteristics.

##### 2. Weld Defect-Fatigue Endurance Correlation

- Incomplete Penetration. Incomplete penetration in 0.25-inch-thick GMA and 1.5-inch-thick EB weldments drastically reduced their fatigue endurance

- Underfills. If root reinforcements are not present, the fatigue endurance of 0.080-inch-thick welds having minor underfills (0.010 to 0.015-inch thick) is comparable to that for weldments having normal as-welded contours. Generation of intentional underfills in 0.25-inch-thick GTA and PA weldments resulted in the creation of root reinforcements which served as failure initiation sites. Underfills in 0.25-inch-thick EB weldments drastically reduced fatigue endurance.
- Undercuts. The fatigue endurance of 0.080-inch-thick welds with minor undercuts (0.005-inch deep) is comparable to that for weldments having normal as-welded contours. Generation of intentional undercuts in 0.25-inch-thick GTA weldments resulted in the creation of root reinforcements which served as failure initiation sites. Plasma-arc weldments (0.25-inch-thick) with 0.005 to 0.015-inch-deep undercuts had a fatigue endurance limit of 60 ksi at  $10^6$  cycles.
- Mismatch. The low fatigue endurance of 0.080-inch-thick GTA and 0.25-inch-thick EB, GTA and PA weldments with mismatches is not due to the mismatches themselves but rather to the resultant extensive changes in weld contours. Blending of weld contours should significantly improve the fatigue endurance of these weldments.
- Inclusions. The fatigue endurance of 0.080 and 0.25-inch-thick GTA welds with internal tungsten inclusions was comparable to that for inclusion-free specimens having similar contours. Tungsten inclusions exposed to the surface did cause a drastic reduction in fatigue endurance.
- Surface Contamination. Slight yellowish discolorations in EB and PA weldments made by approved processes did not result in a significant decrease in fatigue endurance. Bluish-gray discolorations on GTA weldments may indicate extensive pickup of contaminants with resultant susceptibility to cracking and drastic reduction in fatigue endurance.
- Porosity
  - 0.080-Inch-Thick EB Welds
    - Variation in test frequency had no apparent effect on fatigue life
    - A pronounced multiple-failure initiation pattern was evident above the 100-ksi stress level. There was no apparent correlation between radiographic and fractographic findings and fatigue endurance above this stress level.
    - Linear radiographic indications were related to porosity concentration in the face or root portions of the weld. The fatigue endurance of specimens with linear radiographic indications was in the lower portion of the obtained data band. Specimens exhibiting these indications would be rejectable in terms of the proposed standards.
    - Fatigue endurance values predicted by assigning  $K_t$  factors to individual pores (Reference 2) could not be verified by experimental data. This lack of correlation could be attributed to appreciable differences in the weld defect characteristics considered.
  - 0.25-Inch-Thick EB Welds
    - Linear porosity within the limits of the proposed specifications did not significantly reduce fatigue endurance

- Surface porosity considerably reduced fatigue endurance. Depth of porosity was found to affect the extent of such reduction.
  - Double-line radiographic indications were associated with massive porosity which is rejectable in terms of the proposed specifications. Specimens exhibiting these indications had low fatigue endurance.
  - Fatigue endurance of weldments containing porosity greater than 0.010 inch in diameter exhibited a pronounced dependence on the location of pores with respect to the surface
- 0.25-Inch-Thick PA Welds
- Porosity in all weldments was located within a 0.030-inch-wide band, 0.010 to 0.040-inch from the face-side of the surface
  - Close proximity of pores to the surface significantly reduces fatigue endurance
  - Specimens tested above the (maximum) 85-ksi stress level exhibited rather high fatigue endurance despite the presence of rejectable defects. Specimens tested below the 70-ksi stress level, however, exhibited a significant reduction in fatigue endurance due to the presence of rejectable defects.
- 0.080-Inch-Thick GTA Welds
- Most of the specimens containing internal porosity within the limits of the proposed specifications exhibited fatigue endurance comparable to that for flawless specimens
  - The fatigue endurance of specimens with rejectable defects was generally below the  $K_t = 2$  level except for those specimens tested at a stress level of 80 ksi (maximum) and above which had moderately high fatigue endurance despite the presence of rejectable defects.
  - Most of the rejectable welds were rejected because of maximum pore size limitations.
- 0.25-Inch-Thick GTA Welds
- The fatigue endurance of specimens with internal porosity acceptable in terms of the proposed specifications was either within the range for flawless specimens or within 12 to 15 ksi of the lower boundary of the data band for flawless welds.
  - Most of the rejectable specimens exceeded the limits for both maximum linear porosity area and maximum size of individual pores
  - Surface porosity and the presence of clusters did affect fatigue characteristics.
- 0.25-Inch-Thick GMA Weldments
- Correlation of fatigue endurance of porosity containing weldments with quality, as determined by the proposed acceptance criteria, was not as successful as that for weldments produced by the other fusion processes. Although most of the fatigue data for specimens having acceptable quality in terms of the proposed specifications was in close proximity to the data band for flawless specimens, some of the data points fell in the middle of the  $K_t = 2$  to  $K_t = 3$  range for the base-metal. Fractography indicated that the lower fatigue endurance of these specimens was associated with either multiple failure initiations or linear porosity clusters.

- Specimens with rejectable defects exhibited consistently low fatigue endurance.

## B. RECOMMENDATIONS

- Acceptance criteria for titanium fusion welds could be relaxed when production-nondestructive-inspection-techniques capable of determining the precise locations of defects with respect to weldment surfaces are developed. Ultrasonic surface scanning methods now under development might be potentially useful for this application.
- Mathematical relationships between fatigue endurance and the size and location of defects in critical subsurface layers should be developed. Data on the initiation and propagation of internal failures should be generated to facilitate the use of fracture mechanics analytical techniques that would be required to develop these relationships. Acoustic emission monitoring of fatigue test specimens by recently developed techniques could be used to generate such data.
- Considerably more fatigue data should be generated to permit statistical analysis of test results, especially those in the marginal quality range as determined by nondestructive inspection techniques.
- In future weld quality studies, defect-generation methods based on intentional variation of processing parameters should be supplemented by other techniques when precise reproducibility of defect locations is required for statistical evaluations.

## REFERENCES

1. R. W. Messler, Jr., Grumman Aerospace Corporation, Unpublished data.
2. D. V. Lindh and G. M. Peshak - "Influence of Weld Defects on Performance", Welding Research Suppl. to the Welding Journal, Feb. 1969.

APPENDIX A  
DATA - PHASE 1



Figure A-2. Identification and Test Report on 0.25-Inch-Thick Ti-6Al-4V STOA Plate (First Shipment)

TEST REPORT												PAGE 1 OF 1		
 <b>RMI Company - NILES, OHIO</b>	DATE	MILL ORDER NO.	GRADE	PACKING LIST NO.										
	Feb. 21, 1973	16279	6A1-4V	76050										
	CUSTOMER NAME			CUSTOMER ORDER NO.										
	Grumman Aerospace Corp.			10-58908										
MATERIAL														
M.R. Solution Treated & Overaged Ti Plate														
SPECIFICATION														
Mil-T-9046F Type 3 Cond C														
IDENTIFICATION REFERENCE	INGOT NO.	LOT	S-R	INGOT NO.	LOT	S-R	INGOT NO.	LOT	S-R	INGOT NO.	LOT	S-R		
MATERIAL NUMBER	890146	07	00											
TRAVEL CARD NO.	30316													
CHEMISTRY	INGOT	AVERAGE OF TOP-CENTER-BOTTOM					FINAL PRODUCT							
C		.02												
N		.012												
Fe		.17												
Al		6.3												
V		4.0												
Cr														
Sr														
Mn														
Mo														
FINAL PRODUCT	O	.142												
	H	.130												
PROPERTIES														
ULTIMATE TENSILE	L	145.3/146.4												
	T	145.1/150.7												
YIELD STRENGTH	L	131.8/132.5												
	T	130.8/140.5												
ELONGATION	L	12.0/12.0												
	T	11.0/12.0												
REDUCTION OF AREA	L													
	T													
HARDNESS	L													
	T													
HEAT TREATMENT	Prod. STOA. 1750°F 15 min. A.C. + Solution 1150°F 4 hrs. A.C.													
OTHER DATA														
REMARKS														
8 & 1 T.P.														
1284.03 & .54														
.250 x 36 x 96														
.250 x 4x4														

THIS IS TO CERTIFY THAT THE ABOVE TEST RESULTS ARE IN ACCORDANCE WITH THE RECORDS OF THE COMPANY

SIGNED

Figure A-3. Identification Data and Test Report on 0.25-Inch-Thick Ti-6Al-4V STOA Plate (Second Shipment)

TEST REPORT										PAGE 1 OF 1			
 <b>RMI Company - NILES, OHIO</b>		DATE	MILL ORDER NO	GRADE	PACKING LIST NO								
		March 29, 1973	16279	6Al-4V	76571								
		CUSTOMER NAME			CUSTOMER ORDER NO								
		Grumman Aerospace Corp.			10-58908								
MATERIAL													
N.R. Solution Treated & Overaged Ti Plate													
SPECIFICATION													
Mil-T-9046F Type 3 Comp C Sol. Tr. & Overaged													
IDENTIFICATION & REFERENCE		INGOT NO	LOT	S-R	INGOT NO	LOT	S-R	INGOT NO	LOT	S-R	INGOT NO	LOT	S-R
MATERIAL NUMBER		890146	07	10									
TRAVEL CARD NO		74815											
CHEMISTRY													
INGOT (AVERAGE OF TOP-CENTER-BOTTOM) <input type="checkbox"/> FINAL PRODUCT													
	C %	.02											
	N	.012											
	Fe	.17											
	Al	6.3											
	V	4.0											
	Cu												
	Sn												
	Mn												
	Mo												
	O	.138											
FINAL PRODUCT	H	.134											
PROPERTIES													
ULTIMATE KSI	L	148.9/149.7											
	T	149.7/148.4											
YIELD KSI	L	138.1/138.9											
	T	138.9/141.6											
% ELONGATION	L	11.0/11.0											
	T	11.0/12.0											
% REDUCTION	L												
	T												
BEND 108°	L												
	T												
HARDNESS													
STATIC NOTCH													
IMPACT													
ULTRASONIC													
BETA TRANSUS													
VERY FORGE													
PROCEDURE													
As Prod STOA 1750° 7 15 min. A.C. A minimum 1250° 2 hrs. A.C.													
OTHER DATA													
SHIPPED													
NO OF PIECES	A A I T P.												
WEIGHT	424.08 & .3754												
SIZE	.250x36x54												
TEST PIECES	.250x4x4												

FORM NO. 44 REV. 1/71

THIS IS TO CERTIFY THAT THE ABOVE TEST RESULTS ARE CORRECT AS CONTAINED IN THE RECORDS OF THE COMPANY.

SIGNED

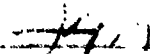


Figure A-4. Identification Data and Test Report on 1½-Inch-Thick Ti-6Al-4V STOA Plate  
(Sheet 1 of 2)



**Timet**

First in Titanium  
P. O. BOX 109 TORONTO, ONTARIO M5R 1A4

1973

NY139  
NS1278 3/2  
APPLIES APPLIES 204-7967  
OOR 03 31059.40  
LATEST  
CUSTOMER ORDER NUMBER 10-58910  
15326543  
DATE 04 TORONTO  
SALES ORDER NUMBER 122772 1 973 16-66663

GRUMMAN AEROSPACE CORPORATION  
P O BOX 54  
HICKSVILLE L.I. NEW YORK 11803

GRUMMAN AEROSPACE CORPORATION  
CENTRAL RECEIVING  
BETHPAGE L.I. NEW YORK 11714

**CERTIFICATE OF TEST  
NOTICE OF SHIPMENT**

TI-6AL-4V STORAGED TO MIL T 9046 F TYPE 3 COMP C ALPHA BETA ROLLED  
GUARANTEE ULTRASONIC CAPABILITY AND 3/16 OVERALL FLATNESS (SEE BELOW)  
SPECIAL MARKING

		764331			April 17, 1973	
QTY	SIZE	NO PCS	SQUARE FEET	WEIGHT	NET WT	GROSS WT
1	1-1/2" x 36" x 24"			2,722	83.0	2,639.0
	PM1, 1-1	2		1,740.0		
	Heat N-1430					
	Test L-0223					
	PM1	1		890.0		
	Heat N-1430					
	Test L-0226					
14	1-1/2" x 4" x 4" Test Pcs (1 Pair Each Heat)	2		9.0		

16-02663-01(1)-01(1)

CERTIFIED CHEMICAL ANALYSIS AND MECHANICAL PROPERTIES  
ON REQUEST SEE

INSTRUCTIONS FOR THE USER OF THIS CERTIFICATE OF TEST ARE GIVEN ON PAGE 2 OF 4

Figure A-4. Identification Data and Test Report on 1½-Inch-Thick Ti-6Al-4V STOA Plate  
(Sheet 2 of 2)

*Titanium Metals Corporation of America*

**CERTIFICATE OF TEST**

**CHEMICAL ANALYSIS**

HEAT NO.	C	Fe	N	Al	Va	Ca	Mo	H	Zr	Sr	Mn	O
B-1430	.022	.15	.013	6.4	4.3			.006				.19

**MECHANICAL PROPERTIES**

HEAT NO.	TEST NO.	SIZE OR GAUGE	MECHANICAL PROPERTIES				HARDNESS	BEND TEST
			YIELD STRENGTH	TENSILE STRENGTH	ELONG.	A & %		
			<b>.25</b>					
		1-1/2"	KSI	KSI				
-1430	L-8826	L	137	151	15	29		
		T	143	153	15	37		
-1430	L-8823	L	138	151	17	32		
		T	143	154	17	41		

*STOA*

Material inspected for micro and acceptable  
Material capable of meeting all requirements of QPS 16100a  
Class A

IN ADDITION TO THESE TESTS

RESULTS TO BE SUBMITTED  
To the Chief Metallurgist of America

4-13-73

*116 Puddy*

Figure A-5. Identification Data and Test Report on 1 1/2-Inch-Thick Ti-6Al-4V STOA Plate  
(Sheet 1 of 2)



*Titanium Metals Corporation of America*

TMCA 1480

First in Titanium

190 CLINTON ROAD WEST CALDWELL, NEW JERSEY 07006

APPLIES APPLIES  
 001 33 1059 40 1622643 04 TORONTO  
 LATEST SALES ORDER  
 CUSTOMER ORDER NUMBER AND DATE 10-38910 122772 1 1973  
 NUMBER 16-66663

GRUMMAN AEROSPACE CORPORATION  
 P O BOX 94  
 NICKSVILLE L.I. NEW YORK 11803

GRUMMAN AEROSPACE CORPORATION  
 CENTRAL RECEIVING  
 BETHPAGE L.I. NEW YORK 11714

**CERTIFICATE OF TEST  
 NOTICE OF SHIPMENT**

TI-6AL-4V STOVENAGED TO MIL T 9046 F TYPE 3 CORP C ALPHA BETA ROLLED  
 GUARANTEES ULTRASONIC CAPABILITY AND 3/16 OVERALL FLATNESS (SEE BELOW)  
 SPECIAL MARKING

				INVOICE NUMBER	DATE		
				704300	April 6, 1973		
QTY	DESCRIPTION	NO. PCS	SQUARE FEET	BILLING BY PER PIECE OR SQ. FT.	WEIGHT	PRICE	TOTAL
						3,630.0	2,430.0
1	1-1/2" x 36" x .001"	1			697.0		
	Part N-1430 Part L-0023						
	2191-1	2			1,733.0		
	Part N-1430 Part L-0024						
	2191,1-1						
1A	1-1/2" x 36" x .001" Stock Exp	13			6.0		
	Part N-1430 Part L-0023						
	Part N-1430 Part L-0024						
S/W Inv. 704300							
24-66663-0003-00(1)							

CERTIFIED CHEMICAL ANALYSIS AND MECHANICAL PROPERTIES ON REQUEST 5100

Reproduced from best available copy.

Figure A-5. Identification Data and Test Report on 1 1/2-Inch-Thick Ti-6Al-4V STOA Plate  
(Sheet 2 of 2)

*Titanium Metals Corporation of America*  
**CERTIFICATE OF TEST**  
**CHEMICAL ANALYSIS**

HEAT NO	C	Fe	N	Al	Va	Co	Mo	H	Zr	Sn	Mn	
												02
H-1430	.022	.15	.013	6.4	4.3			.004				.19
H-1409	.022	.20	.016	6.6	4.2			.005				.18

HEAT NO	TEST NO	SIZE OR GAUGE	MECHANICAL PROPERTIES				HARDNESS	BEND TEST
			YIELD STRENGTH	TENSILE STRENGTH	ELONG	A 1/2		
		1-1/2"	KSI	KSI				
H-14	1-6825	T	138	156	15	34		
		T	140	162	16	38		
H-14	1-6824	T	139	154	13	32		
		T	144	150	14	33		

STOA 7000.

Material ultrasonic inspected to Dimension #3 F28

Supplied to the Customer by the Seller on

Date

6-6-73

Results as above certified  
 Titanium Metals Corporation of America

*W. J. Priddy*

Reproduced from  
 best available copy.

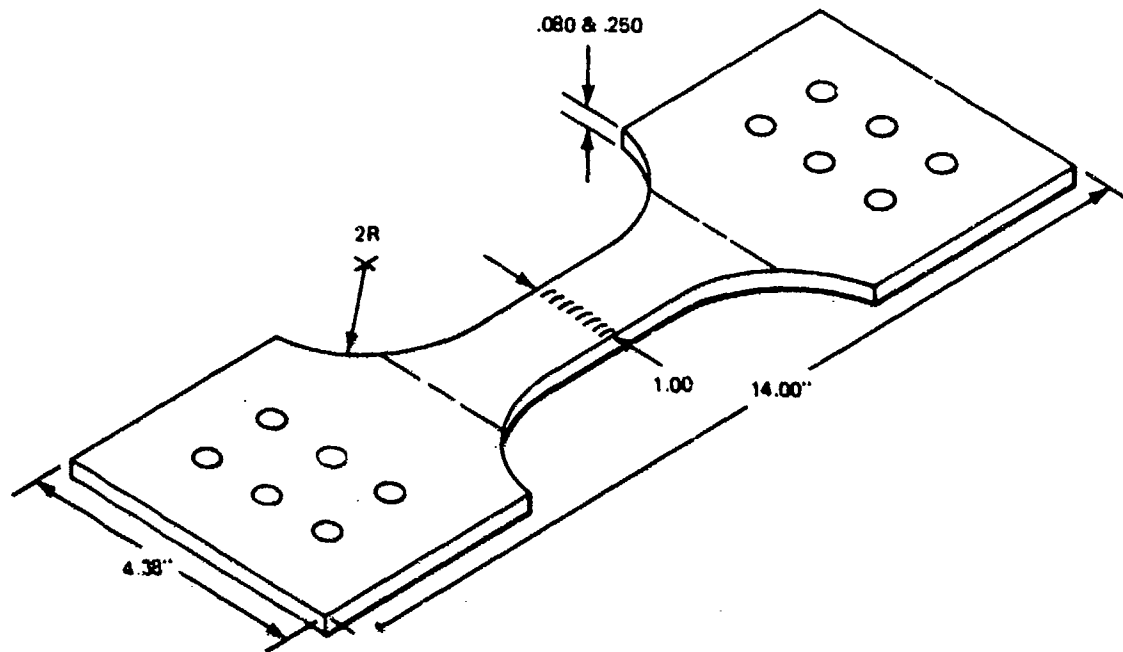


Figure A-6. Butt Welded Fatigue Specimen (0.080- and 0.250-Inch Thick)

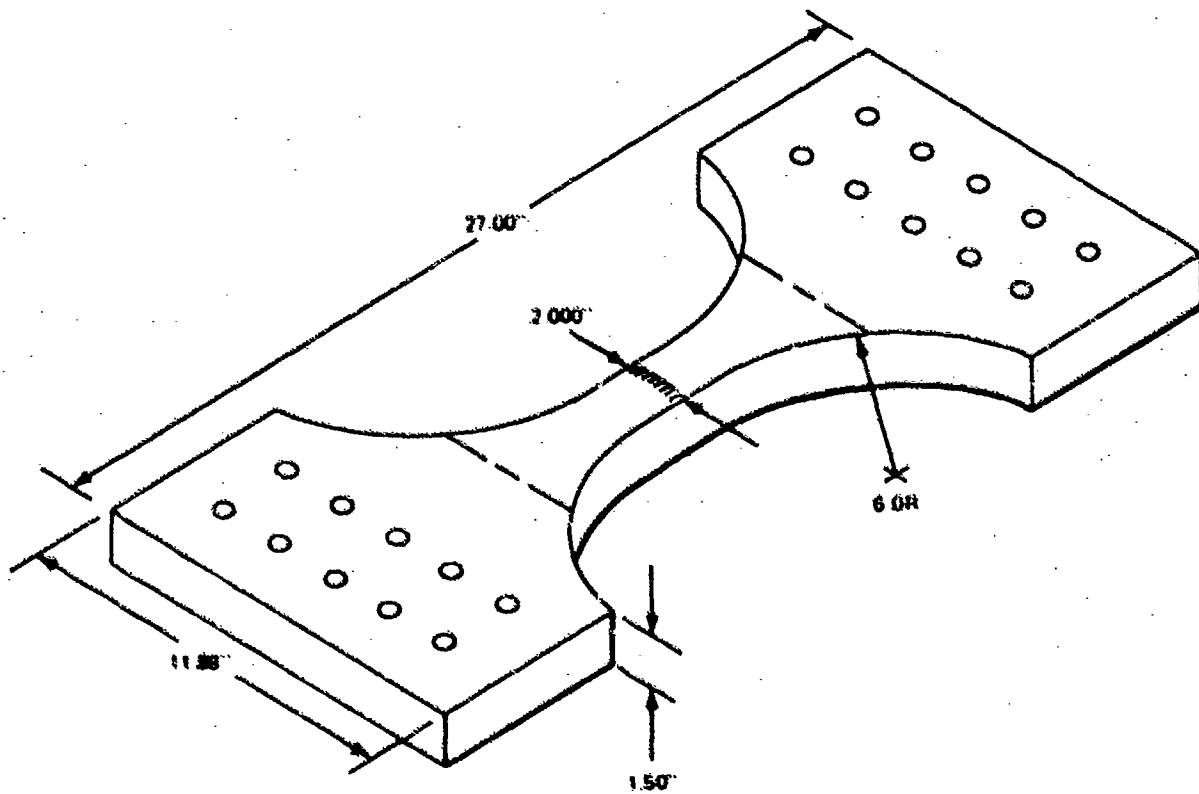


Figure A-7. Butt Welded Fatigue Specimen (1.5-Inch Thick)

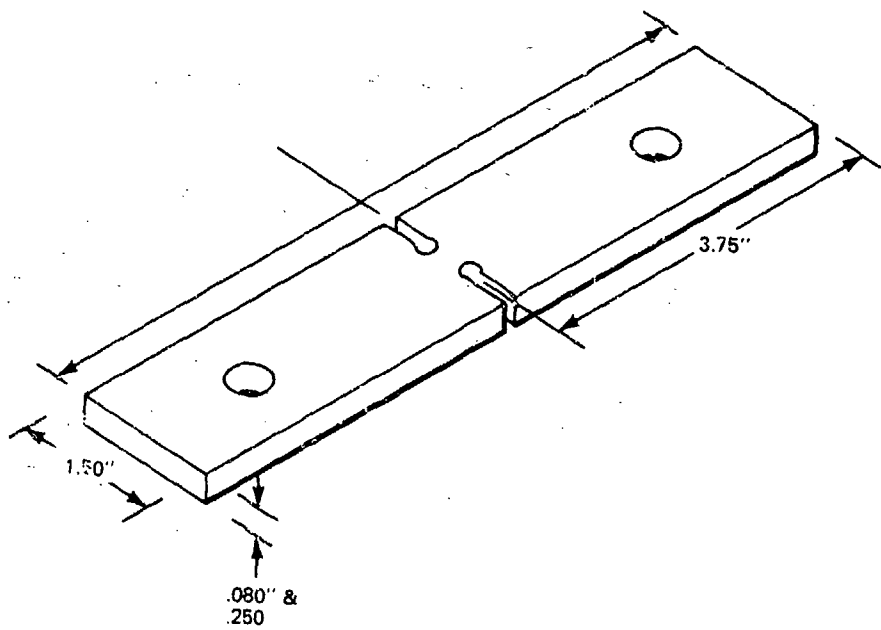


Figure A-8. Edge-Notched-Base Metal Fatigue Specimen (0.080-and 0.250-Inch Thick)

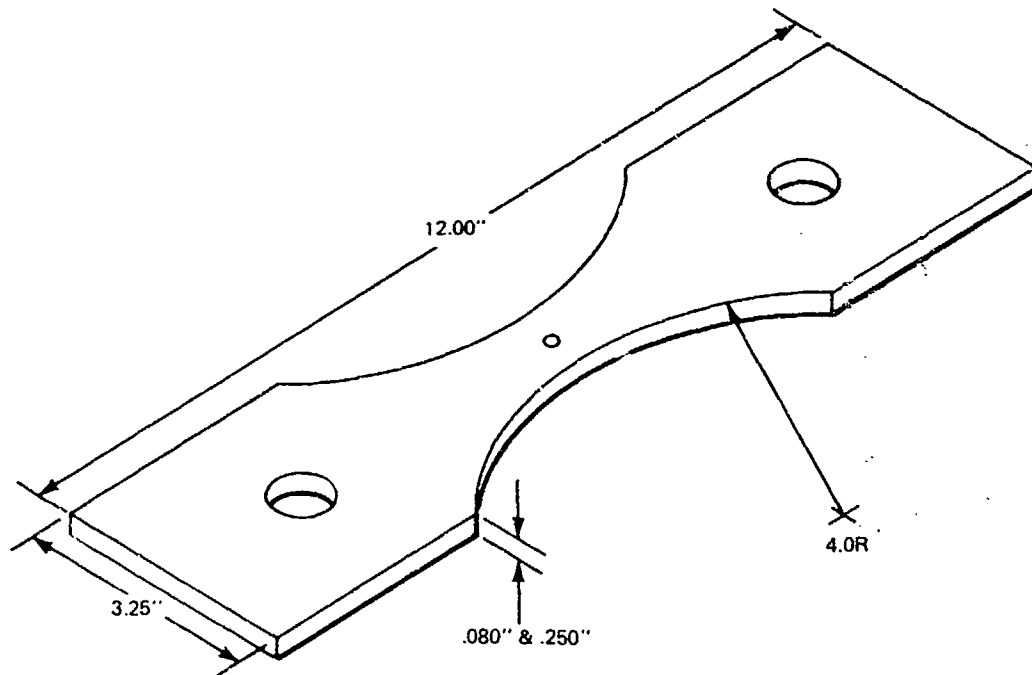


Figure A-9. Center-Notched-Base-Metal Fatigue Specimen (0.080- and 0.250-Inch Thick)

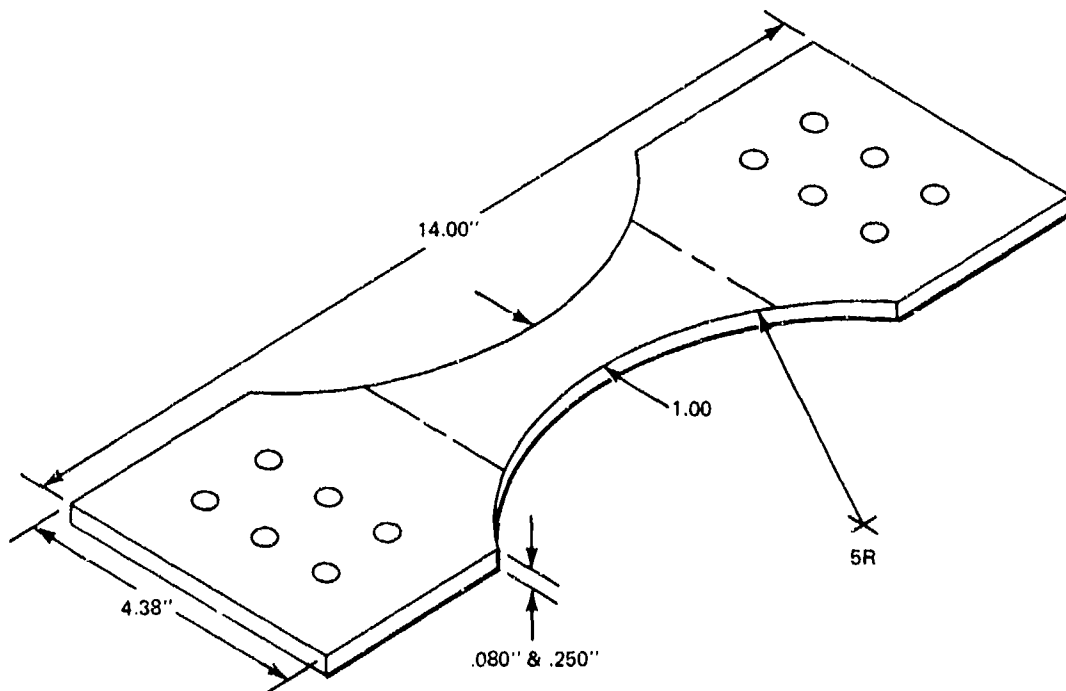


Figure A-10. Unnotched Base-Metal Fatigue Specimen (0.080- and 0.250-Inch Thick)

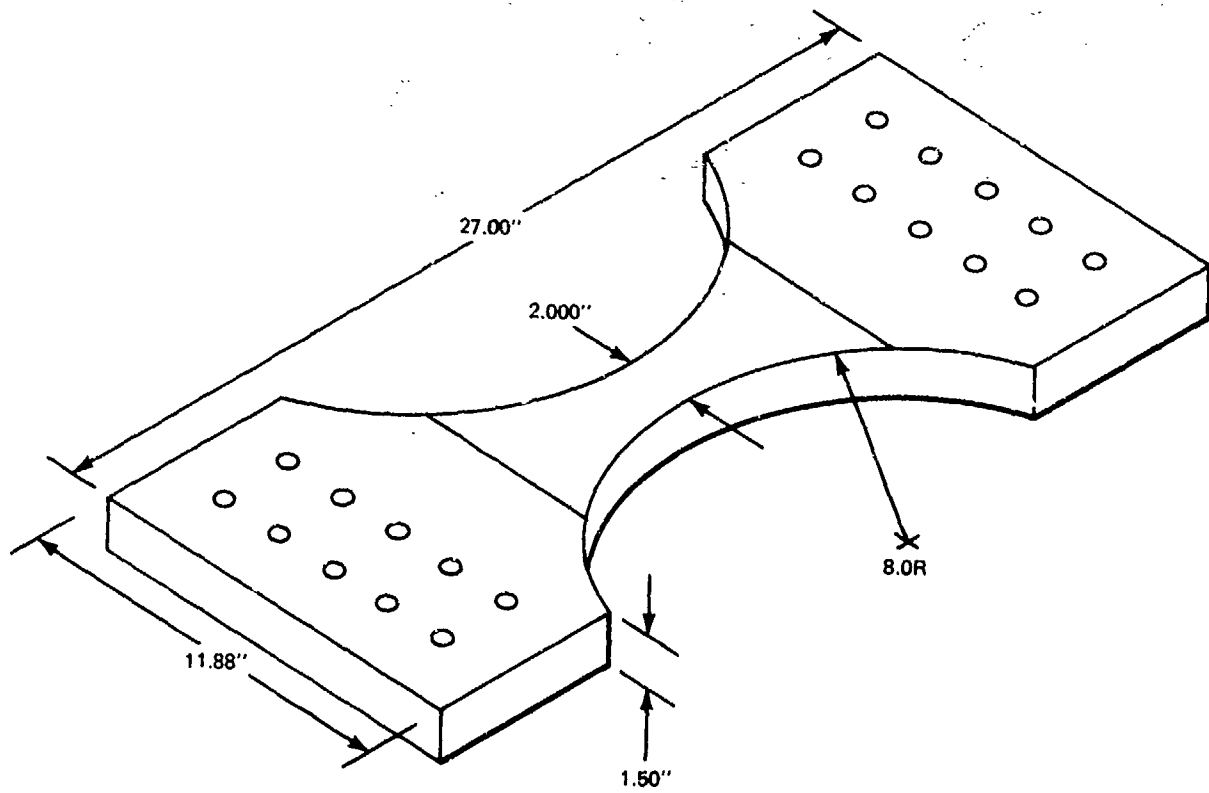


Figure A-11. Unnotched, Base-Metal Fatigue Specimen (1.5-Inch Thick)

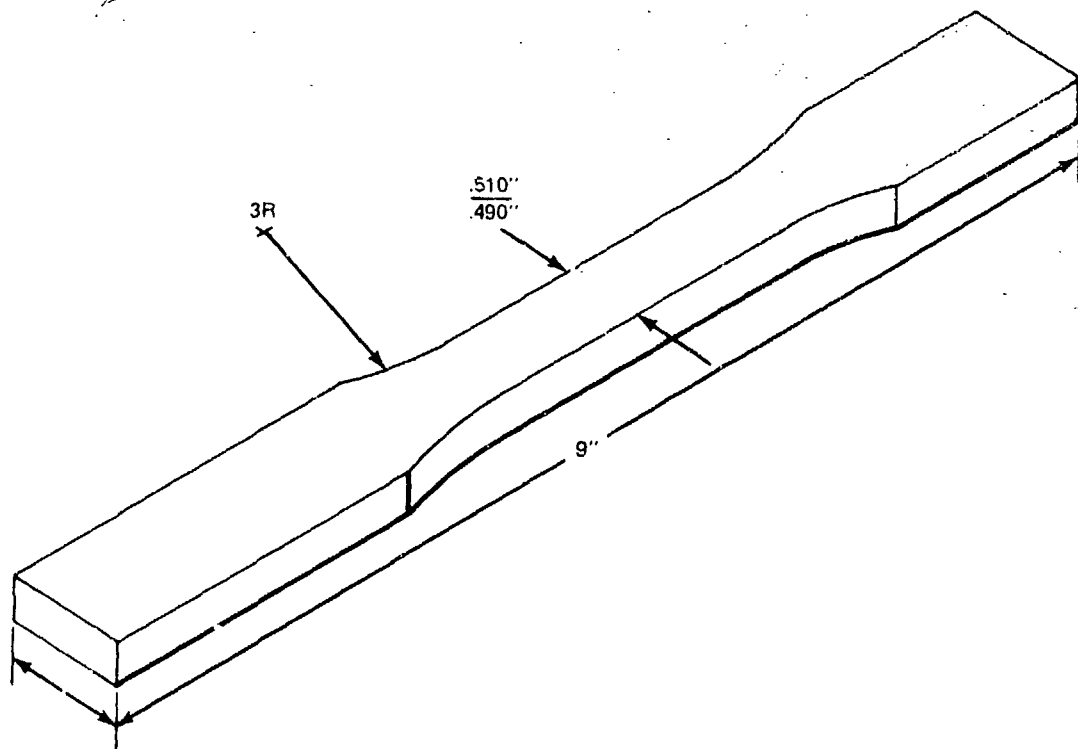


Figure A-12. Base-Metal Tensile Specimen (0.080- and 0.250-Inch Thick)

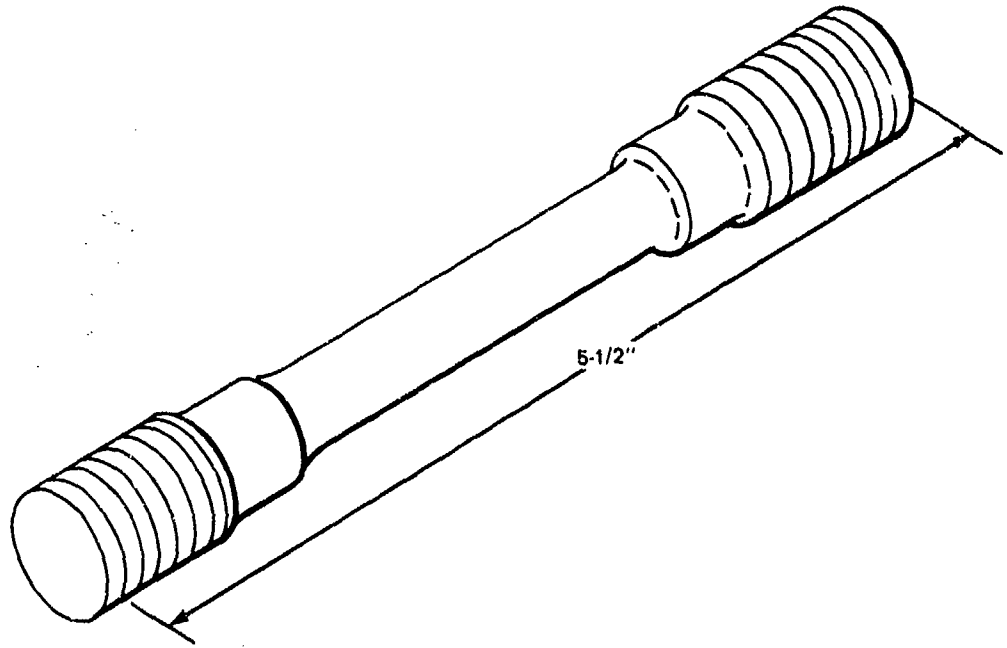


Figure A-13. Base-Metal Tensile Specimen (1.5-Inch Thick)

Table A-1. Phase 1 - 0.250-Inch-Thick Electron Beam Welding (Sheet 1 of 5)

WELD IDENT	NO. OF PASSES	OBJECT	SUCCESS		TECHNIQUE	DEFECT SIZE RANGE	WELD PARAMETERS				WELD BEAD				DEFECT LEVEL	COMMENTS, TEST RESULTS	
			Y	N			TRAVEL SPEED IPM	FOCUS CURRENT AMP	HEAT INPUT KJ	MACHINED		X-RAY		METAL LOGOGRAPHY			
										Y	N	Y	N	Y			N
FLAWLESS WELDS																	
4EB-FX-1 FM-1	1	FLAWLESS	X			1 PORE/QUARTER SPECIMEN ZONE OK	40	5.15	7.875	X		X			X	61,000 CYCLES 100KSI R++ 1	
4EB-FX-2 FM-2	1	"	X			SPECIMEN ZONE OK	40	5.15	7.875	X		X			X	58,000 CYCLES 100KSI R++ 1	
4EB-FX-3 FM-3	1	"	X			SPECIMEN ZONE OK	40	5.15	7.875	X		X			X	58,000 CYCLES 100KSI R++ 1	
POROSITY WELDS																	
4EB-PX-1	1	POROSITY	X		SAND BLAST NOT ACID CLEANED	.005 MAX V V F LIN. POR	40	5.15	7.875		X	X		X		1-PLATE	
4EB-PX-2 PM 2	1	POROSITY	X		SAND BLAST NOT ACID CLEANED	SCATTERED L P .005-.010	40	5.15	7.875	X		X		X		1 PLATE	
4EB-PX-3	1	POROSITY	X		SAND BLAST NOT ACID CLEANED	3-4Q 1.2Q OK PORES	40	5.15	7.875	X		X		X		2 PLATES	
4EB-PX-4	1	POROSITY		X	ROTARY WIRE BRUSH BURNISHED NOT ACID CLEANED	CLEAN	40	5.15	7.875	X		X		X			
4EB-PX-5	1	POROSITY		X	SAME AS ABOVE	CLEAN	40	5.15	7.875	X		X		X			
4EB-PX-6	1	POROSITY	X		SAW CUT EDGES NOT CLEANED	SOME .020 LP .005/.015	40	5.15	7.875	X		X	X				
4EB-PX-7	1	POROSITY		X	ACID CLEANING RESIDUE	CLEAN	40	5.15	7.875	X		X		X			
4EB-PX-8	1	POROSITY	X		ACID CLEANING RESIDUE	CLEAN	40	5.15	7.875	X		X		X			
4EB-PX-9	1	POROSITY	X		SAW CUT EDGES NOT CLEANED	POR. .005/.015	40	5.15	7.875	X		X		X		SOLVENT WIPE	
4EB-PX-10	2	POROSITY		X	1-LACK OF PEN. 1-SAME SIDE F.P.	3Q. PORES 1.2,4Q-OK	40	5.10	6.7	X		X		X		1ST PASS. SEE (4EB L.P.X. - 4)	

Table A-1. Phase 1 - 0.250-Inch-Thick Electron Beam Welding (Sheet 2 of 5)

WELD IDENT	NO. OF PASSES	OBJECT	SUCCESS		TECHNIQUE	DEFECT SIZE RANGE	WELD PARAMETERS				WELD READ				DEFECT LEVEL	COMMENTS, TEST RESULTS
			Y	N			TRAVEL SPEED IPM	FOCUS CURRENT AMP	HEAT INPUT KJ	MACH. INED	X-RAY	METAL LOGOGRAPHY	Y	N		
4EB-PX-11	2	POROSITY	X		1-LACK OF PEN 1-SAME SIDE FP	CLEAN	40	5.10	6.7	X	X	X	X	X	1ST PASS SEE 4EB-LPX-5	
4EB-PX-12	1	POROSITY	X		1 WK IN TAP H <sub>2</sub> O	CLEAN	40	5.10	6.75	X	X	X	X	X		
4EB-PX-13	1	POROSITY	X		24 HR IN 35HNO <sub>3</sub> /H <sub>2</sub> O	CLEAN	40	5.10	6.75	X	X	X	X	X		
4EB-PX-14	1	POROSITY	X		1WK IN 35 HNO <sub>3</sub> / H <sub>2</sub> O	CLEAN	40	5.10	6.75	X	X	X	X	X		
4EB-PX-15	1	POROSITY	X		RAISE WELD SPEED	L.P. 3-4Q 002/015	80	5.10	6.00	X	X	X	X	X		
4EB-PX-16	2	POROSITY	X		1 LACK OF PEN. 1 REV. SIDE FP	1-Q.L.P. 005 3Q-1P VSL POROSITY	40	5.10	6.75	X	X	X	X	X		
4EB-PX-17	1	POROSITY	X		SAW-CUT SOLVENT WIPE - NO ACID	ALL SIZES. LP-002/005 PORES .010-.020	80	5.10	6.00	X	X	X	X	X		
4EB-PX-18	1	POROSITY	X		SAW CUT-SOLVENT WIPE - NO ACID	ALL SIZES LP-.002-.005-.015	40	5.10	6.75	X	X	X	X	X		
4EB-PX-19	1	POROSITY	X		SAW-CUT SOLVENT WIPE-NO ACID	ALL SIZES .005-.020	120	4.80	6.25	X	X	X	X	X		
4EB-PX-20	1	POROSITY	X		SAW CUT-CUTTING OIL - NO ACID	UNUSABLE	120	4.80	6.875	X	X	X	X	X		
4EB-PX-21	1	POROSITY	X		MILLED EDGES CUTTING OIL - NO ACID	ALL SIZES LP-005-.015	120	4.80	6.875	X	X	X	X	X		
SURFACE CONTAMINA- TION WELDS																
4EB-SUX-4 SUM-1	1	SURF CONTAM	X		VACUUM OIL (LIGHT COAT)	1-2-3-4-Q-SL POR 1-4Q-OK 2,3-Q	40	5.15	7.875	X	X	X	X	X	HARDNESS TRAVERSE	
4EB-SUX-2 SUM-2	1	SURF CONTAM.	X		VACUUM OIL (HEAVY COAT, 3-4Q-OK)	SL. POR. 1-2-3-4Q 1-2Q-SL-POR 3-4Q-OK	40	5.15	7.875	X	X	X	X	X	HARDNESS TRAVERSE	
4EB-SUX-3	1	SURF CONTAM.	X		HYDROCARBON OIL	SL. POR 1-3Q	40	5.15	7.875	X	X	X	X	X	HARDNESS TRAVERSE	
4EB-SUX-4	2	SURF CONTAM.	X		VACUUM GREASE	Q.1-3 CL 2 PORES 4 Q.	40 40	5.50 5.10	1.575 6.750	X	X	X	X	X	HARDNESS TRAVERSE	

Table A-1. Phase 1 — 0.250-Inch-Thick Electron Beam Welding (Sheet 3 of 5)

WELD IDENT	NO. OF PASSES	OBJECT	SUCCESS		TECHNIQUE	DEFECT SIZE RANGE	WELD PARAMETERS				WELD BEAD				DEFECT LEVEL	COMMENTS, TEST RESULTS	
			Y	N			TRAVEL SPEED IPM	FOCUS CURRENT AMP	HEAT INPUT KJ	MACH-INED		X-RAY		METAL-LOGRAPHY			
										Y	N	Y	N	Y			N
<b>BURST WELDS</b>																	
4EB-BX 1U	1	BURSTS	X		WELD CHILL VARIATION USING A SQUARE SHAPED OPENING	-	40	5.15	7.875	X		X					
BX 1U-1RW	2						50	5.5	7.6	X		X					
BX 1U-2RW	3						40	5.15	18.6	X		X					
4EB-BX 2U	1	BURSTS	X		WELD CHILL VAR USING A SQUARE SHAPED OPENING	-	40	5.15	7.875	X		X					
BX 2U-1RW	2						50	4.85	7.6	X		X					
BX 2U-2RW	3						50	5.15	18.6	X		X					
4EB-BX 1V	1	BURSTS	X		WELD CHILL VAR USING A DIAMOND SHAPED OPENING	-	40	5.15	7.875	X		X					
BX 1V 1RW	2						50	4.85	7.6	X		X					
BX 1V 2RW	3						50	5.15	18.6	X		X					
4EB-BX 2V	1	BURSTS	X		WELD CHILL VAR USING A DIAMOND SHAPED OPENING	-	40	5.15	7.875	X		X					
BX 2V 1RW	2						50	4.85	7.6	X		X					
BX 2V 2RW	3						50	5.15	18.6	X		X					
4EB-BX 3U	1	BURSTS	X		SAME AS 4EB-BX-1U TRIED COLD WELD	-	40	5.10	6.7	X		X					
4EB-BX 4U	1	BURSTS	X		SAME AS 4EB-BX-1U	-	40	5.10	6.7	X		X					
4EB-BX 3V	1	BURSTS	X		SAME AS 4EB-BX-1V	-	40	5.10	6.7	X		X					
4EB-BX 4V	1	BURSTS	X		SAME AS 4EB-BX-1V	-	40	5.10	6.7	X		X					
4EB-BX 5U	1	BURSTS	X		CHANGED CUTOFF SPACING	-	40	5.10	6.75	X		X					
4EB-BX 6U	1	BURSTS	X		SAME AS 4EB-BX-5U	-	40	5.10	6.75	X		X					
4EB-BX 7U	1	BURSTS	X		SAME AS 4EB-BX-5U	-	40	5.10	6.75	X		X					
4EB2 BX 8U	2	BURSTS	X		LOCKING PASS SQ CUTOFF NO PLUG	-	40	5.15	1.57	X		X					
							40	5.10	6.75	X		X				LOCKING PASS FINAL PASS	

Table A-1. Phase 1 - 0.250-Inch-Thick Electron Beam Welding (Sheet 4 of 5)

WELD IDENT	NO. OF PASSES	OBJECT	SUCCESS		TECHNIQUE	DEFECT SIZE RANGE	WELD PARAMETERS			WELD BEAD				DEFECT LEVEL	COMMENTS, TEST RESULTS		
			Y	N			TRAVEL SPEED IPM	FOCUS CURRENT AMP	HEAT INPUT KJ	MACH. INED		X-RAY				METAL LOGOGRAPHY	
										Y	N	Y	N			Y	N
4EB2-8X-9U	2	BURSTS	X		LOCKING PASS SQ. CUTOUT PLUG INSERT	-	40	5.15	1.57	X		X					
							40	5.10	6.75	X	X						
4EB2-8X-10	2	BURSTS	X		BASELINE LOCKING PASS (LP) + F.P. STAGGERED L.P. + F.P.	-	40	5.15	1.57	X		X					
							40	5.10	6.75	X	X						
4EB2-8X-11	2	BURSTS	X		LOCKING PASS 1/2" HIGH 3/8 DIA T. PLUGS COSMETIC PASS	-	40	5.15	1.57	X		X					
							40	5.15	6.75	X	X						
4EB2-8X-12	3	BURSTS	X		DEEPER LOCKING PASS + FP	-	40	5.15	1.57	X		X					
							40	5.15	6.75	X	X						
4EB2-8X-13	2	BURSTS	X		F.P. LOCKING PASS (STAGGERED) + FULL PEN. PASS	-	40	5.15	1.57	X		X					
							40	5.15	6.75	X	X						
4EB2-8X-14	2	BURSTS	X		3/8 PLUGS IN- SERTED IN WELD (DRILLED HOLES)	-	40	5.15	1.57	X		X					
							40	5.15	6.75	X	X						
4EB2-8X-15	1	BURSTS	X		OFFSET CUTOUTS WITH WELDED PLUGS	-	40	5.15	6.75	X		X			MADE FROM 4EB2-8X-13		
							40	5.15	6.75	X	X						
4EB2-8X-16	2	BURSTS	X		WELD RESTRAINT	-	40	5.15	7.875	X		X					
							40	5.10	7.875	X	X						
SHRINKAGE CRACK WELDS					WELD RESTRAINT	-											
4EB-CX-1	1	CRACKS	X														
	2	CRACKS	X														
4EB-CX-2	1	CRACKS	X														
	2	CRACKS	X														
	3	CRACKS	X														



Table A-2. Phase 1 - 0.090-Inch-Thick Electron Beam Welding

WELD IDENT	NO OF PASSES	OBJECT	SUCCESS		TECHNIQUE	DEFECT SIZE RANGE	WELD PARAMETERS				WELD BEAD				DEFECT LEVEL	COMMENTS, TEST RESULTS	
			Y	N			TRAVEL SPEED IPM	FOCUS CURRENT AMP	HEAT INPUT KJ	MACH. INED		X-RAY		METAL-LOGOGRAPHY			
										Y	N	Y	N	Y			N
FLAWLESS WELDS 9EB-PX-1 FM-1 9EB-PX-2 MM-2 9EB-PX-3 MM-3	2	FLAWLESS	X				60	5.20	0.75							56,000 CYCLES-100 KSI R <sup>+</sup> +1 75,000 CYCLES-100 KSI R <sup>+</sup> +1 71,000 CYCLES-100 KSI R <sup>+</sup> +1	
			X				60	5.20	3.75	X							
				X			60	5.20	0.75								
				X			60	5.20	3.75								
				X			60	5.20	0.75								
				X			60	5.20	3.75								
POROSITY WELDS 9EB-PX-1 9EB-PX-2 9EB-PX-3 9EB-PX-4 9EB-PX-5 9EB-PX-6	2	POROSITY		X	HYDRAULIC OIL	CLEAN	60	5.20	0.75							-	
				X			60	5.20	3.75	X							
	2	POROSITY		X	SAW CUTTING OIL	POROSITY MODERATE 003/007	60	5.20	0.75								
				X			60	5.20	3.75	X							
	2	POROSITY		X	AIR FURN 180°F. 4 DAYS	40 CLEAN 1-2-3-0-1-2 PORES	60	5.20	0.75								
				X			60	5.20	3.75	X							
2	POROSITY		X	AIR FURN 180°F. 7 DAYS	CLEAN	60	5.20	0.75									
			X				60	5.20	3.75	X							
2	POROSITY		X	AIR FURN-14 DAY 10% HUMIDITY	CLEAN	60	5.20	0.75									
			X				60	5.20	3.75	X							
2	POROSITY		X	SAME AS 9EB-PX-5	CLEAN	60	5.20	0.75									
			X				60	5.20	3.75	X							

Table A-3. Phase 1 - 0.250-Inch-Thick Plasma-Arc Welding (Sheet 1 of 3)

WELD IDENT	NO OF PASSES	OBJECT	SUCCESS		TECHNIQUE	DEFECT SIZE RANGE	WELD PARAMETERS				WELD BEAD						DEFECT LEVEL	COMMENTS, TEST RESULTS
			Y	N			TRAVEL SPEED (IPM)	WIRE FEED (IPM)	HEAT INPUT (KJ)	MACHINED		X-RAY		METAL LOGOGRAPHY				
										Y	N	Y	N	Y	N	Y		
FLAWLESS WELDS																		
APAW FX 1 FM 1	1	FLAWLESS	X	X	ACID CLEAN NO WIRE BRUSH	LP 005-010 LP 005-010	30	24 375		X	X	X	X	X	X	X	N/A	SCRAPPED
APAW FX 2 FM 2	1		X	X	NO WIRE BRUSH ACID CLEAN	7 30 CLEAN LP 30 001	30	24 375		X	X	X	X	X	X	X	N/A	SCRAPPED
APAW FX 3 FM 3	1		X	X	ACID CLEAN NO WIRE BRUSH NOT DET ON 2 and X-RAY ONLY	ALL CLEAN 7 30 LP 005	30	24 375		X	X	X	X	X	X	X	N/A	100 KSI R=+1 29,000 CYCLES
APAW FX 4 FM 4	1		X	X	ACID CLEAN WIRE BRUSH	CLEAN 7 30 CLEAN	30	24 375		X	X	X	X	X	X	X	N/A	100 KSI R=+1 50,000 CYCLES
APAW FX 5 FM 5	1		X	X	ACID CLEAN WIRE BRUSH	1 7 1 7 30 CLEAN 1 7 1 7 30 CLEAN	30	24 375		X	X	X	X	X	X	X	N/A	34,000 CYCLES 100 KSI R=+1
APAW FX 6 FM 6	1		X	X	ACID CLEAN WIRE BRUSH	1 7 1 7 30 CLEAN 1 7 1 7 30 CLEAN	30	24 375		X	X	X	X	X	X	X	N/A	NOT USED
POROSITY WELDS																		
APAW FX 1 PM 1	1	POROSITY	X		ACID CLEAN TIME DELAY EXCEEDED	1 2 4 O CLEAN	30	23 906		X	X	X	X	X	X	X		SCRAPPED
APAW FX 2 PM 2	1	POROSITY	X		MACHINE OIL ON BOTTOM 1/2 OF WELD	CONTINUOUS 005-020 010 AVG	30	24 375		X	X	X	X	X	X	X	2	
APAW FX 3 PM 3	1	POROSITY	X		ACID RESIDUE LEFT ON PLATE	CONTINUOUS 010 MAX 005 AVG	30	24 375		X	X	X	X	X	X	X	1	
APAW FX 4	1	POROSITY	X		SAW CUT EDGES		0	25 31		X	X	X	X	X	X	X		NO QUAD SHT
APAW FX 5	1	POROSITY	X		SAW CUT EDGES		0	20 160		X	X	X	X	X	X	X		NO QUAD SHT
APAW FX 6	1	POROSITY	X		SAW CUT/MACH OIL		0			X	X	X	X	X	X	X		NO QUAD SHT

Table A-3. Phase 1 - 0.250-Inch-Thick Plasma-Arc Welding (Sheet 2 of 3)

WELD IDENT	NO. OF PASSES	OBJECT	SUCCESS	TECHNIQUE	DEFECT SIZE RANGE	WELD PARAMETERS					WELD BEAD				DEFECT LEVEL	COMMENTS, TEST RESULTS	
						TRAVEL SPEED IPM	WIRE FEED IPM	HEAT INPUT KJ	MACHINED		X-RAY		METALLOGRAPHY				
									Y	N	Y	N	Y	N			Y
SPAW 1	1	WELD	Y	WELD		24	0									NO QUAD SHT	
SPAW 2	1	WELD	Y	WELD		26	0									NO QUAD SHT	
SPAW SUR 1	1	SURF	Y	WELD	VISUAL	16	28	24.375									HARDNESS TRAVERSE
SPAW SUR 2	1	SURF	Y	WELD	VISUAL	16	28	23.837									HARDNESS TRAVERSE
SPAW SUR 3	1	SURF	Y	WELD	VISUAL	16	28	23.837									HARDNESS TRAVERSE
UNDEMCUT WELDS																	
SPAW UN 1	1	UNDEMCUT CUT	Y	WELD		16	0	26.831									SCRAPPED
SPAW UN 2	1	UNDEMCUT CUT	Y	WELD		16	0	28.760									ORIF FLOW 13 CFH
SPAW UN 3	1	UNDEMCUT CUT	Y	WELD		16	0	28.760									ORIF FLOW 15 CFH
SPAW UN 4	1	UNDEMCUT CUT	Y	WELD		27	0	20.66									ORIF FLOW 17 CFH
SPAW UN 5	1	UNDEMCUT CUT	Y	WELD		27	0	20.66									ORIF FLOW 17 CFH

Table A-1. Phase 1 - 0.250-inch-Thick Plasma-A: Welding (Sheet 3 of 3)

WELDMENT	NO OF PASSES	OBJECT	SUCCESS		TECHNIQUE	DEFECT SIZE RANGE	WELD PARAMETERS				WELD BEAD				DEFECT LEVEL	COMMENTS, TEST RESULTS						
			Y	R			TRAVEL SPEED (IPM)	WIRE FEED (IPM)	HEAT INPUT (KJ)	MACH. (INCH)	Y	N	M	N			Y	N	Y	N		
INSURANCE MANT WELD	1	PIPE FORGE MENT	X		NORMAL	0.06 CRACKING 0.02 DISCR	16	26	24 375	X	X	X	X	X	2	DIFFERENTIAL DUE TO TRAVEL SPEED CHANGES						
																	X	X	X	X	X	X
OPAN CR 2 MANT	1	PIPE FORGE MENT	0		NORMAL	0.02 CRACKING 0.02 DISCR	16*	26	24 375	X	X	X	X	X	1	*ACCURACY OF CONTROLLER QUESTIONED						
																	X	X	X	X	X	X
CRACK WELDS	1	CRACKS	R		WELD RESTRAINT		16	0	72.6	X	X	X	X	X	N/A	REVERSE DIR						
																	X	X	X	X	X	X
																	X	X	X	X	X	X
																	X	X	X	X	X	X
																	X	X	X	X	X	X
																	X	X	X	X	X	X
																	X	X	X	X	X	X
OPAN CR 2 CRACK	1	CRACKS	R		WELD RESTRAINT		16	0	73.6	X	X	X	X	N/A	SPECIMEN 1/2 GOOD							
																X	X	X	X	X	X	
																X	X	X	X	X	X	
																X	X	X	X	X	X	
																X	X	X	X	X	X	
																X	X	X	X	X	X	

Table A-4. Phase 1 -- 0.090-Inch-Thick Gas-Tungsten-Arc Welding (Sheet 1 of 2)

WELD IDENT	NO. OF PASSES	OBJECT	SUCCESS		TECHNIQUE	DEFECT SIZE RANGE	WELD PARAMETERS				WELD BEAD						DEFECT LEVEL	COMMENTS, TEST RESULTS
			Y	N			TRAVEL SPEED IPM	WIRE FEED IPM	HEAT INPUT KJ	MACH-INING		X-RAY		METAL LOGOGRAPHY				
										Y	N	Y	N	Y	N	Y		
FLAWLESS WELDS																		
9GTA-FX-1 FM-1	1	FLAWLESS	X		ACID CLEANED AND SCRAPPED		20	15.6			X				X		53,000 CYCLES 100 KSI R <sub>0.1</sub>	
9GTA-FX-2 FM-2	1	" "	X		ACID CLEANED AND SCRAPPED		20	15.6			X				X		44,000 CYCLES 100 KSI R <sub>0.1</sub>	
9GTA-FX-3 FM-3	1	" "	X		ACID CLEANED AND SCRAPPED		20	15.6			X				X		63,000 CYCLES 100 KSI R <sub>0.1</sub>	
POROSITY WELDS																		
9GTA-PX-1 PM-1	1	POROSITY	X		AIR EXPOSURE 1 WK.	CONTINUOUS 1-4 Q-007/010	6	20	15.6			X			X	1		
9GTA-PX-2	1	POROSITY	X		HYDROCARBON OIL	1-40 010/025 017 AVG.	6	20	15.6			X			X	2		
INCLUSION WELDS																		
9GTA-IX-1	1	W. INCLUSIONS		X	HAND TORCH TACKLING	055 x 040 040 x 030 .110 SPAC	6	20	15.6			X			X		POROSITY ASSOC. WITH W	
9GTA-IX-2	1	W. INCLUSIONS		X	HAND TORCH TACKLING	010 x 010 015 x 005 .025 x 015, 020 x 020, 005 x 002	6	20	16.25			X			X		POROSITY ASSOC. WITH W	
9GTA-IX-3	1	W. INCLUSIONS		X	HAND TORCH TACKLING	040 x 025, 030 x 020, x 025 x 020, 005 x 005	6	20	16.25				X				NO POROSITY BUT LOCATED IN CROWN OR DROP THROUGH	
9GTA-IX-4	2	W. INCLUSIONS		X	UNACCEPTABLE		6	0	15.6			X			X		ROOT PASS PRIOR TO W PLACEMENT 1 COVER PASSES	

Table A-5. Phase 1 — 0.090-Inch-Thick Gas-Tungsten-Arc Welding (Sheet 2 of 2)

WELD IDENT	NO. OF PASSES	OBJECT	SUCCESS		TECHNIQUE	DEFECT SIZE RANGE	WELD PARAMETERS				WELD BEAD				DEFECT LEVEL	COMMENTS, TEST RESULTS
			Y	N			TRAVEL SPEED IPM	WIRE FEED IPM	HEAT INPUT KJ	MACH. INED	X-RAY	METAL LOGOGRAPHY	Y	N		
9GTA-1X-5	2	W. INCLU-SIONS	X		UNACCEPTABLE		6 6	0 20	15.6 16.25		X	X				ROOT PASS PRIOR TO W PASS, 1 COVER PASS
9GTA-1X-6	2	W. INCLU-SIONS	X		T/G TORCH	.060-.100	6 6	0 20	15.6 16.25		X	X	X		1.2	SAME
9GTA-1X-7	2	W. INCLU-SIONS	X		TACKING	.060-.100	6 6	0 20	15.6 16.25		X	X	X		1.2	SAME
UNDERFILL WELDS																
9GTA-UFX-1	1	UNDER-FILL	X		NO FILLER	0.011 UNDERFILL 0.018 DROP	6	0	15.6		X	X	X		2	
9GTA-UFX-2	1	UNDER-FILL	X		NO FILLER - INCR TRAV SPEED	0.0122 UNDERFILL 0.0139 DROP	6	0	11.70		X	X	X		1	
MISMATCH WELDS																
9GTA-MSX-1	1	MISMATCH	X		METAL SHIM-016	NO POROSITY .013 OFFSET	6	20	16.25		X	X	X		1	
9GTA-MSX-2	1	MISMATCH	X		METAL SHIM-025	NO POROSITY .026 OFFSET	6	20	16.25		X	X	X		2	

Table A-5. Phase 1 — 0.250-Inch-Thick Electron Beam Welding-NDI Summary (Sheet 1 of 7)

WELD IDENT	LENGTH	1 <sup>st</sup> QUARTER	2 <sup>nd</sup> QUARTER	3 <sup>rd</sup> QUARTER	4 <sup>th</sup> QUARTER	COMMENTS
4EB-FX-1	12"	1 1/4" IN - 020 PORE SLIGHT WELD UNDER- CUT	1" FROM END .015 (2" IN)	1 3/4" IN - 010	2" OVER .010	
4EB-FM-1	12"	VIS UNDERFILL CLEAN.	2" IN - 2 PORES - 012, 010	1 3/4" 010	CLEAN	
4EB-FX-2	12"	1/2" IN - .010 CLEAN	CLEAN	1 1/2" IN - 005	CLEAN	
4EB-FM-2	12"	3/4" FROM O2 - TOP-010 B-010	CLEAN	1 1/2" IN - .010 CLEAN	1/2" .010 - B CLEAN	
4EB-FX-3	12"	3/4" IN .015 PORE CLEAN.	CLEAN	1 1/2" IN - 020 LONG-005	CLEAN	
4EB-FM-3	12"	START AREA VISUAL UNDERFILL 1/2 FROM O2 .020	CLEAN	CLEAN	CLEAN	

Table A-5. Phase 1 -- 0.250-Inch-Thick Electron Beam Welding-NDI Summary (Sheet 2 of 7)

WELD IDENT	LENGTH	1st QUARTER	2nd QUARTER	3rd QUARTER	4th QUARTER	COMMENTS
4EB-PX-1	12"	MID & 015 ☉ .010" 1" FROM Q2	TOP - 1 1/2" IN - V.V.F. LIN. POR 1 1/2" LONG .005 MAX MID CLEAN BOT	TOP SAME - ENTIRE LENGTH. MID - 005, 005, 005. BOT - CLEAN	TOP 1" SAME MID - PORE - 020 BOT - OK.	
4EB-PX-2	12"	TOP - SCATTERED LINEAR POROSITY 005 MAX ☉ MID - 010, 1/2" END 015 BOT. CLEAN	TOP - SCAT. LIN. POR. 005 MAX MID - .010 BOT. - CLEAN	TOP - FINE SCAT LIN. POR 005 MAX 1-2 UP TO 010 MID - 005, 010 BOT. CLEAN	TOP - FINE LIN. POROSITY MID-CLEAN BOT. - CLEAN	
4EB-PX-3	12"	CLEAN	CLEAN	& 1/2 IN. - .005	TOP & BOT LIN POR - SMALL 005 MAX	
4EB-PX-4	12"	BOTTOM 6 PORES IN .025 LONG AVG. - .003	CLEAN	CLEAN	CLEAN	
4EB-PX-5	12"	CLEAN	CLEAN	CLEAN	CLEAN	
4EB-PX-6	12"	TOP - LIN. POR 002/.010 - AVG = 005 BOT. (1 1/2 IN.) SPOTTY - 1/4 IN. 002/015 AVG = .007	LIN POR. 0.005/020 AVG = 010 BOT. - 3/4 IN. PORS. 005 MID - 005, END - SPOTTY	LIN. POR. - 0.005/015. AVG = .008 MID - 015, 020, 005, BOT. - SCAT. POROS. ITY 1st 1/2 005/015	LIN. POROSITY - 005/015 BOT. SCAT POROS- ITY 1st 1/2 005/015	
4EB-PX-7	12"	CLEAN	CLEAN	CLEAN	CLEAN	
4EB-PX-8	12"	CLEAN	CLEAN	1 IN. .005 ☉ 1 1/2 IN. .010 ☉	CLEAN	CLEAN

Table A-5. Phase 1 - 0.250-inch-Thick Electron Beam Welding-ND! Summary (Sheet 3 of 7)

WELD IDENT	LENGTH	1 <sup>st</sup> QUARTER	2 <sup>nd</sup> QUARTER	3 <sup>rd</sup> QUARTER	4 <sup>th</sup> QUARTER	COMMENTS
4EB-PX-9	12"	TOP, MID, BOT. SMALL POROSITY THROUGHOUT - 005/015. NOT LINEAR	SIMILAR	SIMILAR	POOR - UNUSABLE PLATE OPENED UP	
4EB-PX-10 REWELD OF 4EB-LPX-4	10"	1 IN. 020 PORE - BOTTOM 2" IN. - 015	CLEAN UNDERFILL	CLEAN	CLEAN	REWELD FROM SAME SIDE.
4EB-PX-11 REWELD OF 4EB LPX-5	10"	CLEAN	CLEAN	1/4 IN. BOT: SERIES OF LITTLE PORES - 050 LONG LINEAR	CLEAN	REWELD FROM SAME SIDE
4EB-PX-12	12"	CLEAN	CLEAN	CLEAN	CLEAN	
4EB-PX-13	10 1/2"	CLEAN	CLEAN	CLEAN	CLEAN	
4EB-PX-14	11"	CLEAN	CLEAN	CLEAN	CLEAN	
4EB-PX-15	11"	CLEAN	CLEAN	MID $\phi$ - .010 PORE TOP 2IN. START .005 BOT - LIN. POR. 005/015	TOP - CLEAN MID 010/020 BOT. FINE L.P. 002/005	
4EB-PX-16	11"	TOP - LIN. POR. 1/2 IN. LONG 005 MAX BOT. CLEAN	CLEAN	TOP - CLEAN MID - 3/4 IN. FROM END - .010 BOT. CLEAN	CLEAN	

Table A-5. Phase 1 - 0.250-Inch-Thick Electron Beam Welding-NDI Summary (Sheet 4 of 7)

WELD IDENT	LENGTH	1st QUARTER	2nd QUARTER	3rd QUARTER	4th QUARTER	COMMENTS
4EB-PX-17	9"	CLEAN	TOP - CLEAN MID - .020, .010, .015 010, 010 BOT - CLEAN	TOP - 010, LIN. POROSITY - 1" LONG 005/010, LIN PORE. 1" - .005 MAX MID - (2 IN.) - 010, 020, BOT. FINE LIN. POROSITY 002/005	TOP - LIN. POROSITY - 1" IN. 002/005 CLEAN	
4EB-PX-18	9"	CLEAN	TOP - 1/4 IN. - .010 LIN. POROSITY - 002/005 MID - CLEAN BOT. SM. LIN. 002/005	TOP - CLEAN. MID - CLEAN BOT - LIN. POR. 1 IN. 010, 010, 015, 015, 1 IN. END - LIN. POR.	TOP - LIN. POR. 1/8 IN. .005 MAX MID - CLEAN BOT. LIN. POR. ENTIRE LENGTH	
4EB-PX-19	9"	CLUSTER OF PORES 1/2 IN. - .015, .030, .025", .025", .010", .015", .020", 3/4" TO 1 1/4" IN-LINE OF 7 PORES AVE. - .015" LAST 1 3/4" SCAT- TERED PORES 1/4" APART (.015") SOME UNDERCUTTING	CLUSTERS OF MINOR LINEAR POROSITY THRU- OUT AVERAGE .005" UNDERCUTTING	FIRST 1 1/4" - HEAVY UNDERCUTTING 1 1/4" - 1 3/4" IN - 6 PORES AVERAGE - .010" REMAINDER - FINE LINE OF SMALL LINEAR POROSITY	LACK OF PENETRATION ENTIRE LENGTH	
4EB-PX-20	9"	UN READABLE - WELD UNSATISFACTORY	UN READABLE - WELD UNSATISFACTORY	UN READABLE - WELD UNSATISFACTORY	UN READABLE - WELD UNSATISFACTORY	
4EB-PX-2	9"	1st 1 1/4" SCAT- TERED POROS- ITY .010" - .025"	1" IN. - 2 PORES .010" LAST 1 3/4" 4 SCATTERED PORES .005"	1" IN - LARGE VOID - 200" x .060" 1 3/4" IN - VOID .020" x .005"	1st 3/8" IN 5 PORES .005" - .015" 1/2" IN - VOID .075" x .050. LAST 2" LACK OF PENETRATION. POROSITY AND VOIDS	

Table A-5. Phase 1 - 0.250-Inch-Thick Electron Beam Welding-NDI Summary (Sheet 5 of 7)

WELD IDENT	LENGTH	1 <sup>st</sup> QUARTER	2 <sup>nd</sup> QUARTER	3 <sup>rd</sup> QUARTER	4 <sup>th</sup> QUARTER	COMMENTS
4EB-LPX-1	12"	HEAVY POROSITY. LAST 1 1/2"	1/4" POROSITY 1/2" ☉ 030, 025, 010, 020 MID - 010, 005, 015, 020, 005, 015	1/2 - 1 1/2" HEAVY LINEAR POROSITY	SMALL PORE - .015 (START)	MISSED SEAM ENTIRE LENGTH.
4EB-LPX-2	12"	CLEAN	CLEAN	CLEAN	1 1/2" IN - 025 ☉ 2" IN 015 ☉ CLEAN	MISSED SEAM ENTIRE LENGTH
4EB-LPX-2	11	CLEAN	CLEAN	CLEAN	CLEAN	MISSED SEAM.
4EB-LPX-3	12"	CLEAN	1/2" - 0/2 PORE-BOT. ☉+TA10 - 015 PORE. CLEAN	1/2" IN 4 PORES - ☉ OF WELD 005, 005, 005, 003. END OF Q3 - 1/4 .010 PORE	GAP WIDENS NOT FOR USAGE	MISSED SEAM ENTIRE LENGTH
4EB-LPX-3	11	1 1/4 IN - .007	1 1/2" IN 015 ON SEAM - 020. 2" IN - ON SEAM - 010 2 1/4" - 015 BELOW SEAM	SCATTERED LINEAR POROSITY ON SEAM .005 TYP. 050, 020 SPAC. WELD METAL 2 1/4 - 005, 010	SEAM OPENS UP - - NOT USABLE -	LACK OF PENETRATION
4EB-LPX-4	10"	CLEAN	1 1/2" IN - 0.015 PORE	CLEAN	BOT. -010 (NOT ROUND)	
4EB-LPX-5	10"	1 1/2" IN 010, 012, 005, 010 020, .005, .010 .015	1/3" IN .025, 010, 005, 010, 015, 015, 020, 025, 010, 020, 005, 010	3/4" IN 010, 010, 015, 010, 010,	1/4" IN 005, 015, 010, 010, 005,	

Table A-5. Phase 1 - 0.250-Inch-Thick Electron Beam Welding-NDI Summary (Sheet 6 of 7)

WELD IDENT	LENGTH	1 <sup>st</sup> QUARTER	2 <sup>nd</sup> QUARTER	3 <sup>rd</sup> QUARTER	4 <sup>th</sup> QUARTER	COMMENTS
4EB-SUX-1	12"	1" FROM END - .005 PORE.	☉ MID - LIN. POR. .002/.005 .125 LONG 1-0.010 PORE 2" IN.	1/2" FROM END - .010 PORE.	.015 1" FROM END	
4EB-SUM-1	11"	(1" CUT OFF) VISUAL UNDERCUT CLEAN	2" IN - .015 PORE	3/4" FROM Q4 - .010 PORE.	CLEAN	
4EB-SUX-2	12"	MID ☉ - .010 1/4" END - .010	1 1/4" IN - .010 ☉ 2" IN .005.	☉ MID - .007	1 1/2 IN - .010	
4EB-SUM-2	11"	(1" CUT OFF) 1/2 IN - .025 PORE. 1 1/2" - .015 PORE. CLEAN	3/4" IN - .020 CLEAN	CLEAN	CLEAN	
4EB-SUX-3	12"	1" IN BOT - .010, .015.	1" IN - .005. ☉ - .005. 1 1/2 IN .010, .010,	☉ 1/4" IN - .005, .005, ☉ .007 MID. .010.	CLEAN	
4EB-SUM-3	11"	(1" CUT OFF) 1 1/2" IN .010-3 PORES	1/4" FROM Q3 - ☉ 005	CLEAN	CLEAN	
4EB-SUX-4	12"	OK VISUAL UNDER- CUTTING	OK VISUAL UNDER- CUTTING	OK VISUAL UNDER- CUTTING	2 - .005" PORES 2 1/2" FROM STOP VISUAL UNDER- CUTTING	

Table A-5. Phase 1 -- 0.250-Inch-Thick Electron Beam Welding-NDI Summary (Sheet 7 of 7)

WELD IDENT	LENGTH	1 <sup>st</sup> QUARTER	2 <sup>nd</sup> QUARTER	3 <sup>rd</sup> QUARTER	4 <sup>th</sup> QUARTER	COMMENTS
4EB-BX-1U	12"					
4EB-BX-2U	12"					
4EB-BX-3U	12"					
4EB-BX-4U	12"					
4EB-BX-5U	12"					
4EB-BX-6U	12"					
4EB-BX-7U	12"					
4EB-BX-1V	12"					
4EB-BX-2V	12"					
4EB-BX-3V	12"					
4EB-BX-4V	12"					
4EB-C-X-1	1/18/73	←	NO	CRACKS	→	HEAVY UNDERFILL
4EB-C-X-2	3/7/73	CLEAN	CLEAN	CLEAN	CLEAN	UNDERFILL
	3/12/73	SEVERAL	QUESTIONABLE AREAS	IN HAZ DYE CHECK	NEGATIVE	UNDERFILL
	3/27/73	NUMEROUS	QUESTIONABLE AREAS	IN HAZ DYE CHECK	NEGATIVE	UNDERFILL

Table A-6. Phase 1 -- 0.090-Inch-Thick Electron Beam Welding-NDI Summary (Sheet 1 of 2)

WELD IDENT	LENGTH	1 <sup>st</sup> QUARTER	2 <sup>nd</sup> QUARTER	3 <sup>rd</sup> QUARTER	4 <sup>th</sup> QUARTER	COMMENTS
9EB-FX-1	14"	CLEAN	CLEAN	CLEAN	CLEAN	
9EB-FM-1	14"	CLEAN	CLEAN	CLEAN	CLEAN	
9EB-FX-2	14"	CLEAN HIGH DENSITY INCLUSION BELOW WELD 0.030 (CB SPLATTER)	CLEAN	TOP - 1" IN .015 INCLUSION. (CB SPLATTER) REST CLEAN	CLEAN	
9EB-FM-2	14"	CLEAN	CLEAN	CLEAN	CLEAN	
9EB-MX-3	14"	CLEAN	TOP 1" FROM Q3 - INCLUSION .010 CLEAN	CLEAN	TOP CLEAN BOT. 3 PORES - 2" FROM Q3 - 007 RUG	
9EB-FM-3	14"	CLEAN	VISUAL UNDERFILL NO POROSITY	VISUAL UNDERFILL .012 PORE - 1" FROM Q4	VISUAL UNDERFILL	

Table A-6. Phase 1 - 0.090-Inch-Thick Electron Beam Welding-NDI Summary (Sheet 2 of 2)

WELD IDENT	LENGTH	1 <sup>st</sup> QUARTER	2 <sup>nd</sup> QUARTER	3 <sup>rd</sup> QUARTER	4 <sup>th</sup> QUARTER	COMMENTS
9EB-PX-1	10"	CLEAN	CLEAN	CLEAN	CLEAN	
9EB-PX-2	10"	TOP - 003, 005, 005, 075, 005, 007, 007, 005, 007, 005, 005, 005, 005, 005, 005, 005, 003, 005, 005, 003, 005, 003, 003, 003, 005, 005, 005, 003, 010, 007, 005, 005, 005, 003, 005, 003, 005, 005, 005, 005 BOT. SIMILAR - 75% CLEANER	TOP - 003, 003, 005, 003, 003, 007, 005, 005 BOT. CLEAN - AT END. $\odot$ 005, 005	TOP - 005, 005, 075, 005 BOT. CLEAN	CLEAN TOP - 005, 005, 005, 075, 005, 005, 005, 005, 005, 005, 005, 005, 005, 005, 010, 007, 005, 006, 005, 005, 005, 005, 005, 007, 005, 005, 005, 005, 005, 007 BOT. CLEAN	
9EB-PX-3	8"	TOP - 005, 005 $\odot$ 003, 003 BOT. CLEAN	TOP - 005 BOT. CLEAN	TOP - 005 $\odot$ BOT. CLEAN	CLEAN	
9EB-PX-4	8"	CLEAN	CLEAN	CLEAN	CLEAN	CLEAN
9EB-PX-5	10"	UNDERFILL, CLEAN	SAME	SAME	SAME	CLEAN
9EB-PX-6	8"	CLEAN	SOME UNDERFILL CLEAN	CLEAN SAME	CLEAN SAME	CLEAN

Table A-7. Phase 1 - 0.250-Inch-Thick Plasma-Arc Welding - NDI Summary (Sheet 1 of 5)

WELD IDENT	LENGTH	1 <sup>st</sup> QUARTER	2 <sup>nd</sup> QUARTER	3 <sup>rd</sup> QUARTER	4 <sup>th</sup> QUARTER	COMMENTS
4PAW-FX-1	12"	LINEAR POROSITY (TOP) AVG .007/000 005/015 C - CLEAN BOT. CLEAN	SIMILAR (LINEAR POROSITY). C - CLEAN C - CLEAN	SAME CLEAN CLEAN	SAME - LESS  CLEAN	SCRAP
4PAW-FM-L	12"	TOP LINEAR POROSITY CONT. AVG .007 015/003 MID. C .007 BOT. - CLEAN	SIMILAR .007 - CLEAN - CLEAN CLEAN	SAME CLEAN CLEAN	SAME 56 LESS  CLEAN	SCRAP
4PAW-FX-2	12"	CLEAN	CLEAN	CLEAN	POROSITY ALONG TOP EDGE - .002 MAX - 005	
4PAW-FM-2	12"	TOP - CLEAN BOT LIN POROSITY AVG .005 010/007	TOP 1 ID 1 BOTTOM CLEAN	TOP - CLEAN BOT. 001 LINEAR POROSITY	TOP CLEAN BOT. SCATT. LIN. PORE 005 010/002.	
4PAW-FX-3	12"	CLEAN	CLEAN	CLEAN	CLEAN	
4PAW-FM-3	12"	CLEAN	TOP - 0.3 LONG 0.3 LINEAR POROSITY .005 MAX. BOT. HAIRLINE POROSITY 005 MAX. 2" LONG	TOP - CLEAN BOT. HAIRLINE POROSITY 005 MAX NEAR Q4 0.10 MAX.	TOP - CLEAN BOT. FINE LINEAR POROSITY - 005 MAX.	SPECIMEN
4PAW-FX-4	12"	TOP - CLEAN BOT. C/S POROSITY	TOP CLEAN BOT. POROSITY 1" IN. V.V.F.	CLEAN	CLEAN	
4PAW-FM-4	12"	TOP - CLEAN BOT. - LAST 1/2" V.F. SPREAD APART POROSITY .005 MAX	TOP - CLEAN BOT. SIMILAR 1" IN REST - OK	CLEAN	TOP - 1 1/2" - 2 - 0.005 BOT. CLEAN	SPECIMEN

Table A-7. Phase 1 - 0.250-Inch-Thick Plasma-Arc Welding - NDI Summary (Sheet 2 of 5)

WELD IDENT	LENGTH	1 <sup>st</sup> QUARTER	2 <sup>nd</sup> QUARTER	3 <sup>rd</sup> QUARTER	4 <sup>th</sup> QUARTER	COMMENTS
4PAW-FX-5		CLEAN	CLEAN	CLEAN BOT. - 1 1/2" IN. LIN. POR. TO Q4. 005/010	CLEAN BOT. 1 1/2" IN. Q4.	
4PAW-FM-5	12"	CLEAN	CLEAN	BOTTOM 1 1/2" IN. LIN. POR. STARTS - TO Q4 005.	BOTTOM 1 1/8" INTO Q4 - OK.	SPECIMEN
4PAW-FX-6	12"	1 PORE - .025/030 (TOP) CLEAN	CLEAN	CLEAN	CLEAN	
4PAW-FM-6	12"	CLEAN	CLEAN	CLEAN	CLEAN	NOT USED.

Table A-7. Phase 1 - 0.250-inch-Thick Plasma-Arc Welding -- NDI Summary (Sheet 3 of 5)

WELD IDENT	LENGTH	1 <sup>st</sup> QUARTER	2 <sup>nd</sup> QUARTER	3 <sup>rd</sup> QUARTER	4 <sup>th</sup> QUARTER	COMMENTS
4PAW-PX-1	12"	-	-	1 PORE - .00F. Q	-	
4PAW-PX-2	12"	BOTTOM - CONTINUOUS - .005 - .020 (POCKETS) MAX-.010 (3/8 SPACING) SOME - .001	SAME	BOTTOM - CONTINUOUS POCKETS .010 MAX	LINEAR - .005 - .020 AVG' - .010	
4PAW-PM-2	10 1/2"	BOTTOM CONTINUOUS MAX - .020 AVG - .010	LINEAR POROSITY - MAX - .010 AVG - .005	FEW - .005 PORES 1ST INCH "LIGHT" LINEAR POROSITY MAX - .005	LIGHT LINEAR POROSITY. MAX - .005 (1ST INCH) REM - HEAVY LINEAR .005 MAX.	
4PAW-PX-3	12"	LINEAR - 1" LONG - .010 MAX .005 AVG.	VERY SMALL LINEAR POROSITY .010 MAX .005 AVG.	LINEAR POROSITY - 1ST 000 - 010 MAX. 005 NOM. FND FEW PORE	FEW PORES .020 BEGINNING - END-LINEAR POROSITY (1") .005 MAX.	
4PAW-PM-3		CLEAN	CLEAN - 1ST 1 1/2 INCH LINEAR INDICATION REM 010 MAX. FEW .015	VERY FINE POROSITY NOT LINEAR - 1ST 1/2 MAX - 015 . AVG. 005 REM - CLEAN	1ST INCH - MAX .005 MANY SMALLER	

Table A-7. Phase 1 - 0.250-Inch-Thick Plasma-Arc Welding - NDI Summary (Sheet 4 of 5)

WELD IDENT	LENGTH	1 <sup>st</sup> QUARTER	2 <sup>nd</sup> QUARTER	3 <sup>rd</sup> QUARTER	4 <sup>th</sup> QUARTER	COMMENTS
4PAW-SUX-1	12"	END OF Q-1. .185 VOID .200 LOF.	0.20 PORE- $\phi$ (MID) CLEAN	IRREGULAR WELD. NO VISIBLE POROSITY	CLEAN	
4PAW-SUM-1	12"	VOID .300 X .085 NO POROSITY	VISUAL VOID - NO POROSITY	CLEAN	CLEAN	
4PAW-SUX-2	12"	CLEAN	MID- $\phi$ 2-007	CLEAN	CLEAN	
4PAW-SUM-2	12"	CLEAN	CLEAN	CLEAN	CLEAN	
4PAW-SUX-3	12"	TOP; END OF Q1 - .025 PORE. .020 PORE.	CLEAN	CLEAN	TOP - 3/4" in 2-.007 CLEAN	
4PAW-SUM-3	1"	CLEAN	CLEAN	CLEAN	CLEAN	
4PAW-UFX-1	12"	CLEAN	MID- $\phi$ 2-.005 PORE	TOP - 1-020 PORE - 1" IN Q3 1/8" IN Q.3 - .005 BOT. CLEAN	CLEAN (1-BURST-IN CUT OFF ZONE)	NO UNDERFILL OR UNDERCUT STOP.
4PAW-UFX-2	12"	CLEAN	CLEAN	START - BOT. .015	CLEAN	
4PAW-UFM-2		CLEAN	CLEAN	CLEAN	CLEAN	
4PAW-UFX-3	12"	CLEAN	CLEAN	CLEAN 2 DEEPER ZONES OF UNDERCUT.	CLEAN	
4PAW-UFM-3		CLEAN	CLEAN	CLEAN	CLEAN	
4PAW-UFX-4	12"	UNDERFILL NO PORES	1/2" IN' .015 PORE UNDERFILL	CLEAN UNDERFILL.	CLEAN UNDERFILL.	
4PAW-UFX-5	12"	POOR - NO WELD	NO WELD	NO WELD LAST 3/4" UNDERFILL NO PORES - LOPSIDED UNDERFILL	GOOD - NO PORES UNDERFILL	

Table A-7. Phase 1 - 0.250-Inch-Thick Plasma-Arc Welding - NDI Summary (Sheet 5 of 5)

WELD IDENT	LENGTH	1 <sup>st</sup> QUARTER	2 <sup>nd</sup> QUARTER	3 <sup>rd</sup> QUARTER	4 <sup>th</sup> QUARTER	COMMENTS
4PAW-RX-1	12"	☉ 0.025" PORE.	CLEAN	TOP. 015. 010 PORE (START OF Q3) REST CLEAN	CLEAN	
4PAW-RM-1	12"	CLEAN	CLEAN	CLEAN	CLEAN	
4PAW-RX-2	12"	CLEAN	CLEAN	CLEAN	CLEAN	
4PAW-CX-1	10"		ALL WELD PASSES CLEAN	ALL WELD PASSES CLEAN - NO CRACKS'		STOPPED AFTER 7TH PASS
4PAW-CX-2	10"	CLEAN		ALL WELD PASSES CLEAN - NO CRACKS.		STOPPED AFTER 6TH PASS

Table A-8. Phase 1 - 0.090-Inch-Thick Gas-Tungsten-Arc Welding - NDI Summary (Sheet 1 of 3)

WELD IDENT	LENGTH	1 <sup>st</sup> QUARTER	2 <sup>nd</sup> QUARTER	3 <sup>rd</sup> QUARTER	4 <sup>th</sup> QUARTER	COMMENTS
9GTA-FX-1	14"	CLEAN	TOP CLEAN BOT. 005	CLEAN	CLEAN	
9GTA-FM-1		CLEAN	TOP CLEAN BOT. 005	CLEAN	TOP - CLEAN BOT. 005	
9GTA-FX-2	14"	TOP - CLEAN BOT. 010, 005, 010, 005.	TOP - CLEAN BOT. 005, 005, 007, 005, 005, 007, 007, 005.	TOP - CLEAN BOT. 010, 015, 005, 003.	TOP 003, 005 BOT. 010, 005, 007, 005.	
9GTA-FM-2		TOP - 003, 005, 005.	TOP - 005.	TOP - 005.	TOP - 003, 007, 005. BOT. 010, 005, 007, 005, 005, 005.	
9GTA-FX-3	14"	CLEAN	CLEAN	CLEAN	CLEAN	
9GTA-FM-3		TOP - CLEAN BOT.	2 INCLUSIONS 1st 1/2" TOP 005. BOT. .003 CLEAN	OK	OK	

Table A-8. Phase 1 - 0.090-Inch-Thick Gas-Tungsten-Arc Welding - NDI Summary (Sheet 2 of 3)

WELD IDENT	LENGTH	1 <sup>st</sup> QUARTER	2 <sup>nd</sup> QUARTER	3 <sup>rd</sup> QUARTER	4 <sup>th</sup> QUARTER	COMMENTS
9GTA-MSX-1	8"	CLEAN	CLEAN	TOP - PORE -010 1" IN 2-005 PORES. NEXT TO IT. REST - CLEAN	CLEAN	
9GTA-MSX-2	8"	CLEAN	CLEAN	CLEAN	CLEAN	
9GTA-UCX-1	8"	CLEAN	CLEAN	CLEAN	CLEAN	
9GTA-UCX-2	8"	CLEAN	TOP - 1 PORE. .007 1/4" O2 CLEAN	CLEAN	CLEAN	

Table A-8. Phase 1 - 0.090-inch-Thick Gas-Tungsten-Arc Welding -- NDI Summary (Sheet 3 of 3)

WELD IDENT	LENGTH	1 <sup>st</sup> QUARTER	2 <sup>nd</sup> QUARTER	3 <sup>rd</sup> QUARTER	4 <sup>th</sup> QUARTER	COMMENTS
9GTA-PX-1	14"	TOP - 010, 007, 005, 007, 010, 007, 005, 007, 015, 010, 010, 005, 010, 010, 015, 007, 010, 010, 015, 015, 010, 007, 010, 015, 010, 010, 017	010, 010, 017, 010, 010, 007, 017, 005, 015, 010, 005, 010, 012, 007, 020, 015, 020, 010, 015, 010, 007, 007, 010, 015, 010, 010, 007, 010, 015, 010, 010, 007, 010, 015, 010, 005, 005, 005, 005	005, 007, 007, 005, 005, 010, 007, 010, 007, 010, 010, 005, 010, 010, 010, 010, 005, 007, 1/2" CLEAN	005, 005, 007, 010, 010, 007, 007, 007, 010, 010, 010, 010, 005, 010, 005, 005, 007, 012, 005, 007, 005, 007, 005, 010, 005, 005, 007, 005, 010, 015, 010, 005, 010, 007, 010, 007, 010, 007, 005, 010, 005, 010, 007, 007, 005	INDIVIDUAL PORES ON TOP - NOT LINEAR
9GTA-PX-2	8"	TOP - 007, 015, 025, 010, 012 BOT. 025	TOP - 020, 012, 020, 017, 025, 017, 015, 015, 015, 015, LAST INCH CLEAN BOT. 005, 007, 015	TOP - 012, 017, 017, 012, 010, 010, 010, 015, 015, 015, 012 BOT. 020, 010, 015, 007, 015, 015, 005	TOP - 010, 010, 007, 015, 015, 015, 007, 010, 010, 010, 015, 010, 006, 010, 010, 015, 007, 020, 007, 020, 007, 005 BOT. 010	BOTTOM - MUCH CLEANER
9GTA-IX-1	8"	CLEAN	2 TUNGSTENS - .015 1-.055x.040 .010 2-.040 x .030 TOP .015 SPACING - .110' .010	CLEAN	CLEAN	
9GTA-IX-2	8"	PORE - TOP - 010 .015 (START AREA)	TOP - .015, 010 PORE - .015. 4 TUNGSTENS - (BOTTOM) .010 x 010 1" AWAY. 005, 025 x 015 .015 x 005	TUNGSTEN - (TOP) 020 X 020 PORE ASSOCIATED WITH IT SMALL TUNGSTEN - (BOTTOM) (.005 x .002)	CLEAN	
9GTA-IX-3	8"	PORE - BOT. 010 TOP .010	W - .040 x 025 LOWER C W - .025 x .020 W - .005 x .005 NO PORES.	CLEAN	W INCL. - (TOP) 2 TOUCHING 030 x 020	NO PORES

Table A-9. Fatigue Properties of the Base Metal

Thickness	Spec No.	$K_t$	CPM	Max Stress, KSI [R = .1]	Cycles
.080 In.	200-1-1	1	1800	115	80,000
.080 In.	200-1-4	1	1800	100	6,630,000 (NF)
.080 In.	200-1-4R	1	1800	130	35,000
.080 In.	200-1-8	1	1800	107.5	5,090,000 (NF)
.080 In.	200-1-2	1	1800	100	74,000
.080 In.	200-1-5	1	1800	110	70,000
.080 In.	200-1-7	1	1800	110	47,000
.080 In.	200-1-3	1	1800	130	30,000
.080 In.	200-1-6	1	1800	110	58,000
.080 In.	200-1-9	1	1800	100	466,000
.080 In.	200-1-10	1	1800	90	648,000
.080 In.	200-1-11	1	1800	100	8,855,000 (NF)
.080 In.	200-1-12	1	1800	120	46,000
.080 In.	200-1-13	1	1800	110	66,000
.080 In.	200-1-14	1	1800	100	84,000
.080 In.	200-1-16	1	1800	90	5,101,000 (NF)
.080 In.	20 <sup>1</sup> -1-17	1	1800	100	187,000
.080 In.	200-1-18	1	1800	95	5,115,000
.080 In.	200-1-18R	1	1800	130	37,000
.080 In.	200-1-15	1	20	140	2,956
.080 In.	200-1-19	1	20	135	13,371
.080 In.	200-1-20	1	20	130	13,180
.080 In.	200-1-21	1	20	140	7,423
.080 In.	199-1-11-1	2.1 Center Notch	1800	65	812,000
.080 In.	199-1-11-2	↓	1800	80	39,000
.080 In.	199-1-11-3		1800	70	291,000
.080 In.	199-1-11-4		1800	60	1,672,000
.080 In.	199-1-11-5		1800	55	5,025,000 (NF)
.080 In.	199-1-11-5R		1800	100	12,000
.080 In.	199-1-11-6		1800	70	53,000
.080 In.	199-1-11-7		1800	80	50,000
.080 In.	199-1-11-8		1800	57.5	574,000
.080 In.	199-1-11-9		1800	70	773,000
.080 In.	199-1-11-1RT		1800	80	35,000
.080 In.	199-1-11-2RT		1800	70	383,000
.080 In.	199-1-11-3RT		1800	60	1,366,000
.080 In.	199-1-11-4RT		1800	70	203,000
.080 In.	198-1-17-1RT		3.0 Edge Notch	1800	45
.080 In.	198-1-17-2RT	↓	1800	65	15,000
.080 In.	198-1-17-3RT		1800	50	82,000
.080 In.	198-1-17-4RT		1800	40	159,000
.080 In.	198-1-17-5RT		1800	50	33,000
.080 In.	198-1-17-6RT		1800	30	6,910,000 (NF)
.080 In.	198-1-17-6RT-R		1800	70	10,000
.080 In.	198-1-17-7RT		1800	40	1,361,000
.080 In.	198-1-17-8RT		1800	65	16,000

Note: NF - No Failure

**APPENDIX B**  
**TEST DATA SUMMARY (PHASE 2)**

**Table B-1. Fatigue Endurance of Flawless 0.080-inch-Thick GTA Welds**

Spec. No.	Fatigue Endurance (1800 cpm Unless Otherwise Indicated), cy-ksi	Fractographic Findings
1-4	61,000-100	Surface Failure Initiation - No Porosity
6-1	55,000-100	Surface Failure Initiation - No Porosity
6-2	7,580,000-90 22,000-120	Surface Failure Initiation - No Porosity
6-3	10,000-120	Surface Failure Initiation - No Porosity
6-4	27,000-95	Surface Failure Initiation - No Porosity
7-1	20,000-110	Surface Failure Initiation - No Porosity
7-2	85,000-90	Surface Failure Initiation - No Porosity
8-2	45,000-100	Surface Failure Initiation - No Porosity
9-1	17,613-120 (20 cpm)	Base Metal Initiation
9-2	21,158-110 (20 cpm)	Base Metal Initiation
9-3	5,197-130 (20 cpm)	Base Metal Initiation

**Table B-2. Fatigue Endurance Fractographic Characteristics of Flawless 0.25-inch-Thick GTA Weldments**

Spec. No.	cpm	Fatigue Endurance		Fractographic Findings
		Cycles	Max Stress, ksi	
1-2	1800	5,036,000 10,000	60* 140	Failure Init. at Surface. No Porosity.
2-3	1800	404,000	70	Failure in the Grip Sect. Disregard.
4-2	1800	3,210,000	80	Failure Init. in Base Metal
7-1	1800	1,083,000	80	Failure Init. at Sfcs. (Root)
7-3	1800	2,797,000	60	Failure at .004" Pore, .080" From Sfcs.
7-4	1800	5,031,000 21,000	50* 130	Failure Init. in Base Metal
8-1	1800	38,000	110	Failure Init. in Base Metal
8-2	1800	88,000	90	Failure Init. in Base Metal
8-3	1800	737,000	80	Failure Init. in Base Metal
8-4	1800	359,000	70	Failure at .004", .10" From Sfcs.
2-1	20	10,234	130	Failure Init. in Base Metal
2-2	20	7,404	135	Failure Init. at Sfcs. (Face)
2-4	20	-	-	Inadvert. Overload. Disregard.
4-1	20	15,420	120	Failure Init at Sfcs (Root)

\*No Failure

**Table B-3. Summary of Pretest Radiography, Fatigue Endurance and Fractography Data on Porous 0.080-Inch Thick GTA Welds**

Spec No.	RT Results	Fatigue Endurance (1800 cpm Unless Otherwise Indicated), cy-ksi	Fractography (Failure Initiation)
2-2	.015"-.020" Pores	81,000-60	Failure Init. at .020" Pore, .020" From Sfce.
2-3	.010-.035" Pores	5,181,000-45* 5,000-110	Failure Init at .030" Pore, .004" From Surface
3-1	.020-.030" Pores	59,000-80	Fail. Init. at .015" Pore, .020" From Surface.
3-2	.010" Porosity	14,000-70	Fail. Init. at .010" Pore, .015" From Surface.
3-3	.010" to .035" Pores	33,000-60	Partially Machined Contour of .030" Pore at Sfce. Init. Site
3-4	.010" to .030" Pores	485,000-50	Init. at .030" Pore, .02" From Sfce.
4-1	.005" to .030" Scat. Por.	45,000-70	Mult. Init. at .020" and .030" Dia. Pores, .025" From Surface
4-2	.005" to .025" Pores	1,811,000-50	Multip. Init. at .010" and .025" Pores
4-3	.005" to .025" Scat. Por.	5,104,000-45* 28,000-100	Primary Init. at .010" Pore, .020" From Surface
5-3	.015" to .030" Pores	54,000-80	Mult. Init. at .010" Pores
6-1	Scat. Por. .015"-.025"	47,000-70	Prim. Init. at .020" Pore, .030" From Surface
6-2	Scat. Por. .015"-.025"	98,000-50	Mult. Init. at .015" Pores, .035" From Surface
6-3	Scat. Por. .015"-.025"	3,069,000-40	Mult. Init. Sites, at .010" to .015" Pores
6-4	Scat. Por. .015"-.025"	5,005,000-35* 11,000-100	Mult. Init. at .015"-.020" Pores
7-2	.015" to .035" Pores	32,000-60	Init. at .030" Pore, .020" From Sfce.
7-4	.010" to .025" Pores	12,307,000-40* 18,000-90	Multiple Init. at .020" and .025" Pores
8-1	Scat. Por. .015" Ave.	727,000-50	Init. at .012" Pore at Edge Subsfce.
8-2	Scat. Por. .015"-.035"	2,526,000-45	Init. at .015" Pore, .020" From Sfce.
9-2	Scat. Por. .010"-.030"	26,000-80	Mult. Init. at .010" to .030" Pores

\*No Failure

Table B-4. Results of Radiographic Evaluations, Fatigue Tests and Fractographic Findings on 0.25-Inch-Thick GTA Welds Containing Porosity (Sheet 1 of 2)

Spec No.	RT	Fatigue Endurance, cy-ksi	Fractography (Failure Initiation)
1-2	Pores, .005"-.010"	35,632-90	Base Metal Initiation
1-3	Pores, .010"-.025"	5,357-100	2 Init. Sites at Internal Porosity. Primary .012" Pore, .030" From Surface
3-1	Scat. Por., .010"-.035"	115,000-60	(2) .015" Pores, .050" Apart, .020" From Surface
3-2	Scat. Por., .010-.035"	30,000-80	Mult. Initiation: .010" to .030" Pores, All Interior
3-3	Scat. Por. .010-.035"	463,000-40	Mult. Init. at .010"-.020" Pores and (4) Pore Cluster - .015" to .020"
3-4	Scat. Por. .010"-.035"	4,704,000-30	(2) .020" Pores, .010" Apart, .040" From Surface
5-2	Scat. Por., .010"-.035"	5,910-90	Mult. Init. Primary - .025" Pore, .075" From Surface
5-3	Scat. Por., .010"-.035"	7,233-80	Mult. Init. at .025"-.030" Pores
5-4	Scat. Por., .010"-.035"	6,459-75	Mult. Init. Sites .010" to .030" Pores
6-1	Scat. Por., .005"-.020"	73,000-70	Mult. Init. at .010" to .015" Pores
6-2	Scat. Por., .005"-.025"	13,000-90	Mult. Init. at .020"-.025" Pores
6-3	Same	104,000-50	Mult. Init. at .020"-.025" Pores
6-4	Same	84,000-40	(2) .025"-.030" Pore Cluster, .006" From Surface
7-1	Light Scat. Por., .005"-.020"	198,000-50	Init. at .015" Surface Pore
7-2	Light Scat. Por., .010"-.025"	166,000-40	Cluster of (4) Pores .020"-.030", .030" From Surface
7-3	Scat. Por., .010"-.025"	5,010,000-30* 11,000-90	Mult. Init. Sites at .020"-.025" Pores
7-4	Light Scat. Por., .005"-.020"	35,000-70	Mult. Init. at .015" Pores
8-1	Scat. Por., .005"-.025"	146,000-60	Mult. Init. at .010"-.020" Pores
8-2	Scat. Por., .005"-.025"	6,929,000-40* 17,000-100	Mult. Init. at .010"-.020" Pores
8-3	Scat. Por., .005"-.010"	240,000-50	Init. at .010" Sfce. Pore
8-4	Scat. Por., .005"-.010"	10,000-10	Mult. Init. at .010"-.025" Pores
9-1	Light Scat. Por.,	4,950-90 (20 cpm)	(2) .015"-.020" Pore Cluster, .001" Apart, .020" From Surface
10-1	Scat. Por., .010"-.030"	47,000-70	Init. at .020" Surface Pore
10-2	Scat. Por., .010"-.030"	267,000-40	Init. at .040" Pore, .020" From Surface
10-3	Scat. Por., .010"-.030"	591,000-30	(2) .015"-.020" Pore Cluster at the Surface
10-4	Scat. Por., .010"-.030"	5,009,000-20* 11,000-90	(3) Sfce. Initiations at .025"-.030" Dia Pores
11-1	Light Scat. Por., .010"-.025"	278,000-60	Mult. Init. Sites at .015"-.025" Pores
11-2	Light Scat. Por., .010"-.025"	31,000-80	Init. at an Isolated .020" Pore Approx. .001" From Surface
11-3	Light Scat. Por., .010"-.025"	97,000-50	Init. at .020" Surface Pore

No Failure

**Table B-4. Results of Radiographic Evaluations, Fatigue Tests and Fractographic Findings on 0.25-Inch-Thick GTA Welds Containing Porosity (Sheet 2 of 2)**

Spec No.	RT	Fatigue Endurance, cy-ksi	Fractography (Failure Initiation)
11-4	Light Scat. Por., .010"-.025"	5,118,000-35	Init. at .025" Pore, .090" From Surface
F1-1	.015" Pore	404,000-70	.012" Pore, .040" From Surface
F1-3	.005"-.010" Pores	51,000-90	Init. at .004" Subsurface Pore
F1-4	.020" Pore	30,000-110	Init. at .020" Pore, .050" From Surface

**Table B-5. Results of Pretest RT, Fatigue Tests, and Fractographic Evaluation of 0.080 and 0.25-Inch-Thick GTA Welds Containing Tungsten Inclusions (Sheet 1 of 2)**

Spec. No.	Pretest RT	Fatigue Endurance, cy-ksi	Fractography
<b>0.080" Welds</b>			
4-1	High-Dens Inclusion .080" x .060"	273,000-40	Inclusion Extending Throughout Thkn. Failure Init. at Incl./Surface Interface
4-2	High-Dens Inclusion .050" x .055"	5,030,000-30* 50,000-60	Same
4-3	High-Dens Inclusion .075" x .050"	19,000-50	Inclusion From Surface to ~ 4/3" of Thickness Failure Init. at W-Ti Interface
5-2	High-Dens. Inclusions .150" x .100", 3/8" Apart	25,000-50	Same
5-3	High-Dens. Inclusion .115" x .075"	1,000-100	Inclusion Extending Throughout Thkn. Failure Init. at Ti-W Interface
6-1	High-Dens. Inclusion .100" x .050"	9,735,000-50* 10,000-105	Failure Initiation at Internal Inclusions
6-3	High-Dens. Inclusion .075" x .060"	5,028,000-70* 3,000-120	Failure Initiation at Internal Inclusion
6-2	High-Dens Inclusion .025" x .015"	373,000-90	Same
<b>0.25" Welds (No Machining)</b>			
1-1	High-Dens. Inclusions (1) .035 x .100" and (1) .075" (Dia)	32,000-50	Root Failure Initiation No Inclusions
1-2	High-Dens. Inclusions (1) .075" x .075" (1) .100" x .075" (1) .125" Dia.	5,003,000-40* 20,000-70	Same
1-3	High-Dens. Inclusion .075" x .050	121,000-45	Same

\*No Failure

**Table B-5. Results of Pretest RT, Fatigue Tests, and Fractographic Evaluations of 0.080- and 0.25-inch-Thick GTA Welds Containing Tungsten Inclusions (Sheet 2 of 2)**

Spec. No.	RT Results	Fat. Endurance (1800 cpm Unless Otherwise Indicated), cy/ksi	Fractography (Failure Initiation)
9-3	Scat. .010-.030" Pores	28,000-60	(2) Pore Cluster (.030" and .008"), .015" From Surface
9-4	.015-.025" Pores	165,000-40	(2) Pore Cluster (.020" and .015"), .020" From Surface
10-1	.010"-.020" Pores	58,000-70	Large (Over .020") Pore, .010" From Surface
10-2	.010" to .020" Pores	4,743-50	Mult. Init. at .025" Pores
10-3	.010-.015" Pores	149,000-60	Init. at .010" Pore, .030" From Surface
10-4	.010"-.040" Pores	7,410,000-40* 24,000-90	.025" Pore, .012" From Surface
1-3	.015"-.030" Pores	3,448-90 (20 cpm)	(2) Pore Cluster - .015" and .007" Pores - .002" Apart
5-1	.005" to .025" Pores	18,936-100 (20 cpm)	.008" Pore, .030" From Surface
7-1	.010" to .025" Pores	9,032-90 (20 cpm)	.030" Pore, .015" From Surface
7-3	.010" to .025" Pores	5,771-85 (20 cpm)	Part. Machined Contour of .030" Dia. Pore on Surface
8-3	.010" to .030" Pores	4,604-90 (20 cpm)	Mult. Init. at .035" and .012" Pores
8-4	.010" to .025" Pores	14,032-75 (20 cpm)	Mult. Init. at .025" and .030" Pores
9-1	.010" to .025" Pores	19,462-80 (20 cpm)	Mult. Init. at .009" to .012" Pores
F1-1	.005" to .010" Pores	7,000-120	.001"-.004" Porosity
F1-3	.015" to .025"	59,000-80	.020" Pore, .025 From Surface
F7-4	.005" Porosity	1,283,000-80	.006" Pore, .020" From Surface
F7-3	.010" Porosity	7,640,000-70* 29,000-110	Surface Init. - No Pores
F8-1	(1) .010" Pore	2,533,000-70	Isolated .010" Pore, .025 From Surface
F8-3	.010" Pore	10,000,000-60* 30,000-110	Surface Init. - No Porosity
F8-4	.010" Porosity	336,000-80	.010" Pore, .025" From Surface
F9-4	.005" Porosity	17,613-120	.005" Pore, .003" From Surface

\*No Failure

**Table B-6. Data on Fatigue Endurance and Fracture Characteristics of Flawless 0.090-Inch-Thick EB Welds**

Spec. No.	Fatigue Endurance	Fractographic Findings
1-1	61,000 Cy at 105 ksi	0.002" Isolated Pore at Initiation Site
1-3	7,538,000 Cy at 80 ksi, N.F. 20,000 Cy at 130 ksi	Base Metal Failure
2-1	50,000 Cy at 115 ksi	Sfce. Initiation - No Pores
2-2	5,083,000 Cy at 85 ksi, N.F. 9,000 Cy at 140 ksi	Base Metal Failure
2-3	682,000 Cy at 90 ksi	0.001" Isolated Pore at Initiation Site
2-4	43,000 Cy at 100 ksi	Corner Initiation Site - No Porosity
3-1	739,000 Cy at 100 ksi	0.003" Isolated Pore at Init. Site
3-2	41,000 Cy at 115 ksi	Base Metal Failure
3-3	568,000 Cy at 105 ksi	Base Metal Failure
3-4	2,650,000 Cy at 95 ksi	0.001" Isolated Pore at Init. Site
10-1F	95,000 Cy at 90 ksi	Corner Initiation - No Pores
5-1	4,744 Cy at 140 ksi	0.002" Isolated Pore at Init. Site
5-2	3,900 Cy at 140 ksi	Base Metal Failure
5-3	10,000 Cy at 130 ksi	Two - 0.001" Pores at Initiation Sites
5-4	13,800 Cy at 130 ksi	0.001" Isolated Pore at Init. Site

**Table B-6. Data on Processing Parameters, Geometric Configuration, Fatigue Properties and Fractographic Findings on 0.25-Inch-Thick EB Weldments with Intentional Underfills**

Spec No.	Joint Gap, In.	RT	Underfill Configuration		W/D Ratio	Fatigue Endurance (a) - 1800 cpm (b) - 20 cpm Cycles/ksi	Fractographic Findings
			Width, In.	Depth, In.			
2-1	0.01	Underfill	.140	.02	7	(a) 7,000/80	Sfce. Init. at UF
2-2	Same	Same	.130	.01	13	(a) 14,000/60	Same
2-3	Same	Same	.130	.02	6.5	(a) 84,000/40	Same
2-4	Same	Same	.140	.02	7	(a) 5,073,000/30 NF 14,000/70	Same
9-1	0.025	Underfill	.17	.014	12	(b) 12,030/70	Root Initiation
9-2	Same	Underfill	.15	.015	10	(b) 12,535/60	Sfce Init. at UF
9-3	Same	Underfill	.13	.050	2.6	(b) 18,994/60	Same
9-4	Same	Underfill	.13	.045	2.9	(b) 5,125/65	Same
10-1	0.040	Same	.13	.035	3.7	(a) 7,702,000/40 10,000/70	Same
10-2	Same	Same	.13	.040	3.3	(a) 12,000/60	Same
10-3	Same	Same	.12	.050	2.4	(a) 22,000/40	Same
10-4	Same	Same	.10	.100	1	(b) 5,052/25	Same
11-1	Same	Same	.090	.065	1.4	(a) 5,087,000/15 (a) 14,000/30 NF	Same Same
11-2	Same	Same	.11	.075	1.6	(a) 14,000/30	Same
11-3	Same	Same	.12	.085	1.4	(a) 32,000/20	Same
11-4	Same	Same	.10	.095	1.05	(a) 12,786,000/10 NF 4,000/30	Same
12-1	.030	Same	.14	.020	7	(b) 32,000/60	Root Initiation
12-2	Same	Same	.14	.040	3.5	(b) 22,178/65	Sfce Init. at UF
12-3	Same	Same	.13	.050	2.4	(a) 5,045,000/25 NF 11,000/60	Same

**Table B-7. Data on Fatigue Endurance Characteristics of Flawless 0.25-Inch-Thick EB Welds**

Spec. No.	Fatigue Endurance (1800 cpm Unless Otherwise Indicated)	Fractographic Findings (Failure Initiation)
1-1	8,200 Cy at 140 ksi [20 cpm]	Base Metal Failure
1-2	9,700 Cy at 140 ksi [20 cpm]	An Isolated 0.004" Pore, 0.025" From the Surface
2-1	738,000 Cy at 80 ksi	0.004" Pore Adjacent to 0.002" Pore at the Mid-Thkn.
2-2	29,000 Cy at 120 ksi	Base Metal Failure
2-3	2,341,000 at 75 ksi	.002" Pore, 0.070" From Surface
2-4	7,565,000 Cy at 70 ksi N.F. 12,000 Cy at 140 ksi	Base Metal Failure
3-1	56,000 Cy at 100 ksi	Base Metal Failure
3-2	411,000 Cy at 85 ksi	(2) .001" Pores – 0.075" From the Surface
3-3	141,000 Cy at 85 ksi	(3) .001" Pores [Cluster] .004" From the Surface
3-4	1,863,000 Cy at 70 ksi	(1) .003" Pore, 0.100" From the Surface
4-1	38,000 Cy at 100 ksi	Two Subsurface Initiation Sites at 0.002" Pores
4-2	56,000 Cy at 75 ksi	0.001" Porosity Throughout
4-3	8,500 Cy at 125 ksi	A Linear Porosity Cluster at Subsurface Consisting of (2) .002" and (4) .001" Dia. Pores
4-4	354,000 Cy at 75 ksi	(1) .002" Pore – .004" Away from the Edge

**Table B-8. Detailed Data on Processing and Evaluation of Porosity—Containing 0.060-Inch-Thick EB Weldments (Sheet 1 of 3)**

Spec. No.	Contamination Method	RT Results	Fatigue Endurance	Fractographic Findings
1-1	Cutting Oil	Extensive Scattered Porosity [Ave Size 0.005" dia] (1) Pore -.010" dia	15,000 Cy at 110 ksi 1800 cpm	Multiple Initiation Sites Extensive Concentration of Fine (.001"-.005") Porosity in the Face-Side of the Weld
1-2	Cutting Oil	Minor Scattering of Pores [Ave Size = .003"]	15,500 Cy at 115 ksi 20 cpm	Multiple Init. Sites Scattered .001"-.003" Porosity
1-3	Cutting Oil	Minor Scattering of Pores [Ave Size -.005"]	23,250 Cy at 115 ksi 20 cpm	Init. Site at a Cluster of (3) .001" Pores - .003" From the Surface
2-1	Cutting Oil	Extensive Double-Line Porosity, .005"-.010"	13,000 Cy at 100 ksi 1800 cpm	No Definite Init Site. Extensive Concentr. of Fine [.001"-.002"] Porosity in the Face Side and Coarser (.003"-.004") Porosity at the Root Side
2-2	Cutting Oil	Same	31,000 Cy at 85 ksi 1800 cpm	Same as 2-1
2-3	Cutting Oil	Double Line Porosity [.003"-.007"] (1) Pore -.010" (2) Voids -.030"	18,600 at 105 ksi 20 cpm	Same as 2-1 Multiple Initiation Sites
2-4	Cutting Oil	Double Line Porosity [.003"-.007"] (1) Pore -.010" (2) Voids -.030"	98,000 Cy at 70 ksi 1800 cpm	Same as 2-1
4-1	Cutting Oil	Linear Porosity [Ave. Size .005"]	248,000 Cy at 60 ksi 1800 cpm	Extensive Concentr. of Fine (.001-.003") Porosity in the Face-side by the Weld. Initiation Site at .002" Pore - .004" from the Surface.
4-2	Cutting Oil	Same	352,000 Cy at 55 ksi 1800 cpm	Init. Site at .003" Pore, .004" From the Surface. Extensive Concentration of Fine (.001-.003") Porosity in the Face Side. .001"-.004" Isolated Porosity Elsewhere.
4-3	Cutting Oil	Extensive Linear Porosity (.005" Ave)	25,000 Cy at 95 ksi 1800 cpm	Extensive Concentr. of Fine Porosity in the Face-Side. (.001"-.003") Isolated .004"-.008" Pores at Root Side.
5-1	Grit Blasting Both Edges with Al <sub>2</sub> O <sub>3</sub>	Scattered Porosity [.005"-.010"]	39,000 at 100 ksi 20 cpm	Init. Site at .008" Pore, .020" From the Surface
5-4	Same	Minor Scattered Porosity [.003" Ave]	53,000 Cy at 100 ksi 20 cpm	Init. Site at .003" Pore, .008" from the Surface

Table B-9. Detailed Data on Processing and Evaluation of Porosity—Containing 0.080-Inch-Thick EB Weldments (Continued) (Sheet 2 of 3)

Spec. No.	Contamination Method	RT Results	Fatigue Endurance	Fractographic Findings
6-1	Same	Scattered Porosity — .005" Ave.	500,000 Cy at 45 ksi N.F. 32,000 Cy at 105 ksi 1800 cpm	Multiple Initiat. Sites. Primary Init. Site — .002" Dia, .002" From Surface
6-2	Same	Same	5,013,000 Cy at 50 ksi N.F. 27,000 Cy at 105 ksi 1800 cpm	Init Site at (3) .003" Pores, .020" From the Surface
6-3	Same	Same	5,078,000 Cy at 55 ksi N.F. 12,000 Cy at 130 ksi 1800 cpm	Multiple Init. Sites
6-4	Grit Blasting Both Edges With Al <sub>2</sub> O <sub>3</sub>	Minor Scattered Porosity (.005" Dia. Ave.)	228,000 Cy at 65 ksi 1800 cpm	Init. Site at .002" Pore at the Surface
7-1	Same	Same	62,000 Cy at 100 ksi 1800 cpm	Init. Site at .002" Pore at the Surface
7-2	Same	Same	102,000 Cy 65 ksi 1800 cpm	(2) Init. Sites — One at .002" From the Sfce One .004" From the First Pore, .001" From the Surface
7-3	Same	Extensive Scattered Porosity [.005" Ave.]	4,800 Cy at 130 ksi 20 cpm	Multiple Init. Sites, Scattered .002"-.005" Pores
7-4	Same	Minor Scattered Porosity [.005" Ave.]	5,000,000 Cy at 60 ksi N.F. 17,000 Cy at 130 ksi 1800 cpm	Init. Site at .003" Pore at the Surface
8-1	Same	Same	67,000 Cy at 95 ksi 1800 cpm	Init. Site at .002" Pore at the Sfce Other .002" Pores in the Interior
8-2	Same	Minor Scattered Porosity [.003" to .007" Range]	367,000 at 60 ksi 1800 cpm	.004" Pore .006" From the corner
8-3	Same	Very Minor Scattered Porosity (.005" Ave.)	18,600 Cy 120 ksi 20 cpm	Multiple Initiation Sites.
10-1	Same	Widely Scattered .005" Porosity	283,000 Cy at 70 ksi 1800 cpm	A Collapsed .004" Pore at the Edge. Other .001"-.004" Pores in the Interior
10-2	Same	Scattered Porosity, .003" to .007"	57,000 Cy at 85 ksi 1800 cpm	A Cluster of (3) .002" Pores at the Surface. Other .003" to .005" Pores in the Interior
12-1	Same	Several .005" Pores	101,000 Cy at 100 ksi 1800 cpm	Multiple Crack Initiation .001" to .006" Pores

**Table B-8. Detailed Data on Processing and Evaluation of Porosity—Containing,  
0.080-Inch-Thick EB Weldments (Continued) (Sheet 3 of 3)**

Spec. No.	Contamination Method	RT Results	Fatigue Endurance	Fractographic Findings
12-2	Grit (Al <sub>2</sub> O <sub>3</sub> ) Blasting Both Faying Surfaces	Linear and Scattered .005" Porosity	26,000 Cy at 120 ksi 1800 cpm	Multiple Init. Sites .001" to .006" Porosity
12-3	Same	Linear and Scattered Porosity [.005" Ave.]	7,200 Cy at 135 ksi 20 cpm	Multiple Init. Sites; Isolated .003" to .005" porosity
13-1	Same	Scattered .005" Porosity	73,000 Cy at 85 ksi 1800 cpm	Primary Init. Site at .002" Pore, .002" From Surface
13-2	Same	Scattered .005" Porosity	188,000 Cy at 65 ksi 1800 cpm	Init. Site at .004" Pore at the Corner. Isolated .003"-.004" Pores in Interior
13-3	Same	Same	1,076,000 Cy at 55 ksi 1800 cpm	Init. Site at .003" Dia Pore .002" From Surface
13-4	Same	Linear Fine Porosity and Scattered .005" Porosity	7,580,000 Cy at 50 ksi N.F. 18,000 Cy at 120 ksi 1800 cpm	Multiple Init. Sites. Primary Site at .002" Pore at the Surface

**Table B-9. Detailed Data on Processing and Evaluation of Porosity—Containing 0.25-Inch-Thick EB Weldments (Sheet 1 of 3)**

Spec. No.	Contamination Method	RT Results	Fatigue (1800 cpm) Endurance	Fractographic Findings
3-1	Sand Blasting of Both Faying Surfaces	Linear Porosity, .003" Ave.	308,000 Cy at 80 ksi	Linear Porosity, 0.035" From the Surface [Face] Sizes — 0.001" to 0.003". Internal Initiation.
3-2	Same	Scattered Porosity — .003" Ave.	62,000 Cy at 70 ksi	Subsurface Initiation at (2) .003" Pores, Approx .004" From the Surface. Linear Porosity [.003" Range] 0.020" From the Surface
3-3F	Same	No Indications	41,000 Cy at 110 ksi	Base Metal Failure
6-1	Grit Blasting One Side	Linear Porosity .005" Ave.	26,000 Cy at 105 ksi	Initiation at (2) .003" Pores Approximately .004" From the Surface
6-1F	Same	No Indications	5,030,000 Cy at 60 ksi N.F. 26,000 Cy at 130 ksi	Base Metal Failure
6-3	Same	Linear Porosity .005" Ave.	5,015,000 Cy at 60 ksi N.F. 52,000 Cy at 100 ksi	Linear Porosity (0.002" to 0.006" Range) Approximately 0.040" From the Surface [face] Internal Initiation at Porosity and External Initiation in the Corner
12-1	Thin Layer of Cutting Oil	Small Linear Indications, 0.005" to 0.040" Long. Possible Missed Seam	10,000 Cy at 80 ksi	Initiation at Partially Missed Seam
12-2	Same	Possible Missed Seam. Some Linear Porosity 0.005" or Less	5,000 Cy at 60 ksi	Failure at Missed Seam
12-3	Same	Fine Linear Indications. Possible Missed Seam	5,041,000 Cy at 40 ksi N.F. 68,000 Cy at 80 ksi	Fine (0.001" or Less) Porosity Throughout the Cross-Section. No Missed Seam
21-1	Cutting Oil Blend With G-1 Pwd	(2) . .015 Pores (1) . .025 Pore	29,000 Cy 70 ksi	Initiation Site Could not be Determined Due to Extensive Rubouts
21-2	Same	Scattered 0.005" to 0.020" Pores	88,000 Cy 50 ksi	Same
21-3	Same	Scattered .010" to .025" Pores	287,000 Cy 40 ksi	Initiation at a 0.020" Surface Pore. Other pores in 0.005" to 0.020" Range
24-1	Grit Blasting and Cutting Oil	Double-Row of 0.005" to 0.010" Porosity	25,000 Cy at 70 ksi	Massive Porosity (0.001 to 0.007" Interior Initiation
24-2	Same	Double-Row of Fine Porosity	48,000 Cy at 60 ksi	Massive (0.001" to 0.004") Porosity Especially at the Root Side of the Weld
24-3	Same	Fine Linear Porosity and Possible Lack of Fusion	285,000 Cy at 45 ksi	No Lack of Fusion. Initiation at 0.007" Surface Pore
24-4	Same	(2) Pores in 0.020" to 0.025" Range	549,000 Cy at 40 ksi	Heavy Concentration of Surface and Subsurface Porosity in .001" to .003" Range
27-1	Cutting Oil with G-11 Powder	Fine Linear Porosity — 0.005" Ave. Visual Sigs. Indications	57,000 Cy at 70 ksi	Massive Porosity Throughout (0.001" to 0.003" Range) Multiple Initiation Sites

Table B-9. Detailed Data on Processing and Evaluation of Porosity—Containing 0.25-Inch-Thick EB Weldments (Continued) (Sheet 2 of 3)

Spec. No.	Contamination Method	RT Results	Fatigue (1800 cpm) Endurance	Fractographic Findings
27-2	Same	Same	175,000 Cy at 50 ksi	Initiation at a Surface Pore -- .007" Dia.
27-3	Same	Fine Linear Porosity	5,032,000 Cy at 40 ksi 22,000 Cy at 100 ksi	Initiation at a Surface Pore, Partially Removed by Machining. Remaining Indentation -- .010" Dia.
27-4	Same	Fine Linear Porosity -- 0.005" Ave.	431,000 Cy at 45 ksi	A Cluster of (3) .002" Pores in Close Proximity of the Surface at the Initiation Site
28-1	Same	2 · .020" Pores	27,000 Cy at 90 ksi	Initiation at 0.015" Isolated Pore Approx. 0.005" From the Surface
28-2	Cutting Oil W. G-1 Powder	Fine Linear Porosity and 10 Scattered Pores [0.020" to 0.025"]	1,176,000 at 45 ksi	A Cluster of 5 Pores (.005", 0.004", (2) .002" and .001") .050" From the Surface at the Initiated Site
28-3	Cutting Oil W. G-1 Powder	Scattered Linear Porosity & Sfce. Indications	49,000 Cy at 60 ksi	Initiation at Partially Removed (On Machining) Sfce Pore; Originally ~ 0.015" Dia.
29-1	Same	Double Row of Heavy Porosity [.005" to .0020"] and Visual Sfce Indications	20,000 Cy at 80 ksi	Initiation at 0.002" Pore, 0.005" From the Surface. Massive Porosity [.001" to .006" Elsewhere]
29-2	Same	Same	107,000 Cy 60 ksi	Initiation at a Large Sfce. Porosity Massive Porosity Throughout
29-3	Same	Same	35,000 Cy at 50 ksi	Massive Porosity and Inclusions Throughout
29-4	Same	Same	5,064,000 Cy at 40 ksi N.F. 20,000 Cy at 90 ksi	Multiple Initiations. Massive Porosity and Inclusions
31-1	Same	Visual Sfce. Indications. (1) · .020" Pore	93,000 Cy at 80 ksi	Initiation at a 0.002" Sfce. Pore. Overload Contour Around 0.022" Pore in the Interior.
31-2	Same	Visual Sfce. Indications. Scattered .005" to .020" Pores	103,000 Cy at 60 ksi	Initiation at 0.006" Surface Porosity. Heavy Concentration of .005" to .010" Pores Elsewhere
31-3	Same	2 · 0.015" Pores 1 · 0.025" Pores	398,000 Cy 45 ksi	Initiation at .008" Pore at the Surface; .015" Pore in the Interior
31-4	Same	Scattered Porosity -- .005" Ave.	5,041,000 Cy at 40 ksi N.F. 7,000 Cy at 115 ksi	Multiple Initiation Sites at .002" to .005" Porosity Clusters
6-2	Grit Blasting (1) Faying Sfce.	Linear Porosity .005" Ave.	4,484 Cy at 130 ksi	Multiple Initiation Sites Concentration of .003" to .005" Porosity
13-1	Grit-Blasting (1) Faying Sfce.	Linear Porosity .005" Ave.	17,058 Cy 110 ksi	Multiple Initiation Sites -- Random
13-2	Grit-Blasting (1) Faying Sfce.	.150" x .175" Void	2,945 Cy at 100 ksi	Large Surface Void Due to Incomplete Removal of the Weld Bead

**Table B-9. Detailed Data on Processing and Evaluation of Porosity-Containing  
0.25-Inch-Thick EB WEldments (Continued) (Sheet 3 of 3)**

Spec. No.	Contamination Method	RT Results	Fatigue (1800 cpm) Endurance	Fractographic Findings
13-3	Grit-Blasting (1) Faying Sfce.	No Indications	13,760 Cy 120 ksi	A Cluster of 2 - .001" and .002" Porosity .010" From the Surface
17-1	Sand-Blasting (1) Faying Sfce.	No Indications	12,624 Cy at 120 ksi	An Isolated .004" Pore at the Surface
17-2	Same	Same	23,277 Cy at 110 ksi	Base Metal Failure
17-3	Same	Same	25,833 Cy at 105 ksi	An Isolated 0.004" Pore, .006" From the Surface
17-4	Same	Same	13,256 Cy at 125 ksi	Isolated .001" Pore, .005" From the Surface

**Table B-10. Results of Fatigue Tests and Fractographic Evaluations of 0.25-Inch-Thick EB Weldments with Mismatched Faying Surfaces**

Spec. No.	Mismatch	RT Results	Fatigue Endurance (1800 cpm)	Fractographic Findings
3-1	0.025"	No Indications	29,000 Cy at 50 ksi	Multiple Surface Initiations at the Face of the Weld
3-2	Same	Same	63,000 Cy at 40 ksi	Mult. Sfce. Initiations at the Root
3-3	Same	Same	10,097,000 Cy at 25 ksi N.F. 12,000 Cy at 60 ksi	Mult. Sfce. Initiations at the Root
3-4	Same	Same	293,000 Cy at 30 ksi	Linear Sfce. Initiations at the Root
4-1	0.015"	No Indications	7,030,000 Cy at 30 ksi N.F. 11,000 Cy At 70 ksi	Linear Sfce. Initiation at the Face
4-3	Same	Same	40,000 Cy at 50 ksi	Multiple Initiations at the Face
4-4	Same	Same	81,000 Cy at 40 ksi	Multiple Initiations at the Root
4-2	Same	Same	5,033,000 Cy at 30 ksi N.F. 17,000 Cy at 60 ksi	

Table B-11. Data on Processing Parameters, Geometric Configuration, Fatigue Properties and Fractographic Findings on 0.25-Inch-Thick EB Weldments with Intentional Underfills

Spec No.	Joint Gap, In.	RT	Underfill Configuration		W/D Ratio	Fatigue Endurance (a) - 1800 cpm (b) - 20 cpm Cycles/ksi	Fractographic Findings
			Width, In.	Depth, In.			
2-1	0.01	Underfill	.140	.02	7	(a) 7,000/80	Stce. Init. at UF
2-2	Same	Same	.130	.01	13	(a) 14,000/60	Same
2-3	Same	Same	.130	.02	6.5	(a) 84,000/40	Same
2-4	Same	Same	.140	.02	7	(a) 5,073,000/30 NF 14,000/70	Same
9-1	0.025	Underfill	.17	.014	12	(b) 12,030/70	Root Initiation
9-2	Same	Underfill	.15	.015	10	(b) 12,535/60	Stce Init. at UF
9-3	Same	Underfill	.13	.050	2.6	(b) 18,994/60	Same
9-4	Same	Underfill	.13	.045	2.9	(b) 5,125/65	Same
10-1	0.040	Same	.13	.035	3.7	(a) 7,702,000/40 10,000/70	Same
10-2	Same	Same	.13	.040	3.3	(a) 12,000/60	Same
10-3	Same	Same	.12	.050	2.4	(a) 22,000/40	Same
10-4	Same	Same	.10	.100	1	(b) 5,052/25	Same
11-1	Same	Same	.090	.065	1.4	(a) 5,087,000/15 (a) 14,000/30 NF	Same Same
11-2	Same	Same	.11	.075	1.5	(a) 14,000/30	Same
11-3	Same	Same	.12	.065	1.4	(a) 32,000/20	Same
11-4	Same	Same	.10	.065	1.05	(a) 12,786,000/10 NF 4,000/30	Same
12-1	.030	Same	.14	.020	7	(b) 32,000/60	Root Initiation
12-2	Same	Same	.14	.040	3.5	(b) 22,178/65	Stce Init. at UF
12-3	Same	Same	.13	.050	2.4	(a) 5,046,000/25 NF 11,000/60	Same

**Table B-12. Data on Radiographic Findings, Fatigue Endurance and Fractographic Analyses of Surface Contaminated 0.25-Inch-Thick EB Welds**

Spec. No.	RT Results	Fatigue Endurance	Fractographic Findings
2-1	OK	54,000 Cy at 60 ksi	No porosity at the Initiation Site. Fine (0.001") Scattered Porosity in the Interior. Linear Sfce Initiation.
2-2	OK	7,178,000 Cy at 45 ksi, N.F. 14,000 Cy at 80 ksi	Linear Sfce. Initiation No Porosity
2-3	OK	7,048,000 Cy at 40 ksi, N.F. 10,000 Cy at 90 ksi	Same

**Table B-13. Fatigue Endurance Values and Results of Fractographic Evaluation of Flawless PAW Specimens**

Spec. No.	Fatigue Endurance 1800 cpm Tests, unless otherwise indicated, CY/KSI	Fractography
1-1	61,000 at 100	Base metal failure
1-2	6,100 at 140 (20 cpm)	Stce init at edge no porosity
1-3	6,500 at 140 (20 cpm)	Init at .003" pore in the linear arrangm approx .035 from the [face-side] surface
1-4	27,200 at 115 (20 cpm)	Mult init sites in 003" pores in linear arrangement .020" from the surface
2-1	128,000 at 85	Init in (2) pore [.002" and .003"] cluster in linear arrangm
2-2	27,000 at 115	Base metal failure
2-3	130,000 at 85	Init at .003" pore in linear arrangm
2-4	36,000 at 115	Base metal failure
3-1	301,000 at 80	Init at .003" pore in linear arrangm
3-2	5,032,000 at 75 NF 20,000 at 130	Base metal failure
3-3	795,000 at 80	Init at .002" pore, .070" from Stce.
3-4	580,000 at 77.5	Init at .003" pore in linear arrangement
Note: NF - No Failure		

Table B-14. Data on Processing, Pre-Test Radiography, and Fractography of Porosity-Containing Weldments Produced by (Mechanized) PAW (Sheet 1 of 2)

Spec. No.	Contamination Method	RT	Fatigue Endurance 1800 cpm Unless Otherwise Indicated	Fractographic Findings				Failure Initiation Site	
				Linear Porosity					
				Yes	No	Width	Porosity Size Range		Distances From Surface
1-1	HNO <sub>3</sub> -HF	Lin. Por. - .005" Ave.	5,050,000 Cy at 45 ksi N.F.	✓		.025"	.002"-.005"	.020"	Multiple Failure Initiations in Lin. Por. Mult. Init.; Primary - .006" Pore, .040" From Sfca. Mult. Init.; Primary - .008" and .002" Pores at .030" Dist. From Sfca. (3) Pore Cluster (.004" to .005"), .040" From the Sfca. (5) Pore Cluster (.002"-.005"), .030" From the Sfca. Mult. Init.; Primary (2) .003" Pores, .030" From the Sfca. Mult. Init. Primary-Can't be Determined .004" Pore .04" From (Edge Sfca.) Mult. Init. Prim - at (2) .004" Pore, .020" From the Surface Mult. Init. Primary - (11) Pore Cluster (.003" to .006"), .025" From Sfca. (3) Pore Cluster (.004" to .005"), .006" From the Edge Sfca. (2) .006" Pores, .003" From (Edge) Sfca. (2) Pores (.005"); .020" From Sfca. (4) Pores (.003" to .005"), .030" From Sfca. Mult. Init., Some Clusters. No Primary Init. .004" Pore, .030" From Sfca.
1-2	HNO <sub>3</sub> -HF	Lin. Por. < .005"	31,000 Cy at 130 ksi	✓		.015"	.002"-.004"	.035"	
1-3	HNO <sub>3</sub> -HF	Fine Lin. Por.	189,000 at 60 ksi	✓		.015"	.002"-.007"	.030"	
2-1	HNO <sub>3</sub> -HF	Lin. Por. < .005"	150,000 Cy at 70 ksi	✓		.010"	.004"-.005"	.040"	
2-2	HNO <sub>3</sub> -HF	Same	16,000 Cy at 100 ksi	✓		.015"	.020"-.005"	.030"	
3-1	Oil on One Side	Lin. Por. - .005"	578,000 Cy at 60 ksi	✓		.020"	.002"-.007"	.020"	
3-2	Oil on One Side	Same	62,000 Cy at 95 ksi	✓		.020"	.004"-.006"	.020"	
4-1	Oil on One Side	Lin. Por. - Top Edge	57,000 Cy at 85 ksi	✓		.020"	.004"-.008"	.020"	
4-2	Oil on One Side	Lin. Por. - .005"	14,000 Cy at 120 ksi	✓		.020"	.002"-.007"	.020"	
5-1	Handling W/O Gloves	Lin. Por. - .005"	31,000 Cy at 110 ksi	✓		.015"	.003"-.004"	.025"	
5-2	Handling W/O Gloves	Same	25,000 Cy at 95 ksi	✓		.020"	.002"-.007"	.030"	
5-3	Handling W/O Gloves	Lin. Por. - Top Edge	111,000 Cy at 60 ksi	✓		.020"	.002"-.006"	.020"	
5-4	Handling W/O Gloves	Lin. Por. - .004"	3,775,000 Cy at 45 ksi	✓		.020"	.002"-.005"	.020"	
6-1	Handling W/O Gloves	Fin. Lin. Por.	2,144,000 Cy at 55 ksi	✓		.015"	.001"-.005"	.030"	
6-3	Handling W/O Gloves	Lin. Por. - .005"	30,000 Cy at 95 ksi	✓		.020"	.003"-.006"	.025"	
7-1	6 Days Exposure and Handl. W/O Gloves	Lin. Por.	93,000 Cy at 70 ksi	✓		.020"	.002"-.007"	.020"	

Table B-14. Data on Processing, Pre-Test Radiography, and Fractography of Porosity—Containing Weldments Produced by (Mechanized) PAW (Sheet 2 of 2)

Spec. No.	Contamination Method	RT	Fatigue Endurance 1800 cpm Unless Otherwise Indicated	Fractographic Findings					
				Linear Porosity			Distance From Surface	Failure Initiation Site	
				Yes	No	Width			Porosity Size Range
7-2	Same	Fine Lin. Por., Some .010" Pores	29,000 Cy at 110 ksi	✓		.010"	.003"-.004"	.010"	(3) .006" Pores, .015" From Sfce.
7-3	Same	Lin. Por. - .010" Ave.	286,000 Cy at 110 ksi	✓		.020"	.002"-.007"	.010"	(8) Pores [.002" to .007"], .006" From Edge
7-4	Same	Fine Lin. Por.	573,000 Cy at 45 ksi	✓			Only Few Pores Exposed		.004" Pore at Root Sfce. Other Visual Pore Indications at Root Sfce.
8-2	Same	Same	135,000 Cy at 70 ksi	✓		.020"	.002"-.006"	.020"	Init. at Partially Machined Edge Pore
8-3	Same	Hvy. Con. of Lin. Por. - .005" Ave.	56,000 Cy at 85 ksi	✓		.020"	.004"-.010"	.020"	.007" Pore, .007" From Edge Sfce.
8-4	Same	Lin. Por. .005" to .007" Ave.	324,000 Cy at 55 ksi	✓		.010"	.002"-.007"	.030"	Mult. Init. Primary .002" Pore, .005" From Edge
3-F	Oil-1 Side	No Indications	5,054,000 at 50 ksi N.F.				Base Metal Failure		
4-F	Same	No Indications	30,000 Cy at 120 ksi 58,000 Cy at 100 ksi	✓					A Very Minor Pore at Sfce. Initiation

**Table B-15. Fatigue Endurance Data on Mismatched 0.25-Inch-Thick PAW Specimens**

<b>Spec. No.</b>	<b>Fatigue Endurance (1800 cpm Tests)</b>	<b>Mismatch, In.</b>
3-1	14,000 Cy at 70 ksi	.016
3-2	41,000 Cy at 50 ksi	.016
3-3	5,002,000 Cy at 40 ksi-N.F. 12,000 Cy at 70 ksi	.016
3-4	61,000 Cy at 45 ksi	.016
4-1	64,000 Cy at 50 ksi	.025
4-2	53,000 Cy at 40 ksi	.025
4-3	7,090,000 Cy at 30 ksi-N.F. 5,000 Cy at 75 ksi	.025
4-4	115,000 Cy at 35 ksi	.025

Figure B-16. Fatigue Endurance of 0.25-Inch-Thick PAW Weldments with Minor Underfill

Spec. No.	Underfill, In.		Fatigue Endurance at 1800 cpm, Unless Otherwise Indicated	Failure Initiation
	Depth	Width		
4F1-1	.010	.15	14,288 Cy at 115 ksi (20 cpm)	Root
1-2	.005	.15	10,593 Cy at 115 ksi (20 cpm)	Root
1-3	.005	.15	13,120 Cy at 115 ksi (20 cpm)	Root
1-4	.010	.13	18,693 Cy at 100 ksi (20 cpm)	Root
2-1	.005	.15	7,029,000 Cy at 60 ksi N.F. 15,000 Cy at 115 ksi	Face (UF)
2-2.005	.15	.15	29,224 Cy at 90 ksi (20 cpm)	Face (UF)
2-3	.010	.16	112,000 Cy at 80 ksi	Base Metal
2-4	.005	.15	21,000 Cy at 100 ksi	Root
3-1	.010	.15	31,000 Cy at 80 ksi	Root
3-2	.005	.15	5,012,000 Cy at 60 ksi-N.F. 22,000 Cy at 100 ksi	Root
3-3	.005	.17	7,183,000 Cy at 70 ksi-N.F. 16,000 Cy at 115 ksi	Root
3-4	.005	.15	462,000 Cy at 75 ksi	Root
4-1	.005	.16	109,000 Cy at 80 ksi (20 cpm)	Base Metal
4-2	.005	.15	22,787 Cy at 100 ksi (20 cpm)	Root
4-3	.005	.17	19,045 Cy at 100 ksi	Root
	Undercut			
LIC1-1	.010	.11	14,000 Cy at 90 ksi	Face (UC)
1-2	.015	.10	9,000 Cy at 70 ksi	Disregard-Grooves on the Sfce.
1-3	.010	.10	30,000 Cy at 70 ksi	Disregard-Grooves on the Sfce.
1-4	.007	.12	2,574,000 Cy at 60 ksi	Subsurface Init. at .005" Pore .040" From (Face/Sfce.)
2-1	.010	.08	57,000 Cy at 80 ksi	Root
2-2	.005	.09	63,000 Cy at 70 ksi	Root
2-3	.005	.07	5,004,000 Cy at 65 ksi N.F. 16,000 Cy at 100 ksi	Root

**Table B-17. Fatigue Endurance of 0.25-Inch-Thick PAW Weldments with Minor Underfills or Undercuts**

Spec. No.	Fatigue Endurance [1800 cpm]	
	Cycles	Max. Stress, ksi
1-1	25,000	80
1-2	67,000	60
1-3	6,990,000 7,000	60-N.F. 95
1-4	5,004,000 15,000	55-N.F. 90
2-1	3,096,000	70
2-2	56,000	90
2-3	13,000	110
2-4	59,000	80

**Table B-18. Processing and Fatigue Endurance of Surface-Contamination  
Type PAW Weldments**

Spec. No.	Surface Contamination	Fatigue Endurance
1-1	Trial Shield Argon Decreased From 100 cfh to 30 cfh	23,000 Cy at 70 ksi
1-2	Trial Shield Argon Decreased From 100 cfh to 30 cfh	14,000 Cy at 80 ksi
1-3	Trial Shield Argon Decreased From 100 cfh to 30 cfh	58,000 Cy at 60 ksi
1-4	Trial Shield Argon Decreased From 100 cfh to 30 cfh	190,000 Cy at 50 ksi
2-1	Trial Shield Argon Decreased From 100 cfh to 30 cfh	105,000 Cy at 60 ksi
2-2	Trial Shield Argon Decreased From 100 cfh to 30 cfh	5,010,000 Cy at 50 ksi-N.F. 7,000 Cy at 100 ksi
2-3	Trial Shield Argon Decreased From 100 cfh to 30 cfh	94,000 Cy at 55 ksi
2-4	Trial Shield Argon Decreased From 100 cfh to 30 cfh	61,000 Cy at 55 ksi
3-1	Eliminate Trail Shield & Torch Shield Normal	7,456,000 Cy at 40 ksi-N.F. 12,000 Cy at 90 ksi
3-2	Eliminate Trail Shield & Torch Shield Normal	161,000 Cy at 50 ksi
3-3	Eliminate Trail Shield & Torch Shield Normal	5,051,000 Cy at 45 ksi-N.F. 11,000 Cy at 90 ksi
3-4	Eliminate Trail Shield & Torch Shield Normal	79,000 Cy at 60 ksi
4-1	Eliminate Trail Shield & Torch Shield Normal	5,004,000 Cy at 55 ksi-N.F. 13,000 Cy at 100 ksi
4-2	Eliminate Trail Shield & Torch Shield Normal	34,000 Cy at 70 ksi
4-3	Eliminate Trail Shield & Torch Shield Normal	9,927,000 at 50 ksi-N.F. 12,000 Cy at 95 ksi
4-4	Eliminate Trail Shield & Torch Shield Normal	20,000 Cy at 80 ksi

**Table B-19. Fatigue and Fractographic Characteristics of Flawless GMA Specimens**

Spec. No.	Fatigue Endurance	Fractographic Findings
1-2	63,000 Cy at 100 ksi	Base Metal Failure
1-3	142,000 Cy at 85 ksi	Sfca. Initiation. No Porosity.
3-1	134,000 Cy at 75 ksi	Init. at 0.002" Sfca. Pore
3-2	4,822,000 Cy at 65 ksi	(1) .002" Internal Pore at Initiation Site.
4-1	24,000 Cy at 120 ksi	Sfca. Initiation. No Porosity.
4-2A	17,480 Cy at 120 ksi	Init. at (2) .002" Internal Pores
4-2B	11,443 Cy at 130 ksi	Multiple Initiation at (2) .002" Internal Pores

**Table B-20. Fatigue Endurance and Fractographic Data on 0.25-Inch-Thick GMA Welds with Lack-of-Penetration and Undercut Defects**

Spec. No.	RT	Fatigue Endurance	Fractography
P5-1	Incompl. Penetr [LP] and Undercut	31,000 Cy at 40 ksi	Failure Init. in Undercut at the Face (Undercut - .005" Deep, .040" Wide)
P5-2	Same	444,000 Cy at 20 ksi	LP .030" to .040", 3/4 of Width
P5-3	Same	5,001,000 Cy at 15 ksi N.F. 13,000 Cy at 50 ksi	LP of .030" to .045" in Depth Failure Init. at LP
6-1	Same	27,000 Cy at 40 ksi	LP of .035 to .050" Failure Init. at LP
6-2	Same	675,000 Cy at 20 ksi	0.032" LP in 1/2 of the Width, Failure Init. at LP
5-1	Same	49,000 Cy at 40 ksi	Init. at Face Undercut (.020" Deep, .075" Wide)
5-2	Same	141,000 Cy at 30 ksi	Init. at Face Undercut (.010" Deep, .075" Wide)
5-3	Same	214,000 Cy at 25 ksi	Init. at Face Undercut (.040" Deep, .125" Wide)
5-4	Same	5,399,000 Cy at 20 ksi N.F. 13,000 Cy at 55 ksi	Init. at Face Undercut
6-3	Same	142,000 Cy at 30 ksi	Init. at Face Undercut (.002" Deep, .070" Wide)
6-4	Same	760,000 Cy at 25 ksi	Failure in 0.006" Deep LP

**Table X1. Fatigue Endurance and Fractographic Data on 0.25-Inch-Thick GMA Welds with Lack-of-Penetration and Undercut Defects**

Spec. No.	Fatigue Endurance 1800 cpm Tests, unless Otherwise Indicated	Fractography
1-1	61,000 Cy at 100 ksi	Base Metal Failure
1-2	6,100 Cy at 140 ksi (20 cpm)	Sfce. Init. at Edge. No Porosity
1-3	6,500 Cy at 140 ksi (20 cpm)	Init. at .003" Pore in Linear Arrangement Approx. .035 From the [Face Side] Surface
1-4	27,200 Cy at 115 ksi (20 cpm)	Mult. Init. Sites in .003" Pores in Linear Arrangement .020" From the Surface
2-1	128,000 Cy at 85 ksi	Init. in (2) Pore (.002" and .003") Cluster in Linear Arrangement
2-2	27,000 Cy at 115 ksi	Base Metal Failure
2-3	130,000 Cy at 85 ksi	Init. at .003" Pore in Linear Arrangement
2-4	36,000 Cy at 115 ksi	Base Metal Failure
3-1	301,000 Cy at 80 ksi	Init. at .003" Pore in Linear Arrangement
3-2	5,032,000 Cy at 75 ksi N.F. 20,000 Cy at 130 ksi	Base Metal Failure
3-3	795,000 Cy at 80 ksi	Init. at .002" Pore, .070" From Sfce.
3-4	580,000 Cy at 77.5 ksi	Init. at .003" Pore in Linear Arrangement

**Table B-21. Fatigue Endurance, and Radiographic and Fractographic Data on Porous GMA Welds**

Spec No.	RT	Fatigue Endurance @ (1800 cpm) cy/ksi	Fractography
4-1	Scattered and Linear Porosity	116,000/50	No Porosity at Sfce. Init. Site
4-2	Same	183,000/40	Internal Cluster of 6 Pores [.004" to .020" Range] at Init. Site
4-3	Incompl. Fusion One .035 Pore	301,000/30	Disregard - Mach. Defect
8-1	Scat. Porosity .003" to .020"	91,000/60	.012" and .008" Pores at Init. Site .050" From Sfce.
8-2	Linear Porosity .005" to .020"	49,000/80	Two .010" Pores, .006" Apart at Init. Site .025" From Sfce
8-3	Scat. Porosity .005" to .010"	7,343,000/40 (2) 17,000/105	.008" Pore at Init. .020" From Sfce. Multiple Init. Sites
9-1	No Porosity	44,000/70	No Porosity at Sfce Init. Site
9-2	.005" - .010" Pores	72,000/90	Base Metal Failure
9-4	.005" - .010" Pores	33,000/70	.015" Pore at Init. .070" From Sfce. Multiple Init. Sites
6-1A	.005" to .020" Pores	134,000/70	Multiple Sfce and Subsfce. Init.
6-2	.005" to .020" Pores	14,000/90	Multiple Sfce and Subsfce Init.
6-3A	Scat. Porosity .005" to .010"	1,589,000/50	.010" and .006" Pores at Interior Init. Site
10-2	.005" to .015" Pores	5,000,000/30 (2) 77,000/80	.009" Pore at Sfce Init. Site
10-3	.005" to .015" Pores	3,351,000/45	Six Pores (.006" to .015") at Subsurface
10-4	.005" to .015" Pores	146,000/60	Sfce. and Subsfce Init. Sites
13-2	Linear Isolated .002" to .015" Pores	5,034,000/50 (2) 11,000/105	Multiple Subsfce Init. Sites
13-3	Same	90,000/70	.007" Pore at Sfce. Initiation
14-1	.075" and .100 Voids	393,000/60	.002" Pore at Sfce Init.
14-2	.010" and .020" Pores	165,000/55	.008" Pore at Sfce Init. Two .003" Pores at Subsfce.
14-3	Two .010" Pores	301,000/30	Rubout Fract. Sfce
6-3B	Damaged Film	21,707/110 (1)	Multiple Interior Init. Sites
6-4	Damaged Film	2,763/125 (1)	Multiple Subsfce Init. Sites
13-1	.005" Pores	26,670/110 (1)	Base Metal Failure
13-4	Scattered, .002" - .020" Pores	6,140/125 (1)	Multiple Interior Init. Sites

Notes: 1) 20 cpm  
2) No Failure